On the mass of black holes with scalar field hair in anti-de Sitter spacetime

Wahiba Toubal

PhD
January 2015

Supervisor: Prof. Elizabeth Winstanley

The University of Sheffield
School of Mathematics and Statistics

Abstract

Since it has been proven that the no-hair conjecture has exceptions, systems of gravity coupled with matter have been of great interest. This thesis studies one of these exceptions: the case of a scalar field with nonconvex self interaction potential minimally coupled with gravity in anti-de Sitter spacetime. By considering a convex potential we prove a no-hair theorem for the four possible scalar field cases. For nonconvex potential however, stable soliton and black hole solutions are found. We focus on the stable black hole solutions. We find the explicit expressions for the mass of these spacetimes in four, five and six dimensions. To obtain a finite mass it is necessary to consider the gravitational and the scalar contribution. The scalar contribution is different for different masses of the scalar field above the Breitenlohner-Freedman bound [31]. The last part of the thesis is concerned with providing a numerical method to calculate the mass for the different spacetimes with two different nonconvex potentials. The mass depends on three parameter a, b and f_{rr}. Each parameter is found by solving a differential equation using mathematica. We present a selection of plots to illustrate our results for the masses.

Contents

Preface

Mass in anti-de Sitter (adS) spacetime is a subtle issue which has raised interest in recent years. Following the definition of the mass in [73], this thesis is here to provide with a method to obtain expressions for the mass of adS gravity minimally coupled to a self interacting scalar field. We provide our own numerical method to calculate it.

We start chapter 1 with a section about black hole hair where we present the context in which hairy black holes emerged. We review some exceptions to the no-hair theorem. In order to understand what lies at the heart of the no-hair theorem we present two Bekenstein's proofs. Finally we introduce the definition of the ADM mass and the Komar integral.

In chapter 2 we investigate three different methods of defining the mass in matter-free asymptotically adS spacetimes. This analysis will help us determine which definition is best suited for the work we want to do. We investigate the 'counter-term' method [14], the method used by Hollands *et al* [81] and finally the Henneaux and Teitelboim method [74]. We calculate the mass of adS and adS-Schwarzschild spacetimes in four and five dimensions. The analysis provides us with a set of boundary conditions on the metric perturbations which guarantees that the masses are finite. These boundary conditions are important in later chapters.

In chapter 3 we investigate the Einstein-scalar system with minimal coupling, where we see that the scalar field has different asymptotic forms depending on its mass. We present a no-hair result when the scalar field has a convex potential. We show that the way to avoid the no-hair conjecture is to consider nonconvex potentials. We obtain soliton and black hole solutions in $D = 4, 5, 6$ where D is the number of spacetime dimensions. We then move on to investigate the stability of the solutions by means of a linear perturbation method.

If one wants to calculate the mass of solutions of gravity minimally coupled to a scalar field, one has to consider the gravitational and the scalar contribution to the total mass [73]. We will show how these two contributions are divergent when taken individually

but by adding them together the divergences cancel and we obtain a finite mass. For the cancelations to happen, the leading order behaviour of the scalar field seen in chapter 3 is not enough. We need to include subleading terms in the expansion of the scalar field. Therefore in chapter 4 we investigate the detailed asymptotics following [73]. We see that as the mass of the scalar field increases more subleading terms appear in the expression for the scalar field. We also see that the presence of the scalar field triggers a back reaction on the metric. We present the different subcases where we see that important coefficients appear. We present our own method based on the field equations to obtain these coefficients using mathematica. We show how the boundary conditions on the metric perturbations found in chapter 2 are crucial in our method.

When we have the subleading terms in the expansion of the scalar field, it becomes possible to obtain finite expressions for the masses for the different subcases. This is what we do in chapter 5 where we calculate the divergent gravitational contribution and the divergent scalar contribution separately. When adding the two contributions together we show that the divergences cancel only when the correct cut-offs have been made to both contributions. We present our method and show the results for all the subcases. We give explicit expressions of the finite masses which have not appeared previously in the literature. These are found to be in agreement with [73] where the explicit expression of the mass is given for one subcase.

Once we obtain the expressions for the masses for all subcases we want to be able to calculate them. In chapter 6 we present our own original numerical method to compute the masses using mathematica. We extract important mass parameters contained in subleading terms. This is done by defining new functions and solving their governing differential equations. We show how it is possible to calculate the mass and obtain mass plots using two nonconvex potentials as an example.

Chapters 3, 5 and 6 will lead to publications in the next few months. I would like to thank my supervisor Elizabeth Winstanley for her excellent supervision during this PhD - this work would not have been possible without her continuous support. I'm also thankful for the support of the Algerian consulate in London and the University of Sheffield.

To my Parents
To my Brothers and Sister
In memory of my Grandmother

Conventions

We use the sign convention of Misner, Thorne and Wheeler for our metric signature $(-,+,+,+)$. We use $c = 1$. In our mathematica code we always set the surface gravity $\kappa = 1$. We have tried to use standard notation as much as possible.

List of Tables

List of Figures

Chapter 1

Black holes: hair and mass

The no-hair theorem, which has been experimentally tested recently [32, 136], was rapidly followed by counter examples when it was first stated almost fifty years ago. It opened up a great research area in theoretical physics. Since the discovery of the existence of black hole hair there has been an extensive literature about the topic which testifies to its relevance. Our research focuses on calculating the masses of asymptotically anti de Sitter (adS) spacetimes with a minimally coupled scalar field. Scalar fields play a significant role in fundamental theories such as string theory and cosmology (particulary in inflation and dark energy models). They have been of particular interest in recent years. On the experimental side the first fundamental scalar particle was discovered [2, 42]. It is important to understand exact theoretical hairy black hole solutions. Being able to calculate some of their properties such as mass or angular momentum can help in the understanding of astrophysical black holes.

In this chapter we give a general review of the no-hair conjecture and some exceptions to this conjecture. We then present proofs of no-hair theorems by Bekenstein [21, 23] to understand the argument that lies behind them. Finally we introduce the ADM mass and the Komar integral. We use the later to obtain a finite expression for the mass of an asymptotically flat spacetime. We show that the Komar intergal is divergent for asymptotically adS spacetimes.

§ 1.1 No hair conjecture and black hole hair

The first black hole uniqueness theorem was announced by Israel in 1967 [87]. He proved that a static, topologically spherical black hole is described by the Schwarzschild solution. It can be characterised by two parameters which are the mass and the charge.

In the years following the statement the focus was to prove uniqueness theorems for four dimensional static or stationary black holes either purely gravitational or minimally coupled to an electromagnetic field. A series of black hole uniqueness theorems in electro-vacuum theories followed [40, 87, 105, 116, 135]. Shortly after, other types of matter were considered and soon the phrase 'black hole has no hair' appeared. This statement was introduced by Ruffini and Wheeler [117] for static spherically symmetric black holes in asymptotically flat spacetimes. It is known as the no-hair conjecture (NHC). The basic idea of the NHC is that black holes are characterised by three parameters only: their mass, angular momentum and a set of conserved charges measurable at infinity [30].

The first no-hair theorem for a minimally coupled massless scalar field was found by Bekenstein in 1972 [21] and generalised in [23]. The theorem was proven for minimally coupled scalar field in asymptotically flat space with static spherically symmetric black holes [77, 80, 124]. The no-hair theorems make some assumptions about the scalar field potential i.e. the potential is convex. When assumptions about the positiveness of the potential are not respected, some soliton and asymptotically flat black hole solutions were found analytically [6, 45, 109] and some solutions were constructed numerically [20, 34, 53].

For nonminimal coupling Saa [118] formulated a new no-hair theorem ruling out a very large class of non-minimally coupled finite scalar dressing of an asymptotically flat, static, and spherically symmetric black hole. One counter example is the Bronnikov-Bocharova-Melnikov-Bekenstein (BBMB) black hole solution [22]. This solution consists of a scalar field with zero self-interaction potential conformally coupled to a spherically symmetric extremal black hole. However it was shown to be unstable [33]. By considering a non-zero self interaction potential an analytic solution was found in asymptotically flat spacetime [91].

In the late 1980s one of the most important counterexample of the no-hair conjecture was found: the colored black hole solution of the Einstein-Yang-Mills (EYM) system [29, 90, 133]. It was found to be unstable but it opened up investigation on non-Abelian black holes [99, 126, 130].

No-hair theorems were tested in spacetimes with more complex asymptotic structures by introducing a cosmological constant. In the case of positive cosmological constant, i.e asymptotically de Sitter (dS) spacetimes, analytical solutions for minimally coupled scalar field have been found in [146]. Numerical solutions were found to be unstable against linear perturbations [128]. No-hair theorems were proved to be true for convex or double well potential, however solutions were found when the potential is nonconvex

[25]. Some non-minimally coupled solutions, analogues of the BBMB solution in four dimensions with a quadratic self interaction potential were found [102] but were proven to be unstable in [56, 66].

Spacetimes with a negative cosmological constant (or anti de Sitter spacetimes), have been of great interest in recent years due to the adS/CFT correspondence [100, 141] which has a direct application in string theory and supergravity theories. Asymptotically adS black holes with scalar hair have been related to superconductors by means of the gravity/gauge duality [82]. The adS/CFT or gauge/gravity correspondence relates a D dimensional conformal field theory to the geometry of an adS space in one higher dimension, it is also referred to as holographic duality. It was originally formulated in the context of string theory [100, 141]. Stable black hole solutions in asymptotically adS spacetimes with minimally coupled scalar field hair have been found in [57, 73, 103, 110, 111, 125, 127, 129]. Moreover, stable solutions were found for the EYM system [137]. The case of non-minimally coupled hair with self-interacting potential was also considered [114, 138]. The topic is still of great interest, recently general classes of exact static hairy black hole solutions have been obtained [4, 5, 8, 9, 10, 58]. Some work has also been done on soliton solutions in adS spacetime [60]. Our work is concerned with soliton and black hole solutions in adS. We do not consider time-dependent hairy black holes but it is worth mentioning that they have attracted recent interest [41, 98, 145].

Topological black holes are black holes with the property that the event horizon is an Einstein space with positive, zero or negative curvature. This opens up many possibilities in terms of new black hole solutions with non-spherical event horizons. These types of black holes were investigated in [28, 92, 93, 94, 103, 132]. We consider topological black holes in our work.

In this thesis we focus on $D \geqslant 4$ but three dimensional gravity has attracted a lot of attention with the Banados, Teitelboim and Zanelli (BTZ) black hole [15, 16]. The BTZ solution is of great interest because it shares interesting features with higher dimensional black holes like the adS/CFT correspondence [100]. The microscopic and semiclassical BTZ black hole entropy of matter-free gravity has been investigated in [123]. It has been extended to different gravity theories with matter sources such as a scalar field [46, 47, 48, 67, 71, 104, 108]. The non-minimally coupled case is considered in [143] and has received a lot of attention [24, 119, 142]. The electrically charged BTZ black hole was considered in [16] and the rotating BTZ black hole with an electromagnetic field was presented in [101]. More recently three dimensional gravity with negative cosmological constant in the presence of a scalar field and Abelian gauge field was considered [38]. Stable solutions are obtained and the conserved charges are

computed using the Hamiltonian method described in [115]. Entropy for topological massive gravity in 3D was also investigated [54, 70, 107].

This allows us to make a transition into black hole thermodynamics. The application of our work is found in black hole thermodynamics since the mass is needed. The study of black hole thermodynamics has been a driving force for developments in general relativity and string theory in the recent decades. In [18] Bardeen, Carter and Hawking establish the four laws of black hole mechanics which are analogous to the laws of thermodynamics. The event horizon area and the surface gravity κ are analogous to the entropy and temperature of the black hole respectively. The role of scalar hair parameters in the first law of thermodynamics has been investigated in [96]. The works of Hawking and Page [69] established that black holes have temperature. They have proven that in adS black holes can be in stable equilibrium with thermal radiation at a fixed temperature. The mass is crucial to study thermodynamic stability. Thermodynamics of black holes with minimally coupled scalar field hair has attracted attention in recent years for its relation with the adS/CFT correspondence [37, 64, 79, 144]. Some work on the mass in adS spacetime has been done recently in [96] where the mass is calculated and the thermodynamic properties of systems with black holes and scalar field in adS are studied. Our approach is different since we use a different way of defining the mass.

§ 1.2 Bekenstein's no-hair proof

1.2.1 Proof for a single scalar field

Here we outline the no-hair proof by Bekenstein [21], also considered by Sudarsky [124]. The proof is based on the scalar field equation and the black hole structure of spacetime only. There is no mention of Einstein's equations. A static black hole spacetime with a scalar field minimally coupled to gravity is considered. The scalar field satisfies the equation of motion:

$$\nabla^{\mu}\nabla_{\mu}\phi = \frac{\partial V}{\partial \phi}. \tag{1.1}$$

The spacetime is endowed with a Killing horizon and t the time coordinate is the killing parameter. By multiplying (1.1) by ϕ and integrating over a region of spacetime bounded by two spacelike hypersurfaces (hypersurfaces of constant t), the region at

infinity and the Killing horizon bifurcation 2-surface one has:

$$\begin{aligned} 0 &= \int \sqrt{-g} d^4x \left(-\phi \nabla^\mu \nabla_\mu \phi + \phi \frac{\partial V}{\partial \phi} \right) \\ &= \int \sqrt{-g} d^4x \left(\nabla_\mu \phi \nabla^\mu \phi + \phi \frac{\partial V}{\partial \phi} \right) - \int \phi \nabla^\mu \phi dS_\mu. \end{aligned} \tag{1.2}$$

The asymptotic region contribution vanishes since ϕ is required to fall-off to zero at infinity. The Killing horizon bifurcation surface has measure zero and the contributions from the two spacelike hypersurfaces with constant t cancel each other. As a result, the surface integral in (1.2) vanishes. For convex potentials with $\phi \frac{\partial V}{\partial \phi} > 0$ the integral $\int \sqrt{-g} d^4x \left(\nabla_\mu \phi \nabla^\mu \phi + \phi \frac{\partial V}{\partial \phi} \right)$ is positive-semidefinite (when the potential is centered at zero). We consider the potential to be time-independent. We therefore must have $\phi \equiv 0$.

The proof above is very important as we will use it to prove a series of no-hair theorems in chapter 3. Bekenstein also considers the no hair proof for multiple fields [23], we present the proof in the next subsection.

1.2.2 Proof for multiple scalar fields

In this section we show how the statement made by Wheeler 'a black hole has no hair' [117] is proved in a particular case by Bekenstein in [23]. In this paper he considers a multiplet of scalar fields, $W, Y, ...$ minimally coupled to gravity. We give an outline of the proof. The system is described by the action:

$$S_{W,Y,...} = -\int \sqrt{-g}\, d^4x\, \mathscr{E}(\mathscr{I}, \mathscr{J}, \mathscr{K}, ..., W, Y, ...) \tag{1.3}$$

where $\mathscr{E}$ is a function and $\mathscr{I} \equiv g^{\alpha\beta} W_{,\alpha} W_{,\beta}, \mathscr{J} \equiv g^{\alpha\beta} Y_{,\alpha} Y_{,\beta}$ and $\mathscr{K} \equiv g^{\alpha\beta} Y_{,\alpha} W_{,\beta}$, with other quantities defined similarly. From now on only two fields are considered and it is assumed that the energy density of the scalar field is non-negative. From $S_{W,Y}$ the energy momentum tensor is:

$$T^\beta_\alpha = -\mathscr{E} g^{\alpha\beta} + 2\frac{\partial \mathscr{E}}{\partial \mathscr{I}} W_{,\alpha} W^{,\beta} + 2\frac{\partial \mathscr{E}}{\partial \mathscr{J}} Y_{,\alpha} Y^{,\beta} + \frac{\partial \mathscr{E}}{\partial \mathscr{K}} W_{,\alpha} Y^{,\beta}. \tag{1.4}$$

An observer with a four velocity $\mathbf{U}^\alpha$ where $\mathbf{U}^\alpha \mathbf{U}_\alpha = -1$ sees the energy density:

$$\rho = \mathscr{E} + 2\left[\frac{\partial \mathscr{E}}{\partial \mathscr{I}} (W_{,\alpha} \mathbf{U}^\alpha)^2 + \frac{\partial \mathscr{E}}{\partial \mathscr{J}} (Y_{,\alpha} \mathbf{U}^\alpha)^2 + \frac{\partial \mathscr{E}}{\partial \mathscr{K}} W_{,\alpha} \mathbf{U}^\alpha Y_{,\beta} \mathbf{U}^\beta \right]. \tag{1.5}$$

In the case of static black hole with scalar field hair the spacetime possesses a time-like Killing vector along which the observer moves, so:

$$\begin{aligned} W_{,\alpha}\mathbf{U}^{\alpha} &= 0 \\ Y_{,\alpha}\mathbf{U}^{\alpha} &= 0 \end{aligned} \tag{1.6}$$

and the energy density reduces to $\rho = \mathscr{E}$. As it was mentioned above, the energy density is assumed to be non negative so $\mathscr{E} \geqslant 0$. The local energy density cannot be negative for any observers, which corresponds to the weak energy condition (WEC).

Now consider a second observer moving with a three-velocity $\mathbf{V}$ relative to the first observer. In the free falling frame of reference of the first observer the second observer has a four-velocity with components:

$$\begin{aligned} U^0 &= \frac{1}{\sqrt{1-\mathbf{V}^2}} \\ \mathbf{U} &= \frac{\mathbf{V}}{\sqrt{1-\mathbf{V}^2}}. \end{aligned} \tag{1.7}$$

When $|\mathbf{V}| \to 1$ the terms containing derivatives in (1.5) become very big and dominate $\mathscr{E}$. Therefore we have conditions:

$$\begin{aligned} \frac{\partial \mathscr{E}}{\partial \mathscr{I}} &> 0 \\ \frac{\partial \mathscr{E}}{\partial \mathscr{J}} &> 0 \end{aligned} \tag{1.8}$$

and

$$\left(\frac{\partial \mathscr{E}}{\partial \mathscr{K}}\right)^2 \leqslant 4\frac{\partial \mathscr{E}}{\partial \mathscr{I}}\frac{\partial \mathscr{E}}{\partial \mathscr{J}} \tag{1.9}$$

in order to satisfy the non-negative assumption.

The next step is to assume the existence of a self consistent asymptotically flat solution of the Einstein and scalar field equations describing a static spherically symmetric black hole. The metric outside the black hole event horizon can be written as:

$$ds^2 = -e^{\zeta}dt^2 + e^{\upsilon}dr^2 + r^2(d\theta^2 + \sin\theta^2 d\phi^2) \tag{1.10}$$

where $\zeta = \zeta(r)$ and $\upsilon = \upsilon(r)$ depend on r only and are $O(r^{-1})$ as $r \to \infty$. The scalar fields also depend only on r assuming they are nontrivial. The energy-momentum tensor is conserved since the action is coordinate invariant:

$$T^{\nu}_{\mu\,;\nu} = 0 \tag{1.11}$$

and the r component is:

$$\frac{\partial(\sqrt{-g}\,T^r_r)}{\partial r} = \frac{\sqrt{-g}}{2}\frac{\partial g_{\alpha\beta}}{\partial r}T^{\alpha\beta}. \tag{1.12}$$

We also have $T^\theta_\theta = T^\phi_\phi$ and T^μ_ν is diagonal because the solution is static and spherically symmetric. Under these conditions (1.12) becomes:

$$\frac{\partial}{\partial r}\left(e^{\frac{\zeta+\upsilon}{2}}r^2T^r_r\right) = \frac{e^{\frac{\zeta+\upsilon}{2}}\,r^2}{2}\left(\zeta' T^t_t + \upsilon' T^r_r + \frac{4}{r}T^\theta_\theta\right). \tag{1.13}$$

where the prime is the partial derivative with respect to the radial coordinate. We have the term $1/2e^{\frac{\zeta+\upsilon}{2}}r^2T^r_r\upsilon'$ on both sides of the equality so they cancel and we are left with:

$$\frac{\partial}{\partial r}\left(e^{\frac{\zeta}{2}}r^2T^r_r\right) = \frac{e^{\frac{\zeta}{2}}\,r^2}{2}\left(\zeta' T^t_t + \frac{4}{r}T^\theta_\theta\right). \tag{1.14}$$

Form the symmetries of the spacetime and the expression for the stress energy tensor in (1.4) we have $T^t_t = T^\theta_\theta = -\mathscr{E}$ which substituted in (1.14) gives:

$$\frac{\partial}{\partial r}\left(e^{\frac{\zeta}{2}}r^2T^r_r\right) = -\frac{\partial}{\partial r}\left(e^{\frac{\zeta}{2}}\,r^2\right)\mathscr{E}. \tag{1.15}$$

Equation (1.15) is then integrated from the black hole event horizon r_h to a generic radius r outside the horizon. At r_h the metric function $e^\zeta = 0$ and in order for the corresponding surface to be a regular horizon it must be the case that

$$T_{\alpha\beta}T^{\alpha\beta} = \left(T^t_t\right)^2 + \left(T^r_r\right)^2 + \left(T^\theta_\theta\right)^2 + \left(T^\phi_\phi\right)^2 \tag{1.16}$$

is finite and so T^r_r and $T^t_t = -\mathscr{E}$ are also finite at the event horizon. After performing the integration:

$$T^r_r = -\frac{e^{\frac{\zeta}{2}}}{r^2}\int_{r_h}^{r}(r^2e^{\frac{\zeta}{2}})'\mathscr{E}\,dr. \tag{1.17}$$

We know that $e^\zeta = 0$ at $r = r_h$ and $e^\kappa > 0$ for $r > r_h$ so the term $r^2\,e^{\zeta/2}$ must grow with r sufficiently close to the event horizon. From (1.17) and using the fact that $\mathscr{E} \geqslant 0$ it can be deduced that $T^r_r < 0$ sufficiently close to the horizon. Now if the differentiation in (1.15) is explicitly carried out one gets:

$$(T^r_r)' = -e^{-\frac{\zeta}{2}}\,r^{-2}\left(r^2\,e^{\frac{\zeta}{2}}\right)'(\mathscr{E} + T^r_r). \tag{1.18}$$

and using the expression for the stress energy tensor in (1.4):

$$\mathscr{E} + T_r^r = 2e^{-\upsilon}\left(\frac{\partial \mathscr{E}}{\partial \mathscr{I}} W_{,r}^2 + \frac{\partial \mathscr{E}}{\partial \mathscr{J}} Y_{,r}^2 + \frac{\partial \mathscr{E}}{\partial \mathscr{K}} W_{,r} Y_{,r}\right). \tag{1.19}$$

Conditions (1.8) and (1.9) ensure the positiveness of $\frac{\partial \mathscr{E}}{\partial \mathscr{I}}$, $\frac{\partial \mathscr{E}}{\partial \mathscr{J}}$ and $\frac{\partial \mathscr{E}}{\partial \mathscr{K}}$ so $\mathscr{E} + T_r^r \geqslant 0$ everywhere. Looking at (1.18) and remembering the analysis made for the term $r^2 e^{\zeta/2}$ earlier it can be concluded that $(T_r^r)' < 0$ close to the event horizon.

Now we consider the infinity region where $e^{\zeta/2} \to 1$. When putting this in (1.18) we have $(T_r^r)' < 0$ at infinity. The next step is to consider the Einstein equations obtained by calculating the components of the Ricci tensor, the relevant ones are:

$$\begin{aligned} e^{-\upsilon}\left(\frac{1}{r^2} - \frac{\upsilon'}{r}\right) - \frac{1}{r^2} &= 8\pi G T_t^t = -8\pi \mathscr{E} \\ e^{-\upsilon}\left(\frac{\zeta'}{r} - \frac{1}{r^2}\right) - \frac{1}{r^2} &= 8\pi G T_r^r. \end{aligned} \tag{1.20}$$

Integrating the first equation gives:

$$e^{-\upsilon} = 1 - \frac{8\pi G}{r}\int_{r_h}^{r} \mathscr{E} r^2 dr - \frac{2GM}{r} \tag{1.21}$$

where M is is constant of integration. The spacetime is asymptotically flat so $\mathscr{E} = O(r^{-3})$ and it follows that $\upsilon = O(r^{-1})$. In order to fix the integration constant M one needs to impose that $e^{\upsilon} \to \infty$ as $r \to r_h$. With this condition we have:

$$GM = \frac{r_h}{2} \tag{1.22}$$

and M can be interpreted as the bare mass of the black hole. So the integral in (1.17) converges and $|T_r^r| = O(r^{-2})$ at infinity but since asymptotically $(T_r^r)' < 0$ then $T_r^r > 0$ and decreases as $r \to \infty$. Since it was shown earlier that near the horizon $T_r^r < 0$ then there must be an interval $[r_a, r_b]$ where $(T_r^r)' > 0$ and T_r^r changes sign at some r_c with $r_a < r_c < r_b$. This is incompatible with Einstein equations since from (1.21) $e^{\upsilon} \geqslant 1$ outside the event horizon. The second Einstein equation in (1.20) can be rewritten as:

$$\frac{e^{-\frac{\zeta}{2}}}{r^2}\left(r^2\, e^{\zeta}\right)' = \left[4\pi G r T_r^r + \frac{1}{2r}\right] e^{\upsilon} + \frac{3}{2r} \tag{1.23}$$

and because

$$\frac{e^{\upsilon}}{2} + \frac{3}{2} > 2 \tag{1.24}$$

the inequality

$$\frac{e^{-\frac{\zeta}{2}}}{r^2}\left(r^2\, e^{\zeta}\right)' > 4\pi G r T_r^r e^{\upsilon} + \frac{2}{r} \tag{1.25}$$

holds. It was found above that in $[r_c, r_b]$ we have $T_r^r > 0$ so there $\frac{e^{-\frac{\zeta}{2}}}{r^2}\left(r^2\, e^{\zeta}\right)' > 0$ and according to (1.18) it means that $(T_r^r)' < 0$ in this interval. However in the bigger interval $[r_a, r_b]$ it was found that $(T_r^r)' > 0$. This is a contradiction and it is resolved by considering constant scalar fields in the region outside the event horizon, so

$$\mathscr{E}(0, 0, 0, ..., W, Y, ...) = 0 \tag{1.26}$$

meaning all components of the stress-energy tensor vanish identically in the black hole exterior. Values satisfying (1.26) must exist for a trivial solution of the scalar field equation to exist.

§ 1.3 Mass in asymptotically flat spacetimes

1.3.1 ADM mass

This section is an outline of the definition of ADM mass found in chapter 4 of [112].

Let us start by giving a definition of a hypersurface. A hypersurface is a $(D-1)$-dimensional submanifold embedded in a D-dimensional spacetime. Hypersurfaces can be spacelike, timelike or null and present intrinsic and extrinsic geometries.

The intrinsic geometry of a hypersurface is specified by an induced metric on the hypersurface with respect to the spacetime metric tensor. In a manifold with a system of coordinates x^α we can specify a hypersurface Σ by either restricting the coordinates on this hypersurface, by defining $\Phi(x^\alpha) = 0$ for one or more functions or introducing a parametric equation $x^\alpha = x^\alpha(y^a)$ where y^a are the intrinsic coordinates on the hypersurface. We also define n^α, the unit normal to the hypersurface with:

$$n^\alpha n_\alpha = \varepsilon \equiv \begin{cases} -1 & \text{if } \Sigma \text{ is spacelike} \\ +1 & \text{if } \Sigma \text{ is timelike} \\ 0 & \text{if } \Sigma \text{ is null.} \end{cases} \quad ' \tag{1.27}$$

Since we are interested in the mass of various spacetimes it is important to mention the Hamiltonian formulation of general relativity and the ADM formalism or $3+1$ decomposition. If we want to express the action of a system in terms of the Hamiltonian we have to foliate spacetime with a family of hypersurfaces, each of which corresponds to

a given time. The system of coordinates on the manifold is x^α and we consider a scalar function $t(x^\alpha)$ such that $t =$ constant corresponds to a family of nonintersecting hypersurfaces Σ_t. We define u_α as the timelike unit normal vector to these hypersurfaces. The coordinates on the hypersurfaces are y^a.

We now consider a congruence, which is a group of curves γ with a tangent vector t^α. Each curve γ intersects each hypersurface Σ_t once and only once but they need not be orthogonal to each other. It is then possible to define a new system of coordinates as follows: we construct a configuration such that a specific curve γ_p intersects a first hypersurface Σ_t at time t, a second hypersurface $\Sigma_{t'}$ at time t' and a third hypersurface $\Sigma_{t''}$ at time t'' and so on. The points of intersection are P, P', P'' respectively. The curve γ_p represents a mapping from P to P' and to P''. If we want to fix the coordinates of P' and P'' we impose $y^a(P) = y^a(P') = y^a(P'')$ and therefore y^a are constant on the curve γ. We can then define a coordinate system (t, y^a) in the spacetime which is related to the original coordinate system by $x^\alpha = x^\alpha(t, y^a)$. We have $t^\alpha = \left(\frac{\partial x^\alpha}{\partial t}\right)_{y^a}$ and we define tangent vectors on Σ_t as $e^\alpha_a = \left(\frac{\partial x^\alpha}{\partial y^a}\right)_t$. This implies that $t^\alpha = \delta^\alpha_t$.

We can define the unit normal to Σ as $u_\alpha = -N\partial_\alpha t$ where N is a constant introduced for normalisation purposes and is called the lapse. We also have $u_\alpha e^\alpha_a = 0$ on each hypersurface. The curves γ are not necessarily orthogonal to Σ_t therefore u^α and t^α may not be parallel. The normal vectors and the tangent vectors provide a basis for the tangent space and we can decompose t^α into lapse and shift as $t^\alpha = Nu^\alpha + N^a e^\alpha_a$, where N^a is called the shift.

Now we want to express the metric in the new coordinate system (t, y^a) defined earlier. We have

$$dx^\alpha = t^\alpha dt + e^\alpha_a dy^a = (Ndt)u^\alpha + (dy^a + N^a dt)e^\alpha_a. \tag{1.28}$$

The line element is:

$$ds^2 = -Ndt^2 + h_{ab}(dy^a + N^a dt)(dy^b + N^b dt) \tag{1.29}$$

where $h_{ab} = g_{\alpha\beta}\, e^\alpha_a\, e^\beta_b$ is the induced metric on Σ_t. This is the ADM decomposition.

The Hamiltonian can be thought of as being the energy of the system so it is natural to consider the Hamiltonian when we want to define the gravitational mass of a spacetime. In general relativity both the gravitational field and matter fields contribute to the action. In this section we only consider the gravitational field. Taking an arbitrary region $\mathcal{M}$ of the spacetime manifold foliated with spacelike hypersurfaces Σ, the gravitational

action is defined as:

$$S[g] = \int_{\mathcal{M}} \left(\frac{R}{16\pi}\right) \sqrt{-g}\, d^4x + \frac{1}{8\pi} \oint_{\partial\mathcal{M}} \varepsilon(K - K_0)\sqrt{|h|}\, d^3y \tag{1.30}$$

where R is the Ricci scalar of the spacetime, ε is defined in (1.27), K is the trace of the extrinsic curvature of Σ embedded in $\mathcal{M}$, K_0 is the extrinsic curvature of Σ embedded in flat spacetime, h is the determinant of the induced metric h_{ab} on Σ and y^a is a system of coordinates defined on Σ. The boundary of a given Σ_t is a closed 2-surface which we call S_t. The Hamiltonian H_G corresponding to (1.30) when the vacuum field equations are satisfied is [112]:

$$H_G = -\frac{1}{8\pi} \oint_{S_t} \left[N(w - w_0) - N_a(K^{ab} - Kh^{ab})r_b\right] \sqrt{\sigma}\, d^2\theta \tag{1.31}$$

where w is the trace of the extrinsic curvature of S_t embedded in Σ_t, w_0 is the extrinsic curvature of S_t embedded in flat spacetime, σ is the determinant of the induced metric σ_{ab} on S_t, r_a is the unit normal to S_t and θ^a are the coordinates defined on S_t. The value of the gravitational Hamiltonian when the vacuum field equations are satisfied corresponds to a boundary term (1.31).

How do we define mass in asymptotically flat spacetimes from the Hamiltonian? We can define the gravitational mass of an asymptotically flat spacetime to be the limit of the gravitational Hamiltonian when the boundary S_t is a 2-sphere at spatial infinity with a specific choice of lapse and shift $N = 1$ and $N^a = 0$. A mass defined in such a way is called the ADM mass [11] and is given by :

$$M = -\frac{1}{8\pi} \lim_{S_t \to \infty} \oint_{S_t} (w - w_0)\sqrt{\sigma}\, d^2\theta \tag{1.32}$$

where σ_{AB} is the metric on S_t, ω_0 is the extrinsic curvature of S_t embedded in flat space and $\omega = \sigma^{AB}k_{AB}$ is the extrinsic curvature of S_t embedded in σ_t.

1.3.2 Komar integral

In general relativity is the Komar approach is used to calculate the mass of asymptotically flat spacetimes. This subsection is based on section 5.3 in [131] and section 6.4 in [39]. We outline the method and apply it to calculate the mass.

Noether's theorem states that in a given spacetime every symmetry corresponds to a conserved current. If we consider $g_{\mu\nu}$ to be the metric of a given spacetime, a vector field $\xi^\mu(x)$ with the property $\pounds_\xi g_{\mu\nu} = 0$ is a Killing vector field, which is associated with

a symmetry of the action and hence according to Noether's theorem, to a conserved charge.

Using the Maxwell equation $\nabla_\nu F^{\mu\nu} = J_e^\mu$ we can define the charge passing through a spacelike hypersurface Σ as:

$$Q = -\int_\Sigma \sqrt{h}\, u_\mu J_e^\mu d^3x = -\int_\Sigma \sqrt{h}\, u_\mu \nabla_\nu F^{\mu\nu} d^3x, \tag{1.33}$$

where $F_{\mu\nu}$ is the electromagnetic field strength tensor, J_e^μ is the electric current four-vector, u_μ is the unit normal vector to Σ. Using Stokes' theorem we obtain:

$$Q = -\int_{\partial\Sigma} \sqrt{\sigma}\, u_\mu r_\nu F^{\mu\nu} d^2x \tag{1.34}$$

where r_ν is the unit vector normal to the boundary $\partial\Sigma$ and σ_{ij} the metric on the boundary.

Now for the total mass, we know that the energy momentum tensor $T_{\mu\nu}$ describes the matter not the geometry of the spacetime. The total energy of a spacetime is associated with a timelike Killing vector ξ^μ. The current is now $J_T^\mu = \xi_\nu T^{\mu\nu}$ which is divergence-free because we know that the energy momentum tensor is conserved. An using the Killing's equation we can therefore find a conserved energy by integrating over the hypersurface Σ:

$$E_T = \int_\Sigma \sqrt{h}\, u_\mu J_T^\mu\, d^3x. \tag{1.35}$$

In the Schwarzschild case, we have a timelike Killing vector and the momentum energy tensor vanishes everywhere, but we know that Schwarzschild spacetime has an inherent energy. To avoid this contradiction we define a new current in terms of the geometry rather than the matter content of spacetime using the Ricci tensor:

$$J_R^\mu = \xi_\nu R^{\mu\nu}, \tag{1.36}$$

and taking the trace of the Einstein equations we obtain:

$$J_R^\mu = 8\pi\xi_\nu(T^{\mu\nu} - \frac{1}{2}T g^{\mu\nu}). \tag{1.37}$$

This current is zero for Schwarzschild spacetime but we will work with the expression in (1.36) for the current. The divergence of the Ricci tensor can be computed from the contracted Bianchi identity:

$$\nabla_\mu R^{\mu\nu} = \frac{1}{2}\nabla^\nu R. \tag{1.38}$$

To see if the current (1.36) is conserved we compute its divergence:

$$\nabla_\mu J^\mu_R = (\nabla_\mu \xi_\nu) R^{\mu\nu} + \xi_\nu (\nabla_\mu R^{\mu\nu}). \tag{1.39}$$

The first term vanishes because $R^{\mu\nu}$ is symmetric and according to Killing's equation $\nabla_\mu \xi_\nu$ is antisymmetric. Using (1.36) and (1.38) we have: $\nabla_\mu J^\mu_R = (1/2)\xi_\nu \nabla^\nu R = 0$ because the derivative of the Ricci scalar vanishes along the Killing vector field. We can now define the conserved quantity which is the energy associated with this current:

$$E_R = \frac{1}{4\pi} \int_\Sigma \sqrt{h}\, u_\mu J^\mu_R d^3x. \tag{1.40}$$

The quantity E_R is independent of the spacelike hypersurface Σ and it is conserved. The advantage of E_R is that it can be written as a surface integral over a 2-sphere at spatial infinity. We know that any Killing vector satisfies:

$$\nabla_\mu \nabla_\nu \xi^\mu = \xi^\mu R_{\mu\nu}, \tag{1.41}$$

so the current and energy become respectively:

$$J^\mu_R = \nabla_\nu (\nabla^\mu \xi^\nu) \tag{1.42}$$

and

$$E_R = \frac{1}{4\pi} \int_\Sigma \sqrt{h}\, u_\mu \nabla_\nu (\nabla^\mu \xi^\nu) d^3x. \tag{1.43}$$

Using Stokes' theorem we have:

$$E_R = \frac{1}{4\pi} \int_{\partial\Sigma} \sqrt{\sigma}\, u_\mu r_\nu (\nabla^\mu \xi^\nu)\, d^2x. \tag{1.44}$$

This is the Komar integral [89] associated with the timelike Killing vector ξ^μ giving the total energy of a static spacetime.

As an example we can calculate the Komar mass for Schwarzschild and Schwarzschild-adS spacetimes. In such spaces the timelike Killing vector is $\xi^\mu = (1, 0, 0, 0)$. For Schwarzschild we consider the metric:

$$ds^2 = -\left(1 - \frac{2M}{r}\right) dt^2 + \left(1 - \frac{2M}{r}\right)^{-1} dr^2 + r^2(d\theta^2 + \sin^2\theta d\phi^2) \tag{1.45}$$

and for adS-Schwarzschild we have:

$$ds^2 = -\left(1 + \frac{2M}{r} + \frac{r^2}{L^2}\right) dt^2 + \left(1 + \frac{2M}{r} + \frac{r^2}{L^2}\right)^{-1} dr^2 + r^2(d\theta^2 + \sin^2\theta d\phi^2) \tag{1.46}$$

where L is the adS radius of curvature. Since u_ν is the vector normal to constant t hypersurfaces Σ and r_μ is the vector normal to the timelike boundary $\partial\Sigma$, we have $u_\mu u^\mu = -1$ and $r_\mu r^\mu = 1$ and the only non-zero components of u_μ and r_μ are:

$$u_0 = -\sqrt{(1-2M/r)}, \quad r_1 = (1-2M/r)^{-1/2}. \tag{1.47}$$

Therefore the $u_\mu \sigma_\nu \nabla^\mu \xi^\nu$ term in (1.44) becomes:

$$\begin{aligned} \nabla^0 \xi^1 &= g^{00} \nabla_0 \xi^1 \\ &= g^{00}(\partial_0 \xi^1 + \Gamma^1_{0\lambda}\xi^\lambda) \\ &= g^{00}\Gamma^1_{00}\xi^0 \\ &= -\frac{M}{r^2}. \end{aligned} \tag{1.48}$$

The metric at infinity on a two sphere is $\sigma_{ij}dx^i dx^j = r^2(d\theta^2 + \sin^2\theta\, d\phi^2)$ so we have $\sqrt{\sigma} = r^2 \sin\theta$ and putting everything together (1.44) becomes:

$$E_R = \frac{1}{4\pi}\int r^2 \sin\theta\, d\theta\, d\phi \frac{M}{r^2} = M, \tag{1.49}$$

which is the mass of Schwarzschild spacetime.

Now for Schwarzschild-adS spacetime, we have:

$$\nabla^0 \xi^1 = -\frac{1}{2}\left(\frac{2M}{r^2} - \frac{2\Lambda r}{3}\right). \tag{1.50}$$

In this case (1.44) becomes

$$E_R = M + \int \left(\frac{\Lambda r}{3}\right) r^2 \sin\theta\, d\theta\, d\phi. \tag{1.51}$$

We see that the integral diverges as $r \to \infty$. The Komar integral is not suitable for asymptotically adS spacetimes.

§ 1.4 Summary

In this chapter we reviewed some of the literature for uniqueness and no-hair theorems. We have seen how hairy black holes constitute a prolific field of research. We mentioned the importance of the mass in black hole thermodynamics which is the main application of our work. We have presented Bekenstein's no-hair proof for a single scalar field. We included a proof of a no-hair theorem for multiple fields, we have seen that it is based

on a mathematical contradiction. Finally, we presented definitions of the mass in asymptotically flat spacetimes. We showed that using the Komar integral to calculate mass in adS spacetime results in a divergent mass. This motivates our introduction to different methods to calculate the mass in adS spacetime in the next chapter.

Chapter 2

Mass in asymptotically anti-de Sitter spacetimes

Defining mass in asymptotically *adS* spacetime is a subtle issue in general relativity. There are many different definitions in the literature. The Hamiltonian definition by Henneaux and Teitelboim [74] is based on the Hamiltonian framework [115], the charges are defined as surface integrals. The method presented by Hollands *et al.* [81] is also based on the Hamiltonian framework [81] but the charges are defined from the electric part of the Weyl tensor. This is similar to the method developed by Ashtekar *et al.* in [13, 12]. This method was used to obtain mass for different hairy configurations [4, 5, 43, 44, 95, 97]. Hollands *et al.* show there is an equivalence between their method, Ashtekar *et al.* method [12] and Henneaux and Teitelboim method [74]. The 'counterterm method' in [14] and [75] is based on adding a counter term action to cancel divergences. There is also the 'pseudotensor' method considered in [3] and the spinor definition proposed by Witten in [140], also used in [61, 62]. We restrict our attention to three methods for defining mass in asymptotically *adS* spacetimes.

In this chapter we are concerned with investigating the definition of the mass in matter-free asymptotically *adS* spacetimes in four and five spacetime dimensions. We begin with the 'counter-term' method [14] based on a counter-term action that is added in order to make divergences cancel. The mass is calculated from the quasilocal stress-energy tensor on the boundary of the spacetime. We then move on to the method of Hollands *et al.* [81], finally we investigate Henneaux and Teitelboim method [74]. To illustrate the three methods we calculate the masses of asymptotically *adS* spacetime and asymptotically *adS*-Schwarzschild systems in four and five dimensions. We end the chapter with a discussion to decide which method is best suited for our work. We

adopt the notion in [81].

§ 2.1 Asymptotically adS spacetimes

Before we begin our analysis some general comments on adS spacetime are needed. Anti-de Sitter spacetime is the maximally symmetric vacuum solution of Einstein's equation with a negative cosmological constant Λ. As its name indicates, an asymptotically adS spacetime looks like the adS spacetime at infinity. We have seen in chapter 2 that if we try to calculate the mass of an asymptotically adS spacetime using the Komar integral divergences arise. The crucial difference between asymptotically flat scapcetimes and asymptotically adS spacetimes lies in the form of the boundary at infinity. As an example we show the conformal diagrams for the Schwarzschild spacetime and the adS-Schwarzschild spacetime in Fig. 2.1. We see from the figure that there is a dramatic difference in the structures at infinity. The conformal boundary of asymptotically adS spacetime has a simple structure. As can be seen in Fig. 2.1b the boundary is timelike.

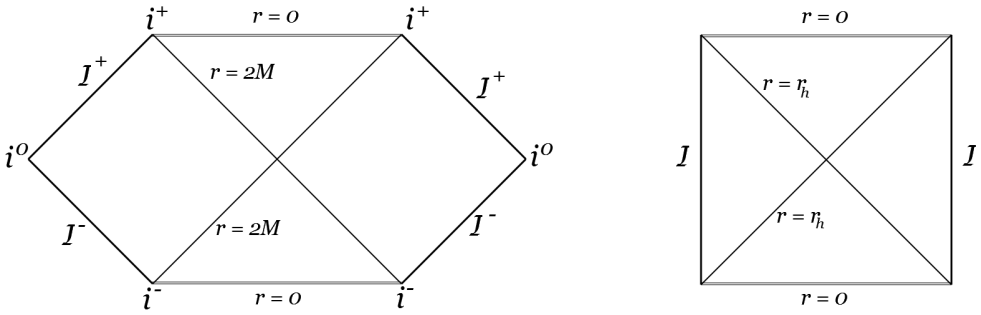

(a) Geometry of Schwarzschild spacetime

(b) Geometry of adS-Schwarzschild spacetime

Figure 2.1: Penrose diagrams showing the difference of the structure at infinity between (a) Schwarzschild spacetime where i^0 is the spatial infinity, i^+ is the future temporal infinity, i^- is the past temporal infinity, I^- is the past null infinity, I^+ is the future null infinity, $r = 0$ surfaces correspond to the singulary (b) adS-Schwarzschild spacetime where the boundaries at infinity are timelike hypersurfaces, $r = 0$ surfaces correspond to the singulary, r_h is the event horizon radius.

An asymptotically adS spacetime is defined as follows [81]:

- One considers a physical spacetime $\widetilde{M}$ with metric $\widetilde{g}_{ab}$ where $\widetilde{M} = M \cup \mathcal{F}$ is a manifold with boundary $\mathcal{F} \equiv \mathbb{R} \times S^{D-2}$. The manifold M has a metric $g_{\alpha\beta}$.

- There exist a smooth function Ω such that:

$$g_{ab} = \Omega^{-2}\widetilde{g}_{ab} \tag{2.1}$$

  and it is assumed that $\Omega = 0$ on $\mathcal{F}$

- and $\widetilde{\nabla}_a\Omega \neq 0$

We say that $\widetilde{M}$ is an asymptotically adS spacetime. The masses in the following sections are defined on such spacetimes.

§ 2.2 The counterterm method

The basic idea of the counterterm method is to cancel divergences by adding counterterms. It has been abundantly used in the literature [14, 26, 27, 51, 52, 76, 121, 122]. We investigate the method presented in [14]. The mass is obtained by integrating the stress energy tensor derived from a counterterm action. The counterterms, as the name indicates, cancels the divergences and a finite mass is obtained. The asymptotic behaviour of the stress energy tensor is determined by the fact that we require a finite mass.

If ξ^μ is a Killing vector of a spacetime, there is an associated conserved charge [35]:

$$Q_\xi = \lim_{C\to\mathcal{F}} \int_C d^{D-1}x\sqrt{\gamma}u^\mu T_{\mu\nu}\xi^\nu \tag{2.2}$$

where C is a sequence of cross sections tending to the adS boundary $\mathcal{F}$ within a hypersurface Σ (see Fig. 2.2). The conserved charge associated with time translation is the mass of the spacetime [14]. According to Brown and York in [35], the quasilocal stress energy tensor is:

$$T^{\mu\nu} = \frac{2}{\sqrt{-\gamma}}\frac{\delta S}{\delta\gamma_{\mu\nu}} \tag{2.3}$$

where $\gamma_{\mu\nu}$ is the metric on the boundary of a given spacetime region and S the gravitational action.

The gravitational action for the counterterm method is [14]:

$$S = -\frac{1}{16\pi G}\int_M d^Dx\sqrt{g}\,(R-2\Lambda) - \lim_{C\to\mathcal{F}}\frac{1}{8\pi G}\int_C d^{D-1}x\sqrt{-\gamma}K + \frac{1}{8\pi G}S_{ct}(\gamma_{\mu\nu}) \tag{2.4}$$

where R is the Ricci scalar, K is the trace of the extrinsic curvature, S_{ct} is the counterterm action that we add to obtain a finite mass, Λ is the cosmological constant expressed

as:

$$\Lambda = -\frac{D(D-1)}{2L^2} \tag{2.5}$$

where L is the adS radius and $K^{\mu\nu}$ is the extrinsic curvature of the boundary defined as:

$$K^{\mu\nu} = -\frac{1}{2}(\nabla^{\mu}\hat{n}^{\nu} + \nabla^{\nu}\hat{n}^{\mu}), \tag{2.6}$$

where $\hat{n}^{\mu}$ is the normal vector to C. The stress energy tensor (2.3) is obtained by the variation of the gravitational action (2.4) with respect to the boundary metric $\gamma_{\mu\nu}$. The only contributions to δS are from the boundary terms since we consider solutions of the equations of motion. The quasilocal tensor becomes [14]:

$$T^{\mu\nu} = \frac{1}{8\pi G}\left[K^{\mu\nu} - K\,\gamma^{\mu\nu} + \frac{2}{\sqrt{-\gamma}}\frac{\delta S_{ct}}{\delta \gamma_{\mu\nu}}\right]. \tag{2.7}$$

As C tends to the adS boundary divergences arise and the counterterm action S_{ct} has to be chosen so these divergences cancel. The counterterm action is defined as [14]:

$$S_{ct} = \int_C L_{ct}, \tag{2.8}$$

where the Lagrangian L_{ct} depends on the number of spacetime dimensions. The Lagrangians for different dimensions are [14]:

$$\begin{aligned}
L_{ct} &= -\frac{1}{L}\sqrt{-\gamma} && \text{for } adS_3 \\
L_{ct} &= -\frac{2}{L}\sqrt{-\gamma}\left(1 - \frac{L^2}{4}R\right) && \text{for } adS_4 \\
L_{ct} &= -\frac{3}{L}\sqrt{-\gamma}\left(1 - \frac{L^2}{12}R\right) && \text{for } adS_5,
\end{aligned} \tag{2.9}$$

where R is the Ricci scalar of the boundary metric $\gamma_{\mu\nu}$. This leads to the following expressions for the stress energy tensor for three, four and five dimensions respectively [14]:

$$T^{\mu\nu} = \frac{1}{8\pi G}\left[K^{\mu\nu} - K\,\gamma^{\mu\nu} - \frac{1}{L}\gamma^{\mu\nu}\right] \tag{2.10}$$

$$T^{\mu\nu} = \frac{1}{8\pi G}\left[K^{\mu\nu} - K\,\gamma^{\mu\nu} - \frac{2}{L}\gamma^{\mu\nu} - L\mathcal{G}^{\mu\nu}\right] \tag{2.11}$$

$$T^{\mu\nu} = \frac{1}{8\pi G}\left[K^{\mu\nu} - K\,\gamma^{\mu\nu} - \frac{3}{L}\gamma^{\mu\nu} - \frac{L}{2}\mathcal{G}^{\mu\nu}\right], \tag{2.12}$$

where $\mathcal{G}_{\mu\nu} = R_{\mu\nu} - \frac{1}{2}R\,\gamma_{\mu\nu}$ is the Einstein tensor associated with the boundary metric

$\gamma_{\mu\nu}$. The number of counterterms required to make the charges finite increases with the dimension of the spacetime. In the following sections we will consider the counterterm method explained above in vacuum adS spacetimes but it can also be used in the presence of matter [49]. We show how to obtain boundary conditions on the perturbations to obtain a finite mass.

2.2.1 Calculating the mass of asymptotically adS_4 spacetime

In [14] the metric is defined in Poincare form as follows:

$$ds^2 = \frac{L^2}{r^2}dr^2 + \frac{r^2}{L^2}(-dt^2 + dx_i dx_i)$$

where $i = 1, 2$. For an asymptotically adS_4 spacetime (2.2) becomes:

$$M = \int d^2x\sqrt{g_{xx}}\xi^t u^t T_{tt} = \int d^2x \frac{r}{L}T_{tt} \tag{2.13}$$

where $d^2x = O(1)$ as $r \to \infty$. For the mass to be finite we need $T_{tt} = O(r^{-1})$.

We consider the adS_4 metric in global coordinates:

$$ds^2 = -\left(1 + \frac{r^2}{L^2}\right)dt^2 + \frac{dr^2}{\left(1 + \frac{r^2}{L^2}\right)} + r^2(d\theta^2 + \sin^2\theta\, d\phi^2). \tag{2.14}$$

The three-dimensional boundary metric is:

$$ds^2 = -\left(1 + \frac{r^2}{L^2}\right)dt^2 + r^2(d\theta^2 + \sin^2\theta\, d\phi^2) \tag{2.15}$$

and the unit vector normal to the boundary is:

$$n_\mu = \sqrt{\frac{L^2}{L^2 + r^2}}\delta_{\mu,r}. \tag{2.16}$$

We calculate the different components of the boundary stress energy tensor in adS_4 in (2.11) using GR-tensor in Maple [1]. We are interested in the T_{tt} component which will give us the mass, we can write T_{tt} explicitly as:

$$\begin{aligned} 8\pi G T_{tt} &= K_{tt} - K\gamma_{tt} - \frac{2\gamma_{tt}}{L} - L\mathcal{G}_{tt} \\ &= -\nabla_t \hat{n}_t - (K_{tt}\gamma^{tt} + K_{xx}\gamma^{xx} + K_{rr}\gamma^{rr})\gamma_{tt} - 2\frac{\gamma_{tt}}{L} - L\mathcal{G}_{tt} \end{aligned} \tag{2.17}$$

The Einstein tensor associated with (2.15) has the component:

$$\mathcal{G}_{tt} = \frac{L^2 + r^2}{r^2 L^2}. \tag{2.18}$$

The different components of the extrinsic curvature are:

$$\begin{aligned} K_{tt} &= \frac{\sqrt{L^2 + r^2}}{L^3} r \\ K_{xx} &= -\frac{\sqrt{L^2 + r^2}}{L} r \\ K_{rr} &= \frac{\sqrt{L^2 + r^2}}{L} r \sin^2\theta \end{aligned} \tag{2.19}$$

and hence the trace of the extrinsic curvature is:

$$K = \frac{1}{rL^2}\left[\sqrt{\frac{L^2}{L^2 + r^2}}(3r^2 + 2L^2)\right]. \tag{2.20}$$

Putting everything together we obtain:

$$\begin{aligned} 8\pi G T_{tt} &= \frac{L}{4r^2} + \frac{L^3}{8r^4} - \frac{3L^5}{64r^6} + ... \\ 8\pi G T_{\theta\theta} &= \frac{L^3}{4r^2} - \frac{L^5}{4r^4} + \frac{15L^7}{64r^6} + ... \\ 8\pi G T_{\phi\phi} &= \frac{L^3}{4r^2}\sin^2\theta - \frac{L^5}{4r^4}\sin^2\theta + \frac{15L^7}{64r^6}\sin^2\theta + ... \end{aligned} \tag{2.21}$$

Putting the expression for T_{tt} in (2.13) we see that the integral tends to zero when $r \to \infty$. We have found the mass of adS_4 spacetime to be zero. This is consistent with [14].

We can also apply the definition of the mass to adS_4 with small perturbations:

$$ds^2 = -\left(1 + \frac{r^2}{L^2} + \delta g_{tt}\right) dt^2 + \frac{dr^2}{1 + \frac{r^2}{L^2} + \delta g_{rr}} + (r^2 + \delta g_{\theta\theta}) d\theta^2 + (r^2 + \delta g_{\phi\phi}) \sin^2\theta \, d\phi^2. \tag{2.22}$$

For this metric we obtain long expressions for the different terms in (2.11) using GR-Tensor in Maple. The expressions for T_{tt}, $T_{\theta\theta}$ and $T_{\phi\phi}$ all contain the perturbations δg_{tt}, δg_{rr}, $\delta g_{\theta\theta}$ and $\delta g_{\phi\phi}$. The conditions on the perturbations at the boundary can be obtained by studying the asymptotic behaviour of one perturbation at a time, i.e. setting all but one perturbation to zero. For example, taking T_{tt} and setting all the

perturbations to zero except δg_{tt}, we obtain:

$$T_{tt}^{\delta g_{tt}\neq 0} = \left(\frac{L}{r^2} - \frac{2}{L} + \frac{2r}{L^2}\sqrt{\frac{L^2}{L^2+r^2}} + \frac{2}{r}\sqrt{\frac{L^2}{L^2+r^2}}\right)\delta g_{tt} \tag{2.23}$$

and (2.13) becomes the leading order:

$$M = \int d^2x \frac{r}{L}\frac{\delta g_{tt}}{r^2}. \tag{2.24}$$

For the mass to be finite $\delta g_{tt} = O(r^{-1})$. Following the same reasoning for the other perturbations the conditions on the perturbations at the boundary are found to be:

$$\delta g_{rr} = O(r^{-5}), \quad \delta g_{\theta\theta} = O(r^{-1}), \quad \delta g_{\phi\phi} = O(r^{-1}). \tag{2.25}$$

As an example we can calculate the mass of Schwarzschild-adS_4. The metric of this spacetime is:

$$ds^2 = -\left(1 + \frac{r^2}{L^2} - \frac{r_0}{r}\right)dt^2 + \left(1 + \frac{r^2}{L^2} - \frac{r_0}{r}\right)^{-1} dr^2 + r^2(d\theta^2 + \sin^2\theta\, d\phi^2) \tag{2.26}$$

and we find the components of the boundary stress energy tensor to be:

$$\begin{aligned} 8\pi G T_{tt} &= \frac{r_0}{Lr} + \frac{L}{4r^2} + \frac{Lr_0}{2r^3} + ... \\ 8\pi G T_{\theta\theta} &= \frac{Lr_0}{2r} + \frac{L^3}{4r^2} - \frac{3}{4}\frac{L^3 r_0}{r^3} + ... \\ 8\pi G T_{\phi\phi} &= \frac{Lr_0}{2r}\sin^2\theta + \frac{L^3}{4r^2}\sin^2\theta - \frac{3L^3 r_0}{4r^3}\sin^2\theta + ... \end{aligned} \tag{2.27}$$

Using (2.13) we obtain the mass of Schwarzschild-adS_4

$$\begin{aligned} M &= \frac{L^2}{8\pi G}\int \frac{r}{L}\frac{r_0}{Lr}\sin\theta\, d\theta\, d\phi \\ &= \frac{1}{8\pi G} 4\pi r_0 = \frac{r_0}{2G}. \end{aligned} \tag{2.28}$$

This is the mass for Schwarzschild-adS_4 and we can see that by setting $r_0 = 2MG$ we recover the standard metric for this spacetime:

$$ds^2 = -\left[1 + \frac{r^2}{L^2} - \left(\frac{2GM}{r}\right)\right]dt^2 + \left[1 + \frac{r^2}{L^2} - \left(\frac{2GM}{r}\right)\right]^{-1} dr^2 + r^2(d\theta^2 + \sin^2\theta\, d\phi^2). \tag{2.29}$$

2.2.2 Calculating the mass of asymptotically adS_5 spacetime

For an asymptotically adS_5 spacetime (2.2) is:

$$M = \int d^3x \frac{r^2}{L^2} T_{tt}. \tag{2.30}$$

First we consider pure adS_5 for which the metric is:

$$ds^2 = -\left(1 + \frac{r^2}{L^2}\right) dt^2 + \frac{dr^2}{1 + \frac{r^2}{L^2}} + r^2(d\theta^2 + \sin^2\theta\, d\phi^2 + \cos^2\theta\, d\alpha^2), \tag{2.31}$$

and by similar method to that outlined above we have:

$$\begin{aligned}
8\pi G T_{tt} &= \frac{3L}{8r^2} - \frac{3L^3}{16r^4} + \frac{9L^5}{128r^6} + ... \\
8\pi G T_{\theta\theta} &= \frac{L^3}{8r^2} - \frac{3L^5}{16r^4} + \frac{25L^7}{128r^6} + ... \\
8\pi G T_{\phi\phi} &= \frac{L^3 \sin^2\theta}{8r^2} + \frac{3L^5 \sin^2\theta}{16r^4} - \frac{25L^7 \sin^2\theta}{128r^6} + ... \\
8\pi G T_{\alpha\alpha} &= \frac{L^3 \cos^2\theta}{8r^2} - \frac{3L^5 \cos^2\theta}{16r^4} + \frac{25L^7 \cos^2\theta}{128r^6} + ...
\end{aligned} \tag{2.32}$$

These expressions agree with [14] and (2.30) becomes:

$$\begin{aligned}
M &= \frac{L^3}{8\pi G} \int \frac{r^2}{L^2} \frac{3L}{8r^2} \sin^2\theta \sin\phi\, d\theta\, d\phi\, d\alpha \\
&= \frac{3\pi L^2}{32G}.
\end{aligned} \tag{2.33}$$

This is the mass of pure adS_5 spacetime. We notice that it is not zero.

Now we consider the following metric:

$$\begin{aligned}
ds^2 \;=\; & -\left(1 + \frac{r^2}{L^2} + \delta g_{tt}\right) dt^2 + \frac{dr^2}{1 + \frac{r^2}{L^2} + \delta g_{rr}} + (r^2 + \delta g_{\theta\theta}) d\theta^2 \\
& + (r^2 + \delta g_{\phi\phi}) \sin^2\theta\, d\phi^2 + (r^2 + \delta g_{\alpha\alpha}) \cos^2\theta\, d\alpha^2.
\end{aligned} \tag{2.34}$$

The expressions for the different components of the boundary stress energy tensor (2.12) are too long to write out here explicitly. Following the same steps as for the previous cases we obtain the following boundary conditions for our perturbations:

$$\delta g_{tt} = O(r^{-2}), \quad \delta g_{rr} = O(r^{-6}), \quad \delta g_{\theta\theta} = O(r^{-2}), \quad \delta g_{\phi\phi} = O(r^{-2}), \quad \delta g_{\alpha\alpha} = O(r^{-2}). \tag{2.35}$$

Now considering the Schwarzschild-adS_5 spacetime whose metric is:

$$\begin{aligned} ds^2 &= -\left[1+\frac{r^2}{L^2}-\left(\frac{r_0}{r}\right)^2\right]dt^2+\left[1+\frac{r^2}{L^2}-\left(\frac{r_0}{r}\right)^2\right]^{-1}dr^2 \\ &\quad +r^2(d\theta^2+\sin^2\theta\, d\phi^2+\cos^2\theta\, d\alpha^2) \end{aligned} \tag{2.36}$$

we have for the different components of the boundary stress energy tensor (2.12):

$$\begin{aligned} 8\pi G T_{tt} &= \frac{3L}{8r^2}+\frac{3r_0^2}{2Lr^2}+... \\ 8\pi G T_{\theta\theta} &= \frac{L^3}{8r^2}+\frac{Lr_0^2}{2r^2}+... \\ 8\pi G T_{\phi\phi} &= \left(\frac{L^3}{8r^2}+\frac{Lr_0^2}{2r^2}\right)\sin^2\theta+... \\ 8\pi G T_{\alpha\alpha} &= \left(\frac{L^3}{8r^2}+\frac{Lr_0^2}{2r^2}\right)\cos^2\theta+... \end{aligned} \tag{2.37}$$

Using (2.30) we obtain for the mass of Schwarzschild-adS_5 spacetime

$$M=\frac{3\pi L^2}{32G}+\frac{3\pi r_0^2}{8G}. \tag{2.38}$$

The first term is the mass of pure adS spacetime in five dimensions which agrees with (2.33) , the second term corresponds to the mass of the Schwarzschild black hole. This result agrees with [14].

This analysis can be extended to higher dimensions by increasing the number of counterterms as the number of dimensions increases. With this method Balasubramanian and Kraus [14] show that it reproduces the masses and angular momenta of various asymptotically adS spacetimes in agreement with [3, 13, 36, 68, 74, 83].

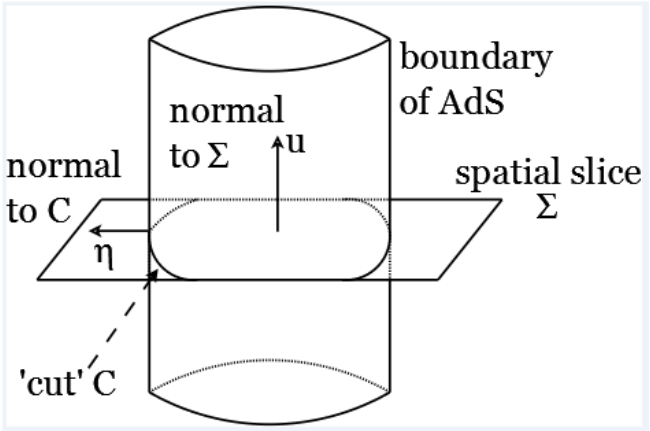

Figure 2.2: *AdS* geometry for the conserved charges

§ 2.3 Hollands *et al* method

Hollands *et al.* method [81] is based on the definition of charges by Wald and Zoupas in [134]. In this section we follow the method in [81] in order to calculate the mass of different spacetimes.

The action corresponding to vacuum general relativity with negative cosmological constant in D dimensions is:

$$S = \int \mathcal{L}\, d^D x = \int \frac{1}{16\pi G}\sqrt{-g}(R - 2\Lambda) d^D x. \tag{2.39}$$

The metric for pure adS spacetime in D dimensions is:

$$ds_0^2 = -\left(1 + \frac{r^2}{L^2}\right) dt^2 + \frac{dr^2}{1 + \frac{r^2}{L^2}} + r^2 d\sigma^2 \tag{2.40}$$

where $d\sigma^2$ is the metric on the S^{D-2} sphere and L is the adS spacetime radius defined by:

$$L = \sqrt{-\frac{(D-1)(D-2)}{2\Lambda}}. \tag{2.41}$$

A new coordinate Ω is defined as a positive analytic function of r:

$$\Omega(r) = -\frac{1}{2}\left(\frac{r}{L} - \sqrt{\frac{r^2 + L^2}{L^2}}\right) \tag{2.42}$$

and the metric (2.40) expressed in terms of Ω is:

$$ds_0^2 = \frac{L^2}{\Omega^2}\left[d\Omega^2 - dt^2 + d\sigma^2 - \frac{\Omega^2}{2}(dt^2 + d\sigma^2) + \frac{\Omega^2}{16}(-dt^2 + d\sigma^2)\right]. \tag{2.43}$$

Hollands *et al.* [81] define the manifold $\tilde{M}$ as being a manifold M to which one attaches a boundary $\mathcal{F}$. The boundary $\mathcal{F}$ consists of points $\Omega = 0$. After a conformal transformation, the unphysical metric is defined as $d\tilde{s}_0^2 = \Omega^2 ds_0^2$ [81]. Writing it explicitly:

$$d\tilde{s}_0^2 = L^2\left[d\Omega^2 - dt^2 + d\sigma^2 - \frac{\Omega^2}{2}(dt^2 + d\sigma^2) + \frac{\Omega^2}{16}(-dt^2 + d\sigma^2)\right]. \tag{2.44}$$

The metric in (2.43) diverges as $\Omega \to 0$ (corresponding to $r \to \infty$) but the unphysical metric is regular there.

The definition in [81] is very technical, here we will give an outline of their method. Hollands *et al* [81] derive an expression for the generator of asymptotic symmetries associated with a vector field ξ^a as:

$$\delta\mathcal{H}_\xi = \sigma_\Sigma(g; \delta g, \mathcal{L}_\xi g) \tag{2.45}$$

where σ_Σ describes the manifold structure of general relativity, g is the unperturbed metric and δg are metric perturbations. Here Σ is a hypersurface whose boundary C is a cut of $\mathcal{F}$, we show it in Fig. 2.2. The expression in 2.45 allows us to see that the mass is defined from geometrical quantities of the spacetime such as the metric or the Lie derivative. The general idea is to rewrite (2.45) in terms of constraints of the theory and Noether's charges. The constraints for the theory vanish when the equations of motion are satisfied. After some complicated mathematics (2.45) leads to the following definition of conserved charges [81, 134]:

$$\mathcal{H}_\xi = \int_\Sigma \xi^a C_a + \int_C I_\xi \tag{2.46}$$

where the C_a in the first term are the constraints of general relativity and I_ξ are the conserved charges. When $C_a = 0$ the constraints are satisfied, the charges $\mathcal{H}_\xi$ reduce to the surface integral. It is also proven [81, 134] that $\mathcal{H}_\xi$ is independent of the cut C.

Hollands *et al* [81] then derive the charges associated with the asymptotic symmetries in terms of the unphysical Weyl tensor:

$$\mathcal{H}_\xi = -\frac{L}{8\pi G}\int_\Sigma \tilde{E}_{ab}\tilde{u}^a\xi^b d\tilde{S} \tag{2.47}$$

where $\tilde{u}^a$ is the unit timelike normal to Σ, $d\tilde{S}$ is the unphysical integration element on the cut C and $\tilde{E}_{ab}$ is the unphysical electric part of the Weyl tensor of the unphysical metric (2.44) defined as:

$$\tilde{E}_{ab} = \frac{1}{D-3}\Omega^{3-D}\tilde{C}_{acbd}\tilde{n}^c\tilde{n}^d \tag{2.48}$$

where $\tilde{n}^a = \tilde{\nabla}^a\Omega$ is a vector field. It can be shown [81] that the electric part of the Weyl tensor is finite at the boundary when the metric satisfies the Einstein equations and the appropriate boundary conditions specified later in this section. According to [81] the charges are defined in the same way in [13] for $D = 4$ and [12] for higher dimensions. The Weyl tensor transforms in such a way that we have $\tilde{C}_{acbd} = \Omega^2 C_{acbd}$ for the unphysical Weyl tensor in terms of the physical Weyl tensor of the metric (2.43).

We are only interested in mass so we consider the following component:

$$M = -\frac{L}{8\pi G}\int_C \frac{1}{d-3}\Omega^{3-D}\tilde{C}_{t\Omega t\Omega}\,\xi^t d\tilde{S}, \tag{2.49}$$

where ξ^t is a timelike Killing vector. We would like to find (2.49) for asymptotically adS_4 and asymptotically adS_5 spacetimes.

2.3.1 Calculating the mass of asymptotically adS_4 spacetimes

In this case (2.49) becomes:

$$M = -\frac{L}{8\pi G}\int_C \Omega^{-1}\Omega^2 C_{t\Omega t\Omega}\,\xi^t d\tilde{S}, \tag{2.50}$$

where we are considering the physical Weyl tensor. The adS_4 metric for our background, to which we add some perturbations which depend on Ω only is:

$$\begin{aligned} ds^2 &= \left(-\frac{L^2}{2} - \frac{L^2}{\Omega^2} - \frac{L^2\Omega^2}{16} + \delta g_{tt}\right)dt^2 + \left(\frac{L^2}{\Omega^2} + \delta g_{\Omega\Omega}\right)d\Omega^2 \\ &\quad + \left(\frac{L^2}{\Omega^2} - \frac{L^2}{2} + \frac{L^2\Omega^2}{16} + \delta g_{\theta\theta}\right)d\theta^2 + \left(\frac{L^2}{\Omega^2} - \frac{L^2}{2} + \frac{L^2\Omega^2}{16} + \delta g_{\phi\phi}\right)\sin^2\theta\, d\phi^2. \end{aligned} \tag{2.51}$$

Using GR-Tensor the boundary conditions are obtained by setting all perturbations to zero except one. We do this for all the perturbations in turn, the general expressions are too long to reproduce here. As an example we can show the expression for the

component $C_{t\Omega t\Omega}$ when only δ_{tt} is non-zero:

$$\begin{aligned} C_{t\Omega t\Omega} &= -\frac{1}{6}\left(\frac{d^2}{d\Omega^2}\delta g_{tt}\right) - \left(\frac{d}{d\Omega}\delta g_{tt}\right)\frac{(2\Omega^6+32\Omega^2+256)}{6[(\Omega^6+4\Omega^4-16\Omega^2-64)\Omega]} \\ &\quad + \frac{\delta g_{tt}(2\Omega^6-24\Omega^4+96\Omega^6-128)}{6[(\Omega^6+4\Omega^4-16\Omega^2-64)\Omega^2]}. \end{aligned} \tag{2.52}$$

In order to find boundary conditions for the perturbations we only consider leading behaviour in Ω as $\Omega \to 0$. In this case (2.49) becomes:

$$M^{\delta g_{tt}\neq 0} \sim -\frac{L}{8\pi G}\int_C \Omega^{-1}\Omega^2\left(-\frac{1}{6}\right)\left[\frac{d^2}{d\Omega^2}\delta g_{tt} + \frac{1}{\Omega}\frac{d}{d\Omega}\delta g_{tt} + \frac{1}{\Omega^2}\delta g_{tt}\right] d\tilde{S} \tag{2.53}$$

and we can see that for the integral to be finite $\delta g_{tt} = O(\Omega)$. Doing the same for all perturbations and requiring that the charge is finite, we obtain boundary conditions on all the perturbations of the metric:

$$\delta g_{tt} = O(\Omega), \quad \delta g_{\Omega\Omega} = O(\Omega), \quad \delta g_{\theta\theta} = O(\Omega), \quad \delta g_{\phi\phi} = O(\Omega). \tag{2.54}$$

These boundary conditions agree with [81] expect for δg_{rr} which was found to be $O(\Omega^5)$ in [81]. However, if $\delta g_{rr} = O(\Omega^5)$ the mass will certainly be finite. The complexity of the expressions for the Weyl tensor makes it hard to check the boundary conditions for the perturbations for the other components of the Weyl tensor.

2.3.2 Calculating the mass of asymptotically adS_5 spacetimes

In this case (2.49) is:

$$M = -\frac{L}{8\pi G}\int_C \Omega^{-2}\Omega^2 C_{t\Omega t\Omega}\,\xi^t d\tilde{S}, \tag{2.55}$$

and we consider the adS_5 metric to which we add some perturbations which depend on Ω only:

$$\begin{aligned} ds^2 &= \left(-\frac{L^2}{2} - \frac{L^2}{\Omega^2} - \frac{L^2\Omega^2}{16} + \delta g_{tt}\right)dt^2 + \left(\frac{L^2}{\Omega} + \delta g_{\Omega\Omega}\right)d\Omega^2 \\ &\quad + \left(\frac{L^2}{\Omega} - \frac{L^2}{2} + \frac{L^2\Omega^2}{16} + \delta g_{\theta\theta}\right)d\theta^2 + \left(\frac{L^2}{\Omega^2} - \frac{L^2}{2} + \frac{L^2\Omega^2}{16} + \delta g_{\phi\phi}\right)\sin^2\theta\, d\phi^2 \\ &\quad + \left(\frac{L^2}{\Omega^2} - \frac{L^2}{2} + \frac{L^2\Omega^2}{16} + \delta g_{\alpha\alpha}\right)\sin^2\theta\sin^2\phi\, d\alpha^2. \end{aligned} \tag{2.56}$$

Following the same method as above, we obtain for the charge, where we set all the perturbations to zero except δg_{tt}:

$$M^{\delta g_{tt}\neq 0} \sim -\frac{L}{8\pi G}\int_C -\Omega^{-1}\Omega^2\frac{1}{4}\left[\frac{d^2}{d\Omega^2}\delta g_{tt}+\frac{1}{\Omega}\frac{d}{d\Omega}\delta g_{tt}+\frac{1}{\Omega^2}\delta g_{tt}\right]d\tilde{S}. \tag{2.57}$$

For the mass to be finite we need $\delta g_{tt} = O(\Omega^2)$. Doing the same for all perturbations in turn and requiring that the charge is finite, we obtain boundary conditions on all the perturbations of the metric. The boundary conditions are:

$$\delta g_{tt} = O(\Omega^2), \quad \delta g_{\Omega\Omega} = O(\Omega^2), \quad \delta g_{\theta\theta} = O(\Omega^2), \quad \delta g_{\phi\phi} = O(\Omega^2), \quad \delta g_{\alpha\alpha} = O(\Omega^2). \tag{2.58}$$

The same comments as for the asymptotically adS_4 case apply here. This analysis can be extended to D dimensions.

§ 2.4 Henneaux and Teitelboim method

Here we will introduce the Henneaux and Teilteboim definition of conserved charges [74]. The spacetime is D-dimensional adS with perturbations:

$$ds^2 = ds_0^2 + h_{\mu\nu}\,dx^\mu\,dx^\nu, \tag{2.59}$$

where

$$ds_0^2 = -\left(1+\frac{r^2}{L^2}\right)dt^2 + \frac{dr^2}{1+\frac{r^2}{L^2}} + r^2\,d\sigma^2_{D-2,k} \tag{2.60}$$

is the pure adS metric, L is the radius of curvature of the adS spacetime and $r^2\,d\sigma^2_{D-2,k}$ is the line element of a $(D-2)$-dimensional sphere with constant curvature. It is demanded that the perturbations obey the following conditions:

$$\begin{aligned} h_{tt} &= O(r^{-D+3}) \\ h_{rr} &= O(r^{-D-1}) \\ h_{tr} &= O(r^{-D}) \\ h_{r\theta^i} &= O(r^{-D}) \\ h_{t\theta^i} &= O(r^{-D+3}) \\ h_{\theta^i\theta^j} &= O(r^{-D+3}) \end{aligned} \tag{2.61}$$

where θ^i are the angular coordinates. The Henneaux and Teitelboim charge is defined as [73, 74]:

$$\begin{aligned}\mathcal{Q}_0 &= \int_\Sigma \mathcal{C}^a\xi_a + \lim_{C\to\mathcal{F}}\frac{1}{16\pi G}\int_C G_a{}^{bdc}[\xi^e\hat{u}_e\mathcal{D}_b h_{cd} - h_{cd}\mathcal{D}_b(\xi^e\hat{u}_e)]\hat{\eta}^a dS \\ &\quad + \lim_{C\to\mathcal{F}}\frac{1}{4\pi G}\int_C(\kappa_{ab}-\kappa q_{ab})K^a\hat{\eta}^b dS \end{aligned} \tag{2.62}$$

where the notation in [81] has been used. We have plotted the geometry in Fig. 2.2. In (2.62) $\mathcal{C}^a$ are the constraints of the theory and:

- h_{ab} are the perturbations of the background metric
- ξ^a is a Killing vector field of unperturbed adS spacetime
- $\hat{u}^a$ is the unit normal to the hypersurface Σ
- C is the boundary of Σ and a cut in $\mathcal{F}$ (see Fig. 2.2)
- $\hat{\eta}^a$ is the unit normal to C within the hypersurface Σ
- $q_{ab} = g_{ab} + \hat{u}_a\hat{u}_b$ is the induced metric on Σ
- $\mathcal{D}_a$ is the spatial derivative operator associated with q_{ab}
- $\kappa_{ab} = -q_a^c q_b^d \nabla_c \hat{u}_d$ is the extrinsic curvature of Σ
- $G_{abcd} = \frac{1}{2}(q_{ac}q_{bd} + q_{ad}q_{bc} - 2q_{ab}q_{cd})$.

The expression in (2.62) is the definition of the conserved quantity associated with ξ^a in a spacetime satisfying the asymptotic conditions (2.61). These asymptotic conditions ensure the finiteness of the charges Q_0. In particular, the mass is the conserved charge associated with the timelike Killing vector ξ^t. In order to calculate the mass using this method, all the individual terms in (2.62)were calculated. As for the previous section we calculate (2.62) for asymptotically adS_4 and asymptotically adS_5 spacetimes.

2.4.1 Calculating the mass for asymptotically adS_4 spacetimes

We only consider a restricted class of perturbations, corresponding to static spherically symmetric geometries. We write the metric in (2.59) explicitly for the 4-dimensional case:

$$ds^2 = -\left(1+\frac{r^2}{L^2}+\delta g_{tt}\right)dt^2 + \frac{dr^2}{1+\frac{r^2}{L^2}+\delta g_{rr}} + (r^2+\delta g_{\theta\theta})d\theta^2 + (r^2+\delta g_{\phi\phi})\sin^2\theta\, d\phi^2. \tag{2.63}$$

The normalised time component of the unit normal to the $t = constant$ hypersurface Σ is

$$\hat{u}_t = \sqrt{\left(1 + \frac{r^2}{L^2}\right) + \delta g_{tt}}, \tag{2.64}$$

where $\hat{u}_\mu \hat{u}^\mu = -1$. The other components of u^μ are zero. The normalised space component of the unit normal η_μ to the cross section C within Σ is:

$$\hat{\eta}_r = \sqrt{\frac{1}{1 + \frac{r^2}{L^2}} + \delta g_{rr}}. \tag{2.65}$$

and the other components of η_μ are zero. The induced metric q_{ab} on Σ is:

$$q_{ab}dx^a dx^b = \left(\frac{1}{1 + \frac{r^2}{L^2}} + \delta g_{rr}\right) dr^2 + (r^2 + \delta g_{\theta\theta})d\theta^2 + (r^2 + \delta g_{\phi\phi}) \sin^2\theta \, d\phi^2. \tag{2.66}$$

Using GR-Tensor in Maple all the components of G_{abcd} have been calculated. It has been found that all components of κ_{ab} vanish and (2.62) reduces to:

$$\begin{aligned} \mathcal{Q}_0 \quad = \quad & \lim_{C \to \mathcal{F}} \frac{1}{16\pi G} \int_C \frac{1}{r^3 L^4} \left[(2L^4 r^2 + 2r^6)\delta g_{rr} + (2r^2 L^2 + 3L^4)\delta g_{\theta\theta} + \left(\frac{d}{dr}\delta g_{\theta\theta}\right)\right] \\ & + \frac{1}{r^3 L^4} \left[(3L^4 + 2r^2 L^2)\delta g_{\phi\phi} + (rL^4 + r^3 L^2) \left(\frac{d}{dr}\delta g_{\phi\phi}\right)\right] dS. \end{aligned} \tag{2.67}$$

Considering only the leading order behaviour in r:

$$\mathcal{Q}_0 = \lim_{C \to \mathcal{F}} \frac{1}{16\pi G} \int_C \left(2r^3 \delta g_{rr} + \frac{2\delta g_{\theta\theta}}{L^2 r} + \frac{2\delta g_{\phi\phi}}{L^2 r} + \frac{d}{dr}\delta g_{\theta\theta} + \frac{1}{L^2}\frac{d}{dr}\delta g_{\phi\phi} \right) dS. \tag{2.68}$$

We want to obtain finite charges and we know that $dS = r^2 \sin\theta \, d\theta \, d\phi$ in four dimensions. We see that δg_{tt} does not appear in this mass. We can obtain suitable boundary conditions by setting all the perturbations to zero except one, doing it for each the perturbation in turn we have the following set of boundary conditions:

$$\delta g_{rr} = O(r^{-5}), \quad \delta g_{\theta\theta} = O(r^{-1}), \quad \delta g_{\phi\phi} = O(r^{-1}) \tag{2.69}$$

and δg_{tt} is finite as $r \to \infty$.

As an example we can consider the Schwarzschild-adS_4 spacetime for which the metric is:

$$ds^2 = -\left[1 + \frac{r^2}{L^2} - \frac{r_0}{r}\right] dt^2 + \left[1 + \frac{r^2}{L^2} - \frac{r_0}{r}\right]^{-1} dr^2 + r^2(d\theta^2 + \sin^2\theta \, d\phi^2). \tag{2.70}$$

In this case the normalised time component of the unit normal to Σ is:

$$\hat{u}_t = \sqrt{1 + \frac{r^3 - r_0 L^2}{L^2 r}}, \tag{2.71}$$

and

$$\hat{\eta}_r = \sqrt{\frac{L^2 r}{L^2 r + r^3 - r_0 L^2}}. \tag{2.72}$$

The induced metric on Σ is:

$$q_{ab}dx^a dx^b = \left(\frac{L^2 r}{L^2 r + r^3 - r_0 L^2}\right) dr^2 + r^2 d\theta^2 + r^2 \sin^2\theta \, d\phi^2. \tag{2.73}$$

Using GR-Tensor we have for the charge:

$$\mathcal{Q}_0 = \lim_{C \to \mathcal{F}} \frac{1}{16\pi G} \int_C \frac{2(L^2 r + r^3 - r_0 L^2)^2 r_0}{r^8} dS. \tag{2.74}$$

Considering only leading behaviour in r we obtain:

$$\mathcal{Q}_0 = \lim_{C \to \mathcal{F}} \frac{1}{16\pi G} \int_C \frac{2r_0}{r^2} dS. \tag{2.75}$$

The charge associated with the timelike Killing vector is the mass of the spacetime:

$$M = \frac{1}{16\pi G} \frac{2r_0}{r^2} 4\pi r^2 = \frac{r_0}{2G} \tag{2.76}$$

which is the mass of Schwarzschild-adS_4 spacetime. This result is in agreement with (2.28).

2.4.2 Calculating the mass of asymptotically adS_5 spacetimes

The metric in this case is:

$$\begin{aligned} ds^2 &= -\left(1 + \frac{r^2}{L^2} + \delta g_{tt}\right) dt^2 + \frac{dr^2}{1 + \frac{r^2}{L^2} + \delta g_{rr}} + (r^2 + \delta g_{\theta\theta}) d\theta^2 \\ &\quad + (r^2 + \delta g_{\phi\phi}) \sin^2\theta \, d\phi^2 + (r^2 + \delta g_{\alpha\alpha}) \cos^2\theta \, d\alpha^2. \end{aligned} \tag{2.77}$$

Using the same method and reasoning as for the four-dimensional case and considering leading behaviour in r we have for the mass:

$$\mathcal{Q}_0 = \lim_{C \to \mathcal{F}} \frac{1}{16\pi G} \int_C \left(r^3 \delta g_{rr} + \frac{\delta g_{\theta\theta}}{r} + \frac{\delta g_{\phi\phi}}{r} + \frac{\delta g_{\alpha\alpha}}{r}\right) dS. \tag{2.78}$$

Following the same steps as in the previous case we have the following asymptotic conditions for the mass to be finite:

$$\delta g_{rr} = O(r^{-6}), \quad \delta g_{\theta\theta} = O(r^{-2}), \quad \delta g_{\phi\phi} = O(r^{-2}), \quad \delta g_{\alpha\alpha} = O(r^{-2}). \tag{2.79}$$

We notice that δg_{tt} does not appear in the expression for the mass.

Now we consider the Schwarzschild-adS_5 spacetime with metric:

$$\begin{aligned} ds^2 &= -\left[1 + \frac{r^2}{L^2} - \left(\frac{r_0}{r}\right)^2\right] dt^2 + \left[1 + \frac{r^2}{L^2} - \left(\frac{r_0}{r}\right)^2\right]^{-1} dr^2. \\ &\quad + r^2 d\theta^2 + r^2 \sin^2\theta \, d\phi^2 + r^2 \cos^2\theta \, d\alpha^2 \end{aligned} \tag{2.80}$$

We have for the non- zero components of the normal unit vectors:

$$\hat{u}_t = \sqrt{1 + \frac{r^2}{L^2} - \frac{r_0}{r^2}} \tag{2.81}$$

and

$$\hat{\eta}_r = \sqrt{\frac{L^2 r^2}{L^2 r^2 + r^4 - r_0^2 L^2}}. \tag{2.82}$$

The induced metric on Σ is:

$$q_{ab} = \left(\frac{L^2 r^2}{L^2 r^2 + r^4 - r_0^2 L^2}\right) dr^2 + r^2 d\theta^2 + r^2 \sin^2\theta \, d\phi^2 + r^2 \cos^2\theta \, d\alpha^2. \tag{2.83}$$

Using GR-Tensor we have for the mass:

$$\mathcal{Q}_0 = \lim_{C \to \mathcal{F}} \frac{1}{16\pi G} \int_C \frac{(3L^2 r^2 + r^4 - r_0 L^2)^2 r_0^2}{r^{11}} dS \tag{2.84}$$

and considering only leading behaviour in r we obtain:

$$\mathcal{Q}_0 = \lim_{C \to \mathcal{F}} \frac{1}{16\pi G} \int_C \frac{3r_0^2}{r^3} dS. \tag{2.85}$$

The charge associated with the timelike Killing vector is the mass of the spacetime:

$$M = \frac{3\pi r_0^2}{8G} \tag{2.86}$$

which is the mass of Schwarzschild-adS_5 spacetime. We notice that as $r_0 \to 0$ the mass of pure adS_5 is zero. These results are in agreement with [73, 81]. It is interesting to notice that the mass of Schwarzschild-adS_5 is not zero when we use the counterterm method.

§ 2.5 Comparing methods

We presented three methods to determine the mass of an asymptotically adS spacetime where the mass is defined as the conserved quantity associated to the timelike Killing vector. We first investigated the counterterm method [14], which defines the mass from a quasilocal boundary stress energy tensor. A counterterm action is added to the action of the theory to make the quasilocal stress energy tensor finite, leading to finite mass. The mass of adS_4 and adS_5 were found to be finite in agreement with [14]. We then considered the definition of Hollands *et al.* [81] where the mass is defined using the electric part of the Weyl tensor. We found the conditions on the perturbations so that the mass of adS spacetimes in four and five dimensions are finite. We finally used the definition of Henneaux and Teitelboim in [74]. We calculated the masses for Schwarzschild-adS_4 and Schwarzschild-adS_5 and the masses of adS spacetime with general perturbations were found to be finite. The boundary conditions we found when deriving the Henneaux and Teitelboim method agree with [74].

The important point that this analysis reveals is that we need to impose boundary conditions on the perturbations in order for the mass to be finite. The boundary conditions on the metric perturbations $h_{\mu\nu}$ defined in (2.59) for asymptotically adS spacetime can be summarised as:

$$h_{rr} = O(r^{-D-1}), \quad h_{mn} = O(r^{-D+3}) \tag{2.87}$$

where m, n include the time coordinate t and the $(D-2)$ angles. These boundary conditions guarantee that the mass of the spacetime is finite.

Comparing our calculations for the three methods we found the concept behind the counterterm method easy to understand and the calculations straightforward. Since the method involves adding more counterterms as the number of dimensions increases this method would not be very convenient to implement for higher dimensions as it is 'ad-hoc'. The Hollands *et al.* [81] method is elegant since the charges are defined from the electric part of the Weyl tensor. However in practice this method leads to rather lengthy expression for the Weyl tensor. This makes it hard to obtain the expressions for the finite mass. Moreover in practice, the fact that there is a change in coordinates (Ω is used instead of r) and that we work with physical and unphysical metrics makes it challenging. In the Henneaux and Teitelboim method [74] the expression for the conserved charge involves various geometric quantities. Although this method seems the most complex it is the most elegant and the most convenient. We will be using the definition of Henneaux and Teitelboim [74] charges when we introduce a scalar field

in the theory in chapter 3. In [81] Hollands *et al.* show that their method and the Henneaux and Teitelboim [74] method are equivalent, Hollands *et al* also consider the case of gravity coupled with matter in [81]. When we consider the definition of the mass for gravity with a scalar field in chapter 3 we will use the fact that the mass of matter free adS is related to $\delta g_{rr} = h_{rr}$.

§ 2.6 Summary

In this chapter we have seen that there are different definitions for the mass in asymptotically adS spacetimes. We investigated three methods and we have decided to select the Henneaux and Teitelboim method [74]. This method has been extended to include a scalar field in [73]. This is discussed in detail in chapter 5.

Chapter 3

Einstein scalar system in anti-de Sitter spacetime

In this chapter we present our model which consists of adS gravity minimally coupled to a massive scalar field with self interacting potential. Our work is concerned with static, spherically symmetric black hole and soliton solutions in $D \geqslant 4$ spacetime dimensions for different event horizon topologies (i.e. $k = -1, 0, 1$ where k is related to the event horizon topology). We begin by describing the model with the action and the field equations. We then consider the behaviour of the scalar field as $r \to \infty$. By considering different constraints on the scalar field mass m we find four possible asymptotic expressions for the scalar field. The no hair theorem is then tested, we show that hair cannot exist if the potential is convex. We then move on to showing that for nonconvex potentials soliton and black hole solutions exist. We present plots which show agreement with the statement in [129] that the local maximum of the potential acts as an asymptotic attractor for the scalar field. We end this chapter by testing the stability of our solutions under linear perturbations.

§ 3.1 Description of the theory and field equations

We consider gravity minimally coupled to a scalar field in asymptotically adS spacetime. We assume a static and spherically symmetric spacetime. The model is described by the following action:

$$I[g, \phi] = \int d^D x \sqrt{-g} \left[\frac{R - 2\Lambda}{16\pi G} - \frac{1}{2}(\nabla\phi)^2 - V(\phi) \right] \tag{3.1}$$

where the scalar field $\phi(r)$ only depends on the radial coordinate r and has a self interaction potential $V(\phi)$. The cosmological constant Λ is related to the adS radius of curvature L:

$$\Lambda = -\frac{(D-1)(D-2)}{2L^2}. \tag{3.2}$$

We define the gravitational coupling κ as $\kappa = 16\pi G$ where G is the universal gravitational constant. Following [73] we expand the potential in this form for small ϕ:

$$V(\phi) = \frac{m^2\phi^2}{2} + C_3\phi^3 + C_4\phi^4 + C_5\phi^5 + O(\phi^6), \tag{3.3}$$

where the constants C_3, C_4, C_5 are fixed by the type of potential we choose. When we vary the action (3.1) with respect to the field variables we obtain the Einstein and scalar field equations:

$$\begin{aligned} G_{\mu\nu} + \Lambda g_{\mu\nu} &= \nabla_\mu\phi\nabla_\nu\phi - \frac{1}{2}g_{\mu\nu}(\nabla\phi)^2 - g_{\mu\nu}V(\phi) \\ \nabla_\mu\nabla^\mu\phi &= \frac{\partial V}{\partial\phi}. \end{aligned} \tag{3.4}$$

We consider the metric ansatz [28, 85]

$$ds^2 = -H(r)e^{2\delta(r)}dt^2 + H(r)^{-1}dr^2 + r^2\, d\sigma^2_{D-2,k}, \tag{3.5}$$

where $H(r)$ and $\delta(r)$ are metric functions and

$$d\sigma^2_{D-2,k} = d\theta^2 + f_k^2(\varphi)\, d\Omega^2 \tag{3.6}$$

is the line element of the $(D-2)$-dimensional horizon with constant curvature. The function $f_k(\varphi)$ depends on k as follows:

$$f_k(\varphi) = \begin{cases} \sin\varphi & \text{for } k = 1 \\ \varphi & \text{for } k = 0 \\ \sinh\varphi & \text{for } k = -1. \end{cases} \tag{3.7}$$

In adS space the parameter k is related to the topology of the horizon. If $k = 1$ the horizon is spherical, if $k = 0$ the horizon is flat and if $k = -1$ the horizon is hyperbolic.

To find the field equations of this theory we substitute the ansatz (3.5) and $\phi(r) = \phi$

in (3.4). We obtain:

$$0 = H\phi'' + \left[H' + H\delta' + (D-2)\frac{H}{r}\right]\phi' - \frac{\partial V}{\partial \phi} \tag{3.8}$$

$$0 = \frac{D-2}{2r}\left[H' + (H-k)\frac{(D-3)}{r}\right] + \frac{1}{2}H\phi'^2 + \Lambda + V(\phi) \tag{3.9}$$

$$0 = (D-2)\frac{\delta'}{r} - \phi'^2. \tag{3.10}$$

We see that the field equations depend on H, H', δ', they also depend on the potential of the scalar field and its derivative. We can see that the dependence on ϕ' is nonlinear which means the expression for $\phi(r)$ will have a complicated structure. There is no dependence on δ which means one can add an arbitrary constant to δ by rescaling the time variable. As a result one can set the values of δ_0 at the origin or of δ_h at the horizon to constants without loss of generality. These field equations are in agreement with [85] when $\xi = 0$ where ξ is the coupling between the Ricci scalar and the scalar field. Solving these equations will give us soliton or black hole solutions but we first need to investigate the boundary conditions at the origin ($r \to 0$), the black hole horizon (r_h) and at infinity ($r \to \infty$).

§ 3.2 Boundary conditions

Boundary conditions at the origin $r = 0$, at the black hole event horizon $r = r_h$ and at infinity $r \to \infty$ have to be specified before proceeding to solve the field equations because the equations (3.8-3.10) are singular at these points. We need to define expansions around the singular points in order to be able to study the behaviour of the metric functions and the scalar field near those points. At the origin we are looking for soliton solutions. Possible black hole solutions are found at the black hole event horizon.

3.2.1 Boundary conditions at the origin

At the origin solutions exist when $k = 1$ since the Ricci scalar diverges at the origin [85] if $k \neq 1$. The field variables near the origin can be expanded as follows:

$$\begin{aligned} H(r) &= H_0 + H_1 r + H_2 r^2 + H_3 r^3 + H_4 r^4 + O(r^5) \\ \phi(r) &= \phi_0 + \phi_1 r + \phi_2 r^2 + \phi_3 r^3 + \phi_4 r^4 + O(r^5) \\ \delta(r) &= \delta_0 + \delta_1 r + \delta_2 r^2 + \delta_3 r^3 + \delta_4 r^4 + O(r^5). \end{aligned} \tag{3.11}$$

Putting these expressions back into the field equations (3.8-3.10) and using the Frobenius method, we identify coefficients of the same power and find the coefficients to be:

$$\begin{aligned} H_0 &= 1 \\ H_2 &= -\frac{2(V(\phi_0)+\Lambda)}{(D-2)(D-1)} \\ \phi_2 &= \frac{1}{2(D-2)}\frac{\partial V}{\partial \phi}(\phi_0) \\ \delta_4 &= \frac{\phi_2^2}{D-2}, \end{aligned} \tag{3.12}$$

with $H_1 = H_3 = \phi_1 = \phi_3 = \delta_1 = \delta_2 = \delta_3 = 0$. Putting (3.12) back in (3.11) we have:

$$\begin{aligned} H &= 1 - \frac{2(V(\phi_0)+\Lambda)}{(D-2)(D-1)} r^2 + O(r^4) \\ \delta &= \delta_0 + \frac{\phi_2^2}{D-2} r^4 + O(r^6) \\ \phi &= \phi_0 + \frac{1}{2(D-2)}\frac{\partial V}{\partial \phi}(\phi_0) r^2 + O(r^4). \end{aligned} \tag{3.13}$$

At this stage δ_0 and ϕ_0 are free parameters, δ_0 will be fixed by the boundary conditions at infinity.

3.2.2 Boundary conditions at the black hole event horizon

For a black hole with a regular event horizon at $r = r_h$ we have $H(r_h) = 0$. The field variables can be Taylor expanded around r_h as:

$$\begin{aligned} H(r) &= H'(r_h)(r - r_h) + O(r - r_h)^2 \\ \delta(r) &= \delta_h + \delta'(r_h)(r - r_h) + O(r - r_h)^2 \\ \phi(r) &= \phi_h + \phi'(r_h)(r - r_h) + O(r - r_h)^2. \end{aligned} \tag{3.14}$$

When we put these expressions in the field equations (3.8-3.10) we obtain:

$$\begin{aligned} H'(r_h) &= \frac{2r_h}{D-2}\left[(D-2)(D-3)\frac{k}{2r_h^2} - \Lambda - V(\phi_h)\right] \\ \delta'(r_h) &= \frac{\phi'^2(r_h)r_h}{D-2} \\ \phi'(r_h) &= \frac{V_h'}{H'(r_h)}. \end{aligned} \tag{3.15}$$

The constant ϕ_h is arbitrary, and $V_h' = \frac{\partial V(\phi_h)}{\partial \phi}$.

3.2.3 Boundary conditions at infinity

The boundary conditions at infinity are the most subtle. At infinity the scalar field minimally coupled to adS has the form [73]:

$$\phi(r) = \phi_\infty + \psi(r) \tag{3.16}$$

where $\psi(r) \to 0$ as $r \to \infty$ and ϕ_∞ is a constant representing the value of the scalar field at infinity. Since the field equations only depend on ϕ', ϕ'' and $V(\phi)$ we can consider $\phi_\infty = 0$, without loss of generality. In order to have a spacetime that is asymptotically adS we write $H(r)$ as:

$$H = \frac{r^2}{L^2} + k + J(r) \tag{3.17}$$

where

$$J(r) \sim r^{-\Sigma} \tag{3.18}$$

is subleading compared to the r^2/L^2 term. The function $\phi(r)$ would normally be expanded as:

$$\psi = \frac{a_0}{r^\Delta} + \frac{a_1}{r^{\Delta+1}} + O(r^{-\Delta+2}), \tag{3.19}$$

but because of the nonlinearity of the field equations (3.8-3.10) the expansion of the scalar field has a more complicated structure which will be investigated in the next chapter.

For the moment we write the scalar field as:

$$\psi = \frac{a_0}{r^\Delta} + ... \tag{3.20}$$

The potential can be expanded as:

$$V(\phi) = V(\phi_\infty + \psi) = V(\phi_\infty) + \frac{\partial V(\phi_\infty)}{\partial \phi}\psi + \frac{1}{2!}\frac{\partial^2 V}{\partial \phi^2}(\phi_\infty)\psi^2 + O(\psi^3) \tag{3.21}$$

and

$$\frac{\partial V(\phi)}{\partial \phi} = \frac{\partial^2 V(\phi_\infty)}{\partial \phi^2}\psi + O(\psi^2). \tag{3.22}$$

Since it has been proven in [129] that ϕ_∞ takes an extremum value of the potential so $\frac{\partial V(\phi_\infty)}{\partial \phi} = 0$ and we define:

$$\frac{\partial^2 V(\phi_\infty)}{\partial \phi^2} = m^2, \tag{3.23}$$

where we are not assuming that m^2 is positive. The expression in (3.23) is in agreement with (3.3) for small $\phi(r)$. Putting (3.17-3.23) in (3.8) we find

$$\Sigma = -2\Delta + 2 \tag{3.24}$$

and considering the leading order behaviour in r we obtain the following quadratic equation for Δ:

$$\frac{1}{L^2}\Delta(\Delta + 1) - \frac{D}{L^2}\Delta - m^2 = 0. \tag{3.25}$$

Solving for Δ we have two roots:

$$\Delta = \Delta_\pm = \frac{(D-1)}{2}\left[1 \pm \sqrt{1 + \frac{4m^2L^2}{(D-1)^2}}\right]. \tag{3.26}$$

We write a more general form for the leading order behaviour function $\psi(r)$:

$$\psi = ar^{-\Delta_-} + br^{-\Delta_+} + ... \tag{3.27}$$

Looking at 3.17 we see that the adS term r^2/L^2 is dominant provided that the term $J(r)$ is subdominant. This is the case when $\Delta_- < 2$ which is always the case for the cases we want to investigate. In our plots the values for dm will be chosen so $J(r)$ is subdominant. Before moving to the different possible asymptotic forms of the scalar field, we consider the function δ. From (3.10) and using the leading behaviour in (3.27) we have:

$$\delta = \frac{a^2\Delta_-}{D-2}\int r^{-2\Delta_- - 1} \tag{3.28}$$

where we see that $\delta = O(r^{-2\Delta_-})$. The metric function δ will always be very small compared to $H(r)$ and $\phi(r)$. This is seen in all the plots for δ in section 3.4.2.

Let us now consider the asymptotic behaviour of the scalar field which depends on the

mass and the roots (3.26). The roots can be real or imaginary. We use the Frobenius method to find the different asymptotic forms of $\phi(r)$.

- **Real solutions**

From (3.26) we see that the solutions are real if:

$$1 + \frac{4m^2L^2}{(D-1)^2} \geqslant 0 \tag{3.29}$$

so the mass of the scalar field is:

$$m^2 \geqslant -\frac{(D-1)^2}{4L^2}. \tag{3.30}$$

This is the Breitenlohner-Freedman bound [31] which will be discussed in more detail in the next chapter.

Now we consider the case where $m^2 > 0$. For this case the potential has a minimum at $\phi = 0$. It is clear that $\Delta_- < 0$ and so the a branch in (3.27) is divergent as $r \to \infty$. In this case the expression for the scalar field reduces to the b branch:

$$\phi(r) = \frac{b}{r^{\Delta_+}} + ... \tag{3.31}$$

The a branch is dominant unless there is some fine tuning, meaning we set $a = 0$ [129]. In the case where $m^2 < 0$, the potential has a maximum at $\phi = 0$. We have:

$$0 < 1 + \frac{4m^2L^2}{(D-1)^2} < 1 \tag{3.32}$$

since we only want real solutions and we have $\Delta_- > 0$. In this case providing the roots $\Delta_\pm$ are not separated by an integer, both a and b branches are included and the scalar field has the form (3.27). If they are separated by an integer p i.e. $\Delta_+ - \Delta = p$ we have:

$$\phi = ar^{-\Delta_-} + br^{-\Delta_+} + c\ln(r)r^{-\Delta_+} + ... \tag{3.33}$$

- **Imaginary solutions**

We can also use the Frobenius method to find solutions with complex roots. The roots are complex when:

$$m^2L^2 < -\frac{(D-1)^2}{4}. \tag{3.34}$$

In this case the roots are complex conjugates i.e. $\Delta_+ = \overline{\Delta}_-$ and have the form $\Delta_\pm =$

case	m^2L^2	$\Delta_\pm$	$\phi(r)$
case 1	> 0	$\Delta_+ > 0, \Delta_- < 0$ $\Delta_+, \Delta_- \in \mathbb{R}$	$br^{-\Delta_+} + ...$
case 2	< 0 $> -\frac{(D-1)^2}{4}$ $\neq \frac{p^2-(D-1)^2}{4}$	$\Delta_+ > 0, \Delta_- > 0$ $\Delta_+, \Delta_- \in \mathbb{R}$	$ar^{-\Delta_-} + ... + br^{-\Delta_+} + ...$
case 3	< 0 $> -\frac{(D-1)^2}{4}$ $= \frac{p^2-(D-1)^2}{4}$	$\Delta_+ > 0, \Delta_- > 0$ $\Delta_+ - \Delta_- \in \mathbb{Z}^+$	$ar^{-\Delta_-} ... + br^{-\Delta_+} + ... + c\ln(r)r^{-\Delta_+}$
case 4	$< -\frac{(D-1)^2}{4}$	$\Delta_+ = \overline{\Delta}_-$ $\Delta_\pm = \gamma \pm i\omega$	$ar^\gamma \cos[\omega \ln(r)] + ...$

Table 3.1: Summary of the different roots of (3.25) and different asymptotics for the scalar field.

$\gamma \pm i\omega$ where γ and ω are real. The scalar field is oscillatory and has the form:

$$\phi = ar^\gamma \cos[\omega \ln(r)] + ... \tag{3.35}$$

We see that we have four possible cases for the asymptotic form of the scalar field which we present in Table 3.1. In [129] the four cases are mentioned for $D = 4$ and $k = 1$. Our analysis is a generalisation to $D \geqslant 4$ and for all k. We also present a more systematic analysis for all the cases.

§ 3.3 No-hair results

We want to investigate the possible existence of hair for the cases in Table 3.1 for convex potentials which satisfy $\frac{\partial V}{\partial \phi}\phi > 0$. We use the approach described in chapter 1 for a single field. First we multiply (3.8) by $\phi r^{D-2}e^\delta$ and then integrate by part using different limits corresponding to different boundaries. We have:

$$\begin{aligned} 0 &= \int_x^y dr \left[\frac{\partial V}{\partial \phi}\phi r^{D-2}e^\delta - \phi\left(H\phi' r^{D-2}e^\delta\right)'\right] \\ &= \int_x^y dr\, r^{D-2}e^\delta \left(\frac{\partial V}{\partial \phi}\phi + H\phi'^2\right) - \left[H\phi\phi' r^{D-2}e^\delta\right]_x^y. \end{aligned} \tag{3.36}$$

We restrict our attention to convex potentials for which $\frac{\partial V}{\partial \phi}\phi > 0$, and we assume that $H > 0$ for $x < r < y$. We want to evaluate (3.36) for the different cases, if the boundary term is zero then the rest of the integral must be equal to zero since the sum of two positive terms cannot be zero. As a consequence $\phi =$ constant so we do not have hair. We consider the behaviour of the boundary term for three different boundary points:

- **For** $r = 0$

For this case $x = 0$ and the metric functions H, ϕ and δ are all $O(1)$ according to the boundary conditions at the origin defined in (3.13). Since $\phi' = O(r)$ the boundary term is $O(r^{D-1})$ and the boundary term in (3.36) vanishes as $r \to 0$.

- **For** $r = r_h$

For this case $x = r_h$. We have $H = 0$ at $r = r_h$ therefore the boundary term will vanish if all the other terms are finite at $r = r_h$.

- **For** $r = \infty$

We set $y = \infty$. We will consider the four cases in Table 3.1 separately. We first consider case 1 where

$$\begin{aligned} \phi &= br^{-\Delta_+} + ... \\ \phi' &= -b\Delta_+ r^{-\Delta_+ - 1} + ... \end{aligned} \tag{3.37}$$

As $r \to \infty$ the boundary term in (3.36) is:

$$-\frac{b^2}{L^2} e^{\delta} r^{-2\Delta_+ + D - 1} \tag{3.38}$$

and we have

$$-2\Delta_+ + D - 1 = -(D-1)\sqrt{1 + \frac{4m^2L^2}{(D-1)^2}} < 0, \tag{3.39}$$

the exponent of r is negative so the boundary term (3.38) vanishes as $r \to \infty$.

We now consider case 2 from Table 3.1 but only the leading behaviour:

$$\phi = ar^{-\Delta_-} + ... \tag{3.40}$$

and we have:

$$\phi' = -a\Delta_- r^{-\Delta_- - 1} + ... \tag{3.41}$$

In this case the boundary term in (3.36) becomes:

$$-\frac{a^2}{L^2}\Delta_- e^{\delta} r^{-2\Delta_- + D - 1} \tag{3.42}$$

where the exponent of r, namely $-2\Delta_- + D - 1$, is positive. In this case the boundary term is negative so (3.36) is the sum of two positive terms which can never be zero. This is a mathematical contradiction and therefore for case 3 there is no hair.

Finally, we consider case 4:

$$\begin{aligned} \phi &= ar^{\gamma}\cos[\omega \ln(r)] + ... \\ \phi' &= a\gamma r^{\gamma-1}\cos[\omega \ln(r)] - ar^{\gamma}\sin[\omega \ln(r)]\left(\frac{\omega}{r}\right) + ... \end{aligned} \tag{3.43}$$

For nontrivial solutions we need the boundary term to be positive since the sum of two positive terms can never be zero. We can see that the first derivative of ϕ oscillates, it is negative and positive alternatively. Therefore the condition $\phi(r)\phi'(r) > 0$ is not satisfied since for this case it can sometimes be negative we conclude that there is no hair.

These no hair results rule out the existence of scalar field hair for convex self-interacting potentials such as: $V(\phi) = \frac{1}{2}m^2\phi^2$ or $V(\phi) = \lambda\phi^4$ but not potentials such as the Higgs potential. As mentioned above, our work generalises the results in [129] as we consider D dimensions and $k = -1, 0, 1$. Solutions may exist for nonconvex potentials, we investigate this in the next session.

§ 3.4 Soliton and black hole solutions

By considering nonconvex potentials it was proven in [129] that stable black hole solutions exist. Torri *et al.* consider the Higgs potential in $D = 4$ with $k = 1$. Our approach is more systematic, we find soliton and black hole solutions for $D \geqslant 4$ for any k with two nonconvex potentials.

3.4.1 The method

We want to find numerical solutions near the origin and the black hole horizon using NDSolve in Mathematica. We therefore need to find suitable expressions for the differential equations governing the functions of the theory, namely $\phi(r)$, $J(r)$ and $\delta(r)$ and then integrate those. Here we present the method used to obtain soliton solutions, spherically symmetric black holes and topological black hole solutions for $4 \leqslant D \leqslant 6$

with two different potentials.

We begin by considering the metric function $H(r)$ as given in (3.17). The field equations (3.8-3.10) can be written in a simpler form in terms of $J(r)$:

$$0 = \frac{(D-2)}{2r}\left[J' + \frac{(D-3)}{r}J\right] + \frac{1}{2}\left[k + \frac{r^2}{L^2} + J\right]\phi'^2 + V(\phi) \tag{3.44}$$

$$\begin{aligned} 0 = &\left[k + \frac{r^2}{L^2} + J\right]\phi'' \\ &+ \left[\left(\frac{2r}{L^2} + J'\right) + \left(k + \frac{r^2}{L^2} + J\right)\delta' + \frac{(D-2)}{r}\left(k + \frac{r^2}{L^2} + J\right)\right]\phi' - \frac{\partial V(\phi)}{\partial \phi} \end{aligned} \tag{3.45}$$

$$0 = (D-2)\frac{\delta'}{r} - \phi'^2. \tag{3.46}$$

The mass of the scalar field is defined as [73]:

$$m^2 = m_*^2 + dm^2 \tag{3.47}$$

where

$$m_*^2 = -\frac{(D-1)^2}{4L^2} \tag{3.48}$$

is the Breitenlohner-Freedman mass bound [31]. We then write down the expressions for the potential and its derivative. In our work we investigate the Higgs potential expressed as:

$$V(\phi) = \frac{\alpha_0}{4}(\phi^2 - v^2)^2 \tag{3.49}$$

and the TWI potential from cosmology [50]:

$$V(\phi) = M^4\left[1 - A\left(\frac{\phi}{\phi_0}\right)^2 e^{-\phi/B_0}\right] \tag{3.50}$$

which is also a nonconvex potential.

The equation that we numerically solve for $J(r)$ is:

$$J' = -\frac{D-3}{r}J - \frac{r}{D-2}\left(k + \frac{r^2}{L^2} + J\right)\phi'^2 - \frac{2r}{D-2}V, \tag{3.51}$$

for the scalar field $\phi(r)$ we have:

$$\begin{aligned}\phi'' &= -\frac{\phi'}{k+\frac{r^2}{L^2}+J}\left[\frac{2r}{L^2}+J'+\left(k+\frac{r^2}{L^2}+J\right)\delta'+\frac{(D-2)}{r}\left(k+\frac{r^2}{L^2}+J\right)\right] \\ &\quad +\frac{V'}{k+\frac{r^2}{L^2}+J}\end{aligned} \tag{3.52}$$

and for the function $\delta(r)$ we use:

$$\delta' = \frac{r\phi'^2}{D-2}. \tag{3.53}$$

We want to start integrating at $r = 0$ or at $r = r_h$ but the field equations are singular at these points. Therefore we start integrating at $r = \epsilon$ for soliton solutions, or $r = r_h + \epsilon$ for black hole solutions, where $\epsilon << 1$. The power series (3.11) and (3.14) give us suitable initial conditions. In the expression for Λ in (3.2) we set the adS radius of curvature $L = 1$. The other parameters we fix are the number of spacetime dimensions D, the gravitational coupling κ that we set to one and the the potential parameters v and α and A and M for the Higgs (3.49) and the TWI (3.50) potentials respectively. We give more details about how we fix the parameters below.

Higgs potential

The Higgs potential is:

$$V = \frac{\alpha}{4}(\phi^2 - v^2)^2. \tag{3.54}$$

In order to match Henneaux *et al.* definition [73] for the generic potential (3.3), we write the Higgs potential as:

$$V = \frac{\alpha_0}{4}\left(\phi^2 - v^2\right)^2 - \frac{\alpha_0 v^4}{4}. \tag{3.55}$$

It follows that:

$$V' = \alpha_0\left(\phi^3 - v^2\phi\right). \tag{3.56}$$

We present the plots for the possible shapes of the Higgs potential in Figs. 3.1a and 3.1b. This potential is considered in [129] where it has been shown that he scalar field is asymptotically attracted to the local maximum of the potential as $r \to \infty$. For $m^2 > 0$ which corresponds to case 1 we see from Fig. 3.1a that the local maximum occurs at $\phi = v$ and there is a local minimum occurring at zero. In this case the scalar field should converge to one at infinity. From Fig. 3.1b we see that for $m^2 < 0$, the maximum occurs at $\phi = 0$, the local minimum is located at $\phi = v$. In this case the

scalar field should go to zero at infinity, this behaviour should be seen for cases 2 and 3 in the next section. In the Mathematica code we set $v = 1$ without loss of generality.

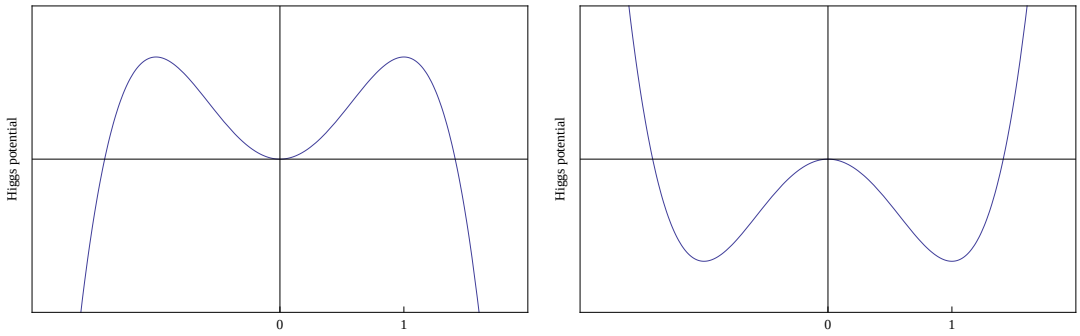

(a) Higgs potential with $m^2 > 0$ (b) Higgs potential with $m^2 < 0$

Figure 3.1: (a) Higgs potential for case 1 with $m^2 > 0$ and $v = 1$, stationary points happen at $\phi = 0$ and $\phi = v$. (b) Higgs potential for cases 2 and case 3 with $m^2 < 0$ and $v = 1$, stationary points happen at $\phi = 0$ and $\phi = v$.

The next step is to define initial conditions for soliton and black hole solutions. The initial conditions for the metric functions are given in (3.13) and (3.15) respectively. Here we only give the quantities which are specific to the potential. At the origin, for the Higgs potential we have:

$$\begin{aligned} \delta_{origin} &= \delta_0 + \frac{1}{D-2}\left[\frac{\alpha_0}{2(D-2)}(\phi_0^3 - v^2\phi_0)^2\right] r^4 + ... \\ \phi_{origin} &= \phi_0 + \frac{\alpha_0}{2(D-2)}(\phi_0^3 - v^2\phi_0)^2 r^2 + ... \end{aligned} \tag{3.57}$$

The quantities at the horizon have the same form as in (3.15).

TWI potential

We extend our work to another nonconvex potential found in cosmology [50] called Twisted Inflation potential (TWI) with the form:

$$V(\phi) = M^4\left[1 - A\left(\frac{\phi}{B_0}\right)^2 e^{-\phi/B_0}\right]. \tag{3.58}$$

where M and B_0 are parameters that we can fix, the parameter B_0 can be set to one without loss of generality. In order for the TWI potential to match (3.3) we take off

the M^4 term and set $M = 1$, we obtain:

$$V(\phi) = -A\left(\frac{\phi}{B_0}\right)^2 e^{-\phi/B_0}. \tag{3.59}$$

We have have:

$$\frac{\partial V}{\partial \phi} = -A\left(\frac{\phi}{B_0^2}\right) e^{-\phi/B_0}\left(2 - \frac{\phi}{B_0}\right). \tag{3.60}$$

The stationary points happen at $\phi = 0$ and $\phi = 2B_0$ as we illustrate in Figs. 3.2a, 3.2b where we set $B_0 = 1$ without loss of generality. To find the expression of A in terms of parameters of the generic potential (3.3) we expand the exponential function so the potential has the form:

$$V = -A\phi^2 + A\phi^3 - \frac{A}{2!}\phi^4 + \frac{A}{3!}\phi^5 + ... \tag{3.61}$$

By identification of coefficients in (3.3) we have:

$$\begin{aligned} \frac{m^2}{2} &= -A \\ C_3 &= A \\ C_4 &= -\frac{A}{2!} \\ C_5 &= \frac{A}{3!}. \end{aligned} \tag{3.62}$$

The quantities at the origin and horizon are defined as in (3.13) and (3.15) respectively. We plot the TWI potential for $m^2 > 0$ in Fig. 3.2a and $m^2 < 0$ in Fig. 3.2b. When $m^2 > 0$ the maximum occurs at $\phi = 2B_0$ and the minimum occurs at $\phi = 0$. According to [129] for this case the potential should converge to two at infinity. When $m^2 < 0$ the maximum occurs at $\phi = 0$ and the minimum occurs at $\phi = 2B_0$, for this case the potential should go to zero infinity.

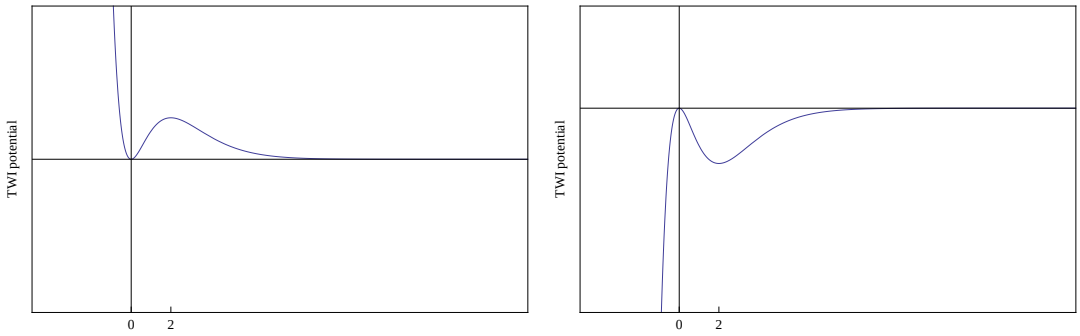

(a) TWI potential with $m^2 > 0$ (b) TWI potential with $m^2 < 0$

Figure 3.2: (a) TWI potential for case 1 with $m^2 > 0$ and $B_0 = 1$, stationary points happen at $\phi = 0$ and $\phi = 2B_0$. (b) TWI potential for cases 2 and case 3 with $m^2 < 0$ and $B_0 = 1$, stationary points happen at $\phi = 0$ and $\phi = 2B_0$.

§ 3.5 Example solutions

Due to the large number of cases we cannot present them all, we therefore illustrate every case by selected plots. We limit the number of dimensions to $4 \leqslant D \leqslant 6$ which covers all the cases in chapter 4. We set $v = 1$ for all cases. For the Higgs potential we have $\alpha_0 = -m^2/v^2$ and for the TWI potential we have $A = -m^2/2$.

3.5.1 Cases 1

In Figs. 3.3a-3.3c we present black hole solutions for case 1 with the Higgs potential (3.55) for $D = 4$ where we vary ϕ_h. In Fig. 3.3a the scalar field oscillates then converges to $v = 1$ which corresponds to the maximum of the Higgs potential for $m^2 > 0$, this is in agreement with Fig. 3.1a. The function $J(r)$ presented in Fig. 3.3b decreases rapidly for all values of ϕ_h and $\delta(r)$ converges at infinity as shown in Fig. 3.3c. We see similar effects for $D = 5, 6$ but with damped oscillations. When we consider topological black holes with $k \neq 1$ for $D = 4$ we do not observe significant changes in ϕ and $J(r)$ diverges to $-\infty$ in the same way for all k. However we see that the function $\delta(r)$ converges to a higher value when $k = -1$, this can be seen in Figs. 3.3d-3.3f. The function δ (3.28) was expected to be small and converge quickly, this is confirmed in Fig. 3.3c. Similar behaviour as for $D = 4$ is seen for $D = 5, 6$. We also found soliton solutions for the Higgs potential, the plots in $D = 4, 5, 6$ have a similar behaviour as the black hole solutions shown in Figs. 3.3a-3.3f.

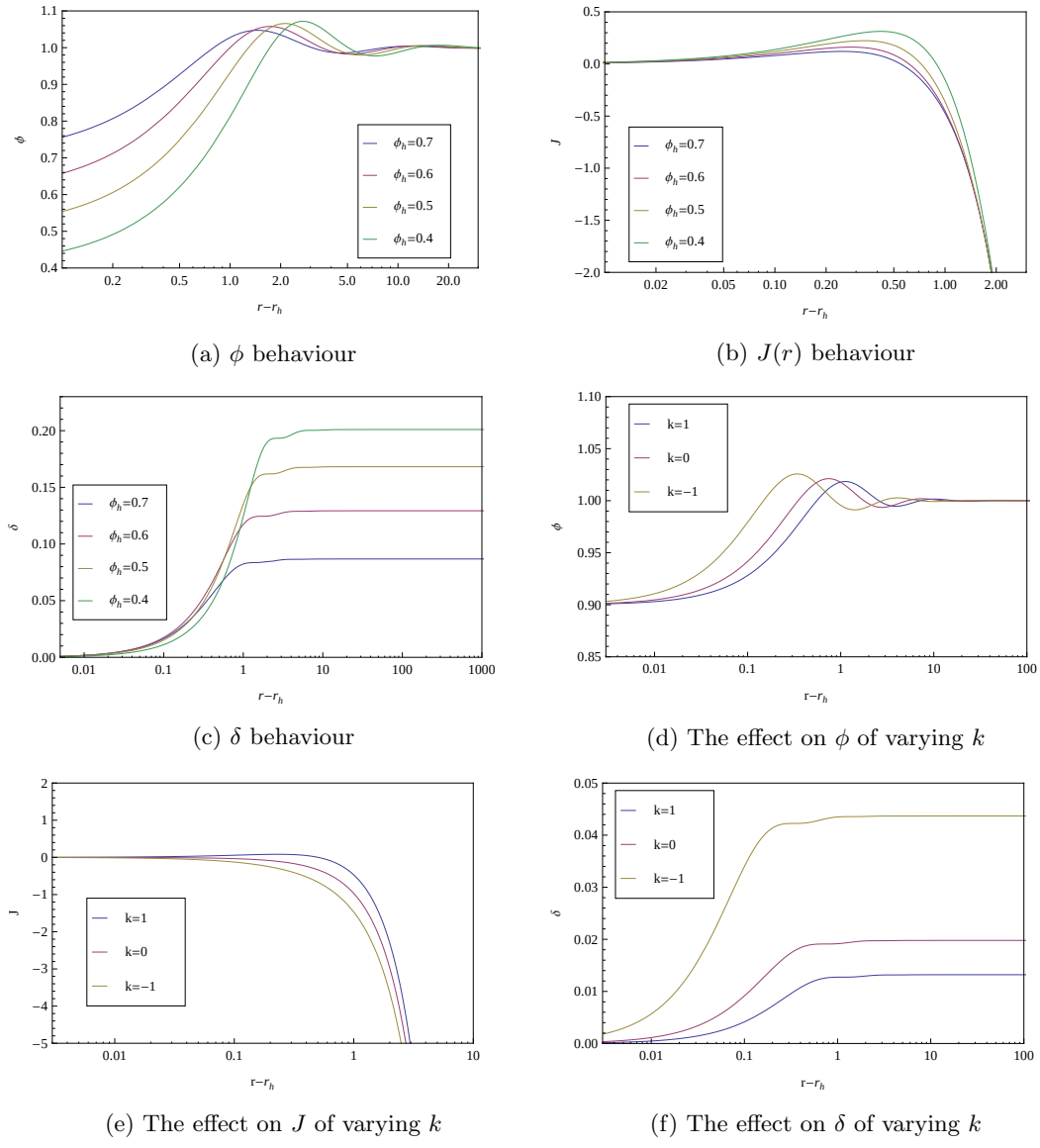

(a) ϕ behaviour

(b) $J(r)$ behaviour

(c) δ behaviour

(d) The effect on ϕ of varying k

(e) The effect on J of varying k

(f) The effect on δ of varying k

Figure 3.3: Case 1 with Higgs potential (a,b,c) plots showing the effect on ϕ, J and δ of varying ϕ_h for four-dimensional black hole solutions with $dm = 27/10L$, $v = 1$, $L = 1$ $k = 1$, $\kappa = 1$, $r_h = 1$. (d, e, f) plots showing the effects on ϕ, J and δ of varying k for four-dimensional black hole solutions with $dm = 27/10L$, $v = 1$, $L = 1$, $\kappa = 1$, $r_h = 1$, $\phi_h = 0.9$.

For the TWI potential, the solutions are similar to the Higgs potential except they have no oscillations as can be seen in Figs. 3.4a-3.4c. We can see that the function ϕ converges to two as expected from Fig. 3.2a since the maximum happens at $2B_0$ (we set $B_0 = 1$). The metric function $J(r)$ diverges to $-\infty$ and δ converges as $r \to \infty$. The soliton solutions have a similar behaviour as 3.4a-3.4c. When we consider higher

dimensions we obtain similar results for soliton and black hole solutions.

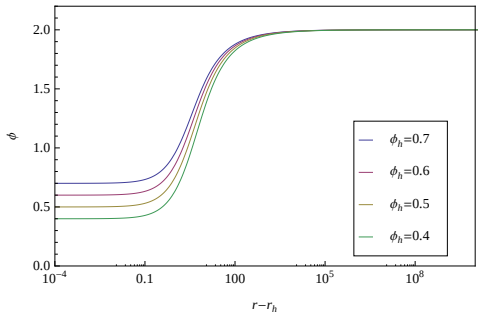

(a) ϕ when varying ϕ_h

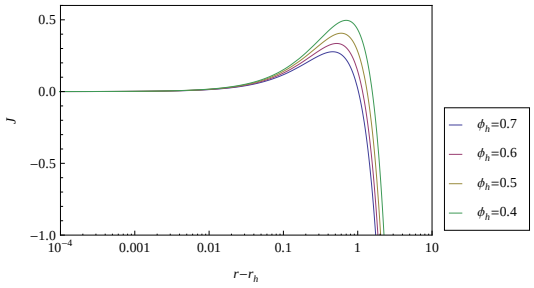

(b) $J(r)$ when varying ϕ_h

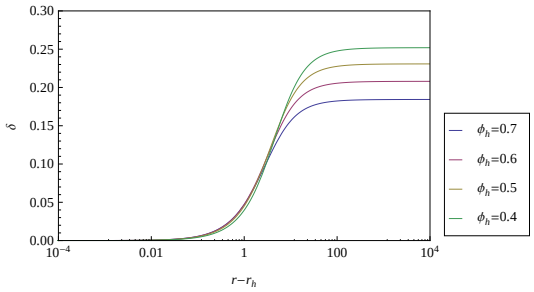

(c) δ when varying ϕ_h

Figure 3.4: Case 1 with TWI potential (a) the effect on the scalar field ϕ of varying ϕ_h is shown for four-dimensional black hole solutions with $dm = 27/10L$, $v = 1$, $k = 1$, $B_0 = 1$ (b) the effect on on the metric function J of varying ϕ_h is shown for four-dimensional black hole solutions with $dm = 27/10L$, $v = 1$, $k = 1$, $\kappa = 1$ $L = 1$, $B_0 = 1$ (c) the effect on the metric function δ of varying ϕ_h is shown for four-dimensional black hole solutions with $dm = 27/10L$, $v = 1$, $k = 1$, $\kappa = 1$, $L = 1$, $B_0 = 1$.

3.5.2 Case 2

In Fig. 3.5 we present a black hole solution for case 2 for $D = 4$ with Higgs potential. We can see ϕ vanishing at infinity, $J(r)$ diverges at infinity and $\delta(r)$ converges for all values of ϕ_h. For the TWI potential we have similar results. To illustrate this we show how the three functions vary when we vary the values of ϕ_h for $D = 6$. We see in Fig. 3.6a that the scalar field goes to zero at infinity, Fig. 3.6b shows the behaviour of $J(r)$ which for this case converges to two at infinity. Fig. 3.6c shows the behaviour of δ function which converges at infinity. We also investigate topological black holes for this case with $D = 4$ for TWI potential. We see in Fig. 3.6d how the scalar field is not very affected by the change in k. Similar comments apply to $J(r)$ and $\delta(r)$ as can be seen in Figs. 3.6e and 3.6f. We see that $J(r)$ is divergent which is similar to the behaviour

of $J(r)$ for Higgs potential.

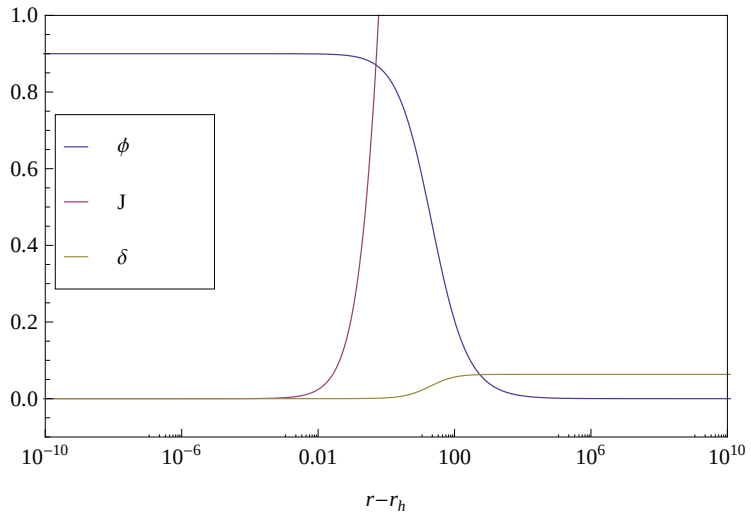

Figure 3.5: Case 2: Example of four-dimensional black hole solutions with $\Delta_- = 5/4$, $\Delta_+ = 11/4$, $\phi_h = 9/10$, $L = 1$ and $k = 1$, $\kappa = 1$ with Higgs potential

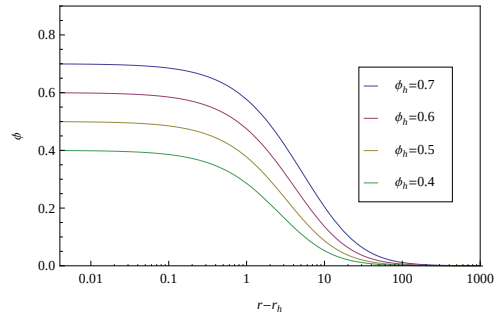

(a) ϕ behaviour when varying ϕ_h

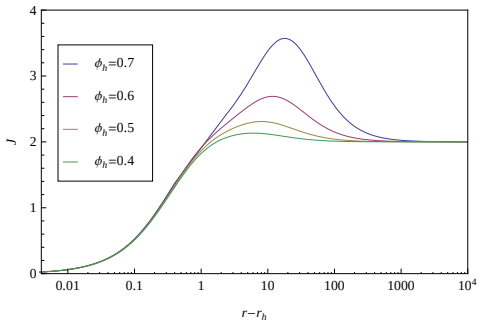

(b) $J(r)$ behaviour when varying ϕ_h

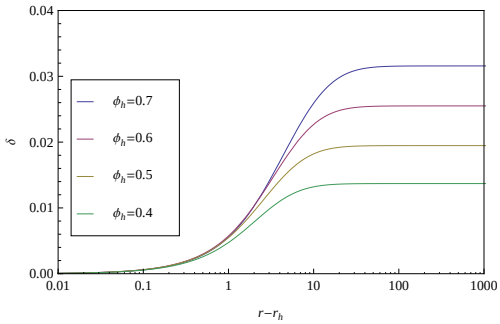

(c) δ behaviour when varying ϕ_h

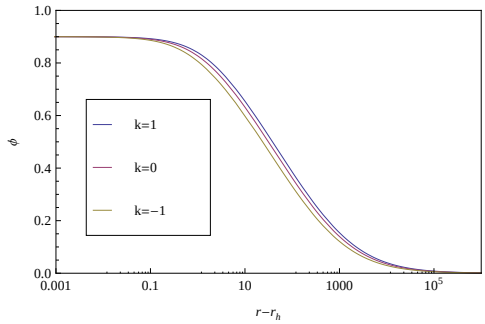

(d) The effect on ϕ of varying k

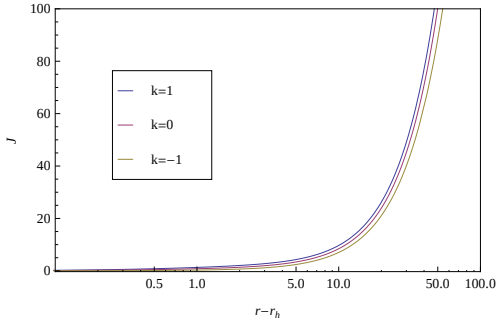

(e) The effect on J of varying k

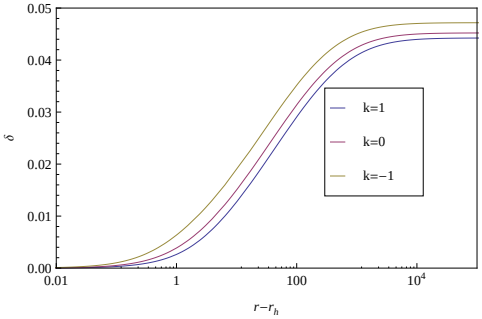

(f) The effect on δ of varying k

Figure 3.6: Case 2 with TWI potential (a,b,c) plots of six-dimensional black hole solution showing the effect of varying ϕ_h on ϕ, J and δ, with $dm = 3/4L$, $k = 1$, $L = 1$, $\delta_h = 0$, $\kappa = 1$, $r_h = 1$, $\Delta_- = 3/4$, $\Delta_+ = 9/4$, $B_0 = 1$ (d, e, f) plots of four-dimensional black hole solution showing the effect of changing k on $\phi(r)$, $J(r)$ and $\delta(r)$ with with $dm = 3/4L$, $\Delta_- = 3/4$, $\Delta_+ = 9/4$, $L = 1$, $\delta_h = 0$, $\phi_h = 0.9$, $\kappa = 1$, $r_h = 1$, $B_0 = 1$.

3.5.3 Case 3

For case 3 we found that for soliton solutions for $D = 4$ with TWI potential, $J(r)$ diverges as can be seen in Fig. 3.7c. A similar effect is observed for Higgs potential. The functions ϕ and δ converge as it can be seen in Figs. 3.7b and Fig. 3.7d. We have

also investigated solutions in higher dimensions, the functions ϕ and δ have similar behaviour as in four dimensions but the function J converges in higher dimensions as we can see in Fig. 3.7a. This is true for soliton and black hole solutions for Higgs potential. When we investigated topological black holes for this case the behaviour was found to be similar to case 2 seen in Figs. 3.6d-3.6f.

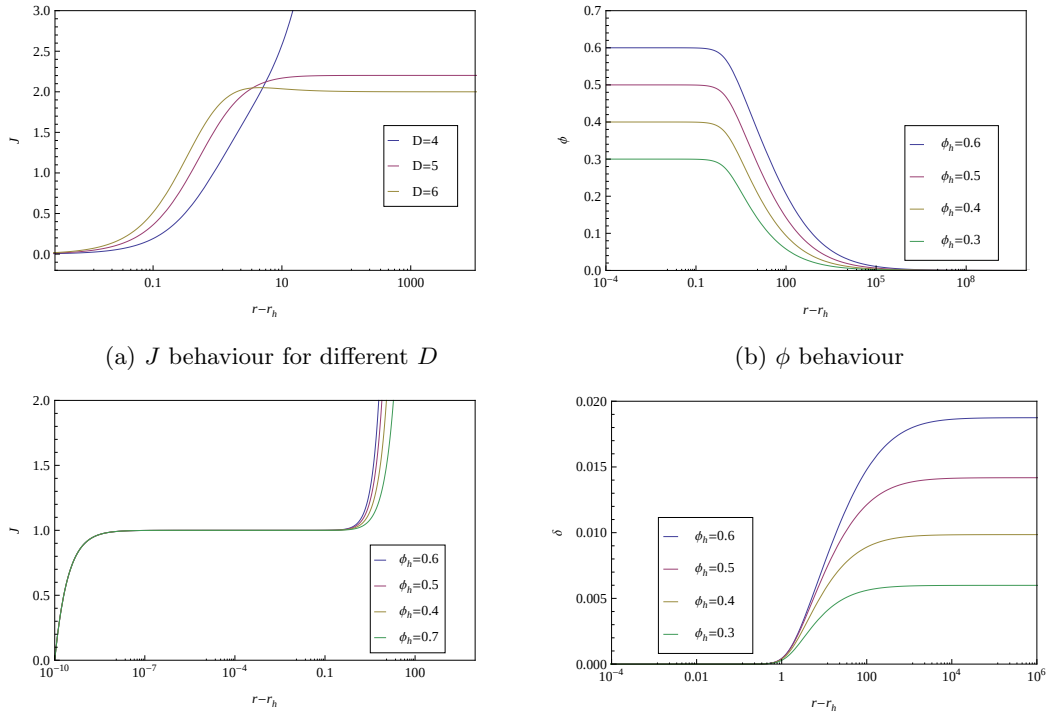

(a) J behaviour for different D

(b) ϕ behaviour

(c) $J(r)$ behaviour

(d) δ behaviour

Figure 3.7: Case 3 (a) plot for four-dimensional black hole solution showing the metric function J for different dimensions with $L = 1$, $r_h = 1$, $\kappa = 1$, $k = 1$, $v = 1$, $\delta_h = 0$, $\phi_h = 0.4$, $dm = 1/L$ with Higgs potential (b, c, d) plots of four-dimensional soliton solution showing the effect of varying ϕ_h on ϕ, J and δ with with $dm = 1/L$, $L = 1$, $\delta_0 = 0$, $k = 1$, $\kappa = 1$, $\delta_0 = 0$ $\Delta_- = 3/2$, $\Delta_+ = 11/4$, with TWI potential.

3.5.4 Case 4

We have plotted graphs of soliton and black hole solutions for case 4 with four, five and six dimensions. The oscillations are damped as we increase the number of dimensions as it can be seen by comparing Fig. 3.8a and Fig. 3.8a. For this case ϕ, $J(r)$ and $\delta(r)$ converge when we vary ϕ_0 or ϕ_h. This is true for all dimensions and for both Higgs and TWI potentials as we illustrate it in Figs. 3.8a - 3.8f. We also investigated topological black holes with $D = 4$ for Higgs potential. We see in Fig. 3.9a how the scalar field is not very affected by the change in k. The difference is more significant for the metric

functions $J(r)$ and $\delta(r)$ as it can be seen in Fig. 3.9b and Fig. 3.9c.

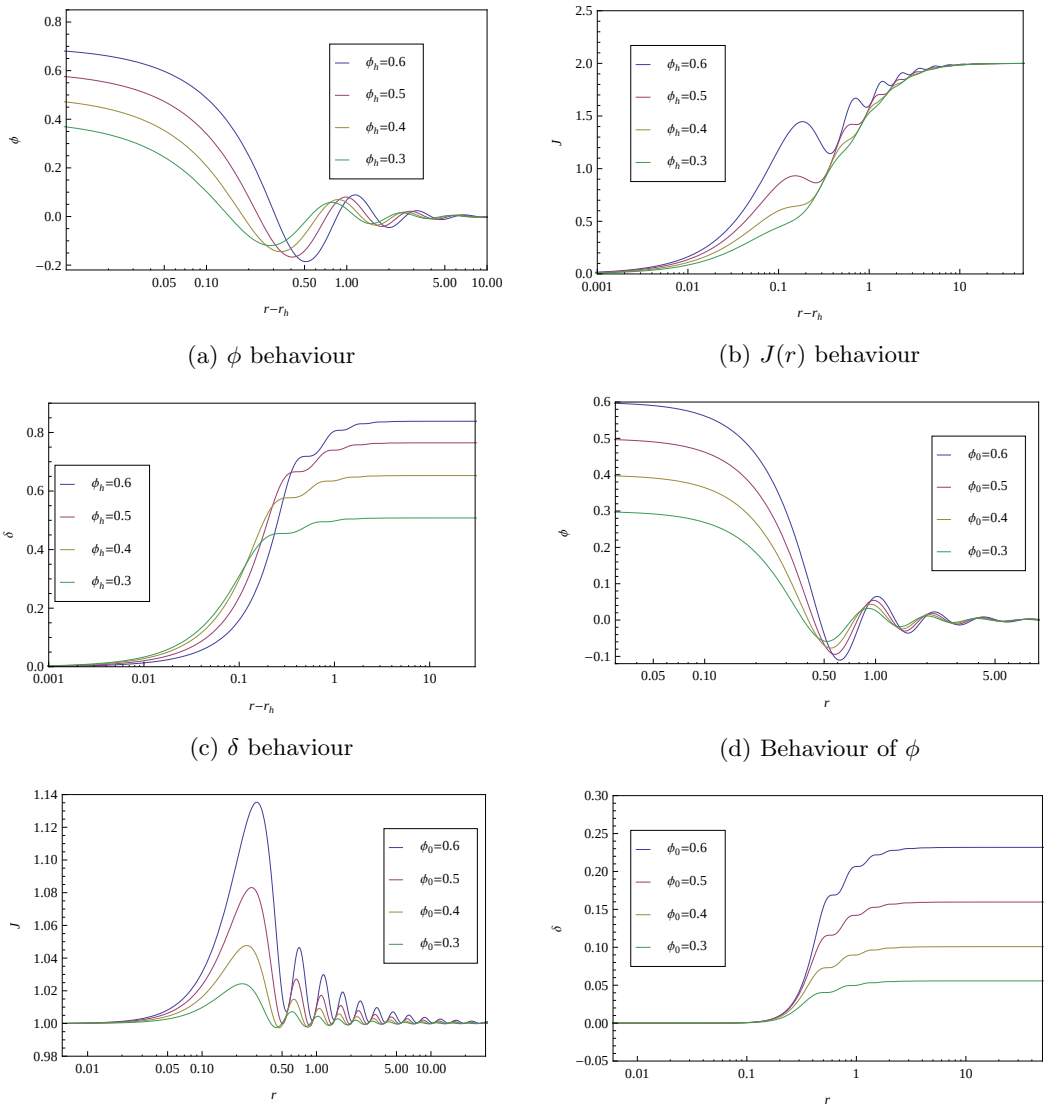

(a) ϕ behaviour

(b) $J(r)$ behaviour

(c) δ behaviour

(d) Behaviour of ϕ

(e) Behaviour of J

(f) Behaviour of δ

Figure 3.8: Case 4 (a,b,c) plots showing the effect on ϕ, J, δ of varying ϕ_h for five-dimensional black hole solutions with $\Delta_- = 3/2 - 10i$, $\Delta_+ = 3/2 + 10i$, $L = 1$ and $k = 1$, $\kappa = 1$, $r_h = 1$ with Higgs potential (d, e, f) plots showing the effect on ϕ, J, δ of varying ϕ_0 for four-dimensional soliton solutions with $\Delta_- = 3/2 - 10i$, $\Delta_+ = 3/2 + 10i$, $L = 1$ and $k = 1$, $\delta_0 = 0$ with TWI potential

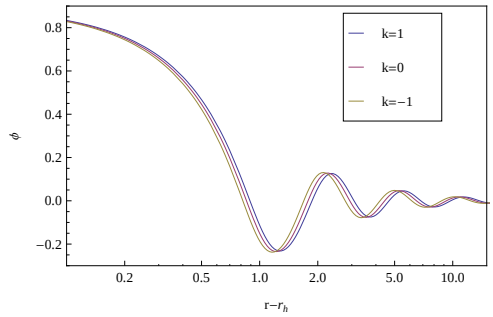

(a) ϕ when varying k

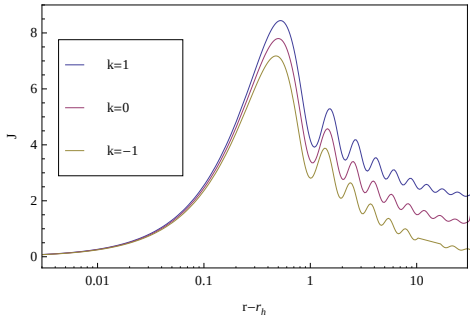

(b) $J(r)$ when varying k

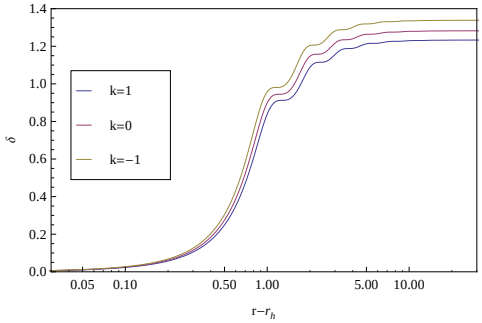

(c) δ when varying k

Figure 3.9: Case 4 (a) the effect on the scalar field ϕ of varying k is shown for four-dimensional black hole solutions with $\Delta_- = 3/2 - 10i$, $\Delta_+ = 3/2 + 10i$, $L = 1$ and $\phi_h = 9/10$ with Higgs potential (b) the effect on the the metric function J of varying k is shown for four-dimensional black hole solutions with $\Delta_- = 3/2-10i$, $\Delta_+ = 3/2+10i$, $L = 1$ and $\phi_h = 9/10$ with Higgs potential (c) the effect on the the metric function δ of varying k is shown for four-dimensional black hole solutions with $\Delta_- = 3/2 - 10i$, $\Delta_+ = 3/2 + 10i$, $L = 1$ and $\phi_h = 9/10$ with Higgs potential.

§ 3.6 Stability analysis

In this section we investigate the stability of the soliton and black hole solutions.

3.6.1 Perturbation Potential

We adopt the same approach as in [114, 129]. So far we have considered spatial dependance only for $\phi(r)$, $H(r)$ and $\delta(r)$. We now consider linear perturbations depending on r and t for these three functions as follows. We consider the perturbation Einstein field equations:

$$G_{\mu\nu} + \Lambda g_{\mu\nu} = \nabla_\mu \phi \nabla_\nu \phi - \frac{1}{2} g_{\mu\nu} (\nabla \phi)^2 - g_{\mu\nu} V(\phi) \tag{3.63}$$

and the scalar equation:

$$\nabla_\mu \nabla^\mu \phi - \frac{dV}{d\phi} = 0. \tag{3.64}$$

The perturbed functions are:

$$\begin{aligned} \phi &= \phi(r) + \delta\phi(t,r) \\ H &= H(r) + \delta H(t,r) \\ \delta &= \delta(r) + \delta\delta(t,r) \end{aligned} \tag{3.65}$$

where $\delta\phi(t,r)$, $\delta H(t,r)$ and $\delta\phi(t,r)$ are the time and space-dependent perturbations. We will outline the key steps of the analysis.

From the (tr) component of the Einstein equation (3.63) we obtain:

$$\begin{aligned} \dot{H} &= -\frac{-2rH\phi'\dot{\phi}}{D-2} \\ \Rightarrow \delta H &= -\frac{2rH\phi'}{D-2}\delta\phi + \mathcal{F}(r) \end{aligned} \tag{3.66}$$

where the prime is the derivative with respect to r and the dot is the derivative with respect to t and $\mathcal{F}$ is an arbitrary function depending on r only. For the function δ we consider the (tt) component and the (rr) component of the Einstein equation (3.63), by subtracting them we have:

$$\delta'(D-2) = r\phi'^2 - \frac{1}{H^2 e^{2\delta}}\dot{\phi}^2, \tag{3.67}$$

taking the linear perturbation of (3.67) we have:

$$\delta\delta' = \frac{2r\phi'}{D-2}\delta\phi'. \tag{3.68}$$

Now considering the linearised tt component of (3.63) and perturbing it we obtain:

$$\frac{\delta H}{2r^2}(D-2)(D-3) + \frac{(D-2)}{2r}\delta H' = -\frac{1}{2}\delta H\phi'^2 - H\phi'\delta\phi' - \frac{\partial V}{\partial\phi}\delta\phi. \tag{3.69}$$

Using the equation for δH in (3.66) and differentiating it, we obtain an expression for $\delta H'$. We use these new expressions for δH and $\delta H'$ in (3.69) and after some algebra using the equilibrium field equations we obtain a differential equation for the function $\mathcal{F}(r)$:

$$\mathcal{F}' + \left(\frac{D-3}{r} + \frac{r\phi'^2}{D-2}\right)\mathcal{F} = 0. \tag{3.70}$$

This is a first order differential equation so we can use an integrating factor to obtain:

$$\mathcal{F} = \mathcal{A} r^{-(D-3)} e^{-I_1} \tag{3.71}$$

where

$$I_1 = \int \frac{r\phi'^2}{D-2} dr \tag{3.72}$$

and $\mathcal{A}$ is a constant. At the origin $\mathcal{A} = 0$ if $\mathcal{F}$ is regular. Assuming that e^{-I_1} is regular and setting $\mathcal{F} = 0$ at the event horizon for example ensures that the only possibility is $\mathcal{F} \equiv 0$. So the metric perturbation in (3.66) is then:

$$\delta H = -\frac{2rH\phi'\delta\phi}{D-2}. \tag{3.73}$$

We need to find the scalar perturbation equation now by linearising the scalar field equation as follows:

$$\delta[\nabla_\mu \nabla^\mu \phi] - \frac{d^2V}{d\phi^2}\delta\phi = 0, \tag{3.74}$$

using (3.68) and (3.73) the perturbation equation is:

$$\begin{aligned} 0 &= -\frac{e^{-2\delta}}{H}\ddot{\delta\phi} + H\delta\phi'' + \left[H' + H\delta' + (D-2)\frac{H}{r}\right]\delta\phi' \\ &\quad + \left[\frac{2r\phi'}{D-2}\left[2\frac{\partial V}{\partial\phi} - H'\phi' - H\delta'\phi' - (D-3)\frac{H}{r}\phi'\right] - \frac{\partial^2 V}{\partial\phi^2}\right]\delta\phi. \end{aligned} \tag{3.75}$$

We now introduce the tortoise coordinate r_* defined by:

$$\frac{dr_*}{dr} = \frac{1}{He^\delta} \tag{3.76}$$

so we have:

$$\delta\phi' = \frac{1}{He^\delta}\frac{d}{dr_*}(\delta\phi). \tag{3.77}$$

For black holes, $r_* \in (-\infty, 0]$, more specifically $r_* \to -\infty$ as $r \to r_h$ and $r_* \to 0$ as $r \to \infty$. For solitons $r_* \in [0, r_c]$, more specifically $r_* \to 0$ as $r \to 0$ and $r_* \to r_c = constant$ as $r \to \infty$, by choice of constant of integration [139].

After some substitutions the perturbation equation in terms of the tortoise coordinate becomes:

$$\begin{aligned} 0 &= -\ddot{\delta\phi} + \frac{d^2}{dr_*^2}(\delta\phi) + \frac{He^\delta}{r}(D-2)\frac{d}{dr_*}(\delta\phi) \\ &\quad + He^{2\delta}\left[\frac{2r\phi'}{D-2}\left[2\frac{dV}{d\phi} - H'\phi' - H\delta'\phi' - (D-3)\frac{H}{r}\phi'\right] - \frac{\partial^2 V}{\partial\phi^2}\right]\delta\phi. \end{aligned} \tag{3.78}$$

Letting $\delta\phi = r^n\Psi$ we have $\delta\ddot{\phi} = r^n\ddot{\Psi}$ and substituting it in (3.78) we find that setting

$$n = -\frac{(D-2)}{2} \tag{3.79}$$

eliminates the first order derivative terms. So we write the scalar field equation (3.78) in terms of Ψ:

$$-\ddot{\Psi} + \frac{d^2}{dr_*^2}\Psi + \frac{He^{2\delta}}{r^2}\mathcal{C}\Psi = 0. \tag{3.80}$$

After simplifications using the equilibrium field equations we obtain the following expression for $\mathcal{C}$:

$$\begin{aligned}\mathcal{C} &= H - (D-2)(D-3)\frac{k}{2} + (V+\Lambda)r^2 - \frac{\partial^2 V}{\partial\phi^2}r^2 \\ &\quad -2r^3\phi\frac{\partial V}{\partial\phi} + (D-2)(D-3)r^2\frac{k}{2}\phi'^2 - (V+\Lambda)r^4\phi'^2.\end{aligned} \tag{3.81}$$

Following the approach in [114, 139] we consider time-periodic perturbations $\Psi(t,r) = e^{i\sigma t}\Psi(r)$. We define the perturbation potential to be:

$$\mathcal{U} = -He^{2\delta}r^{-2}\mathcal{C} \tag{3.82}$$

and (3.80) takes the standard Schrödinger equation:

$$-\frac{d^2\Psi}{dr_*{}^2} + \mathcal{U}\Psi = \sigma^2\Psi. \tag{3.83}$$

If the eigenvalue $\sigma^2 > 0$ then σ is real, $U > 0$ because the operator on the LHS is positive and the perturbations are stable. If $\sigma^2 < 0$ this is equivalent to negative energy eigenvalues, σ is imaginary and the perturbations are unstable. If the potential perturbation $\mathcal{U}$ is positive everywhere the solution is stable. if it is not positive everywhere then further analysis is needed. We are interested in the behaviour of the perturbation potential $\mathcal{U}$ (3.82) at the usual three regions of spacetime:‘

- **at** $r = 0$

The initial conditions for the metric functions are (3.13). In this case the perturbation potential (3.82) reduces to:

$$\mathcal{U} = \frac{H_0e^{2\delta_0}}{r^2}\left[\frac{(D-2)(D-3)}{2}k - 1\right] + O(1). \tag{3.84}$$

Since we only consider $k = 1$ at the origin, and $H_0 = 1$ we see that the perturbation

potential diverges to ∞ at the origin except when $D = 4$. For the Higgs potential we can see this by comparing Figs. 3.10a and 3.10b. For the TWI the behaviour is the same as for Higgs at the origin, this can be seen by comparing Figs. 3.10c and 3.10d.

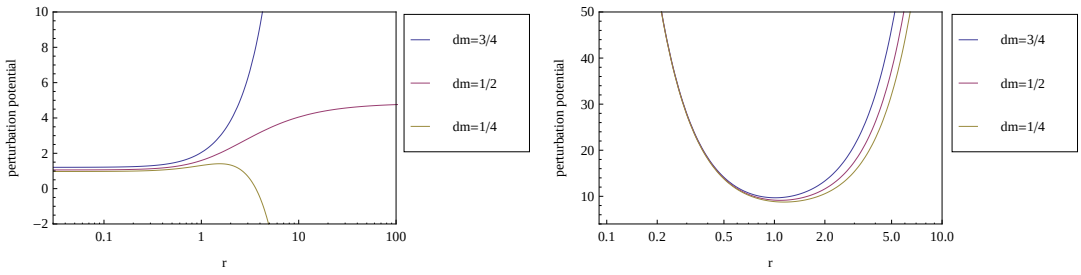

(a) Higgs: potential perturbation in $D = 4$

(b) Higgs: potential perturbation in $D = 5$

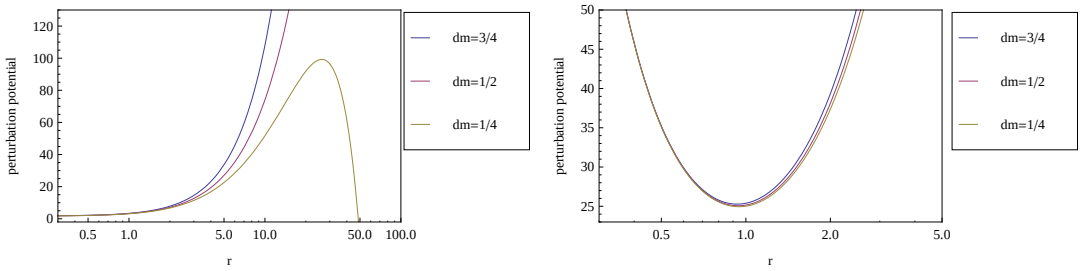

(c) TWI: potential perturbation in $D = 4$

(d) TWI: potential perturbation in $D = 6$

Figure 3.10: (a) Perturbation potential $\mathcal{U}$ (3.82) plotted as a function of r for some four-dimensional solitons with $L = 1$, $\phi_0 = 0.4$, for three different values of dm with the Higgs potential. In this case the potential is finite at the origin. The behaviour of the potential at infinity is in accordance with (3.87). (b) Perturbation potential $\mathcal{U}$ (3.82) plotted as a function of r for some five-dimensional soliton with $L = 1$, $\phi_0 = 0.4$, and three different values of dm with the Higgs potential. In this case the potential is divergent at the origin as expected from equation (3.84). The behaviour of the potential at infinity is in accordance with (3.87). (c) Perturbation potential $\mathcal{U}$ (3.82) plotted as a function of r for some four-dimensional solitons with $L = 1$, $\phi_0 = 0.4$, for three different values of dm with the TWI potential. In this case the potential is finite at the origin. The behaviour of the potential at infinity is in accordance with (3.87). (d) Perturbation potential $\mathcal{U}$ (3.82) plotted as a function of r for some six-dimensional soliton with $L = 1$, $\phi_0 = 0.4$, and three different values of dm with the TWI potential. In this case the potential is divergent at the origin as expected from equation (3.84). The behaviour of the potential at infinity is in accordance with (3.87).

- **at** $r = r_h$

At the black hole event horizon all the metric functions are finite and we have $H(r_h) = 0$ so $\mathcal{U}$ (3.82) vanishes. The behaviour of the potential perturbation for Higgs potential

can be seen in Fig. 3.11a and Figs. 3.11b and for the TWI potentials in Figs. 3.11c and 3.11d.

- **at** $r \to \infty$

We study the asymptotics of (3.82), that is the behaviour of $\mathcal{U}$ as $r \to \infty$. For this we use the expansion for the potential (3.3) and substitute for $H(r)$ using (3.17). We also know that the leading behaviour of the scalar field at infinity is:

$$\phi = ar^{-\Delta_-} + ... \tag{3.85}$$

and

$$\phi' = -a\Delta_- r^{-\Delta_- - 1} + ... \tag{3.86}$$

By putting (3.85), (3.86) and (3.17) in (3.81) we find the leading order terms in $\mathcal{U}$ as $r \to \infty$:

$$\mathcal{U} = -\frac{He^{2\delta}}{r^2}\left[\left(\frac{1}{L^2} + \Lambda - m^2\right) r^2 + 6C_3 a r^{-\Delta_- + 2} + O(1)\right]. \tag{3.87}$$

Therefore the behaviour at infinity is different for each potential.

- **For the Higgs potential**

For this potential $C_3 = 0$. Therefore $\mathcal{U}$ has the general form:

$$\mathcal{U} = -\frac{He^{2\delta}}{r^2}\left[\left(\frac{1}{L^2} + \Lambda - m^2\right) r^2 + O(1)\right]. \tag{3.88}$$

When $m^2 = -2/L^2$ and $D = 4$ the first term in (3.88) vanishes and the potential (3.88) becomes

$$\mathcal{U} = -\frac{He^{2\delta}}{r^2}\left[-\frac{3a^2(1 + 8C_4)}{2L^2}\right] + O(r^{-1}) \tag{3.89}$$

where we write down the term of $O(1)$ explicitly. In this case $\mathcal{U}$ is positive and converges to a constant as $r \to \infty$. This can be seen in Fig. 3.10a and Fig. 3.11a where we see that when $dmL = 1/2$ the potential perturbation $\mathcal{U}$ converges. When $dmL \neq 1/2$ in $D = 4$, we see that the first term in (3.87)

$$\frac{1}{L^2} + \Lambda - m^2 \tag{3.90}$$

is negative when $dmL > 1/2$ and positive when $dmL < 1/2$. Therefore $\mathcal{U}$ diverges to $-\infty$ for all $dm < 1/2$ and diverges to $+\infty$ for all $dm > 1/2$ in $D = 4$. This behaviour can be seen in Figs. 3.10a and 3.11a. For higher dimensions (3.90) is always negative therefore the potential perturbation $\mathcal{U}$ always diverges to $+\infty$ as seen in Figs. 3.10b and 3.11b.

- **For the TWI potential**

For TWI potential the leading order term in (3.87) also vanishes when $dmL = 1/2$ in $D = 4$, but in this case we have $C_3 \neq 0$. For this potential $C_3 > 0$ so the term $6C_3 a r^{-\Delta_- + 2}$ in (3.87) is always positive. In this case $\mathcal{U} < 0$ and it diverges to $-\infty$ as $r \to \infty$. For $dm \neq 1/2$ in $D = 4$ the first term (3.90) is the same as for the Higgs potential case, therefore the same analysis applies. For the TWI potential see Figs. 3.10c and 3.11c. We notice that the potential diverges slower when $dmL = 1/2$ in $D = 4$. For higher dimensions the perturbation potential $\mathcal{U}$ is always positive as can be seen in Figs. 3.10d and 3.11d.

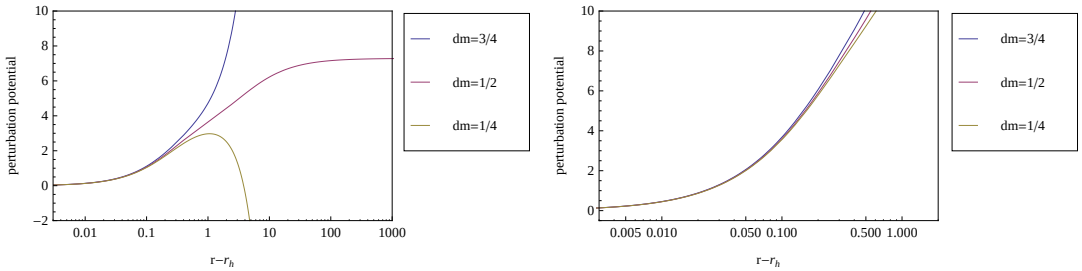

(a) Higgs: potential perturbation in $D = 4$

(b) Higgs: potential perturbation in $D = 5$

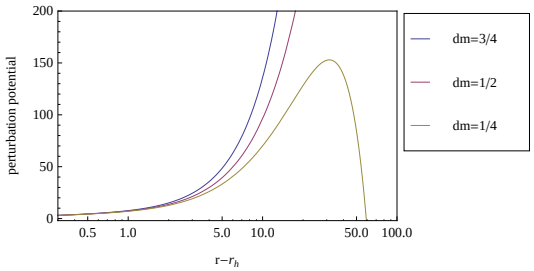

(c) TWI: potential perturbation in $D = 4$

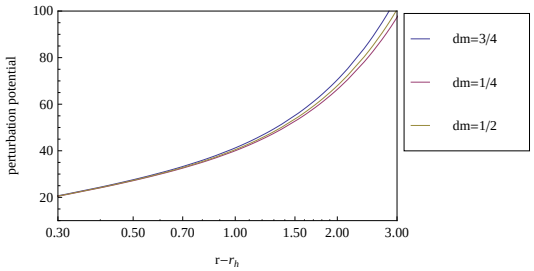

(d) TWI: potential perturbation in $D = 6$

Figure 3.11: (a) Perturbation potential $\mathcal{U}$ (3.82) plotted as a function of r for some four-dimensional black holes with $L = 1$, $\phi_h = 0.4$, for three different values of dm with the Higgs potential. $\mathcal{U} \to 0$ as $r \to r_h$. The behaviour of the potential at infinity is in accordance with (3.87). (b) Perturbation potential $\mathcal{U}$ (3.82) plotted as a function of r for some five-dimensional black holes with $L = 1$, $\phi_h = 0.4$, for three different values of dm with the Higgs potential. $\mathcal{U} \to 0$ as $r \to r_h$. The behaviour of the potential at infinity is in accordance with (3.87). (c) Perturbation potential $\mathcal{U}$ (3.82) plotted as a function of r for some four-dimensional black hole with $L = 1$, $\phi_h = 0.4$, for three different values of dm with the Higgs potential. The behaviour of the potential at infinity is in accordance with (3.87). (d) Perturbation potential $\mathcal{U}$ (3.82) plotted as a function of r for some six-dimensional black holes with $L = 1$, $\phi_h = 0.4$, for three different values of dm with the TWI potential. The behaviour of the potential at infinity is in accordance with (3.87).

3.6.2 Zero mode

If $\mathcal{U} > 0$ everywhere then (3.83) implies that $\sigma^2 > 0$ and the solutions are stable. This is the case in Figs. 3.10b, 3.10d, 3.11b and 3.11d. If (3.83) is not positive everywhere as can be seen in Figs. 3.10a, 3.10c , 3.11a and 3.11c then more investigation is needed. The figures show that $U > 0$ everywhere unless $U \to -\infty$ as $r \to \infty$. In these cases we have to consider the zero mode perturbation Ψ_0 which is the solution of the perturbation equation (3.83) with $\sigma = 0$. The zero mode tells us about the stability of the solutions. If the zero mode has no zeros then the solutions are stable. The more zeros the zero mode function has the more unstable the solution is [114, 139].The perturbation potential is negative when:

$$\frac{1}{L^2} + \Lambda - m^2 > 0$$

which corresponds to:

$$m^2 > -\frac{D(D-3)}{2L^2}.$$

For these values of m^2 the zero mode has to be investigated. We will also do it for the rest of the values of m^2 for a complete analysis. Before we study the behaviour of the zero mode in the usual three regions of spacetime, we write (3.83) in a simpler form. When $\sigma = 0$ we have:

$$-\frac{d^2}{dr_*^2}\Psi_0 - \frac{He^{2\delta}}{r^2}\mathcal{C}\Psi_0 = 0. \tag{3.91}$$

We also have

$$\frac{d}{dr_*}\Psi_0 = \frac{dr}{dr_*}\frac{d}{dr}\Psi_0 = \Psi_0' He^{\delta} \tag{3.92}$$

where the prime is the derivative with respect to the radial coordinate r. Therefore we can write:

$$\frac{d^2}{dr_*^2}\Psi_0 = (\Psi_0' He^{\delta})' He^{\delta} \tag{3.93}$$

so (3.91) becomes:

$$-He^{\delta}\Psi_0'' - (He^{\delta})'\Psi_0' - \frac{e^{\delta}}{r^2}\mathcal{C}\Psi_0 = 0. \tag{3.94}$$

Let us investigate the three regions of spacetime:

- **At the origin**

Near $r = 0$ we can expand Ψ_0 as:

$$\Psi_0 = \Psi_1 r^{\alpha} + \Psi_2 r^{\alpha+1} + \Psi_3 r^{\alpha+2} + ... \tag{3.95}$$

where $\alpha \geqslant 0$. Using the expansions of the function $H(r)$ and $\delta(r)$ in (3.13) we can substitute in (3.94) and obtain the following quadratic equation for α:

$$\alpha^2 - \alpha + \mathcal{C}_0 = 0 \tag{3.96}$$

where $\mathcal{C}_0 = \mathcal{C}(0)$. From (3.84) we have

$$\mathcal{C}_0 = 1 - \frac{(D-2)(D-3)}{2} \tag{3.97}$$

at the origin. Solving (3.96) for α we have:

$$\alpha = \frac{1}{2} \pm \frac{1}{2}\sqrt{2D^2 - 10D + 9}. \tag{3.98}$$

This agrees with the expression found in [85]. In [85], they consider non-minimal coupling and zero potential therefore neither the coupling not the scalar field potential affect (3.98). We want Ψ_0 to be regular at the origin so we choose the positive root when we produce the plots.

- **At the horizon**

At this point of spacetime we require that:

$$\Psi = O(r - r_h) \tag{3.99}$$

as $r \to \infty$. We can see in Figs. 3.12c, 3.12d, 3.13c, 3.13d that the Ψ_0 is regular at the horizon.

- **At infinity**

As $r \to \infty$ we have $\Psi_0 = O(r^{-\beta})$. To find the expression for β we have to consider the leading behaviour of (3.94) at infinity. Substituting (3.17) in (3.94) and considering the leading order terms we have the following quadratic equation to solve for β:

$$-\beta^2 + \beta - (1 + L^2\Lambda + L^2m^2) = 0 \tag{3.100}$$

and the solutions are:

$$\beta = \frac{1}{2} \pm \frac{1}{2}\sqrt{1 + 2D(D-3) + 4m^2L^2}. \tag{3.101}$$

The behaviour of Ψ_0 is subtle. The constant β is real if and only if:

$$\begin{aligned} &1 + 2D(D-3) + 4m^2L^2 > 0 \\ &\Rightarrow m^2 > \frac{-1 - 2D(D-3)}{4L^2}. \end{aligned} \tag{3.102}$$

In this case the dominant behaviour of Ψ_0 will be from taking the negative sign in (3.101). We therefore have:

$$\beta = \frac{1}{2} - \frac{1}{2}\sqrt{1 + 2D(D-3) + 4m^2L^2}. \tag{3.103}$$

Now β is positive if and only if:

$$m^2 < -\frac{D(D-3)}{2L^2}, \tag{3.104}$$

in this case $\Psi_0 \to 0$ as $r \to \infty$. When

$$m^2 > -\frac{D(D-3)}{2L^2} \tag{3.105}$$

the zero mode perturbation Ψ_0 diverges as $r \to \infty$. So when β is real, $\Psi_0 \to 0$ as $r \to \infty$ when

$$\frac{-1 - 2D(D-3)}{4L^2} < m^2 < -\frac{D(D-3)}{2L^2}. \tag{3.106}$$

This can be seen for $D = 4$ in Fig. 3.12a where the zero mode goes to zero as $r \to \infty$ for $dmL = 1/2$. This corresponds to subcase $2a$ in the next chapter. We find that the zero mode has no zeros and so we deduce that there can be no negative eigenvalues $\sigma^2 < 0$ of the perturbation equation (3.83), in other words, the solutions are stable. This can be seen in Figs. 3.12a-3.12d for Higgs potential and in Figs. 3.13a-3.13d for TWI potential.

The constant β is complex when:

$$m^2 < \frac{-1 - 2D(D-3)}{4L^2}. \tag{3.107}$$

We notice that in $D = 4$ this is the same condition on m^2 as for case 4 namely:

$$m^2 < -\frac{(D-1)^2}{4L^2}. \tag{3.108}$$

We see that if $D = 4$ (3.107) and (3.108) are the same so these will give oscillatory solutions illustrated in Fig. 3.12a. However in higher dimensions we see that (3.107) is more negative than (3.108) so for case 4 as we increase the number of dimensions we

will have fewer zeros of the zero modes. This explains why we see damped oscillations in Ψ_0 as we increase the dimensions. This can be seen by comparing Figs. 3.12c and 3.12d for Higgs potential, and comparing Fig. 3.13c and Fig. 3.13d for TWI potential. There is at least one negative eigenvalue $\sigma^2 < 0$ of the perturbation equation (3.83) and the solutions are unstable. This behaviour can be seen for soliton and black hole solutions for Higgs in Figs. 3.12a-3.12d and for TWI potential in Figs. 3.13a-3.13d.

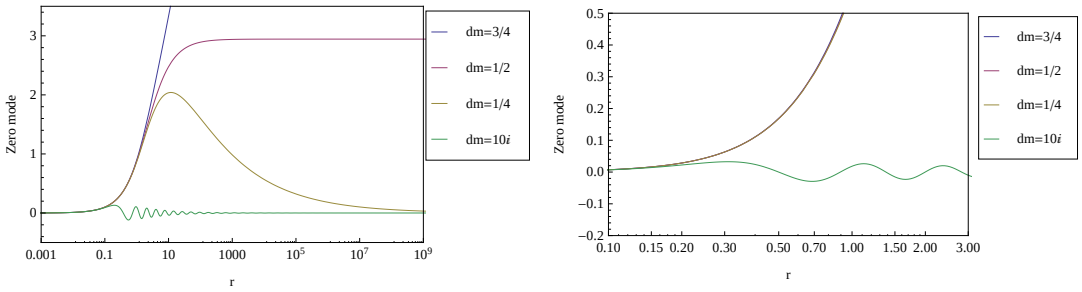

(a) Higgs: Zero mode Ψ_0 in $D = 4$

(b) Higgs: Zero mode Ψ_0 in $D = 5$

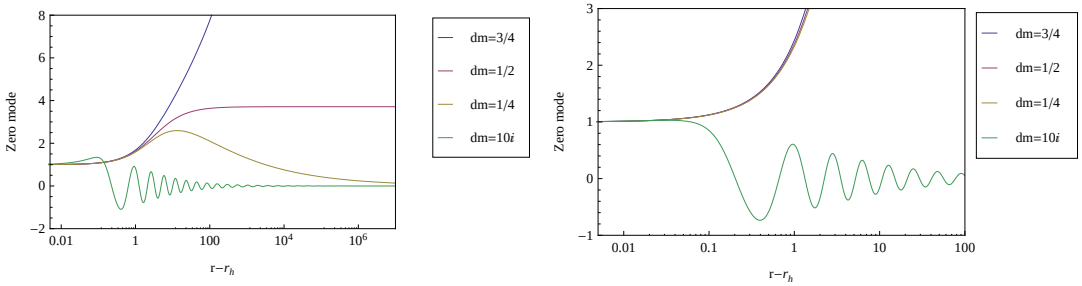

(c) Higgs: Zero mode Ψ_0 in $D = 4$

(d) Higgs: Zero mode Ψ_0 in $D = 5$

Figure 3.12: (a) Zero mode Ψ_0 plotted as a function of r for some four-dimensional soliton solution with $L = 1$, $\phi_0 = 0.4$ with four different values for dm with Higgs potential. (b) Zero mode Ψ_0 plotted as a function of r for some five-dimensional soliton solution with $L = 1$, $\phi_0 = 0.4$ and $dm = 3/4$. with Higgs potential. (c) Zero mode Ψ_0 plotted as a function of r for some four-dimensional black hole solutions with $L = 1$, $\phi_0 = 0.4$ with four different values for dm with Higgs potential. (d) Zero mode Ψ_0 plotted as a function of r for some five-dimensional black hole solution with $L = 1$, $\phi_0 = 0.4$ and $dm = 3/4$. with Higgs potential.

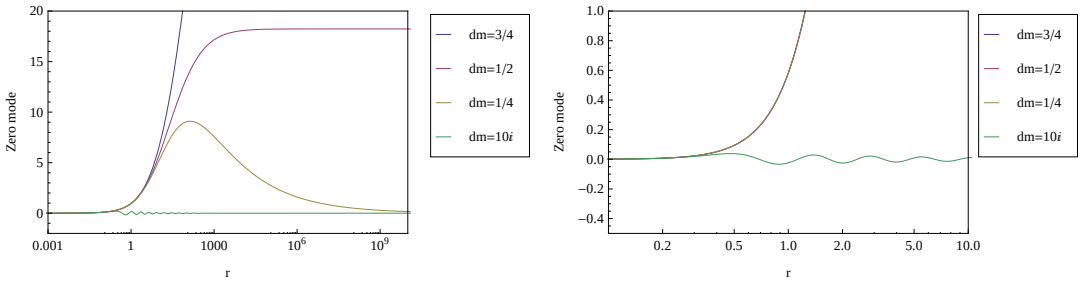

(a) TWI: Zero mode Ψ_0 in $D = 4$

(b) TWI: Zero mode Ψ_0 in $D = 6$

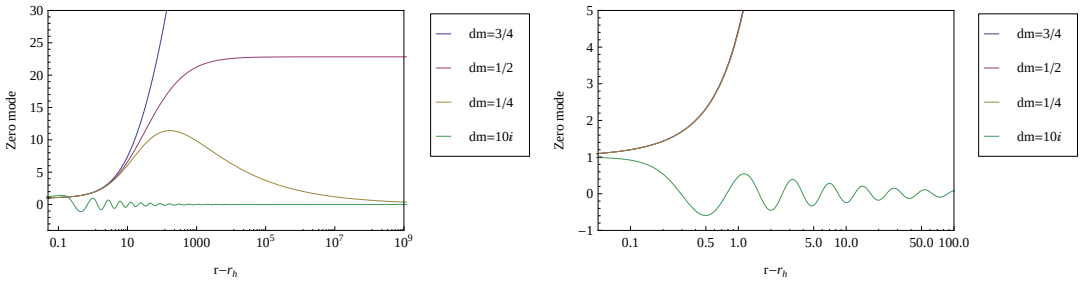

(c) TWI: Zero mode Ψ_0 in $D = 4$

(d) TWI: Zero mode Ψ_0 in $D = 6$

Figure 3.13: (a) Zero mode Ψ_0 plotted as a function of r for some four-dimensional soliton solution with $L = 1$, $\phi_0 = 0.4$ with four different values of dm with TWI potential. (b) Zero mode Ψ_0 plotted as a function of r for some six-dimensional soliton solutions with $L = 1$, $\phi_0 = 0.4$ for four different values of dm with TWI potential. (c) Zero mode Ψ_0 plotted as a function of r for some four-dimensional black hole solutions with $L = 1$, $\phi_0 = 0.4$ with four different values of dm with TWI potential. (d) Zero mode Ψ_0 plotted as a function of r for some six-dimensional black hole solutions with $L = 1$, $\phi_0 = 0.4$ for four different values of dm with TWI potential.

§ 3.7 Results tables

dm	Ψ_0	stability
$dm > \frac{1}{4}$ and $dm \neq \frac{1}{2}$	Ψ_0 divergent, no zeros	Stable
$dm = \frac{1}{2}$	$\Psi_0 \to$ constant, no zeros	Stable
$0 < dm < \frac{1}{4}$	$\Psi_0 \to 0$, no zeros	Stable
Imaginary	Ψ_0 oscillates	Unstable

Table 3.2: Zero mode summary table $D = 4$ for Higgs and TWI potential

dm	Ψ_0	stability
$dm > \frac{1}{4}$ and $dm \neq \frac{1}{2}$	Ψ_0 divergent, no zeros	Stable
$dm = \frac{1}{2}$	Ψ_0 divergent, no zeros	Stable
$0 < dm < \frac{1}{4}$	Ψ_0 divergent, no zeros	Stable
Imaginary	Ψ_0 oscillates	Unstable

Table 3.3: Zero mode summary table $D > 4$ for Higgs and TWI potential

The stability test can be related to the four cases of the scalar field. Cases 2 and 3 are stable, case 4 is unstable since it corresponds to the oscillatory case. Case 1 is different from the rest of the cases since the scalar field does not vanish at infinity therefore the stability analysis presented above is not straightforward to apply. The stability will depend on the behaviour of ϕ, J and δ at equilibrium.

§ 3.8 Summary

In this chapter we have seen that when we consider a scalar field with self interaction potential minimally coupled to gravity, four cases arise at infinity. We have proven some no-hair theorems assuming convex potential. However by considering nonconvex potentials such as the Higgs potential and the TWI potential we have found soliton and black hole solutions. In order to test the stability of the solutions we considered a perturbation potential and we investigated the zero mode. Cases 2 and 3 are stable. Case 4 is unstable, when case 1 shows oscillations we expect it to be unstable.

Chapter 4

Detailed asymptotics at infinity

In this chapter we are concerned with investigating the details of the asymptotic form of the scalar field as $r \to \infty$ by considering the subleading terms. Different subcases arise depending on the mass range of the scalar field. Cases 2 and 3 in Table 3.1 subdivide into several subcases. We will see that the presence of the scalar field has a back reaction on the metric and we will present expressions for the metric perturbation δg_{rr} that we now call h_{rr}. We present the method we used to find the coefficients in the expansion of the scalar field and the expansion of h_{rr}. We start by giving some motivation to explain why we need subleading terms before moving onto studying the detailed asymptotics at infinity and obtaining expressions for the coefficients.

§ 4.1 Motivation

When we include a scalar field in our model the metric asymptotically approaches adS spacetime at infinity slower than in the absence of matter [73]. The mass Q_0 as defined by Henneaux and Teilteboim in (2.62) is no longer finite. The total mass of the spacetime has to be redefined to account for the slow fall off of the scalar field at infinity. For this we need to obtain the subleading terms in the expansion of the scalar field. In the previous chapter we have seen that the scalar field can take four different forms at infinity depending on conditions on its mass and the two roots Δ_- and Δ_+ (3.26) (Table 3.1). When we calculate the mass of the Einstein-Gravity system with a self interaction potential the leading behaviour of the scalar field is not enough. We have to consider subleading terms in the expansion of the scalar field.

In [73] Henneaux *et al.* consider cases 2 and 3. In this chapter we review their results but we use our method based on the field equations to find important coefficients of

the theory. For these two cases the mass of the scalar field is considered to be above the Breitenlohner-Freedman bound [31, 106]:

$$m^2 = m_*^2 + dm^2, \tag{4.1}$$

where

$$m_*^2 = -\frac{(D-1)^2}{4L^2}. \tag{4.2}$$

is the Breitenlohner-Freedman bound [31, 106]. This bound presents interesting physics properties as it is a condition for stability. It is wieldy considered in literature [17, 59, 63, 71, 78, 79, 84, 103, 111, 125].

As the mass m^2 increases the scalar field acquires more subleading terms. We need to keep the a branch and the b branch in the scalar field expression because they contain Δ_- and Δ_+ respectively. The field equations are a set of nonlinear equations, therefore the scalar field will be of the form:

$$\phi(r) = c_1 r^{-\Delta_-} + c_2 r^{-2\Delta_-} + c_3 r^{-3\Delta_-} + ... + c_4 r^{-\Delta_+} + ... \tag{4.3}$$

where $c_1, c_2, ...$ are constants. As we can see in (4.3) we consider terms with powers of r that are multiples of Δ_- such as $r^{-2\Delta_-}$, $r^{-3\Delta_-}$ etc. Since $\Delta_- < \Delta_+$ we have to find all the terms with powers $n\Delta_-$, with $n \in \mathbb{N}$, which are larger than $r^{-\Delta_+}$. These terms are essential to obtain a finite expression for the mass of the spacetime. All the other terms can be ignored.

As a consequence of these extra terms in the scalar field the metric perturbation h_{rr} (2.61) seen in chapter 2 is also going to acquire extra terms due to the scalar field back reaction. We have seen in chapter 2 that in order for the mass to be finite in an asymptotically adS spacetime we need h_{rr} to be $O(r^{-D-1})$ (2.87). When we add a scalar field, the metric perturbation has the form [73]:

$$h_{rr} = y(r) + z(r) \tag{4.4}$$

where

$$z(r) = \frac{f_{rr}}{r^{D+1}} + O\left(r^{-(D+2)}\right). \tag{4.5}$$

In (4.4), the function $y(r)$ arises from the back reaction of the scalar field, f_{rr} is a constant. In the absence of the scalar field, $y(r) = 0$ and we recover the result from asymptotically adS spacetime in chapter 2. We will see that in our calculations in the sections below we need to make sure we always have a f_{rr} term in our expression of the metric perturbation and we need to include all the terms that are larger than

$O(r^{-D-1})$.

We start with case 1 in Table 3.1 which is the simplest case and does not have subcases. For case 2 we have subcases in four dimensions and subcases for higher dimensions. Case 3 groups all the subcases where the logarithmic branch is switched on. Finally we consider case 4 from table 3.1 which is the oscillatory case.

§ 4.2 Details

4.2.1 Case 1

For this case we see in Table 3.1 that $m^2 > 0$ for all D. This case is the simplest case treated. Both roots are real but Δ_- is negative, only the b branch (i.e. the branch containing Δ_+) survives as we have seen in our analysis in chapter 3:

$$\phi(r) = \frac{b}{r^{\Delta_+}} + ... \tag{4.6}$$

and the metric perturbation is:

$$h_{rr} = \frac{f_{rr}}{r^5} + ... \tag{4.7}$$

We see that there is no contribution coming from the scalar field in the expression for h_{rr}. This case does not arise in practice unless there is a fine-tuning to switch off the a branch by setting $a = 0$.

4.2.2 Case 2

We start with the cases for four dimensions, there are four subcases which we will present separately:

Subcase $2a$**:** $0 < dm^2 < \frac{1}{4L^2}$ **in** $D = 4$

For this case $3/2 < \Delta_+ < 2$, and $1 < \Delta_- < 3/2$. The only term that dominates over $r^{-\Delta_+}$ is $r^{-\Delta_-}$ so the expression for the scalar field is:

$$\phi(r) = \frac{a}{r^{\Delta_-}} + \frac{b}{r^{\Delta_+}} + ... \tag{4.8}$$

and the metric perturbation acquires an extra term due to the scalar field back reaction, having the form:

$$h_{rr} = \frac{\kappa L^2}{r^2}(\alpha_1 a^2 r^{-2\Delta_-}) + \frac{f_{rr}}{r^5} + ... \tag{4.9}$$

where α_1 is a coefficient that we will determine in section 4.4.

Subcase 2*b*: $\frac{1}{4L^2} < dm^2 < \frac{9}{16L^2}$ in $D = 4$

In this subcase $2 < \Delta_+ < 9/4$ and $3/4 < \Delta_- < 1$ and the scalar field picks up a term of order $r^{2\Delta_-}$:

$$\phi = ar^{-\Delta_-} + \beta_1 a^2 r^{-2\Delta_-} + br^{-\Delta_+} + ... \tag{4.10}$$

the term of order $r^{-3\Delta_-}$ is smaller than $br^{-\Delta_+}$ so it can be neglected. The metric perturbation is:

$$h_{rr} = \frac{\kappa L^2}{r^2}(\alpha_1 a^2 r^{-2\Delta_-} + \alpha_2 a^3 r^{-3\Delta_-}) + \frac{f_{rr}}{r^5} + ... \tag{4.11}$$

The coefficients β_1, α_1 and α_2 are determined in section 4.4.

Subcase 2*c*: $\frac{9}{16L^2} < dm^2 < \frac{81}{100L^2}$ in $D = 4$

For this range of dm^2 we have $9/4 < \Delta_+ < 12/5$ and $3/5 < \Delta_- < 3/4$. The scalar field picks up yet another term of order $r^{-3\Delta_-}$ and we have:

$$\phi = ar^{-\Delta_-} + \beta_1 a^2 r^{-2\Delta_-} + \beta_2 a^3 r^{-3\Delta_-} + br^{-\Delta_+} + ... \tag{4.12}$$

The next term with the smaller root in it is of order $r^{-4\Delta_-}$ but is smaller than $br^{-\Delta_+}$ so it can be neglected. The metric perturbation has the form:

$$h_{rr} = \frac{\kappa L^2}{r^2}(\alpha_1 a^2 r^{-2\Delta_-} + \alpha_2 a^3 r^{-3\Delta_-} + \alpha_3 a^4 r^{-4\Delta_-}) + \frac{f_{rr}}{r^5} + ... \tag{4.13}$$

where we have three terms coming from the scalar field back reaction, the coefficients $\beta_1, \beta_2, \alpha_1, \alpha_2, \alpha_3$ are determined in section 4.4.

Subcase 2*d*: $\frac{81}{100L^2} < dm^2 < \frac{1}{L^2}$ in $D = 4$

This is the most complicated case, for this case the ranges for the roots are $12/5 < \Delta_+ < 5/2$ and $1/2 < \Delta_- < 5/2$. The scalar field has the form:

$$\phi = ar^{-\Delta_-} + \beta_1 a^2 r^{-2\Delta_-} + \beta_2 a^3 r^{-3\Delta_-} + \beta_3 a^4 r^{-4\Delta_-} + br^{-\Delta_+} + ... \tag{4.14}$$

The term $r^{-5\Delta_-}$ is subleading in this case because it is smaller than $br^{-\Delta_+}$ and does not need to be included. The metric perturbation is:

$$h_{rr} = \frac{\kappa L^2}{r^2}(\alpha_1 a^2 r^{-2\Delta_-} + \alpha_2 a^3 r^{-3\Delta_-} + \alpha_3 a^4 r^{-4\Delta_-} + \alpha_4 a^5 r^{-5\Delta_-}) + \frac{f_{rr}}{r^5} + ... \quad (4.15)$$

where we have included the first power of r which has f_{rr} as a coefficient. It is obvious that terms with $O(r^{-6})$ are subleading.

Subcases $2e$ for $D = 5$ and $2f$ for $D = 6$: $0 < dm^2 < \frac{(D-1)^2}{36L^2}$

For subcase $2e$ we have $2 < \Delta_+ < 7/3$ and $5/3 < \Delta_- < 2$. For subcase $2f$ we have $5/2 < \Delta_+ < 10/3$ and $5/3 < \Delta_- < 5/2$. For these two subcases the scalar field has the form:

$$\phi = ar^{-\Delta_-} + br^{-\Delta_+}. \quad (4.16)$$

We do not need to include the next power in Δ_- as it is smaller than $br^{-\Delta_+}$. The metric perturbation is:

$$h_{rr} = \frac{\kappa L^2}{r^2}(\alpha_1 a^2 r^{-2\Delta_-}) + \frac{f_{rr}}{r^{D+1}} + ... \quad (4.17)$$

where α_1 is determined on section 4.4. This is the only case that arises in $D \geqslant 7$. This is why we consider only $D = 4, 5, 6$ as these dimensions cover all the interesting cases.

Subcases $2g$ in $5D$, $2h$ in $D = 6$: $\frac{(D-1)^2}{36L^2} < dm^2 < \frac{1}{L^2}$

For subcase $2g$ we have $8/3 < \Delta_+ < 3$ and $1 < \Delta_- < 4/3$. For subcase $2h$ the ranges of the roots are $10/3 < \Delta_+ < 7/2$ and $3/2 < \Delta_- < 5/3$ for $2f$. The expression for the scalar field is:

$$\phi = ar^{-\Delta_-} + \beta_1 a^2 r^{-2\Delta_-} + br^{-\Delta_+} + ... \quad (4.18)$$

as the term of order $r^{-2\Delta_-}$ is smaller than $br^{-\Delta_+}$ and the metric perturbation is:

$$h_{rr} = \frac{\kappa L^2}{r^2}(\alpha_1 a^2 r^{-2\Delta_-} + \alpha_2 a^3 r^{-3\Delta}) + \frac{f_{rr}}{r^{D+1}} + ... \quad (4.19)$$

where we have included all the terms that are bigger than $O(r^{-D-1})$ coming from the scalar field back reaction.

We see that cases 2 presented in Table 3.1 subdivides into subcases. The scalar field and the metric perturbation acquire more terms as the mass of the scalar field increases.

4.2.3 Case 3

Let us now consider case 3 from Table 3.1 when the scalar field acquires a logarithmic branch.

Subcases $3a$ for $D = 4$, $3b$ for $D = 5$ and $3c$ for $D = 6$: $dm^2 = \frac{(D-1)^2}{36L^2}$

In this case we have $\Delta_+ = 2\Delta_- = 2(D-1)/3$ the scalar field picks up a logarithmic branch of order $r^{-2\Delta_-}$. The expansion of the scalar field is:

$$\phi(r) = ar^{-\Delta_-} + (D - 1 - 3\Delta_-)\beta_1 a^2 \log(r) r^{-\Delta_+} + br^{-\Delta_+} + ... \tag{4.20}$$

where the term of order $r^{-3\Delta_-}$ is not contributing since we have $\Delta_+ = 2\Delta_-$. The metric perturbation is:

$$h_{rr} = \frac{\kappa L^2}{r^2}\left[\alpha_1 a^2 r^{-2\Delta_-} + (-D + 1 + 3\Delta_-)\alpha_2 \log(r) a^3 r^{-3\Delta_-}\right] + \frac{f_{rr}}{r^{D+1}} + ... \tag{4.21}$$

These expansions are valid for 4, 5 and 6 dimensions.

Subcase $3d$: $dm^2 = \frac{9}{16L^2}$ for $D = 4$

In this case the roots are $\Delta_+ = 3\Delta_- = 9/4$. The scalar field expansion picks up terms of order $r^{-3\Delta_-}$:

$$\phi(r) = ar^{-\Delta_-} + \beta_1 a^2 r^{-2\Delta_-} - (4\Delta_- - 3)\beta_2 a^3 \log(r) r^{-\Delta_+} + br^{-\Delta_+} + ... \tag{4.22}$$

and the term of order $r^{-4\Delta_-}$ does not contribute. The metric perturbation is:

$$\begin{aligned} h_{rr} &= \frac{\kappa L^2}{r^2}\left[\alpha_1 a^2 r^{-2\Delta_-} + \alpha_2 a^3 r^{-3\Delta_-} + \frac{9}{8}(4\Delta_- - 3)\,\beta_2 a^4 \log(r) r^{-4\Delta_-}\right] \\ &\quad + \frac{f_{rr}}{r^5} + ... \end{aligned} \tag{4.23}$$

where coefficients $\beta_1, \beta_2, \alpha_1, \alpha_2$ are determined in section 4.4.

Subcase $3e$**:** $dm^2 = \frac{81}{100L^2}$ **for** $D = 4$

This is the most complicated case with a logarithmic branch, we have $\Delta_+ = 4\Delta_- = 12/5$ and the scalar field has the form:

$$\begin{aligned}\phi &= ar^{-\Delta_-} + \beta_1 a^2 r^{-2\Delta_-} + \beta_2 a^3 r^{-3\Delta_-} - (5\Delta_- - 3)\beta_3 a^4 \log(r) r^{-\Delta_+} \\ &\quad + br^{-\Delta_+} + ... \end{aligned} \tag{4.24}$$

terms of $O(r^{5\Delta})$ and smaller orders do not to be included as they are negligible. For this subcase the metric perturbation is:

$$\begin{aligned}h_{rr} &= \frac{\kappa L^2}{r^2}\left[\alpha_1 a^2 r^{-2\Delta_-} + \alpha_2 a^3 r^{-3\Delta_-} + \alpha_3 a^4 r^{-4\Delta_-} + \frac{24}{25}(5\Delta_- - 3)\beta_3 a^5 \log(r) r^{-5\Delta}\right] \\ &\quad + \frac{f_{rr}}{r^5} + ... \end{aligned} \tag{4.25}$$

where we see that again we have a term of $O(r^{-5})$ which has f_{rr} in its coefficient. The coefficients $\beta_1, \beta_2, \beta_3, \alpha_1, \alpha_2, \alpha_3$ are determined in section 4.4.

4.2.4 Case 4

For this case $dm^2 < 0$ for all D. As we have seen in Table 3.1 in case 4 the roots have the form:

$$\Delta\pm = \gamma \pm i\omega \tag{4.26}$$

where

$$\gamma = \frac{(D-1)}{2} \tag{4.27}$$

and

$$\omega = \sqrt{\frac{-4m^2L^2}{(D-1)^2} - 1} \tag{4.28}$$

where ω is real. The scalar field has the form:

$$\phi(r) = ar^{-\gamma+i\omega} + br^{-\gamma-i\omega} + ... \tag{4.29}$$

and the metric perturbation is:

$$h_{rr} = Ar^{-2\gamma-2+2i\omega} + Br^{-2\gamma-2-2i\omega} + \frac{f_{rr}}{r^{D+1}} + ... \tag{4.30}$$

where A and B are coefficients that we determine in chapter 5. The scalar field and the metric perturbation have oscillatory behaviour.

§ 4.3 Tables of results

The different possibilities are covered in the subcases presented above by considering $D = 4, 5, 6$. For $D \geqslant 7$ only the behaviour of subcases $2e$ and $2f$ appears. That is the scalar field has a mass range $0 < dm^2 < \frac{(D-1)^2}{36L^2}$ and has the form (4.16). The metric perturbation has the form (4.17)). In Table 4.1 we present a summary table of scalar field forms for all the subcases, in Table 4.2 we present the expansions of h_{rr}.

Case	constraints on dm^2	D	$\phi(r)$
1	$dm^2 > -m_*^2$	D	$br^{-\Delta_+} + ...$
$2a$	$0 < dm^2 < \frac{1}{4L^2}$	4	$ar^{-\Delta_-} + br^{-\Delta_+} + ...$
$2b$	$\frac{1}{4L^2} < dm^2 < \frac{9}{16L^2}$	4	$ar^{-\Delta_-} + \beta_1 a^2 r^{-2\Delta} + br^{-\Delta_+} + ...$
$2c$	$\frac{9}{16L^2} < dm^2 < \frac{81}{100L^2}$	4	$ar^{-\Delta_-} + \beta_1 a^2 r^{-2\Delta_-} + \beta_2 a^3 r^{-3\Delta_-} + br^{-\Delta_-} + ...$
$2d$	$\frac{81}{100L^2} < dm^2 < \frac{1}{L^2}$	4	$ar^{-\Delta_-} + \beta_1 a^2 r^{-2\Delta_-} + \beta_2 a^3 r^{-3\Delta_-} + \beta_3 a^4 r^{-4\Delta_-} + br^{-\Delta_+} + ...$
$2e, 2f$	$0 < dm^2 < \frac{(D-1)^2}{36L^2}$	5, 6	$ar^{-\Delta_-} + br^{-\Delta_+} + ...$
$2g, 2h$	$\frac{(D-1)^2}{36L^2} < dm^2 < \frac{1}{L^2}$	5, 6	$ar^{-\Delta_-} + \beta_1 a^2 r^{-2\Delta_-} + br^{-\Delta_+} + ...$
$3a, 3b, 3c$	$dm^2 = \frac{(D-1)^2}{36L^2}$	4, 5, 6	$ar^{-\Delta_-} + (D-1-\Delta_-)\beta_1 a^2 \log(r) r^{-\Delta_+} + br^{-\Delta_+} + ...$
$3d$	$dm^2 = \frac{9}{16L^2}$	4	$ar^{-\Delta_-} + \beta_1 a^2 r^{-2\Delta_-} + (3-4\Delta_-)\beta_2 a^3 \log(r) r^{-\Delta_+} + br^{-\Delta_+} + ...$
$3e$	$dm^2 = \frac{81}{100L^2}$	4	$ar^{-\Delta_-} + \beta_1 a^2 r^{-2\Delta_-} + \beta_2 a^3 r^{-3\Delta_-} - (5\Delta_- - 3)\beta_3 a^4 \log(r) r^{-\Delta_+} + br^{-\Delta_+} + ...$
4	$dm^2 < 0$	D	$ar^{-\gamma+i\omega} + br^{-\gamma-i\omega}$

Table 4.1: Summary table: Asymptotic form of $\phi(r)$ for all the subcases

Case	constraints on dm^2	D	h_{rr}
1	$dm^2 > -m_*^2$	D	$\frac{f_{rr}}{r^{D+1}} + ...$
$2a$	$0 < dm^2 < \frac{1}{4L^2}$	4	$\frac{f_{rr}}{r^5} + \frac{\kappa L^2}{r^2}(\alpha_1 a^2 r^{-2\Delta_-}) + ...$
$2b$	$\frac{1}{4L^2} < dm^2 < \frac{9}{16L^2}$	4	$\frac{f_{rr}}{r^5} + \frac{\kappa L^2}{r^2}(\alpha_1 a^2 r^{-2\Delta_-} + \alpha_2 a^3 r^{-3\Delta_-}) + ...$
$2c$	$\frac{9}{16L^2} < dm^2 < \frac{81}{100L^2}$	4	$\frac{f_{rr}}{r^5} + \frac{\kappa L^2}{r^2}(\alpha_1 a^2 r^{-2\Delta_-} + \alpha_2 a^3 r^{-3\Delta_-} + \alpha_3 a^4 r^{-4\Delta_-}) + ...$
$2d$	$\frac{81}{100L^2} < dm^2 < \frac{1}{L^2}$	4	$\frac{f_{rr}}{r^5} + \frac{\kappa L^2}{r^2}(\alpha_1 a^2 r^{-2\Delta_-} + \alpha_2 a^3 r^{-3\Delta_-} + \alpha_3 a^4 r^{-4\Delta_-} + \alpha_4 a^5 r^{-5\Delta_-}) + ...$
$2e$, $2f$	$0 < dm^2 < \frac{(D-1)^2}{36L^2}$	5, 6	$\frac{f_{rr}}{r^{D+1}} + \frac{\kappa L^2}{r^2}(\alpha_1 a^2 r^{-2\Delta_-}) + ...$
$2g$, $2h$	$\frac{(D-1)^2}{36L^2} < dm^2 < \frac{1}{L^2}$	5, 6	$\frac{f_{rr}}{r^{D+1}} + \frac{\kappa L^2}{r^2}(\alpha_1 a^2 r^{-2\Delta_-} + \alpha_2 a^3 r^{-3\Delta_-}) + ...$
$3a$, $3b$, $3c$	$dm^2 = \frac{(D-1)^2}{36L^2}$	4, 5, 6	$\frac{f_{rr}}{r^{D+1}} + \frac{\kappa L^2}{r^2}\left[\alpha_1 a^2 r^{-2\Delta_-}\right] + \frac{\kappa L^2}{r^2}\left[(D-1-\Delta_-)\alpha_2 \frac{\log(r) a^3}{r^{-3\Delta_-}}\right] + ...$
$3d$	$dm^2 = \frac{9}{16L^2}$	4	$\frac{f_{rr}}{r^5} + \frac{\kappa L^2}{r^2}(\alpha_1 a^2 r^{-2\Delta_-} + a^3 r^{-3\Delta_-} + (4\Delta_- - 3)\,\beta_2 a^4 \frac{9}{8}\log(r) r^{-4\Delta_-}) + ...$
$3e$	$dm^2 = \frac{81}{100L^2}$	4	$\frac{f_{rr}}{r^5} + \frac{\kappa L^2}{r^2}(\alpha_1 a^2 r^{-2\Delta_-} + a^3 r^{-3\Delta_-} + (4\Delta_- 3)\,\beta_2 a^4 \frac{9}{8}\log(r) r^{-4\Delta_-}) + ...$
4	$dm^2 < 0$	D	$\frac{f_{rr}}{r^{D+1}} + A r^{-2\gamma-2+2i\omega} + B r^{-2\gamma-2-2i\omega} + ...$

Table 4.2: Summary table: Asymptotic form of h_{rr} for the different subcases

§ 4.4 Expressions for the constants of the theory

We have seen that the expressions for the scalar field and the metric perturbation contain unknown coefficients. In this section we present our method to obtain the expressions of the coefficients $\alpha_1, \alpha_2, \alpha_3, \alpha_4, \beta_1, \beta_2, \beta_3$ using our own mathematica code. This section is split in two parts. We need to find $J(r)$ (3.18) in terms of h_{rr} first. Then we use the field equations expressed in terms of $J(r)$ (3.44-3.46) to find all the coefficients that appear in the previous section.

4.4.1 Expression for J in terms of h_{rr}

In our calculations we are dealing with different quantities that can be expanded but we want to extract and keep only the information we need. We want to always keep the f_{rr} term that appears in h_{rr} (Table. 4.2) in our expressions for this reason we want to obtain an expression of $J(r)$ where it explicitly depends on h_{rr}. We consider the metric component:

$$g_{rr} = \left(k + \frac{r^2}{L^2} + J(r)\right)^{-1} = \left(k + \frac{r^2}{L^2}\right)^{-1} + h_{rr}. \tag{4.31}$$

It follows that

$$J(r) = \left(k + \frac{r^2}{L^2}\right)\left[\frac{1}{1 + h_{rr}\left(k + \frac{r^2}{L^2}\right)} - 1\right] \tag{4.32}$$

which can be written on terms of a series expansion as:

$$J(r) = \sum_{i=1}^{\infty} (-1)^i \left(k + \frac{r^2}{L^2}\right)^{i+1} h_{rr}^i. \tag{4.33}$$

We have now obtained an expansion form for $J(r)$ in terms of h_{rr}. We do not need all the terms in $J(r)$. We want to make the right cut off for $J(r)$ and keep only the relevant terms. The relevant terms are the first term where f_{rr} coefficient appears and any terms that are larger as $r \to \infty$. This becomes clearer with an example. In this section we show how it is done for the subcase $2a$ but the method is applicable to the rest of the cases.

We consider subcase $2a$ for which $0 < dm^2 < \frac{1}{4L^2}$. We start by defining $\texttt{Jterm}_1$ as:

$$\texttt{Jterm}_1 = h_{rr}\left(k + \frac{r^2}{L^2}\right)$$

for case $2a$ this gives the expression:

$$\texttt{Jterm}_1 \quad = \quad a^2 r^{-5+2dmL}\alpha_1 + a^2 r^{-3+2dmL}\alpha_1 + \frac{f_{rr}}{r^5} + \frac{f_{rr}}{L^2 r^3}$$

where we see f_{rr} appearing. We then want to extract the powers of r in the expression above, for this purpose we use the command `Exponent` which will generate a list of all the exponents that we name `Jterm1PowerList` for convenience:

$$\texttt{Jterm}_1\texttt{PowerList} = \{-5, -3, -5 + 2dmL, -3 + 2dmL\}. \tag{4.34}$$

We see that there are four powers or r and we want to know which ones are too small to keep i.e. the once corresponding to terms that are subdominant. We create a loop with two `For` loops and one `If` loop (Fig. 4.1). The first `For` loop with the index i is

```
For[i = 0, i < 1 + Length[JTerm1PowerList], i++,
 If[Simplify[JTerm1PowerList[[i]] < -3],
  JCasesTest = Cases[Jterm1, _ * r^(JTerm1PowerList[[i]])];
  JCasesLength = Length[JCasesTest];
  JSubtract = 0;
  For[j = 1, j < 1 + JCasesLength, j++,
   JSubtract = JSubtract + JCasesTest[[j]];
  ];
  Jterm1Short = Jterm1Short - JSubtract
 ]
]

Jterm1Short
```

Figure 4.1: Loop to cut off $J(r)$ expression

concerned with the elements in the power list, the index i allows the progression from one element of the list to the next. We see from the expression for $\texttt{Jterm}_1$ in (4.34) that the biggest power of r that has f_{rr} as a coefficient is r^{-3}, this will determine our cut-off. If the element of the power list chosen is smaller than -3 then it is added to a

separated list called `Jsubstract` using the `Cases` command. Finally:

$$\texttt{Jterm}_1\texttt{Short} = \texttt{JtermShort} - \texttt{JSubtract} \tag{4.35}$$

is the final expression for $\texttt{Jterm}_1$ with all necessary cancellations done.

This process is repeated for the other terms in the sum of $J(r)$ (4.33). The next term is called

$$\texttt{Jterm}_2 = (\texttt{Jterm}_1\texttt{Short})^2 \tag{4.36}$$

and we run the same loop for it. In more general terms in `Jterm` ($\texttt{Jterm}_1$, $\texttt{Jterm}_2 = (\texttt{Jterm}_1)^2$, $\texttt{Jterm}_3 = (\texttt{Jterm}_1)^3$ etc) we extract the powers of r, every power is compared with the biggest power of r which has f_{rr} as its coefficient. The reason we need to keep the f_{rr} term is because it appears in the expression for the mass in the matter-free asymptotically adS spacetime mass calculation in chapter 2. From Fig. 4.1 we see that the powers of r smaller than -3 are cut off. We are then only left with relevant terms. The final simplified expression of the sum for J (4.33) has therefore the following structure:

$$\begin{aligned} \texttt{J}_{\texttt{short}} &= -\texttt{Jterm}_1\texttt{short}\left(k+\frac{r^2}{L^2}\right) + [\texttt{Jterm}_1\texttt{short}]^2\left(k+\frac{r^2}{L^2}\right) \\ &- [\texttt{Jterm}_1\texttt{short}]^3\left(k+\frac{r^2}{L^2}\right) + ... \end{aligned} \tag{4.37}$$

The idea is to keep on adding powers of $\texttt{Jterm}_1\texttt{short}$ until no terms survive the cut off. For the subcase $2a$ only $\texttt{Jterm}_1\texttt{short}$ contributes so:

$$\begin{aligned} J(r) &= -\texttt{Jterm}_1\texttt{short}\left(k+\frac{r^2}{L^2}\right) \\ &= -\frac{f_{rr}}{L^2r^3} - \frac{f_{rr}}{L^4r} - \alpha_1\frac{a^2r^{-1+2dmL}}{L} - \alpha_1 a^2 k r^{-3+2dmL}. \end{aligned} \tag{4.38}$$

Since we have multiplied by a factor of r^2, when we run a loop to find the final expression for $J(r)$ we need to change our cut off to $O(r^{-1})$. We finally obtain the most simplified expression:

$$\texttt{Jshort} = -\frac{f_{rr}}{L^4r} - \alpha_1\frac{a^2r^{-1+2dmL}}{L}. \tag{4.39}$$

This method will be used for all the subcases in order to obtain simplified expressions for $J(r)$.

4.4.2 Method for finding the coefficients

The coefficients that appear in the expansions of the scalar field and the metric perturbation in Tables 4.2 and 4.1 are very important for the mass calculations in the next chapter. Here we present our own method of obtaining these coefficients. We give the details for subcase $2d$ but the method is applicable to the rest of the cases.

For case $2d$ we have:

$$\frac{81}{100} < dm^2L^2 < 1 \tag{4.40}$$

and:

$$\Delta_- = \frac{3}{2} - dmL \tag{4.41}$$

$$\Delta_+ = \frac{3}{2} + dmL \tag{4.42}$$

where $L > 0$ and $dmL > 0$. The reason why we chose this subcase is because we can see in (4.14) and (4.15) that it contains the coefficients, β_1, β_2, β_3, α_1, α_2, α_3, α_4. In our code roots $\Delta_\pm$ are defined as in (3.26). We then enter the asymptotic expressions (4.14) for ϕ and (4.15) for h_{rr} for this case.

We consider the field equations expressed in terms of $J(r)$ (3.44):

$$\mathcal{E}_1 = \frac{D-2}{2r}\left[J' + \frac{(D-3)}{r}J\right] + \frac{1}{2}H(\phi')^2 + V(\phi) = 0. \tag{4.43}$$

The way we proceed is to break down (4.43) into two parts that we call

$$\mathcal{E}_{1Part1} = \frac{D-2}{2r}\left[J' + \frac{(D-3)}{r}J\right] \tag{4.44}$$

and

$$\mathcal{E}_{1Part2} = \frac{1}{2}H(\phi')^2. \tag{4.45}$$

We simplify the expression for $J(r)$ using the method described in 4.2.1, that is performing a cut-off at $O(r^{-1})$. The simplified expression for $J(r)$ for subcase $2d$ is:

$$\begin{aligned} \texttt{Jshort} = & -\frac{f_{rr}}{L^4 r} - \frac{a^2 r^{-1+2dmL}\alpha_1}{L^2} - \frac{a^3 r^{-\frac{5}{2}+3dmL}\alpha_2}{L^2} \\ & + \frac{a^4 r^{-4+4dmL}\left({\alpha_1}^2 - \alpha_3\right)}{L^2} + \frac{a^5 r^{-\frac{11}{2}+5dmL}(2\alpha_1\alpha_2 - \alpha_4)}{L^2}. \end{aligned} \tag{4.46}$$

We use $O(r^{-3})$ as our default cut-off as this was the cut off we used for the first term in $J(r)$ that we called $\texttt{Jshort}_1$. We simplify all the terms in (4.44) and (4.45) by

performing cut-offs at $O(r^{-3})$ except for the term $(\phi')^2$ in (4.45) where we had to perform a cut-off at $O(r^{-5})$ for crucial cancelations to happen later. We check that we keep all the terms that we need, in particular we check that after every cut-off we still have f_{rr}, a and b parameters in our expressions. After the cut-offs are performed, much simpler expressions for (4.44) and (4.45) are obtained, these are too long to present here.

Next we consider the general potential $V(\phi)$ defined as:

$$V(\phi) = \frac{1}{2}m^2\phi^2 + C_3\phi^3 + C_4\phi^4 + C_5\phi^5. \tag{4.47}$$

In order to do some necessary simplifications we split the potential as follows:

$$\begin{aligned} V_1 &= \frac{1}{2}m^2\phi^2 \\ V_2 &= C_3\phi^3 \\ V_3 &= C_4\phi^4 \\ V_4 &= C_5\phi^5 \end{aligned} \tag{4.48}$$

and each of these terms is simplified using a cut at $O(r^{-3})$ following Fig. 4.1. For subcase $2d$ all the terms in (4.48) were found to have a contribution. For other subcases not al the terms in (4.48) contribute. Putting together all the simplified terms (4.43) becomes:

$$\begin{aligned} \mathcal{E}_1(\texttt{simplified}) &= \mathcal{E}_{1Part1}(\texttt{simplified}) + \mathcal{E}_{1Part2}(\texttt{simplified}) \\ &\quad + V(\texttt{simplified}) = 0. \end{aligned} \tag{4.49}$$

Now we consider the field equation (3.8):

$$\mathcal{E}_2 = H\phi'' + \left[H' + (D-2)\frac{H}{r}\right]\phi' + H\delta'\phi' - \frac{\partial V}{\partial \phi} = 0. \tag{4.50}$$

We break (4.50) into the following expressions:

$$\begin{aligned} \mathcal{E}_{2Part1} &= H\phi'' \\ \mathcal{E}_{2Part2} &= \left[H' + (D-2)\frac{H}{r}\right]\phi' \\ \mathcal{E}_{2Part3} &= H\delta'\phi'. \end{aligned} \tag{4.51}$$

We perform a cut-off at $O(r^{-3})$ for the equations in (4.51). Similarly to $V(\phi)$ above,

we consider the individual terms of $\frac{\partial V(\phi)}{\partial \phi}$ as follows:

$$\begin{aligned}
\left(\frac{\partial V}{\partial \phi}\right)_1 &= m^2\phi \\
\left(\frac{\partial V}{\partial \phi}\right)_2 &= 3C_3\phi^2 \\
\left(\frac{\partial V}{\partial \phi}\right)_3 &= 4C_4\phi^3 \\
\left(\frac{\partial V}{\partial \phi}\right)_4 &= 5C_5\phi^4
\end{aligned} \tag{4.52}$$

These are also cut-off at $O(r^{-3})$ following the method described in 4.2.1. The simplified version of (4.50) is:

$$\begin{aligned}
\mathcal{E}_2(\texttt{simplified}) &= \mathcal{E}_{2Part1}(\texttt{simplified}) + \mathcal{E}_{2Part2}(\texttt{simplified}) \\
&\quad + \mathcal{E}_{2Part3}(\texttt{simplified}) + \frac{\partial V}{\partial \phi}(\texttt{simplified}) = 0.
\end{aligned} \tag{4.53}$$

To make sure all the cancellations have been made we also perform a cut-off at $O(r^{-3})$ for (4.49) and (4.53). The simplified field equations are too long to be presented here.

For both equations (4.49) and (4.53) we extract the coefficients of every power of r. From (4.49) and (4.53) we obtain the following coefficients:

$$
\begin{aligned}
\texttt{Coefficient}_1 &= a^2dm^2 - \frac{3a^2dm}{2L} - \frac{2a^2dm\alpha_1}{L} \\
\texttt{Coefficient}_2 &= \frac{a^3C_3}{L^2} + \frac{3a^3\alpha_2}{2L^2} - \frac{3a^3dm\alpha_2}{L} \\
&\quad +3a^3dm^2\beta_1 + \frac{9a^3\beta_1}{4L^2} - \frac{6a^3dm\beta_1}{L} \\
\texttt{Coefficient}_3 &= \frac{a^4C_4}{L^2} - \frac{1}{2}a^4dm^2\alpha_1 - \frac{9a^4\alpha_1}{8L^2} + \frac{3a^4dm\alpha_1}{2L} - \frac{3a^4\alpha_1^2}{L^2} + \frac{4a^4dm\alpha_1^2}{L} \\
&\quad +\frac{3a^4\alpha_3}{L^2} - \frac{4a^4dm\alpha_3}{L} + \frac{3a^4C_3\beta_1}{L^2} + \frac{5}{2}a^4dm^2\beta_1^2 + \frac{27a^4\beta_1^2}{8L^2} \\
&\quad -\frac{6a^4dm\beta_1^2}{L} + 4a^4dm^2\beta_2 + \frac{9a^4\beta_2}{2L^2} - \frac{9a^4dm\beta_2}{L} \\
\texttt{Coefficient}_4 &= \frac{a^5C_5}{L^2} - \frac{1}{2}a^5dm^2\alpha_2 - \frac{9a^5\alpha_2}{8L^2} + \frac{3a^5dm\alpha_2}{2L} + \frac{3a^5dm\alpha_2}{2L} \\
&\quad +\frac{3a^5dm\alpha_2}{2L} - \frac{9a^5\alpha_1\alpha_2}{L^2} + \frac{10a^5dm\alpha_1\alpha_2}{L} + \frac{9a^5\alpha_4}{2L^2} \\
&\quad +\frac{9a^5\alpha_4}{2L^2} - \frac{5a^5dm\alpha_4}{L} + \frac{4a^5C_4\beta_1}{L^2} - 2a^5dm^2\alpha_1\beta_1 \\
&\quad -\frac{9a^5\alpha_1\beta_1}{2L^2} + \frac{6a^5dm\alpha_1\beta_1}{L} + \frac{3a^5C_3\beta_1^2}{L^2} + \frac{3a^5C_3\beta_2}{L^2} \\
&\quad +7a^5dm^2\beta_1\beta_2 + \frac{45a^5\beta_1\beta_2}{4L^2} - \frac{18a^5dm\beta_1\beta_2}{L} + 5a^5dm^2\beta_3 \\
&\quad +\frac{27a^5\beta_3}{4L^2} - \frac{12a^5dm\beta_3}{L} \\
\texttt{Coefficient}_5 &= -\frac{3a^2C_3}{L^2} + 3a^2dm^2\beta_1 + \frac{9a^2\beta_1}{4L^2} - \frac{6a^2dm\beta_1}{L} \\
\texttt{Coefficient}_6 &= \frac{9}{4}a^3dm^2 - \frac{27a^3}{16L^2} - \frac{4a^3C_4}{L^2} + \frac{27a^3dm}{8L} + \frac{1}{2}a^3dm^3L - 3a^3dm^2\alpha_1 \\
&\quad -\frac{9a^3\alpha_1}{4L^2} + \frac{6a^3dm\alpha_1}{L} - \frac{6a^3C_3\beta_1}{L^2} + 8a^3dm^2\beta_2 + \frac{9a^3\beta_2}{L^2} - \frac{18a^3dm\beta_2}{L} \\
\texttt{Coefficient}_7 &= -\frac{5a^4C_5}{L^2} - 4a^4dm^2\alpha_2 - \frac{9a^4\alpha_2}{2L^2} + \frac{9a^4dm\alpha_2}{L} - \frac{27}{2}a^4dm^2\beta_1 \\
&\quad -\frac{81a^4\beta_1}{8L^2} - \frac{12a^4C_4\beta_1}{L^2} + \frac{81a^4dm\beta_1}{4L} + 3a^4dm^3L\beta_1 - 8a^4dm^2\alpha_1\beta_1 \\
&\quad -\frac{9a^4\alpha_1\beta_1}{L^2} + \frac{18a^4dm\alpha_1\beta_1}{L} - \frac{3a^4C_3\beta_1^2}{L^2} - \frac{6a^4C_3\beta_2}{L^2} \\
&\quad +15a^4dm^2\beta_3 + \frac{81a^4\beta_3}{4L^2} - \frac{36a^4dm\beta_3}{L}
\end{aligned}
\tag{4.54}
$$

The different coefficients come from different powers of r: $\texttt{Coefficient}_1$, $\texttt{Coefficient}_2$, $\texttt{Coefficient}_3$, $\texttt{Coefficient}_4$ are obtained from (4.49), they are the coefficients of $r^{-3+2dmL}$, $r^{-9/2+3dmL}$, $r^{-6+4dmL}$ and $r^{-15/2+dmL}$ respectively. From the field equation (4.53) we obtain the rest of the coefficients $\texttt{Coefficient}_5$, $\texttt{Coefficient}_6$, $\texttt{Coefficient}_7$ which are the coefficients of $r^{-3+2dmL}$, $r^{-9/2+3dmL}$, and $r^{-6+4dmL}$. By setting each of the $\texttt{Coefficients}$ in 4.54 to zero we find the expressions of $\alpha_1, \alpha_2, \alpha_3, \alpha_4, \beta_1, \beta_2, \beta_3$. We are effectively solving a system of simultaneous equations. For example from $\texttt{Coefficient}_1$ we obtain:

$$\alpha_1 = -\frac{3}{4} + \frac{1}{2}dmL \tag{4.55}$$

and using (4.42) we can express it in terms of Δ_- as:

$$\alpha_1 = -\frac{\Delta_-}{2}, \tag{4.56}$$

in agreement with [73]. For the rest of the coefficients we proceed in a similar way. For example we see that we can use $\texttt{Coefficient}_5$ to obtain an expression for β_1:

$$\beta_1 = \frac{4C_3}{3 - 8dmL + 4dm^2L^2} \tag{4.57}$$

and substituting (4.57) in $\texttt{Coefficient}_2$ we find the expression for α_2:

$$\alpha_2 = \frac{16C_3}{-6 + 12dmL}. \tag{4.58}$$

We have proceeded with a similar method for the other subcases and we obtained consistent results for all the coefficients, i.e. the same coefficients $\alpha_1, \alpha_2, \alpha_3, \alpha_4, \beta_1, \beta_2, \beta_3$ appear in all the different subcases. We present all the expressions for the coefficients in a more elegant form in the next section.

4.4.3 Expressions for the coefficients

The expressions for the coefficients are neater when presented as follows:

$$\begin{aligned}
\alpha_1 &= -\frac{\Delta_-}{D-2} \\
\alpha_2 &= -\frac{8}{3(D-2)}\Delta_-\beta_1 \\
\alpha_3 &= -\frac{\Delta_-}{4}\left(-\frac{\kappa\Delta_-}{2} + 6\beta_2 + 4\beta_1^2\right) \\
\alpha_4 &= -\frac{\Delta_-}{5}\left(8\beta_3 + 12\beta_1\beta_2 - \frac{10}{3}\kappa\Delta_-\beta_1\right).
\end{aligned} \tag{4.59}$$

where we see that only α_1 does not depend on β_1, β_2 nor on β_3. For these coefficients we have:

$$\begin{aligned}
\beta_1 &= \frac{C_3}{\Delta_-(\Delta_- - (D-1)/3)} \\
\beta_2 &= \frac{2C_4}{\Delta_-(4\Delta_- - 3)} + \frac{3C_3^2}{\Delta_-^2(\Delta_- - 1)(4\Delta_- - 3)} + \kappa\frac{\Delta(3-2\Delta_-)}{4(4\Delta_- - 3)} \\
\beta_3 &= \frac{5C_5}{3\Delta_-(5\Delta_- - 3)} + \frac{4C_3C_4(5\Delta_- - 4)}{\Delta_-^2(\Delta_- - 1)(4\Delta_- - 3)(5\Delta_- - 3)} \\
&\quad + \frac{C_3^3(10\Delta_- - 9)}{\Delta_-^3(5\Delta_- - 3)(4\Delta_- - 3)(\Delta_- - 1)^2}, \\
&\quad + \kappa\frac{C_3(-153 + 327\Delta_- - 170\Delta_-^2)}{18(\Delta_- - 1)(4\Delta_- - 3)(5\Delta_- - 3)}
\end{aligned} \tag{4.60}$$

We see that all the coefficients depend on Δ_-. We stress that the expressions of the coefficients above are valid for all the different subcases.

§ 4.5 Summary

In this chapter we have considered the subleading terms in the asymptotic behaviour of the scalar field as $r \to \infty$. Whenever the mass of the scalar field is considered to be within a certain range, the expressions for the scalar field and the metric perturbation h_{rr} acquire new terms in their expansion but the logarithmic branch remains switched off. When the mass of the scalar field is exactly equal to certain values, $\phi(r)$ and h_{rr} acquire extra terms containing a logarithmic branch. We have presented our own method of finding the coefficients of the theory $\alpha_1, \alpha_2, \alpha_3, \alpha_4, \beta_1, \beta_2, \beta_3$. In the next chapter we focus on obtaining the expression for the spacetime mass for all the subcases using the asymptotic expressions that we presented in this chapter.

Chapter 5

Calculating the mass of the spacetimes

When the scalar field has a slow fall off at infinity it induces a strong back reaction on the metric. It has been proven that the scalar field mass contributes to the mass of hairy black hole solutions [7, 17, 19, 59, 72, 73, 78]. In the previous chapter we have obtained explicit expressions for the asymptotics of the scalar field and the metric perturbations. We have seen that there exist many subcases corresponding to different ranges of the scalar field mass. We use the detailed asymptotics presented in chapter 4 to obtain finite expressions for the mass. In [73] Henneaux *et al.* show that when a scalar field is added to the theory it will have crucial contributions. It will make the divergences cancel when added to the divergent gravitational contribution. In this chapter we show how to obtain the expressions for the masses for all the subcases. We will present the resulting finite expressions for the spacetime mass in a summary table.

§ 5.1 More about Henneaux and Teiltelboim mass in adS

Before we consider what happens in the case when we add a scalar field we would like to give an outline of the gravitational mass defined by Henneaux and Teltelboim [74]. In chapter 2 we have decided that the Henneaux and Teitelboim definition for a conserved charge in asymptotically adS sapcetime (2.62) is the definition we found the most adapted to our work. We have seen that the mass is defined in the Hamiltonian framework. Killing vector fields are associated with a symmetry of the action and hence according to Noether's theorem to a conserved charge of the spacetime. The mass is the conserved charge associated with the timelike Killing vector. Here we will give an outline of where the definition of Q_0 (2.62) comes from rather than a rigorous

mathematical derivation.

As we have seen in chapter 2 the conserved charges in [74] are defined as:

$$\begin{aligned}\mathcal{Q}_0 &= \int_\Sigma \mathcal{C}^a\xi_a + \lim_{C\to\mathcal{F}}\frac{1}{16\pi G}\int_C G_a{}^{bdc}[\xi^e\hat{u}_e\mathcal{D}_b h_{cd} - h_{cd}\mathcal{D}_b(\xi^e\hat{u}_e)]\hat{\eta}^a dS \\ &\quad + \lim_{C\to\mathcal{F}}\frac{1}{4\pi G}\int_C(\kappa_{ab}-\kappa q_{ab})\xi^a\hat{\eta}^b dS \end{aligned} \tag{5.1}$$

where all of the quantities are defined in chapter 2. The first integral involves constraint generators $\mathcal{C}^a$ of general relativity [11, 55, 65, 74]. The second and third integrals are surface integrals over a two dimensional surface at infinity. The expression in (5.1) is an improved Hamiltonian [74]. In order for a Hamiltonian to give the right equations of motion we want it to be well defined. It has to give well-defined functional derivatives with respect to the canonical variables (the spatial metric and the conjugate momentum). This means that when we vary the Hamiltonian it should only give us a volume term and no surface integrals. Henneaux and Teitelboim [74] show that if the Hamiltonian is only defined from constraints of the theory as

$$\mathcal{H}_\xi = \int_\Sigma \mathcal{C}^a\xi_a, \tag{5.2}$$

then when it is varied, it gives a volume term but also a surface integral term. In order to cancel these surface integrals, extra terms have to be added to the Hamiltonian in (5.2) to obtain what is called an improved Hamiltonian [74]. The improved Hamiltonian has the form:

$$\mathcal{H}_\xi = \int_\Sigma \mathcal{C}^a\xi_a + Q_0. \tag{5.3}$$

The extra terms added are the conserved charges. They are surface integrals defined on a $D-2$ hypersurface at infinity. They satisfy the boundary conditions described in (2.61), in particular $h_{rr} = O(r^{-D-1})$. The conserved charge associated with the timelike Killing vector is the mass. These asymptotic conditions hold in the absence of matter or for matter fields which fall off sufficiently fast at infinity so they do not contribute to the charges. However as we have seen in the previous chapter when the scalar field has a mass greater than the Breitenlohner-Freedman bound [31], h_{rr} has a different form.

5.1.1 Gravitational and scalar contribution

When we add a scalar field it has a back reaction and (5.1) no longer gives a finite mass [73]. This expression is no longer finite for our h_{rr} terms which have an extra

contribution from the presence of the scalar field as can been seen in Table 4.2. The total mass of the spacetime becomes [73]:

$$Q(\xi) = Q_G(\xi) + Q_\phi(\xi) \tag{5.4}$$

where $Q_G(\xi)$ is the gravitational contribution defined as $Q_G(\xi) = Q_0 + \Delta Q$ with

$$\Delta Q = -\frac{3}{4\kappa}\int \frac{r^6}{L^5}\xi^t h_{rr}^2 dS. \tag{5.5}$$

The extra contribution ΔG to the gravitational mass is a non-linear correction in the deviation from the background metric. This term is essential to cancel some divergences for some subcases and is added specifically to obtain a finite mass [73]. Q_G is divergent and Q_ϕ, the scalar contribution is also divergent. When we add the two divergent contributions the divergences cancel and we obtain a finite mass. We emphasise that the challenge is to obtain the correct divergent gravitational and scalar contributions for every subcase by performing the right cut-off as we will explain in the next section. Calculating Q_0 using (5.1) is very challenging when we consider the detailed asymptotics of the scalar field and the metric perturbation. Using our maple code and mathematica, we have found that Q_0 can be written in terms of quantities which we can expand. We found after some cancelations that Q_0 can be expressed as:

$$Q_0 = J\, u_t\, \eta^r \left(k + \frac{r^2}{L^2}\right)^{-1} \frac{(D-2)}{r}. \tag{5.6}$$

where η^r is the non zero component of the space unit vector, u_t is the non zero component of time unit vector:

$$\hat{\eta}_r = \sqrt{\frac{1}{1+\frac{r^2}{L^2}+h_{rr}}} \tag{5.7}$$

$$u_t = \frac{r}{L}\sqrt{1+\frac{L^2}{r^2}(k-h_{tt})}, \tag{5.8}$$

and $J(r)$ is defined in (4.33). We can obtain expansions for the unit vectors and then perform the right cut-offs to keep the only necessary contributions (for the function $J(r)$ we have already shown how to perform the cut-offs in the previous chapter).

The scalar contribution is specifically defined to cancel the divergences of the gravitational part and has the form [73]:

$$Q_\phi(\xi) = \frac{1}{6L}\int r^2 \xi_t u^t [L^2(\eta^r\partial_r\phi)^2 - m^2L^2\phi^2 + k_3\phi^3 + k_4\phi^4 + k_5\phi^5]\, dS \tag{5.9}$$

where $\xi_t = \frac{\partial}{\partial t}$ and u_t (5.8) are the only non-zero components of the time-like Killing vector and time-like unit vector respectively.

We are integrating (5.9) over the angular coordinates and k_3, k_4, k_5 are constants given by [73]:

$$\begin{aligned} k_3 &= -2C_3 \\ k_4 &= -2C_4 - \kappa\frac{3}{8}\Delta_-^2 \\ k_5 &= -2C_5 - \kappa\frac{C_3\Delta_-}{2(\Delta_- - 1)}. \end{aligned} \tag{5.10}$$

The scalar contribution was calculated in the same way as the gravitational contribution, that is by performing the right cut-offs. For some cases we do not need to go down further than ϕ^3 to obtain the correct scalar contribution. The masses for all cases described in the previous chapter were calculated using our own method. Every case was treated separately. Because of the large number of subcases we cannot go through the derivation of every case. We will present the calculation in detail for subcase $2a$. A similar approach was taken for the other cases but we will explain any differences. We will also present the expressions of the gravitational and scalar contribution for all the cases except for case $2d$ where the expressions are too lengthy. We will however mention how the calculations were done.

§ 5.2 Method for subcase $2a$

We illustrate the key ideas of our method for calculating the mass by considering subcase $2a$. For this subcase $0 < dm^2 < \frac{1}{4L^2}$ and

$$\phi(r) = \frac{a}{r^{\Delta_-}} + \frac{b}{r^{\Delta_+}} + ... \tag{5.11}$$

with

$$h_{rr} = \frac{\kappa L^2}{r^2}(\alpha_1 a^2 r^{-2\Delta_-}) + \frac{f_{rr}}{r^5} + ... \tag{5.12}$$

and $1 < \Delta_- < 3/2$ and $3/2 < \Delta_+ < 2$. In order to calculate the gravitational contribution to the total mass, all the terms in (5.6) were calculated. Our work consisted in finding series expansions for all the quantities and cutting off unnecessary terms at every stage. Here we give an example of the work that had to be done for one important quantity, the timelike unit vector u_t (5.8).

For the timelike unit vector an expression for h_{tt} is required. From the metric (3.5) we have:

$$g_{tt} = -He^{2\delta(r)} = -\left(k + \frac{r^2}{L^2}\right) + h_{tt} \tag{5.13}$$

so

$$h_{tt} = \left(k + \frac{r^2}{L^2}\right)\left(1 - e^{-2\delta(r)}\right) - J(r)e^{2\delta(r)}, \tag{5.14}$$

where the expression for the $\delta(r)$ function is obtained from the field equations (3.10):

$$\delta(r) = \int \frac{[\phi']^2}{(D-2)} r\, dr. \tag{5.15}$$

which we easily calculate using mathematica. We begin by expanding the term $e^{2\delta}$ in (5.14) and perform cut-offs. From the exponential series expansion we have:

$$e^{2\delta} = 1 + 2\delta + \frac{(2\delta)^2}{2!} + \frac{(2\delta)^3}{3!} + ... \tag{5.16}$$

We call:

$$\mathtt{exp_1} = 2\delta. \tag{5.17}$$

We calculate this term and use a FOR loop as we did in chapter 4 for $J(r)$ to cut off all the terms that are smaller than $O(r^{-3})$. We do the same for the next term in the exponential expansion (5.16) which we define as:

$$\mathtt{exp_2} = \frac{(2\delta)^2}{2!}. \tag{5.18}$$

After we perform the cut-off on this term we find out that all the terms are smaller than $O(r^{-3})$. Therefore there is no contribution from this term to (5.16) or from any subsequent terms in the expansion. The only term that contributes is $\mathtt{exp_1}$. We can hence write:

$$\mathtt{e^{2\delta}short} = 1 + \mathtt{exp_1}. \tag{5.19}$$

For case $2a$ we have:

$$\mathtt{e^{2\delta}short} = 1 - \frac{ab}{r^3}\left(\frac{2}{3}dm^2\, L^2 - \frac{3}{2}\right) + \frac{a^2}{2}\left(dmL - \frac{3}{2}\right) r^{-3+2dmL} \tag{5.20}$$

we see that both parameters a and b appear.

Now we go back to the expression (5.14) and break it down into several terms on which

we perform cut-offs individually. The first of these is:

$$\texttt{Term}_1 = k + \frac{r^2}{L^2} \tag{5.21}$$

this term does not need further simplification. The next term is $(1 - e^{-2\delta})$ but we have just worked that only the first term of the exponential expansion contributes, the following terms are too small. We can use the simplified version $\texttt{e}^{2\delta}\texttt{short}$ and write:

$$\texttt{Term}_2 = 1 - \texttt{e}^{2\delta}\texttt{short} \tag{5.22}$$

Now we define:

$$\texttt{Term}_3 = \texttt{Term}_1\,\texttt{Term}_2 \tag{5.23}$$

and perform a cut-off at $O(r^{-3})$ to make sure all unnecessary terms are disregarded, the term we obtain is defined as $\texttt{Term}_3(\texttt{simplified})$. The last term in the expansion is $J(r)e^{2\delta}$ but since we have a simplified version for both $J(r)$ and $e^{2\delta(r)}$ we can use them:

$$\texttt{Term}_4 = \texttt{Jshort}\,\texttt{e}^{2\delta(\texttt{r})}\texttt{short} \tag{5.24}$$

and we also obtain $\texttt{Term}_4\texttt{short}$ after running the cut-off for $\texttt{Term}_4$. We have calculated all the terms in (5.14) and we can obtain the simplified expression for h_{tt}:

$$h_{tt}(\texttt{simplified}) = \texttt{Term}_3\texttt{short} - \texttt{Term}_4\texttt{short}. \tag{5.25}$$

This expression can now be used to calculate the time-like unit vector where the only non-zero component is:

$$u_t = \frac{r}{L}\sqrt{1 + \frac{L^2}{r^2}(k - h_{tt})}. \tag{5.26}$$

We expand this expression using the series expansion for the square root. The series we obtain is:

$$u_t = \frac{r}{L}\left[1 + \frac{1}{2}\left[\frac{L^2}{r^2}(k - h_{tt})\right] - \frac{1}{8}\left[\frac{L^2}{r^2}(k - h_{tt})\right]^2 + \frac{1}{16}\left[\frac{L^2}{r^2}(k - h_{tt})\right]^3 - ...\right] \tag{5.27}$$

The important aspect to understand is that every term of the expansion is calculated individually and cuts are performed to cancel any unnecessary terms. We begin with the first term:

$$\texttt{Timeunit}_1 = \frac{L^2}{r^2}(k - h_{tt}) \tag{5.28}$$

and the simplified expression for this term after we perform a cut-off at $O(r^{-3})$ is named $\texttt{Timeunit}_1\texttt{short}$.

We notice that (5.27) can be written as:

$$\begin{aligned} u_t &= \frac{r}{L}\left[1+\frac{1}{2}[\texttt{Timeunit}_1\texttt{short}]-\frac{1}{8}[\texttt{Timeunit}_1\texttt{short}]^2\right] \\ &\quad +\frac{r}{L}\left[\frac{1}{16}[\texttt{Timeunit}_1\texttt{short}]^3-...\right] \end{aligned} \tag{5.29}$$

and we define:

$$\texttt{Timeunit}_2 = [\texttt{Timeunit}_1\texttt{short}]^2. \tag{5.30}$$

Again the simplified expression is called $\texttt{Timeunit}_2\texttt{short}$ and was found to be zero. So for this case there are no contributions from the subsequent term (which would be $\texttt{Timeunit}_3$) as the terms become too small. The most simplified expression for the time-like unit vector component is therefore:

$$u_t = \frac{r}{L}\left(1+\frac{1}{2}\texttt{Timeunit}_1\texttt{short}\right). \tag{5.31}$$

We give the expression for subcase $2a$ here:

$$\begin{aligned} u_t &= \frac{-18f_{rr}+abL^2\left(9-4dm^2L^2\right)}{24Lr^4}-\frac{6f_{rr}+abL^2\left(9-4dm^2L^2\right)}{12L^3r^2} \\ &\quad -\frac{L^3}{8r^3}+\frac{L}{2r}+\frac{r}{L}-\frac{1}{16}a^2L(-3+2dmL)r^{-4+2dmL}(1+3\kappa) \\ &\quad -\frac{a^2(-3+2dmL)r^{-2+2dmL}(1+\kappa)}{8L} \\ &\quad +\frac{a^4(3-2dmL)^2r^{-5+4dmL}\left(-1-6\kappa+3\kappa^2\right)}{128L}. \end{aligned} \tag{5.32}$$

We see that we have f_{rr}, a and b parameters in the expression for u_t.

Now for the space-like unit vector we do exactly the same as for the time-like unit vector. The only non-zero component is

$$\hat{\eta}_r = \sqrt{\frac{1}{1+\frac{r^2}{L^2}+h_{rr}}}. \tag{5.33}$$

Using the relationship between $J(r)$ and $h_r r$ (4.33) and expanding the squareroot, we

obtain

$$\begin{aligned}\hat{\eta}_r &= \frac{r}{L}\left[1+\frac{1}{2}\left[\frac{L^2}{r^2}(k+\texttt{Jshort})\right]-\frac{1}{8}\left[\frac{L^2}{r^2}(k+\texttt{Jshort})\right]^2\right] \\ &+ \frac{r}{L}\left[\frac{1}{16}\left[\frac{L^2}{r^2}(k+\texttt{Jshort})\right]^3-...\right]. \end{aligned} \tag{5.34}$$

Here, `Jshort` is the $J(r)$ function after the cut-off. We define

$$\texttt{Spaceunit}_1 = k + \texttt{Jshort}. \tag{5.35}$$

and we call the simplified version of (5.35) $\texttt{Spaceunit}_1\texttt{short}$. The rest of the terms are defined as:

$$\texttt{Spaceunit}_2 = [\texttt{Spaceunit}_1\texttt{short}]^2. \tag{5.36}$$

When we cut-off all the terms smaller than $O(r^{-3})$ we obtain the simplified expression $\texttt{Spaceunit}_2(\texttt{simplified})$. We have found that there is no contribution from $\texttt{Spaceunit}_2\texttt{short}$ or higher order terms so:

$$\hat{\eta}_r = \frac{r}{L}\left(1+\frac{1}{2}\texttt{Spaceunit}_1(\texttt{simplified})\right). \tag{5.37}$$

For subcase $2a$ we have:

$$\begin{aligned}\hat{\eta}_r &= \frac{3f_{rr}}{4Lr^4}-\frac{L^3}{8r^3}-\frac{f_{rr}}{2L^3r^2}+\frac{L}{2r}+\frac{r}{L} \\ &-\frac{1}{4}a^2dmr^{-2+2dmL}\kappa+\frac{3a^2r^{-2+2dmL}\kappa}{8L}-\frac{9}{32}a^4dmr^{-5+4dmL}\kappa^2 \\ &+\frac{27a^4r^{-5+4dmL}\kappa^2}{128L}+\frac{3}{32}a^4dm^2Lr^{-5+4dmL}\kappa^2 \end{aligned} \tag{5.38}$$

where we see the parameters f_{rr} and a. We have now performed all the necessary cut-offs and we can put all the terms together to calculate Q_0. For subcase $2a$ (5.6) becomes:

$$Q_0 = \frac{a^2}{2L}\left(dm-\frac{3}{2L}\right)r^{2dmL}+\frac{f_{rr}}{L^4\kappa}. \tag{5.39}$$

We notice here that we have a and f_{rr} but no b which will come from the scalar contribution. Since $dm > 0$ the expression (5.39) diverges as $r \to \infty$.

The other gravitational contribution ΔQ has the form (5.5):

$$\Delta Q = \frac{3\,r^6\,u_t\,h_{rr}^2}{4\kappa L^5}. \tag{5.40}$$

but for subcase $2a$ this term is zero. We will see that for other subcases this term is non-zero.

We are now left with the scalar contribution to the total conserved charge which is:

$$Q_\phi(\xi) = \frac{1}{6L}\int r^2 \xi_t u^t [L^2(\eta^r \partial_r \phi)^2 - m^2 L^2 \phi^2 + k_3\phi^3 + k_4\phi^4 + k_5\phi^5]\, dS \tag{5.41}$$

We split the expression into pieces and define new terms:

$$\begin{aligned} \texttt{scalar}_1 &= L^2\eta^2\phi'^2 \\ \texttt{scalar}_2 &= m^2L^2\phi^2 \\ \texttt{scalar}_3 &= k_3\phi^3 \\ \texttt{scalar}_4 &= k_4\phi^4 \\ \texttt{scalar}_5 &= k_5\phi^5. \end{aligned} \tag{5.42}$$

We run a `For` loop for each of these new terms with a cut-off at $O(r^{-3})$. We find that only $\texttt{scalar}_1$ and $\texttt{scalar}_2$ contribute towards the final expression for the scalar contribution, all the other terms are too small. So we have:

$$Q_\phi \texttt{short} = \frac{r^{D-2}}{2(D-1)L} u_t \texttt{short}(\texttt{scalar}_1\texttt{short} - \texttt{scalar}_2\texttt{short}). \tag{5.43}$$

For subcase $2a$ case we have:

$$Q_\phi = \frac{ab}{2L^2} - \frac{2}{3}abdm^2 - \frac{a^2}{2L}\left(dm - \frac{3}{2L}\right) r^{2dmL}. \tag{5.44}$$

The terms (5.39) and (5.44) are divergent but we see that adding them together we have:

$$Q = -\frac{2abdm^2}{3} + \frac{3ab}{L^2} + \frac{f_{rr}}{L^4\kappa}. \tag{5.45}$$

The mass is finite, in agreement with the mass calculated in [73] for a different subcase. This illustrates how by performing the right cut-offs at every step we obtain the expressions for the gravitational and the scalar contribution. When we add them together all the divergences cancel.

§ 5.3 Explicit expressions for Q_G and Q_ϕ for the other subcases

In this section we discuss the other subcases in detail.

5.3.1 Cut offs for the rest of the cases

In the previous section we have seen the details of the method we have used to obtain finite expressions for the spacetime mass. For the rest of the subcases presented we have used the same method. The challenge we encountered is to find the right cut-off so as to only include the necessary terms. The most challenging subcase was $2d$, for the time-like unit vector and the space-like unit vector we had to go down to $O(r^{-4})$ in the expansions and we performed cut-offs at $O(r^{-5})$. For subcases $2b$ and $2c$ any term in the time-like unit vector or the space-like unit vector with $O(r^{-3})$ or smaller does not contribute to the simplified expressions, the cut off was done at $O(r^{-3})$ as for subcase $2a$. For higher dimensions, the subcases had different cut-offs in five and six dimensions. In five dimensions we only needed to go as far as $O(r^{-2})$ in the expansions of the unit vectors and perform a cut-off at $O(r^{-4})$. In six dimensions we went down to $O(r^{-3})$ for the expansions with a cut-off at $O(r^{-6})$.

For the subcases with a logarithmic branch in four dimensions the cut-offs were $O(r^{-3})$ and the unit vectors contribute to $O(r^{-2})$ except for subcase $3a$ where only $O(r^{-1})$ contributes. The subcase $3a$ is also valid in five and six dimensions where the cut-offs are $O(r^{-4})$ and $O(r^{-5})$ respectively and the unit vector contributions are $O(r^{-2})$ for both. With these cut-offs we obtained finite masses for all the cases which have never been explicitly given in literature. We have done the calculations for all k and have found that this parameter does not affect the final expressions for the mass. We present the results in Table 5.1.

The other gravitational contribution is from ΔQ, we found it to be non-zero for subcases $2c$, $2d$, $3b$ and $3c$. For the scalar contribution we had to go as far as ϕ^5 for subcases $2d$ and $3c$. For cases $2b$ and $3c$ we needed ϕ^4 to make sure all the divergences cancel whereas for cases $2b$, $2h$ for both five and six dimensions we only needed to go as far as ϕ^3 as there were no contributions from ϕ^4. Finally for case $2e$ we only needed ϕ^2 in five and six dimensions.

In the next subsection we give the expressions of the different components for all the subcases except for case $2d$ where the expressions are too long to write out explicitly.

5.3.2 Explicit expressions

Subcase $2b$

The gravitational and scalar contribution were calculated in the same way as the method described above. We obtained

$$\begin{aligned} Q_0 &= \frac{a^2(-3+2dmL)r^{2dmL}}{4L^2} + \frac{8a^3C_3r^{-\frac{3}{2}+3dmL}}{3L^2(-1+2dmL)} + \frac{f_{rr}}{L^4\kappa} \\ Q_\phi &= -\frac{a^2(-3+2dmL)r^{2dmL}}{4L^2} + \frac{8a^3C_3r^{-\frac{3}{2}+3dmL}}{3L^2(1-2dmL)} \\ &\quad -\frac{2}{3}abdm^2 + \frac{3ab}{2L^2}. \end{aligned} \tag{5.46}$$

There is no contribution from ΔQ in this case. We see that Q_0 and Q_ϕ are divergent but when we add them together they give a finite mass:

$$Q = -\frac{2abdm^2}{3} + \frac{3ab}{2L^2} + \frac{f_{rr}}{L^4\kappa}. \tag{5.47}$$

Subcase $2c$

For this subcase the expressions are significantly longer and are not very elegant. The gravitational contribution is:

$$\begin{aligned} Q_0 &= \frac{a^2(-3+2dmL)r^{2dmL}}{4L^2} + \frac{8a^3C_3r^{-\frac{3}{2}+3dmL}}{3L^2(-1+2dmL)} + \frac{f_{rr}}{L^4\kappa} \\ &\quad -\frac{3a^4\left(27+448{C_3}^2+96C_4+576dm^2L^2+640C_4dm^2L^2\right)r^{-3+4dmL}}{32L^2(1-2dmL)^2(-3+2dmL)(-3+4dmL)} \\ &\quad +\frac{a^4dm\left[1088{C_3}^2+3\left[99+424dm^2L^2+32C_4\left(7+4dm^2L^2\right)\right]\right]r^{-3+4dmL}}{16L(1-2dmL)^2(-3+2dmL)(-3+4dmL)} \\ &\quad -\frac{a^4r^{-3+4dmL}\left[2000dm^4L^4-800dm^5L^5+128dm^6L^6+243\kappa+4212dm^2L^2\kappa\right]}{32L^2(1-2dmL)^2(-3+2dmL)(-3+4dmL)} \\ &\quad -\frac{3a^4dm\left[-135-456dm^2L^2+316dm^3L^3-112dm^4L^4+16dm^5L^5\right]r^{-3+4dmL}\kappa}{8L(1-2dmL)^2(-3+2dmL)(-3+4dmL)} \end{aligned} \tag{5.48}$$

and the scalar contribution is:

$$\begin{aligned}
Q_\phi &= \frac{ab\left(9-4dm^2L^2\right)}{6L^2}-\frac{a^2(-3+2dmL)r^{2dmL}}{4L^2}+\frac{8a^3C_3r^{-\frac{3}{2}+3dmL}}{3L^2(1-2dmL)}\\
&+\frac{3a^4\left[64{C_3}^2\left(63+1424dm^2L^2\right)+3\left(81+64(99+214C_4)dm^2L^2\right)\right]r^{-3+4dmL}}{32L^2(3-4dmL)^2(1-2dmL)^4(3-2dmL)^2}\\
&-\frac{9a^4\left[12C_4(-3+32dmL)+dmL\left(135+1280{C_3}^2+2688dm^2L^2\right)\right]r^{-3+4dmL}}{4L^2(3-4dmL)^2(1-2dmL)^4(3-2dmL)^2}\\
&+\frac{a^4dm^3L\left[32{C_3}^2(-383+263dmL)+3(4377dmL+16C_4(-193+269dmL))\right]}{(3-4dmL)^2(1-2dmL)^4(3-2dmL)^2r^{3-4dmL}}\\
&+\frac{8a^4dm^5L^3\left[-2379-272{C_3}^2+2329dmL+24C4(-54+23dmL)\right]r^{-3+4dmL}}{(3-4dmL)^2(1-2dmL)^4(3-2dmL)^2}\\
&+\frac{8a^4dm^7L^5\left[-1520-96C_4+633dmL-152dm^2L^2+16dm^3L^3\right]r^{-3+4dmL}}{(3-4dmL)^2(1-2dmL)^4(3-2dmL)^2}\\
&+\frac{81a^4\left[27-324dmL+1680dm^2L^2-4928dm^3L^3+8992dm^4L^4\right]r^{-3+4dmL}\kappa}{64L^2(3-4dmL)^2(1-2dmL)^4(3-2dmL)^2}\\
&-\frac{18a^4dm^5L^3\left[743-562dmL+264dm^2L^2-70dm^3L^3+8dm^4L^4\right]r^{-3+4dmL}\kappa}{(3-4dmL)^2(1-2dmL)^4(3-2dmL)^2}.
\end{aligned} \tag{5.49}$$

We found that for this case there is a ΔQ (5.5)contribution:

$$\begin{aligned}
\Delta Q &= -\frac{2187a^4\left(9-174dmL+1540dm^2L^2-8264dm^3L^3+30016dm^4L^4\right)r^{-3+4dmL}\kappa}{64L^2(1-2dmL)^6(-3+2dmL)^3(-3+4dmL)^3}\\
&-\frac{3a^4dm^5L^3\left(-888489+1702314dmL-2441220dm^2L^2+2631524dm^3L^3\right)\kappa}{(1-2dmL)^6(-3+2dmL)^3(-3+4dmL)^3r^{3-4dmL}}\\
&-\frac{24a^4dm^9L^7\left(-265107+157194dmL-66484dm^2L^2+18960dm^3L^3\right)\kappa}{(1-2dmL)^6(-3+2dmL)^3(-3+4dmL)^3r^{3-4dmL}}\\
&-\frac{1536a^4dm^{13}L^{11}(-51+4dmL)r^{-3+4dmL}\kappa}{(1-2dmL)^6(-3+2dmL)^3(-3+4dmL)^3}.
\end{aligned} \tag{5.50}$$

The term (5.50) is crucial in order for the mass to be finite. When we add (5.48), (5.49) and (5.50) together, we obtain a finite mass:

$$Q=-\frac{2abdm^2}{3}+\frac{3ab}{2L^2}+\frac{f_{rr}}{L^4\kappa}. \tag{5.51}$$

Subcase $2d$

As mentioned earlier the explicit expressions for Q_0, Q_ϕ and ΔQ are too long to present here. The expressions are significantly longer that the expressions for subcase $2c$ but

by performing the right cut-off as described at the beginning of this section we obtain a finite mass which is:

$$Q = -\frac{2abdm^2}{3} + \frac{3ab}{2L^2} + \frac{f_{rr}}{L^4\kappa}. \tag{5.52}$$

We notice here that the masses in $D = 4$, (5.45), (5.47), (5.51), (5.52) have same expression, this is a good consistency check.

Subcases $2e$ and $2f$

For the subcase $2e$ in $D = 5$ we have for the gravitational and scalar contributions:

$$\begin{aligned} Q_0 &= \frac{a^2(-2+dmL)r^{2dmL}}{2L^2} + \frac{3f_{rr}}{2L^4\kappa} \\ Q_\phi &= -\frac{a^2(-2+dmL)r^{2dmL}}{2L^2} - \frac{1}{2}abdm^2 + \frac{2ab}{L^2} \end{aligned} \tag{5.53}$$

and there is no contribution from ΔQ, and the final mass is:

$$Q = -\frac{abdm^2}{2} + \frac{2ab}{L^2} + \frac{3frr}{2L^4\kappa}. \tag{5.54}$$

Now for the subcase $2f$ in $D = 6$ we have:

$$\begin{aligned} Q_0 &= \frac{a^2(-5+2dmL)r^{2dmL}}{4L^2} + \frac{2f_{rr}}{L^4\kappa} \\ Q_\phi &= -\frac{a^2(-5+2dmL)r^{2dmL}}{4L^2} - \frac{2}{5}abdm^2 + \frac{5ab}{2L^2} \end{aligned} \tag{5.55}$$

and there is no contribution from ΔG. The total mass is:

$$Q = -\frac{2}{5}abdm^2 + \frac{5ab}{2L^2} + \frac{2f_{rr}}{L^4\kappa}. \tag{5.56}$$

where we see that all divergences cancel to give a finite mass.

Subcases $2g$ and $2h$

For subcase $2g$ the gravitational and scalar contributions are:

$$\begin{aligned} Q_0 &= \frac{a^2(-2+dmL)r^{2dmL}}{2L^2} + \frac{4a^3C_3r^{-2+3dmL}}{L^2(-2+3dmL)} + \frac{3f_{rr}}{2L^4\kappa} \\ Q_\phi &= -\frac{1}{2}abdm^2 + \frac{2ab}{L^2} - \frac{a^2(-2+dmL)r^{2dmL}}{2L^2} - \frac{4a^3C_3r^{-2+3dmL}}{L^2(-2+3dmL)} \end{aligned} \tag{5.57}$$

and there is no contribution coming from ΔQ leading to the total mass:

$$Q = -\frac{abdm^2}{2} + \frac{2ab}{L^2} + \frac{3frr}{2L^4\kappa}. \tag{5.58}$$

Subcase $2h$ is in $D = 6$ and we have:

$$\begin{aligned} Q_0 &= \frac{a^2(-5+2dmL)r^{2dmL}}{4L^2} + \frac{8a^3C_3r^{-\frac{5}{2}+3dmL}}{L^2(-5+6dmL)} + \frac{2f_{rr}}{L^4\kappa} \\ Q_\phi &= -\frac{2}{5}abdm^2 + \frac{5ab}{2L^2} - \frac{a^2(-5+2dmL)r^{2dmL}}{4L^2} - \frac{8a^3C3r^{-\frac{5}{2}+3dmL}}{L^2(-5+6dmL)} \end{aligned} \tag{5.59}$$

with no contribution from ΔQ. The total mass is:

$$Q = -\frac{2}{5}abdm^2 + \frac{5ab}{2L^2} + \frac{2f_{rr}}{L^4\kappa} \tag{5.60}$$

We notice that the masses in $D = 5$ for subcases $2e$ and $2g$ are the same. The masses for subcases $2f$ and $2h$ in $D = 6$ are also the same.

Subcases $3a$, $3b$ and $3c$

For subcase $3a$ in $D = 4$ we have:

$$\begin{aligned} Q_0 &= -\frac{a^2r}{2L^2} + \frac{f_{rr}}{L^4\kappa} + \frac{4a^3C_3\log[r]}{L^2} \\ Q_\phi &= \frac{4ab}{3L^2} + \frac{2a^3C_3}{3L^2} + \frac{a^2r}{2L^2} - \frac{4a^3C_3\log[r]}{L^2} \end{aligned} \tag{5.61}$$

and in this case $\Delta Q = 0$. The total mass is:

$$Q = \frac{4ab}{3L^2} + \frac{2a^3C_3}{3L^2} + \frac{f_{rr}}{L^4\kappa}. \tag{5.62}$$

For subcase $3b$ in $D = 5$ we have:

$$Q_0 = -\frac{2a^2r^{4/3}}{3L^2} + \frac{3f_{rr}}{2L^4\kappa} + \frac{4a^3C_3\log[r]}{L^2} \tag{5.63}$$

$$Q_\phi = \frac{16ab}{9L^2} + \frac{a^3C_3}{2L^2} + \frac{2a^2r^{4/3}}{3L^2} - \frac{4a^3C_3\log[r]}{L^2} \tag{5.64}$$

and the ΔQ contribution is zero. And the mass is:

$$Q = \frac{16ab}{9L^2} + \frac{a^3C_3}{2L^2} + \frac{3f_{rr}}{2L^4\kappa}. \tag{5.65}$$

Finally for the subcase $3c$ in $D = 6$ the gravitational and scalar contributions are:

$$\begin{aligned} Q_0 &= -\frac{5a^2r^{5/3}}{6L^2} + \frac{2f_{rr}}{L^4\kappa} + \frac{4a^3C_3\log[r]}{L^2} \\ Q_\phi &= \frac{20ab}{9L^2} + \frac{2a^3C_3}{5L^2} + \frac{5a^2r^{5/3}}{6L^2} - \frac{4a^3C_3\log[r]}{L^2} \end{aligned} \tag{5.66}$$

with no ΔQ contribution and the total mass is:

$$Q = \frac{20ab}{9L^2} + \frac{2a^3C_3}{5L^2} + \frac{2f_{rr}}{L^4\kappa}. \tag{5.67}$$

All the masses (5.62), (5.65), (5.67) depend on parameters a, b, f_{rr} and C_3.

Subcase $3d$

The expressions in this case are more complicated than the previous subcase. For the gravitational contribution we have

$$\begin{aligned} Q_0 &= -\frac{9a^4}{128L^2} + \frac{16a^3C_3r^{3/4}}{3L^2} - \frac{3a^2r^{3/2}}{8L^2} + \frac{f_{rr}}{L^4\kappa} \\ &\quad -\frac{9a^4\kappa}{32L^2} - \frac{24a^4{C_3}^2\log[r]}{L^2} + \frac{3a^4C_4\log[r]}{L^2} + \frac{81a^4\kappa\log[r]}{256L^2} \end{aligned} \tag{5.68}$$

and for the scalar contribution we have:

$$\begin{aligned} Q_\phi &= \frac{9a^4}{128L^2} + \frac{9ab}{8L^2} + \frac{56a^4{C_3}^2}{3L^2} + \frac{a^4C_4}{3L^2} - \frac{16a^3C_3r^{3/4}}{3L^2} \\ &\quad +\frac{3a^2r^{3/2}}{8L^2} + \frac{9a^4\kappa}{64L^2} + \frac{24a^4{C_3}^2Log[r]}{L^2} - \frac{3a^4C4\log[r]}{L^2} \\ &\quad -\frac{81a^4\kappa\log[r]}{256L^2}. \end{aligned} \tag{5.69}$$

There is also an extra gravitational contribution to make the divergences cancel:

$$\Delta Q = \frac{27a^4\kappa}{256L^2}. \tag{5.70}$$

Adding the three contributions (5.68), (5.69), (5.70) together gives us a finite mass:

$$Q = \frac{9ab}{8L^2} + \frac{56a^4C_3^2}{3L^2} + \frac{a^4C_4}{3L^2} + \frac{f_{rr}}{L^4\kappa} - \frac{9a^4\kappa}{256L^2}. \tag{5.71}$$

The mass for this subcase depends in a, b, f_{rr}, C_3 and C_4.

Subcase $3e$

This subcase is in $D = 4$. This is the most complicated logarithmic case. For the gravitational contribution we have:

$$\begin{aligned} Q_0 &= \frac{a^5 C_3}{L^2} + \frac{10a^3 C_3 r^{6/5}}{3L^2} - \frac{3a^2 r^{9/5}}{10L^2} + \frac{f_{rr}}{L^4\kappa} + \frac{4a^5 C_3 \kappa}{L^2} \\ &\quad + r^{3/5}\left(-\frac{9a^4}{200L^2} - \frac{125a^4 {C_3}^2}{3L^2} + \frac{5a^4 C_4}{L^2} + \frac{27a^4\kappa}{100L^2}\right) \\ &\quad - \frac{400a^5 C_3 C_4 \log[r]}{9L^2} + \frac{8a^5 C_5 Log[r]}{3L^2} - \frac{4a^5 C_3 \kappa \log[r]}{L^2} + \frac{1250a^5 {C_3}^3 \log[r]}{9L^2} \end{aligned} \tag{5.72}$$

and for the scalar one we have:

$$\begin{aligned} Q_\phi &= \frac{24ab}{25L^2} - \frac{a^5 C_3}{L^2} - \frac{8125a^5 {C_3}^3}{36L^2} + \frac{800a^5 C_3 C_4}{27L^2} \\ &\quad + \frac{2a^5 C_5}{9L^2} - \frac{10a^3 C_3 r^{6/5}}{3L^2} + \frac{3a^2 r^{9/5}}{10L^2} + \frac{13a^5 C_3 \kappa}{15L^2} \\ &\quad + r^{3/5}\left(\frac{9a^4}{200L^2} + \frac{125a^4 {C_3}^2}{3L^2} - \frac{5a^4 C_4}{L^2} - \frac{27a^4\kappa}{80L^2}\right) \\ &\quad + \frac{400a^5 C_3 C_4 \log[r]}{9L^2} - \frac{8a^5 C_5 \log[r]}{3L^2} + \frac{4a^5 C_3 \kappa \log[r]}{L^2} \\ &\quad + \frac{3125a^5 {C_3}^3}{108L^2} - \frac{1250a^5 {C_3}^3 \log[r]}{9L^2}. \end{aligned} \tag{5.73}$$

There is also an extra gravitational contribution:

$$\Delta Q = -\frac{3a^5 C_3 \kappa}{2L^2} + \frac{27a^4 r^{3/5}\kappa}{400L^2} \tag{5.74}$$

When we add everything together we have:

$$\begin{aligned} Q &= \frac{24ab}{25L^2} - \frac{8125a^5 C_3^3}{36L^2} + \frac{800a^5 C_3 C_4}{27L^2} \\ &\quad + \frac{2a^5 C_5}{9L^2} + \frac{f_{rr}}{L^4\kappa} + \frac{101a^5 C_3 \kappa}{30L^2} + \frac{3125a^5 C_3^3}{108L^2} \end{aligned} \tag{5.75}$$

we see that the coefficients C_3, C_4, C_5 appear. As for the other subcases the mass also depends on the parameters a, b and f_{rr}.

5.3.3 Summary table

We have seen that all the masses for all the subcases are finite. The correct gravitational and scalar contributions are different for every subcase. By adding these two contributions the divergent terms vanish. All masses depend on parameters a, b and f_{rr}. The coefficient C_3 appears in the masses for subcases $3a, 3b, 3c, 3d, 3e$, the coefficient C_4 appears in subcases $3d$ and $3c$. Finally the coefficient C_5 only appears in subcase $3e$. We summarise all the results in the following table:

Case	constraints on dm^2	dimension	mass
$2a$	$0 < dm^2 < \frac{1}{4L^2}$	4	$-\frac{2abdm^2}{3} + \frac{3ab}{2L^2} + \frac{f_{rr}}{L^4\kappa}$
$2b$	$\frac{1}{4L^2} < dm^2 < \frac{9}{16L^2}$	4	$-\frac{2abdm^2}{3} + \frac{3ab}{2L^2} + \frac{f_{rr}}{L^4\kappa}$
$2c$	$\frac{9}{16L^2} < dm^2 < \frac{81}{100L^2}$	4	$-\frac{2abdm^2}{3} + \frac{3ab}{2L^2} + \frac{f_{rr}}{L^4\kappa}$
$2d$	$\frac{81}{100L^2} < dm^2 < \frac{1}{L^2}$	4	$-\frac{2abdm^2}{3} + \frac{3ab}{2L^2} + \frac{f_{rr}}{L^4\kappa}$
$2e$	$0 < dm^2 < \frac{(d-1)^2}{36L^2}$	5	$-\frac{abdm^2}{2} + \frac{2ab}{L^2} + \frac{3f_{rr}}{2L^4\kappa}$
$2f$	$0 < dm^2 < \frac{(d-1)^2}{36L^2}$	6	$-\frac{2}{5}abdm^2 + \frac{5ab}{2L^2} + \frac{2f_{rr}}{L^4\kappa}$
$2g$	$\frac{(d-1)^2}{36L^2} < dm^2 < \frac{1}{L^2}$	5	$-\frac{abdm^2}{2} + \frac{2ab}{L^2} + \frac{3f_{rr}}{2L^4\kappa}$
$2h$	$\frac{(d-1)^2}{36L^2} < dm^2 < \frac{1}{L^2}$	6	$-\frac{2}{5}abdm^2 + \frac{5ab}{2L^2} + \frac{2f_{rr}}{L^4\kappa}$
$3a$	$dm = \frac{(d-1)^2}{36L^2}$	4	$\frac{4ab}{3L^2} + \frac{2a^3C_3}{3L^2} + \frac{f_{rr}}{L^4\kappa}$
$3b$	$dm = \frac{(d-1)^2}{36L^2}$	5	$\frac{16ab}{9L^2} + \frac{a^3C_3}{2L^2} + \frac{3f_{rr}}{2L^4\kappa}$
$3c$	$dm = \frac{(d-1)^2}{36L^2}$	6	$\frac{20ab}{9L^2} + \frac{2a^3C_3}{5L^2} + \frac{2f_{rr}}{L^4\kappa}$
$3d$	$dm = \frac{9}{16L^2}$	4	$\frac{9ab}{8L^2} + \frac{56a^4C_3^2}{3L^2} + \frac{a^4C_4}{3L^2} - \frac{9a^4\kappa}{256L^2} + \frac{f_{rr}}{L^4\kappa}$
$3e$	$dm = \frac{81}{100L^2}$	4	$\frac{24ab}{25L^2} - \frac{8125a^5C_3^3}{36L^2} + \frac{800a^5C_3C_4}{27L^2}$ $+ \frac{2a^5C_5}{9L^2} + \frac{101a^5C_3\kappa}{30L^2} + \frac{3125a^5C_3^3}{108L^2} + \frac{f_{rr}}{L^4\kappa}$

Table 5.1: Summary of mass expressions

5.3.4 Cases 1 and 4

We briefly discuss cases 1 and 4. These are not stable cases as seen in chapter 3. They will not be considered for further investigation. The simplest case is case 1, this case does not arise in practice as it has been discussed in chapter 3. For this case in $D = 4$:

$$Q = \frac{f_{rr}}{L^4\kappa} \tag{5.76}$$

For case 4 we found the mass to be:

$$\begin{aligned} Q(\xi) &= \frac{13}{27}abdm^2 + \frac{3ab}{2L^2} + \frac{f_{rr}}{L^4\kappa} \\ &+ \left(\frac{5}{54}dm^2 + \frac{3}{4L^2} - \frac{i}{3L}dm + \frac{27i}{32dmL^3\kappa} + \frac{3i}{8L\kappa}dm\right) a^2 r^{\frac{4}{3}idmL} \\ &+ \left(\frac{5}{54}dm^2 + \frac{3}{4L^2} - \frac{i}{3L}dm - \frac{27i}{32dmL^3\kappa} - \frac{3i}{8L\kappa}dm\right) b^2 r^{-\frac{4}{3}idmL} \end{aligned} \tag{5.77}$$

and the coefficients A and B in Table 4.2 were found to be:

$$\begin{aligned} A &= \frac{27iL}{32dm}a^2 + \frac{3}{8}ia^2dmL^3 \\ B &= -\frac{27iL}{32dm}b^2 - \frac{3}{8}ib^2dmL^3. \end{aligned}$$

It is not possible to determine if a finite mass exists for this case. There are three possibilities. The first one is that there is a fundamental relation between the scalar field parameters a and b which will give a limit to the mass function. The second possibility is that we need another counterterm that will make the mass finite. Finally it is also possible that for this case there is no limit, the mass function oscillates without converging. In this case a mass cannot be determined.

§ 5.4 Summary

In this chapter we have seen how to obtain finite expressions for the spacetime mass. We have seen that there are two contribution, a gravitational contribution and a scalar contributions. The expressions for these two contributions are not finite as $r \to \infty$. We showed how to perform the right cut-offs to obtain expressions for both. As we have seen in our example the gravitational (5.39) and the scalar contribution (5.44) diverge when $r \to \infty$ but when we add them together we obtain a finite mass. We emphasis the fact that the cut-off is different for every case. Cases were treated separately to ensure that the final mass is finite. The expressions for the mass we obtained contain

the a, b and f_{rr} parameters. In order to calculate the masses that we found we need to compute these parameters numerically.

Chapter 6

Calculation of the mass and numerical method

In this chapter we restrict our attention to black holes. We are interested in calculating the masses of spacetimes which have black hole hair. One can see from Table 5.1 that the expressions for the masses contain b and f_{rr} which are hard to obtain. The reason is because they appear in subleading terms in ϕ and h_{rr} as can be seen in Tables 4.1 and 4.2. In this chapter we present a method of finding these parameters. This method comes from a similar problem faced when dealing with the peeling property of perturbations of Kerr black holes [88]. Ingoing and outgoing waves have different r behaviour for large r, the amplitude for ingoing and outgoing waves depend on different powers of r. This problem is dealt with numerically by performing a transformation to make ingoing and outgoing waves have the same amplitudes [120]. We are faced with a similar situation where b and f_{rr} are contained in subleading terms which are small compared to the leading order behaviour which contains a. We follow the approach of Press and Teukolsky [113] by defining new functions $\xi(r)$ and $\psi(r)$ whose leading behaviour is proportional to b and f_{rr} respectively. We show how to analytically obtain the differential equations for these functions for a particular subcase. We then implement the steps in mathematica and produce code to solve the resulting differential equations for Higgs (3.49), TWI and pseudo-TWI (3.50) potentials. We find a, b and f_{rr} which allows us to calculate the mass and study it for different subcases.

§ 6.1 Equation for $\xi(r)$

We want to define a function whose leading behaviour at infinity depends on b so when we numerically integrate it we obtain the value of the parameter b. We start by

constructing such a function for subcase $2a$. We will show the detailed calculations for this subcase.

Let us start with the asymptotic form of the scalar field in subcase $2a$:

$$\phi = \frac{a}{r^{\Delta_-}} + \frac{b}{r^{\Delta_+}} + ... \tag{6.1}$$

Dividing (6.1) by the leading order behaviour we have:

$$\frac{\phi}{r^{-\Delta_-}} = a + \frac{b}{r^{\Delta_+ - \Delta_-}} + ... \tag{6.2}$$

where we see that in order to obtain a function whose leading order behaviour is proportional to b we have to differentiate (6.2). Hence we define:

$$\xi(r) = \left(\frac{\phi}{r^{-\Delta_-}}\right)' \tag{6.3}$$

where the prime indicates differentiation with respect to r. The asymptotic form of $\xi(r)$ is:

$$\xi = (-\Delta_+ + \Delta_-) b r^{-\Delta_+ + \Delta_- - 1} + ... \tag{6.4}$$

In order to obtain values of the parameter b we need to find an ordinary differential equation for $\xi(r)$ which is suitable for numerical integration. We write (6.3) as:

$$\xi = \phi' r^{\Delta_-} + \Delta_- \phi r^{\Delta_- - 1} \tag{6.5}$$

and taking the derivative with respect to r gives

$$\xi' = \frac{\phi''}{r^{-\Delta_-}} + \frac{2\phi'\Delta_-}{r^{-\Delta_-+1}} + \frac{\Delta_-(\Delta_- - 1)\phi}{r^{-\Delta_-+2}}. \tag{6.6}$$

From the field equation (3.8):

$$\phi'' = -\left(\frac{H'}{H} + \delta' + \frac{2}{r}\right)\phi' + \frac{1}{H}\frac{\partial V}{\partial \phi} \tag{6.7}$$

and substituting for ϕ'' in (6.6):

$$\xi' = -\frac{\phi'}{r^{-\Delta_-}}\left(\frac{H'}{H} + \delta' + \frac{2}{r}\right) + \frac{r^{\Delta_-}}{H}\frac{\partial V}{\partial \phi} + \frac{2\phi'\Delta_-}{r^{-\Delta_-+1}} + \frac{\Delta_-(\Delta_- - 1)\phi}{r^{-\Delta_-+2}}. \tag{6.8}$$

To eliminate ϕ' from (6.8) we write (6.5) as:

$$\frac{\phi'}{r^{-\Delta_-}} = \xi(r) - \frac{\Delta_-\phi}{r^{-\Delta_-+1}} \tag{6.9}$$

and we rearrange (6.8) to obtain:

$$H\xi' + \left[H' + H\delta' + \frac{2H}{r}(1-\Delta_-)\right]\xi = \Delta_- r^{\Delta_- -1}\phi\left[H' + H\delta' + \frac{2H}{r}(1-\Delta_-)\right] + r^{\Delta_-}\frac{\partial V}{\partial \phi} + \Delta_-(\Delta_- - 1)Hr^{\Delta_- -2}\phi. \quad (6.10)$$

In order to make the leading order term obvious as $r \to \infty$, we want to express $H(r)$ in terms of $J(r)$ and $V(\phi)$ in terms of $U(\phi)$, we remind here for convenience that:

$$V = \frac{1}{2}m^2\phi^2 + U \quad (6.11)$$

and

$$\frac{\partial V}{\partial \phi} = m^2\phi + \frac{\partial U}{\partial \phi} \quad (6.12)$$

where

$$U(\phi) = C_3\phi^3 + C_4\phi^4 + C_5\phi^5. \quad (6.13)$$

The metric function $H(r)$ is:

$$H = \frac{r^2}{L^2} + k + J \quad (6.14)$$

with the derivative with respect to r being:

$$H' = \frac{2r}{L^2} + J'. \quad (6.15)$$

After we perform the substitutions, (6.10) becomes

$$\begin{aligned} H\xi' + \left[H' + H\delta' + \frac{2H}{r}(1-\Delta_-)\right]\xi \\ = r^{\Delta_-}\phi\left[\frac{2\Delta_-}{L^2} + \frac{\Delta_- J'}{r} + \frac{\Delta_- H\delta'}{r} + \frac{2\Delta_-}{r^2}(1-\Delta_-)\left(\frac{r^2}{L^2} + k + J\right)\right] \\ + r^{\Delta_-}\phi\left[m^2 + \frac{\Delta_-(\Delta_- - 1)}{r^2}\left(\frac{r^2}{L^2} + k + J\right)\right] + r^{\Delta_-}\frac{\partial U}{\partial \phi} \end{aligned} \quad (6.16)$$

and after some simplification the right hand side of (6.16) becomes:

$$\begin{aligned} H\xi' + \left[H' + H\delta' + \frac{2H}{r}(1-\Delta_-)\right]\xi \\ = r^{\Delta_-}\phi\left[\frac{\Delta_- J'}{r} + \frac{\Delta_- H\delta'}{r} + \frac{\Delta_-(1-\Delta_-)(k+J)}{r^2}\right] \\ + r^{\Delta_-}\phi\left[-\frac{\Delta_-^2}{L^2} + \frac{3\Delta_-}{L^2} + m^2\right] + r^{\Delta_-}\frac{\partial U}{\partial \phi}. \end{aligned} \quad (6.17)$$

Now using the quadratic equation (3.25) for $D = 4$, the last term in square brackets vanishes and the differential equation for $\xi(r)$ simplifies to:

$$H\xi' + \left[H' + H\delta' + \frac{2H}{r}(1-\Delta_-)\right]\xi \\ = r^{\Delta_-}\phi\left[\frac{\Delta_- J'}{r} + \frac{\Delta_- H\delta'}{r} + \frac{\Delta_-(1-\Delta_-)(k+J)}{r^2}\right] + r^{\Delta_-}\frac{\partial U}{\partial \phi}. \quad (6.18)$$

This is done in order to check if the apparent leading terms cancel or if they are indeed the leading order terms. The right hand side of (6.18) can no longer be simplified. Now let us check the leading order behaviour of the expression in square bracket on the left hand side. Again writing $H(r)$ and $H'(r)$ as in (6.14) and (6.15) respectively we obtain:

$$H' + H\delta' + \frac{2H}{r}(1-\Delta_-) = \frac{2r}{L^2}(2-\Delta_-) + H\delta' + J' + \frac{2(k+J)}{r}(1-\Delta_-) \quad (6.19)$$

and putting this back into (6.18) we obtain the differential equation for $\xi(r)$:

$$H\xi' + \left[\frac{2r}{L^2}(2-\Delta_-) + H\delta' + J' + \frac{2(k+J)}{r}(1-\Delta_-)\right]\xi \\ = r^{\Delta_-}\phi\left[\frac{\Delta_- J'}{r} + \frac{\Delta_- H\delta'}{r} + \frac{\Delta_-(1-\Delta_-)(k+J)}{r^2}\right] + r^{\Delta_-}\frac{\partial U}{\partial \phi}. \quad (6.20)$$

Because the expressions for the scalar field are more complicated we first wrote a mathematica code to solve for case $2a$ algebraically then extended the code to the rest of the cases. The asymptotic forms for the function ξ can be found in table (6.1).

§ 6.2 Equation for $J''(r)$

Before we move onto defining the other function $\psi(r)$ we need to find an expression for $J''(r)$ that we will use in the next subsection. The function $J(r)$ can be written in terms of metric perturbation h_{rr} as shown in (4.33). We need to find an expression for $J''(r)$ from the field equation (3.44).

From (3.44) we have:

$$J' = -\frac{(D-3)}{r}J - \frac{r}{(D-2)}H\phi'^2 - \frac{2r}{D-2}V. \quad (6.21)$$

Differentiating it with respect to r gives

$$\begin{aligned} J'' &= \frac{(D-3)}{r^2}J - \frac{(D-3)}{r}J' - \frac{1}{(D-2)}H\phi'^2 - \frac{r}{(D-2)}H'\phi'^2 - \frac{2rH}{(D-2)}\phi'\phi'' \\ &\quad -\frac{2V}{(D-2)} - \frac{2r}{(D-2)}\frac{\partial V}{\partial \phi}\phi'. \end{aligned} \tag{6.22}$$

Now using the scalar field equation (3.8):

$$\frac{2r}{D-2}H\phi'\phi'' = -\frac{2r}{(D-2)}\left[H' + H\delta' + (d-2)\frac{H}{r}\right]\phi'^2 + \frac{2r}{(D-2)}\frac{\partial V}{\partial \phi}\phi' \tag{6.23}$$

and substituting into (6.22)

$$\begin{aligned} J'' &= \frac{D-3}{r^2}J - \frac{(D-3)}{r}J' - \frac{4r}{(D-2)}\frac{\partial V}{\partial \phi}\phi' \\ &\quad -\frac{2V}{(D-2)} + \frac{r\phi'^2}{(D-2)}\left[H' + 2H\delta' + \frac{H}{r}(2D-5)\right]. \end{aligned} \tag{6.24}$$

In order to obtain an equation that does not depend on J we use (6.21) to write:

$$\frac{(D-3)}{r^2}J = -\frac{J'}{r} - \frac{H\phi'^2}{(D-2)} - \frac{2V}{(D-2)}. \tag{6.25}$$

The final expression for J'' that will be used in the field equations for the new function $\psi(r)$ is:

$$J'' = -\frac{(D-2)}{r}J' + \frac{r\phi'^2}{D-2}\left[H' + 2H\delta' + \frac{2H}{r}(D-3)\right] - 2r\phi'\frac{\partial V}{\partial \phi} - V. \tag{6.26}$$

§ 6.3 Equation for $\psi(r)$

We want to define a function whose leading order behaviour contains f_{rr}. We have seen in chapter 5 that h_{rr} and $J(r)$ are related by (4.33). We have seen how to simplify $J(r)$ using mathematica, always keeping the f_{rr} term. Let us call J_{short} the simplified expression for $J(r)$. In the subcase $2a$ the form of J_{short} is:

$$J_{short} = a_0 r^{\sigma} + f_{rr} b_0 r^{\sigma_1} \tag{6.27}$$

where a_0, b_0 are parameters, and σ, σ_1 have real values and depend on the value of dm. Using the same reasoning as for $\xi(r)$ in section 7.1, we start by dividing J_{short} by its leading order behaviour:

$$\frac{J_{short}}{a_0 r^{\sigma}} = 1 + \frac{f_{rr} b_0 r^{\sigma_1}}{a_0 r^{\sigma}}. \tag{6.28}$$

If we differentiate (6.28) with respect to r we obtain

$$\left(\frac{J_{short}}{a_0 r^\sigma}\right)' = \frac{f_{rr} b_0}{a_0}(\sigma_1 - \sigma) r^{\sigma_1 - \sigma - 1} + ... \tag{6.29}$$

We can see that the leading order behaviour in (6.29) contains f_{rr}.

Motivated by (6.29) we define a new function $\psi(r)$ for subcase $2a$:

$$\psi(r) = \left(\frac{J}{r^\sigma}\right)' = \frac{J'}{r^\sigma} - \frac{\sigma J}{r^{\sigma+1}} \tag{6.30}$$

where

$$\sigma = -1 + 2dmL = 2 - 2\Delta_-. \tag{6.31}$$

Differentiating (6.30):

$$\psi'(r) = \frac{J''}{r^\sigma} - \frac{2\sigma J'}{r^{\sigma+1}} + \frac{\sigma(\sigma+1)J}{r^{\sigma+2}} \tag{6.32}$$

where we see that the term J'' appears. Rewriting (6.32), we have:

$$r^{\sigma+2}\psi' + (\sigma+2) r^{\sigma+1}\psi = r^2 J'' + rJ'(2-\sigma) - J\sigma. \tag{6.33}$$

Now using (6.24) with $D = 4$:

$$r^2 J''(r) = J(r) - rJ'(r) - 2r^3\phi' \frac{\partial V}{\partial \phi} - r^2 V + \frac{r^2\phi'^2}{2}\left(rH' + 3H + 2rH\delta'\right). \tag{6.34}$$

Next we define:

$$r^{\sigma+2}\psi' + (\sigma+2) r^{\sigma+1}\psi' = \mathcal{D} \tag{6.35}$$

where the right-hand-side is:

$$\mathcal{D} = rJ'(1-\sigma) + (1-\sigma)J - 2r^3\phi' \frac{\partial V}{\partial \phi} - r^2 V + \frac{r^2\phi'^2}{2}\left[rH' + 3H + 2rH\delta'\right]. \tag{6.36}$$

From the field equation (3.44) with $D = 4$:

$$rJ' + J = -\frac{1}{2} H r^2 \phi'^2 - r^2 V, \tag{6.37}$$

so $\mathcal{D}$ becomes:

$$\mathcal{D} = -2r^3\phi' \frac{\partial V}{\partial \phi} - (2-\sigma) r^2 V + \frac{1}{2} r^2 \phi'^2 \left[rH' + 2rH\delta' + (2+\sigma)H\right]. \tag{6.38}$$

To simplify this further and make the leading order behaviour explicit we write H and V as in (6.11) and (6.14) we also use (6.5) to write:

$$r\phi' = r^{1-\Delta_-}\xi - \Delta_-\phi. \tag{6.39}$$

After these substitutions we obtain:

$$\begin{aligned}\mathcal{D} &= \left[2\Delta_- m^2 - \left(1-\frac{\sigma}{2}\right)m^2 + \frac{\Delta_-^2}{L^2}\left(2+\frac{\sigma}{2}\right)\right] r^2\phi - 2r^{3-\Delta_-}\xi\left(m^2\phi + \frac{\partial U}{\partial\phi}\right) \\ &+\frac{1}{2}\left(r^{2-2\Delta_-}\xi^2 - 2\Delta_- r^{1-\Delta_-}\xi\phi\right)\left[(4+\sigma)\frac{r^2}{L^2} + rJ' + 2rH\delta' + (2+\sigma)(k+J)\right] \\ &+\frac{1}{2}\Delta_-^2\phi^2\left(rJ' + 2rH\delta' + (2+\sigma)(k+J)\right) + 2r^2\Delta_-\phi\frac{\partial U}{\partial\phi} - (2-\sigma)r^2U. \end{aligned}\tag{6.40}$$

We name the leading order coefficient $\mathcal{D}_0$:

$$\mathcal{D}_0 = 2\Delta_- m^2 - \left(1-\frac{\sigma}{2}\right)m^2 + \frac{\Delta_-^2}{L^2}\left(2+\frac{\sigma}{2}\right). \tag{6.41}$$

Now, we consider the quadratic equation (3.25) for Δ_- in $D=4$ which has the form:

$$\frac{\Delta_-^2}{L^2} - \frac{3\Delta_-}{L^2} - m^2 = 0 \tag{6.42}$$

so we have:

$$\Delta_-^2 = 3\frac{\Delta_-}{L^2} + m^2 \tag{6.43}$$

and substituting this in (6.41) we obtain:

$$\mathcal{D}_0 = m^2\left(2\Delta_- + 1 + \sigma\right) + \frac{3\Delta_-}{L^2}\left(2+\frac{\sigma}{2}\right). \tag{6.44}$$

The general expression for the scalar field mass is:

$$m^2 = -\frac{(D-1)^2}{4L^2} + dm^2 \tag{6.45}$$

so in $D=4$ the mass is given by

$$m^2 = -\frac{9}{4L^2} + dm^2. \tag{6.46}$$

Putting this into (6.42) we have:

$$\frac{\Delta_-^2}{L^2} - \frac{3\Delta_-}{L^2} + \frac{9}{4L^2} - dm^2 = 0 \tag{6.47}$$

and from this we can check that the smaller root is:

$$\Delta_- = \frac{3}{2} - dmL. \tag{6.48}$$

Using the equation (6.31) for σ we have

$$2 + \frac{\sigma}{2} = 3 - \Delta_- \tag{6.49}$$

and substituting (6.48) and (6.49) in (6.44) we obtain

$$\mathcal{D}_0 \;=\; 3m^2 + \frac{9}{L^2} - \frac{3\Delta_-^2}{L^2} = 0 \tag{6.50}$$

The above calculations show that we obtained the cancellation of the apparent leading behaviour. Therefore we have a new expression for $\mathcal{D}$:

$$\begin{aligned}
\mathcal{D} \;=\; & -\mathcal{D}_1 2r^{3-\Delta_-}\xi\phi - 2r^{3-\Delta}\xi\phi\frac{\partial U}{\partial\phi} + 2r^2\Delta_-\phi\frac{\partial U}{\partial\phi} - (2-\sigma)r^2U \\
& + \frac{1}{2}r^{2-2\Delta_-}\xi^2\left[(4+\sigma)\frac{r^2}{L^2} + rJ' + 2rH\delta' + (2+\sigma)(k+J)\right] \\
& - \Delta_- r^{1-\Delta_-}\xi\phi\left[(4+\sigma)\frac{r^2}{L^2} + rJ' + 2rH\delta' + (2+\sigma)(k+J)\right] \\
& + \frac{1}{2}\Delta_-^2\phi^2\left[rJ' + 2rH\delta' + (2+\sigma)(k+J)\right]
\end{aligned} \tag{6.51}$$

where

$$\mathcal{D}_1 \;=\; -2m^2 - (4+\sigma)\frac{\Delta_-}{L^2} = 2\left(\frac{\Delta_-^2}{L^2} - \frac{3\Delta_-}{L^2} - m^2\right) = 0. \tag{6.52}$$

So $\mathcal{D}_1$ also cancels and we can simplify (6.51):

$$\begin{aligned}
\mathcal{D} \;=\; & 2\frac{\partial U}{\partial\phi}\left(r^2\Delta_-\phi - r^{3-\Delta_-}\xi\right) - (2-\sigma)r^2U \\
& + \frac{1}{2}r^{2-2\Delta_-}\xi^2\left[(4+\sigma)\frac{r^2}{L^2} + rJ' + 2rH\delta' + (2+\sigma)(k+J)\right] \\
& + \left(\frac{1}{2}\Delta_-^2\phi^2 - \Delta_- r^{1-\Delta_-}\xi\phi\right)\left[rJ' + 2rH\delta' + (2+\sigma)(k+J)\right].
\end{aligned} \tag{6.53}$$

Putting (6.53) back into (6.35) we obtain the field equation for $\psi(r)$:

$$r^{\sigma+2}\psi' + (\sigma+2)r^{\sigma+1}\psi = 2\frac{\partial U}{\partial \phi}\left(r^2\Delta_-\phi - r^{3-\Delta_-}\xi\right) - (2-\sigma)r^2U + \frac{1}{2}r^{2-2\Delta_-}\xi^2\left[(4+\sigma)\frac{r^2}{L^2} + rJ' + 2rH\delta' + (2+\sigma)(k+J)\right] + \left(\frac{1}{2}\Delta_-^2\phi^2 - \Delta_- r^{1-\Delta_-}\xi\phi\right)\left[rJ' + 2rH\delta' + (2+\sigma)(k+J)\right]. \quad (6.54)$$

All possible cancellations have been performed algebraically so (6.54) is the right form for the field equation for $\psi(r)$ that we can implement in mathematica.

For the other cases the expressions for $\xi(r)$ and $\psi(r)$ are more complex because the expressions for the asymptotic behaviour of $\phi(r)$ and h_{rr} contain more terms as can be seen in Tables 4.1, 4.2. The analysis for subcase $2a$ shown above allowed us to write a mathematica code to extend the method and obtain algebraic expressions for ξ and ψ. We present these expressions in Table 6.1. In order to better understand how to extend the above analysis to the more complex subcases we discuss subcase $2b$ in the next section.

Case	dm	$\xi(r)$	$\psi(r)$
$2a$	$0 < dm < \frac{1}{2}$	$-\frac{2bdm}{a} r^{-1-2dm}$	$-\frac{2dmf_{rr}}{a^2} r^{-1-2dm}$
$2b$	$\frac{1}{2} < dm < \frac{3}{4}$	$-\frac{2bdm}{a} r^{-1-2dm}$	$-\frac{2dmf_{rr}}{a^2} r^{-1-2dm}$
$2c$	$\frac{3}{4} < dm < \frac{9}{10}$	$-\frac{2bdm}{a} r^{-1-2dm}$	$-\frac{2dmf_{rr}}{a^2} r^{-1-2dm}$
$2d$	$\frac{9}{10} < dm < 1$	$-\frac{2bdm}{a} r^{-1-2dm}$	$-\frac{2dmf_{rr}}{a^2} r^{-1-2dm}$
$2e$	$0 < dm < \frac{2}{3}$	$-\frac{2bdmL}{a} r^{-1-2dmL}$	$\frac{2dmf_{rr}}{a^2 L\alpha_1} r^{-1-2dmL}$
$2f$	$0 < dm < \frac{5}{6}$	$-\frac{2bdmL}{a} r^{-1-2dmL}$	$\frac{2dmf_{rr}}{a^2 L\alpha_1} r^{-1-2dmL}$
$2g$	$\frac{2}{3} < dm < 1$	$-\frac{2bdmL}{a} r^{-1-2dmL}$	$\frac{2dmf_{rr}}{a^2 L\alpha_1} r^{-1-2dmL}$
$2h$	$\frac{5}{6} < dm < 1$	$-\frac{2bdmL}{a} r^{-1-2dmL}$	$\frac{2dmf_{rr}}{a^2 L\alpha_1} r^{-1-2dmL}$
$3a$	$1/2$	$-\frac{b}{a} r^{-2}$	$\frac{2f_{rr}}{a^2L^2} r^{-2}$
$3b$	$2/3$	$-\frac{4b}{3a} r^{-7/3}$	$\frac{2f_{rr}}{a^2L^2} r^{-7/3}$
$3c$	$5/6$	$-\frac{3b}{5a} r^{-8/3}$	$\frac{2f_{rr}}{a^2L^2} r^{-8/3}$
$3d$	$3/4$	$-\frac{3b}{2a} r^{-5/2}$	$\frac{4f_{rr}}{a^2L^2} r^{-5/2}$
$3e$	$9/10$	$-\frac{9b}{5a} r^{-14/5}$	$\frac{6f_{rr}}{a^2L^2} r^{-14/5}$

Table 6.1: leading order behaviour of $\xi(r)$ and $\psi(r)$

§ 6.4 Numerical method

We are interested in the behaviour of ϕ, ξ and ψ at infinity and we want to extract the values of the mass parameters a, b and f_{rr}. For this purpose we use NDSolve in mathematica to solve the differential equations for $\phi(r)$, $\xi(r)$ (6.3) and $\psi(r)$ (6.30) using our own numerical code. We present the method in detail for subcase $2a$ and we explain how we extended it to the rest of the cases. Similarly, for the plots showing our results, we present the plots for subcase $2a$ in detail. For the rest of the cases we present a selection of plots and comment on interesting features. We used the Higgs potential as defined in (3.55). For the TWI potential as defined in (3.58) we faced numerical problems when trying to obtain the plots. We therefore considered a modified potential that we refer to as a pseudo-TWI potential defined as:

$$V(\phi) = A\phi^2 + A\phi^3 + A\frac{\phi^4}{2!} + A\frac{\phi^5}{3!} \tag{6.55}$$

where

$$A = \frac{m^2}{2}. \tag{6.56}$$

The shape of the potential is:

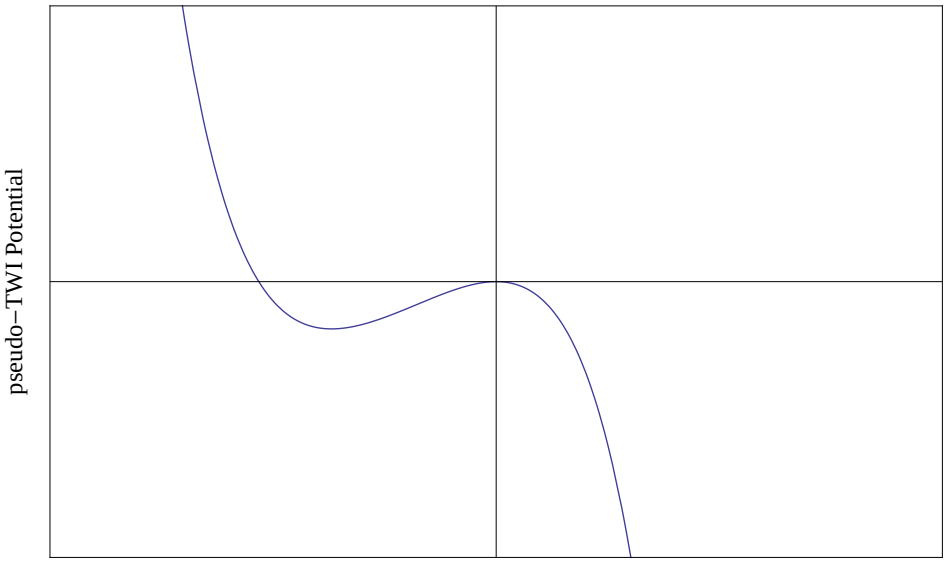

Figure 6.1: Shape of the pseudo-TWI potential with $m^2 < 0$, showing a maximum at $\phi = 0$

We see from Fig. 6.1 that the pseudo-TWI in nonconvex, it therefore has the required feature. It has a local maximum at $\phi = 0$ to which the scalar field will be attracted at infinity [129]. In the plots we will make clear which potential we used (TWI or pseudo-TWI).

6.4.1 Solving for ξ and ψ numerically

Subcase $2a$

We describe the numerical implementation for solving the differential equations for subcase $2a$ for the Higgs potential (3.55) with $k = 1$. We first begin by fixing parameters such as D and dm, in the subcase case $2a$ with Higgs potential we choose $dm = 1/4$ and we set $\kappa = L = 1$. We put in the details for the asymptotics for $\phi(r)$ and h_{rr} for case $2a$ which we can see in Tables 4.1 and 4.2. We obtain a simplified expression for the function $J(r)$ using the loop described in chapter 4. In this case for J_{Short} we have:

$$J_{Short} = -\frac{f_{rr}}{r} + \frac{5a^2}{8} r^{-1/2}. \tag{6.57}$$

We then define $\xi(r)$ as in (6.3) which gives us the leading behaviour as $r \to \infty$:

$$\xi = -\frac{b}{2a} r^{-3/2} + ... \tag{6.58}$$

and we call $\sigma_3 = 3/2$. We see that b is contained in the coefficient of the leading behaviour of ξ, we can define:

$$\xi_{Coeff} = -\frac{b}{2a} \tag{6.59}$$

and b is then just

$$b = -2a\xi_{Coeff}. \tag{6.60}$$

We also see that as $r \to \infty$:

$$\xi r^{\sigma_3} = -\frac{b}{2a} + ... \tag{6.61}$$

so when plotting (6.61) we should see it converging to ξ_{Coeff}.

Similarly for the function ψ we have:

$$\psi = \frac{4f_{rr}}{5a^2} r^{-3/2} + ..., \tag{6.62}$$

where we define $\sigma_4 = 3/2$. We see that f_{rr} is contained in the coefficient of the leading behaviour of ψ. We define:

$$\psi_{Coeff} = \frac{4f_{rr}}{5a^2} \tag{6.63}$$

and we can extract the expression for f_{rr}:

$$f_{rr} = \frac{\psi_{Coeff} 5a^2}{4}. \tag{6.64}$$

When we plot:

$$\psi r^{\sigma_4} \to \frac{4 f_{rr}}{5a^2 L^2} \tag{6.65}$$

as $r \to \infty$ we should observe a convergence to ψ_{Coeff}.

The next step is to write the differential equations for ξ and ψ in the same form as in (6.20) and (6.54) respectively. In our mathematica code we make substitutions so that the differential equation for ξ will depend on ϕ and $J(r)$ functions only. The differential equation for ψ is then written in terms of ξ. We write a mathematica code that solves the differential equation for ϕ to find a and then solves the differential equations for ξ (6.20) and ψ (6.54). As can be seen in (6.60) and (6.64) both b and f_{rr} depend on a. We solve the differential equations (6.20) and (6.54) using NDSolve.

The rest of the cases

In subcase $2a$ we can define ξ and ψ so they do not depend on a. This is also true for subcases $2e, 2f$ in five and six dimensions respectively. For the subcases with more complicated asymptotic behaviour the functions ξ and ψ will depend on the parameter a. Let us consider subcase $2b$ as an example. For this subcase we have from Tables 4.1 and 4.2:

$$\phi = a r^{-\Delta_-} + \beta_1 a^2 r^{-2\Delta} + b r^{-\Delta_+} + ... \tag{6.66}$$

and

$$h_{rr} = \frac{\kappa L^2}{r^2}(\alpha_1 a^2 r^{-2\Delta_-} + \alpha_2 a^3 r^{-3\Delta_-}) + \frac{f_{rr}}{r^5} + ... \tag{6.67}$$

In this case the function $\xi(r)$ has the form:

$$\xi = \left(\frac{\phi}{a r^{-\Delta_-} + \beta_1 a^2 r^{-2\Delta}} \right)' \tag{6.68}$$

where the denominator includes all the terms in (6.66) expect the term with the parameter b in its coefficient. The asymptotic form of ξ is:

$$\xi = -\frac{2bdm}{a} r^{-1-2dm} + ... \tag{6.69}$$

where we see that ξ depends on has parameters a and b.

For the function $\psi(r)$ we first need to find the expression for J_{Short} using the cut-off

loop described in chapter 4. For case $2b$ with $dmL = 2/3$ we have:

$$J_{Short} = -\frac{f_{rr}}{L^4 r} - \frac{8a^3 C_3}{L^2 r^{1/2}} + \frac{5a^2 r^{1/3}}{12L^2} \tag{6.70}$$

$$\psi = \left(\frac{J_{Short}}{-\frac{8a^3 C_3}{L^2 r^{1/2}} + \frac{5a^2 r^{1/3}}{12L^2})} \right)' \tag{6.71}$$

where the denominator in this case included all the terms in (6.70) except the term with f_{rr} in its coefficient. The asymptotic form for ψ is:

$$\psi = -\frac{2dm f_{rr}}{a^2} r^{-1-2dm} + ... \tag{6.72}$$

where we wee that the function ψ has coefficients a and f_{rr}.

We see that the functions ξ and ψ depend on a, therefore we have to find a first to be able to find b from (6.68) and f_{rr} from (6.71). The more subleading terms a subcase contains the more complex the expressions for ξ and ψ are. Because of complexity of the forms of the the ξ and ψ functions, we use mathematica to define these functions and solve their governing differential equations. In order to obtain good results for parameters b and f_{rr} we want to obtain the best value for a. For this purpose we build a convergence test that we describe in the next subsection.

6.4.2 Parameters and mass when varying ϕ_h and r_h

We want to understand how the mass parameters a, b and f_{rr} change with r_h and ϕ_h. For this purpose we repeat the procedure described in the previous subsection so as to obtain several black hole solutions. We solve the differential equation for ϕ first in order to obtain a value for the parameter a. Then we solve the differential equations for ξ and ψ simultaneously to obtain values for parameters b and f_{rr}.

- keeping r_h constant and varying ϕ_h

We choose fixed values for $r_h = 1, 10, 100$ and for each of these we vary ϕ_h. We create a first loop shown in Fig. 6.2 to solve the differential equation for ϕ and obtain the best value of the parameter a. In the loop we have:

$$\phi_h = \frac{i}{100} \tag{6.73}$$

where $1 < i < 300$. We therefore obtain a value for a for each i which gives us a table of 300 values for a. For every a, we want the best value, for this purpose we perform a

convergence test. For every value of ϕ_h we want to compare n values of the parameter a where n is an integer and corresponds to $x_{final} = 10^n$. We see in Fig. 6.2 that we go up to $x_{final} = 10^{40}$ to reduce numerical error by obtaining the best value for a. We define $aconverg$ to evaluate the ratio between two successive values for a. We then check which ratio is nearest to the value of 1 and find the position at which this occurs. This will then be the value that we keep for the parameter a that will contribute the the mass. Once the values of a are obtained, we construct another `FOR` loop seen in Fig. 6.3 and perform a similar convergence test for b and f_{rr} in order to extract the best numerical value for these parameters for each ϕ_h. The graphs obtained are presented and commented in the next section. This is done for the three fixed values of r_h. We therefore obtain tables for a, b and f_{rr} of 300 values each and from those we calculate the corresponding mass. We can now plot the graphs of a, b f_{rr} and the mass.

- keeping ϕ_h constant and varying r_h

We want to see how the parameters vary with r_h. We follow the same procedure as described above but this time we vary r_h for three fixed values of $\phi_h = 0.2, 0.5, 0.7$, performing the same convergence test for the mass parameters. The results are presented and commented in the next section.

```
rh = 1
1

For[i = 1, i < 300, i++,
 Print[i];
 ϕh = (i / 300) * v;
 xinitial = ϵ;
 xfinal = 10^40;
 NumSolBH =
  NDSolve[{ϕ''[x] == ϕprimeprime[x], Jt'[x] == Jprime[x], δ'[x] == δprime[x], rvar'[x] == 1,
    Jt[xinitial] == Jhorizon,
    ϕ[xinitial] == ϕhorizon,
    ϕ'[xinitial] == ϕhprimehorizon,
    δ[xinitial] == δhorizon, rvar[xinitial] == rh + xinitial}, {rvar, Jt, ϕ, δ},
   {x, xinitial, xfinal}, PrecisionGoal → 25, AccuracyGoal → 25, WorkingPrecision → 50,
   Method → "Extrapolation" , InterpolationOrder → All];
 For[j = 1, j < 40, j++,
  aconverg[[j]] = (ϕ[xfinal / 10^(j - 1)] * (xfinal / 10^(j - 1) + rh)^(Δminus) /. NumSolBH[[1]]) /
     (ϕ[xfinal / 10^j] * (xfinal / 10^j + rh)^(Δminus) /. NumSolBH[[1]]);
 ];
 anearest = Nearest[aconverg, 1];
 jposition = Position[aconverg, anearest[[1]][[1]][[1]]];
 a = ϕ[xfinal / 10^jposition] * (xfinal / 10^jposition + rh)^(Δminus) /. NumSolBH[[1]];
```

Figure 6.2: Loop to find parameter a as we vary ϕ_h, for $r_h = 1$ with Higgs potential and $k = 1$.

```
NumSolBH1 = NDSolve[{ϕ''[x] == ϕprimeprime[x], Jt'[x] == Jprime[x], δ'[x] == δprime[x],
    rvar'[x] == 1, ξ'[x] == ξprime[x], ψ'[x] == ψprime1[x],
    Jt[xinitial] == Jhorizon,
    ϕ[xinitial] == ϕhorizon,
    ϕ'[xinitial] == ϕhprimehorizon,
    ξ[xinitial] == ξhorizon,
    ψ[xinitial] == ψhorizon,
    δ[xinitial] == δhorizon, rvar[xinitial] == rh + xinitial}, {rvar, Jt, ϕ, δ, ξ, ψ},
  {x, xinitial, xfinal}, PrecisionGoal → 25, AccuracyGoal → 25, WorkingPrecision → 50,
  Method → "Extrapolation" , InterpolationOrder → All];
For[j = 1, j < 40, j++,
 bconverg[[j]] = (ξ[xfinal / 10^(j - 1)] * (xfinal / 10^(j - 1) + rh)^(σ1) /. NumSolBH1[[1]]) /
    (ξ[xfinal / 10^j] * (xfinal / 10^j + rh)^(σ1) /. NumSolBH1[[1]]);];
bnearest = Nearest[bconverg, 1];
jposition = Position[bconverg, bnearest[[1]]][[1]][[1]];
ξcoeff = ξ[xfinal / 10^jposition] * (xfinal / 10^jposition + rh)^(σ1) /. NumSolBH1[[1]];
For[j = 1, j < 40, j++,
 frrconverg[[j]] = (ψ[xfinal / 10^(j - 1)] * (xfinal / 10^(j - 1) + rh)^(σ2) /. NumSolBH1[[1]]) /
    (ψ[xfinal / 10^j] * (xfinal / 10^j + rh)^(σ2) /. NumSolBH1[[1]]);];
frrnearest = Nearest[frrconverg, 1];
jposition = Position[frrconverg, frrnearest[[1]]][[1]][[1]];
ψcoeff = ψ[xfinal / 10^jposition] * (xfinal / 10^jposition + rh)^(σ2) /. NumSolBH1[[1]];
b = bCoeff;
frr = frrCoeff;
mass = (frr / (L^4 * κ) + 3 * a * b / (2 * L^2) - 2 * a * b * dm^2 / 3);
ϕhtable[[i]] = ϕh;
atable[[i]] = a;
btable[[i]] = b;
frrtable[[i]] = frr;
masstable[[i]] = mass;]
```

Figure 6.3: Loop to find b and f_{rr} as we vary ϕ_h, for $r_h = 1$ with Higgs potential and $k = 1$.

§ 6.5 Results for subcase $2a$

6.5.1 Behaviour of ξ and ψ

We plot the functions ξ and ψ to see how they behave at infinity. These are example plots to show typical behaviour.

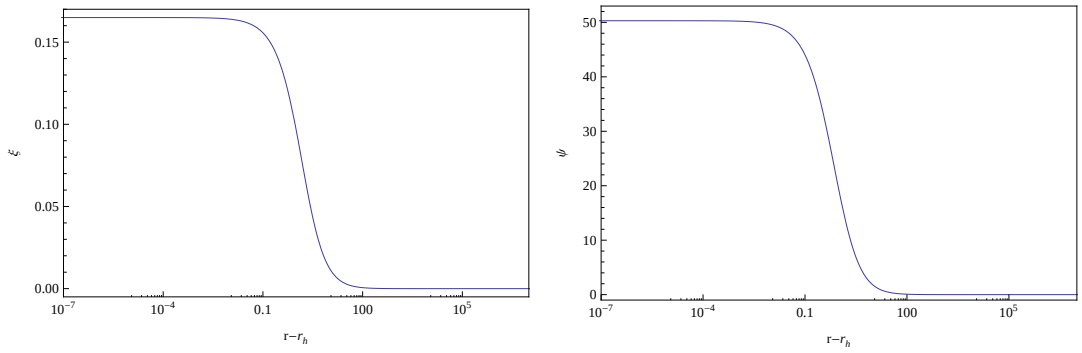

(a) $\xi(r)$ (b) $\psi(r)$

Figure 6.4: Subcase 2a with TWI potential for $k = 1$, $\kappa = 1$, $dm = 1/4L$, $L = 1$, $r_h = 1$, $\delta_h = 0$ (a) behaviour of ξ (b) behaviour of ψ.

We see in Figs. 6.4a and 6.4b that ξ and ψ go to zero as $r \to \infty$. We plot the functions ϕr^{Δ_-}, ξr^{σ_3} and ψr^{σ_4} to verify that these converge when r is large.

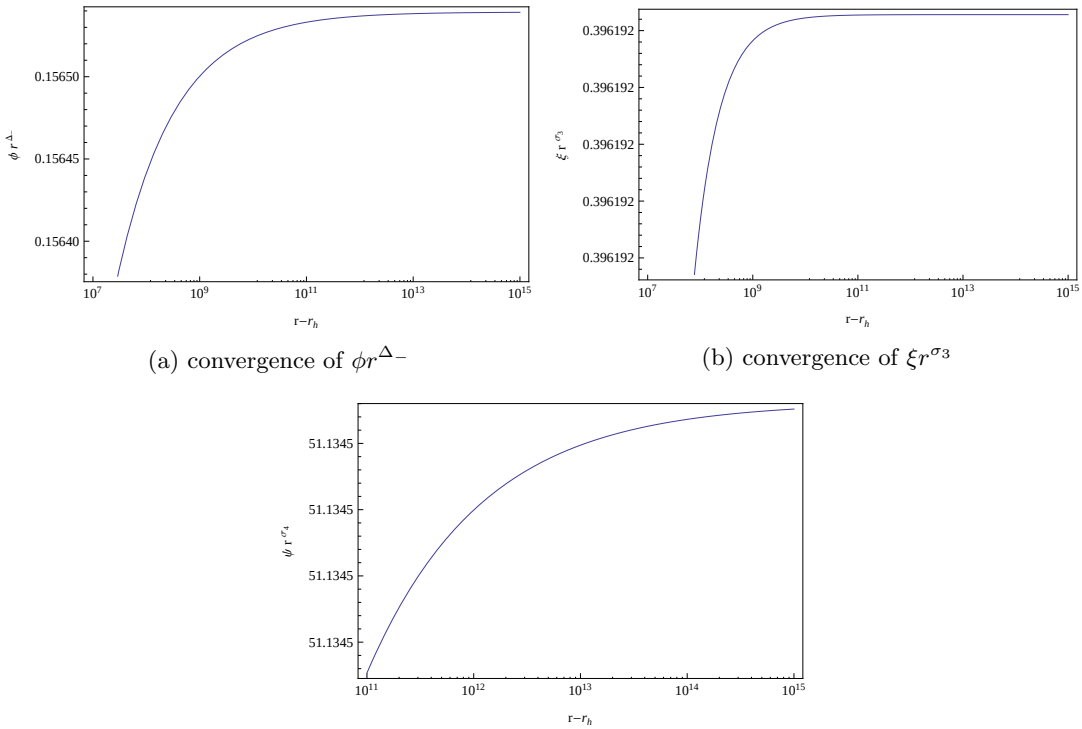

(a) convergence of ϕr^{Δ_-}

(b) convergence of ξr^{σ_3}

(c) convergence of ψr^{σ_4}

Figure 6.5: Subcase 2a for TWI potential with $k = 1$, $\kappa = 1$, $dm = 1/4L$, $L = 1$, $r_h = 1$, $\delta_h = 0$ (a) convergence of ϕr^{Δ_-} (b) convergence of ξr^{σ_3} (c) convergence of ψr^{σ_4}.

These functions converge to constant values which contain a, b and f_{rr} in them respectively as seen in Figs. 6.5a, 6.5b, 6.5c. The convergence is good, for example as can be seen in Figs. 6.5b and 6.5c the values shown are the same to six significant figures.

6.5.2 Results when varying ϕ_h

We present here the results for subcase $2a$ with Higgs potential.

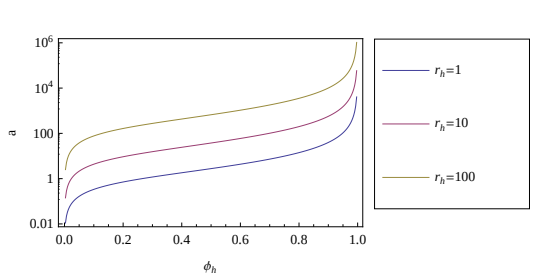

(a) parameter a

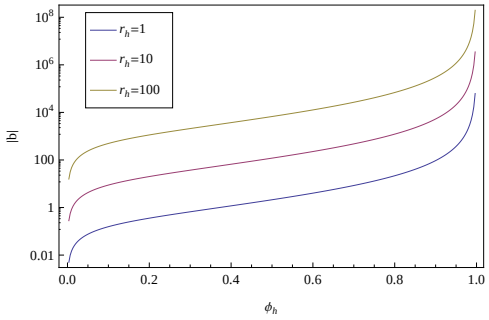

(b) parameter b

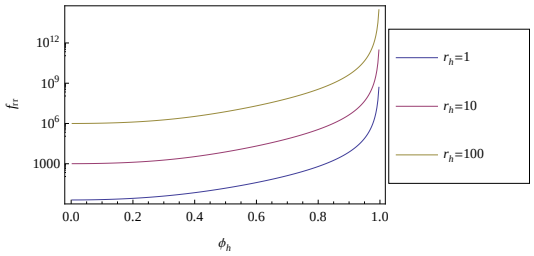

(c) parameter f_{rr}

Figure 6.6: Subcase $2a$ for Higgs potential with $k = 1$, $\kappa = 1$, $dm = 1/4L$, $L = 1$, $\delta_h = 0$ (a) parameter a as we vary ϕ_h for three different values of r_h (b) parameter b as we vary ϕ_h for three different values of r_h (c) parameter f_{rr} as we vary ϕ_h, for three different values of r_h.

Fig. 6.6a shows a parameter space where we have plotted the parameter a for three fixed values of r_h. We see that the parameter a increases as ϕ_h increases and $a \to 0$ as $\phi_h \to 0$. The parameter a is positive because ϕ is positive everywhere. The value of a increases rapidly as r_h increases. The curves have similar shape for all r_h for this reason for the other subcases we only consider two values for for r. We see that for the Higgs potential as $\phi_h \to v$, the scalar field needs more and more energy to get out of the potential well. We have plotted in the log scale because the values are big.

We see from Fig. 6.6b that the parameter b is negative for all ϕ_h and $b \to 0$ as $\phi_h \to 0$.

Moreover $|b|$ increases rapidly as $\phi_h \to v$. We also see that $|b|$ increases as r_h increases. The curves have similar shape to the ones for the parameter a in Fig. 6.6a. In Fig. 6.6c we see that f_{rr} is always positive and as $\phi_h \to 0$, f_{rr} tends to a constant which corresponds to the Schwarzschild-adS parameter in the absence of scalar field. We see that f_{rr} increases as r_h increases. The curves have very similar shapes for all r_h.

Now we can obtain the mass plots where every point is a black hole solution:

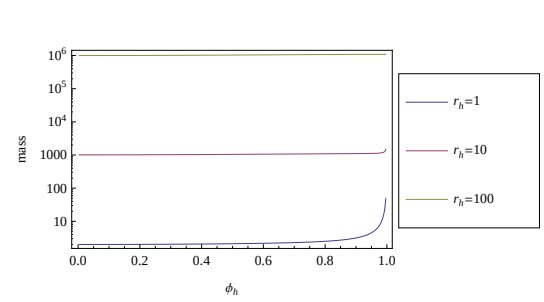

(a) Mass

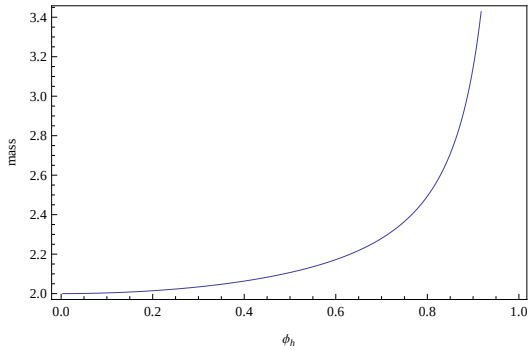

(b) Mass for $r_h = 1$

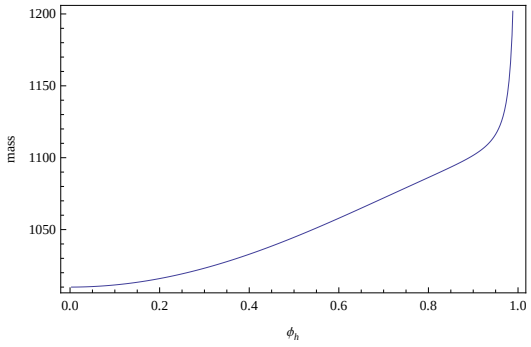

(c) Mass for $r_h = 10$

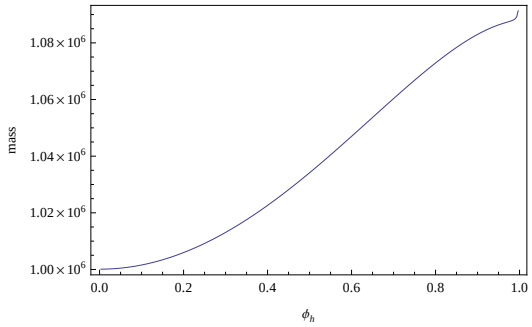

(d) Mass for $r_h = 100$

Figure 6.7: Subcase 2a for Higgs potential with $k = 1$, $dm = 1/4$, $\kappa = 1$, $L = 1$ (a) mass plot where ϕ_h is varied for three different values of r_h with (b) mass plot where ϕ_h is varied with $r_h = 1$ (c) mass plot where ϕ_h is varied for $r_h = 10$ (d) mass plot where ϕ_h is varied for $r_h = 100$.

Fig. 6.7a shows that the shape of the mass is not the same for all r_h. We see it in more details in Figs. 6.7b-6.7d. For $r_h = 1$ we see that we start with a mass of roughly 2 at $\phi_h = 0$ this corresponds to the mass of the Schwarzschild adS spacetime. As we increase ϕ_h we see that the final value of the mass is roughly 3.4 so the contribution to the mass from the black hole and from the scalar field are similar. However for Fig. 6.7c we see that the starting value of the mass is about 1000, that is the Schwarzschild adS mass and we see that the contribution of the scalar field mass is less important

than for $r_h = 1$. This is even clearer when $r_h = 100$ in Fig. 6.7d, the black hole is very big and the mass contribution from the scalar field is less important than in the previous cases. This is explained by the fact that as we increase the size of the event horizon the size of the black hole will increase and its contribution to the total mass will be more important than the scalar field contribution. We see that the scalar field always has a positive contribution to the total mass.

6.5.3 Results when varying r_h

Now when we vary r_h for three fixed values of ϕ_h the plots for the mass parameters are:

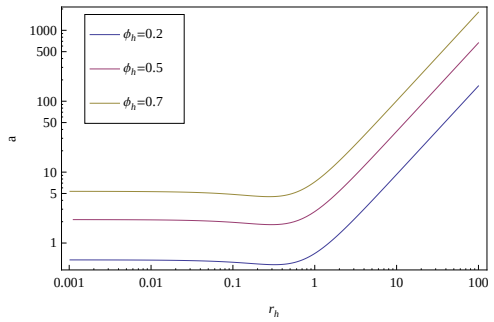

(a) parameter a

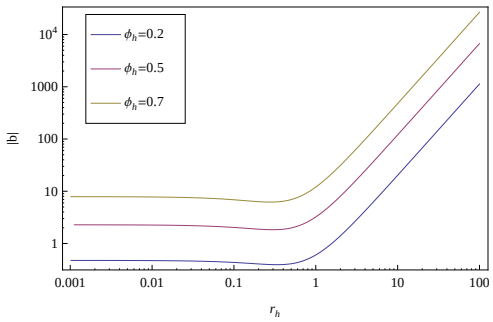

(b) parameter b

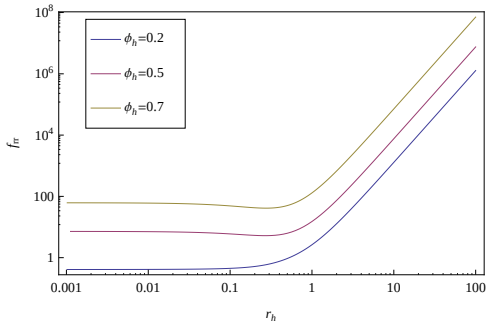

(c) parameter f_{rr}

Figure 6.8: Subcase 2a with Higgs potential for $k = 1$, $dm = 1/4L$ (a) parameter a as we vary r_h, for three different values of ϕ_h (b) parameter b as we vary r_h, for three different values of ϕ_h (c) parameter f_{rr} as we vary r_h, for three different values of ϕ_h.

In Fig. 6.8a we see that the parameter a is positive and that the shape is similar for all ϕ_h. For $r_h < 1$ the parameter a is fairly flat with a slight dip just before $r_h = 1$. We see a change of behaviour when $r_h \sim 1$. For $r_h > 1$, a increases, it looks like a straight line in a log log plot. In Fig. 6.8b we plot the absolute value of b, the parameter b

being negative. We see that b is about an order of magnitude bigger than a for large r_h. The shape of the plot is similar to the plot for a. The parameter space for f_{rr} is presented in Fig. 6.8c where we see that f_{rr} is positive. The behaviour is again similar to the plots for a and b. However, for large r_h, f_{rr} is a lot bigger than a and b. The expression for the mass for case $2a$ is:

$$-\frac{ab}{3}dm^2 + \frac{3ab}{2L^2} + \frac{f_{rr}}{L^4\kappa}. \tag{6.74}$$

By comparing the values for a, b and f_{rr} at $r_h = 100$ in Figs. 6.8a-6.8c we see that f_{rr} is a factor of 10 bigger than ab so we deduce that for large r the black hole mass dominates the total mass. This confirmed by the graph in Fig. 6.9 where we see that for $r_h > 1$ the scalar field does not make much difference to the total mass. For this reason we decide to focus on smaller values of r_h for the rest of the results.

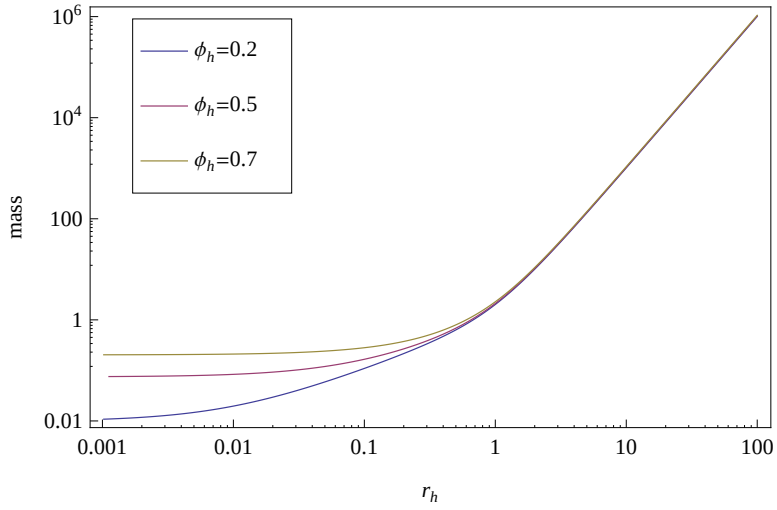

Figure 6.9: Mass plot for subcase $2a$ as we vary r_h, for three different values of ϕ_h.

6.5.4 Topological black holes

We investigate topological black holes for which $k \neq 1$. As for the case when $k = 1$, we first varied ϕ for fixed values of r_h. Then we varied r_h for fixed values of ϕ_h.

$k = 0$

We plot the mass parameters and the when we vary ϕ_h:

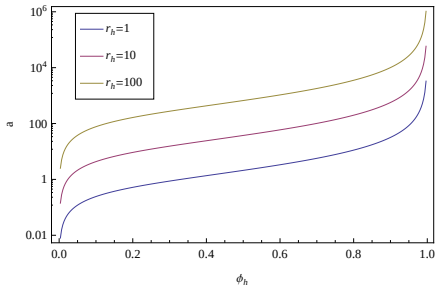

(a) Parameter a

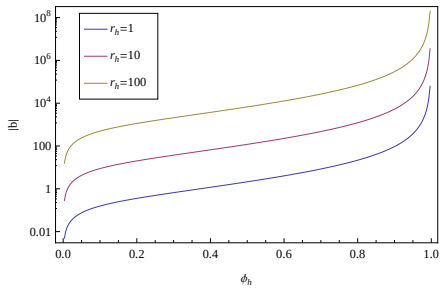

(b) Parameter b

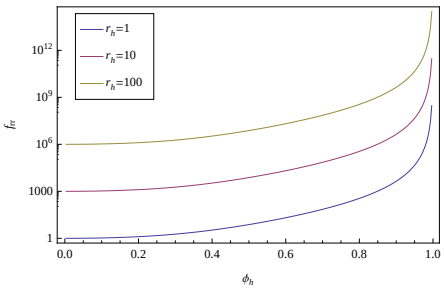

(c) Parameter f_{rr}

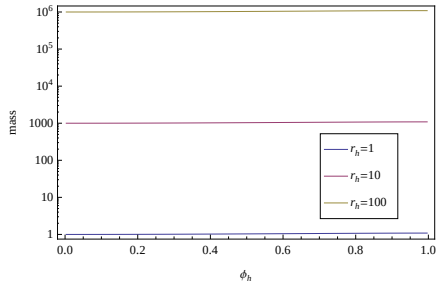

(d) Mass plot

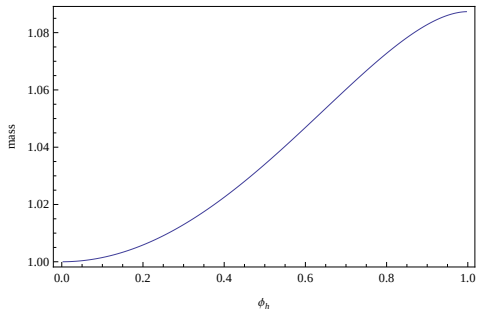

(e) Mass for $r_h = 1$

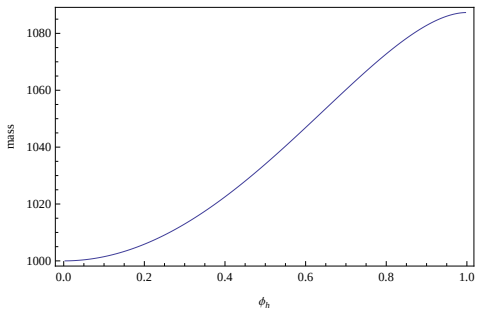

(f) Mass for $r_h = 10$

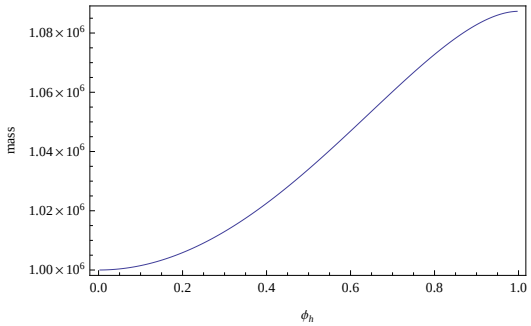

(g) Mass for $r_h = 100$

Figure 6.10: Subcase 2a with Higgs potential for $k = 0$, $\kappa = 1$, $dm = 1/4L$, $L = 1$, $v = 1$, $\alpha_0 = 35/16L^2v^2$ (a) effect on parameter a as we vary ϕ_h, for three different values of r_h (b) effect on parameter b as we vary ϕ_h, for three different values of r_h (c) effect on parameter f_{rr} as we vary ϕ_h, for three different values of r_h (d) mass plot as we vary ϕ_h, for three different values of r_h (e) mass as we vary ϕ_h, for $r_h = 1$ (f) mass as we vary ϕ_h, for $r_h = 10$ (g) mass as we vary ϕ_h, for $r_h = 100$.

In Fig. 6.10a we see that the parameter a is positive, it has a similar shape as for the $k = 1$ case seen in Fig. 6.6a. The plots for the parameters b and f_{rr} seen in Figs. 6.10b and 6.10c are also identical to the ones for $k = 1$. The parameter b is always negative and f_{rr} tends to a constant when $\phi \to 0$. However we see from Fig. 6.10d that the mass has a similar shape for the three values of r_h. This is confirmed in Figs. 6.10e-6.10g where we see that the shapes of the mass plots are exactly the same for all r_h. The mass is roughly one for $r_h = 1$. For $r_h = 100$ the mass is of order 10^6.

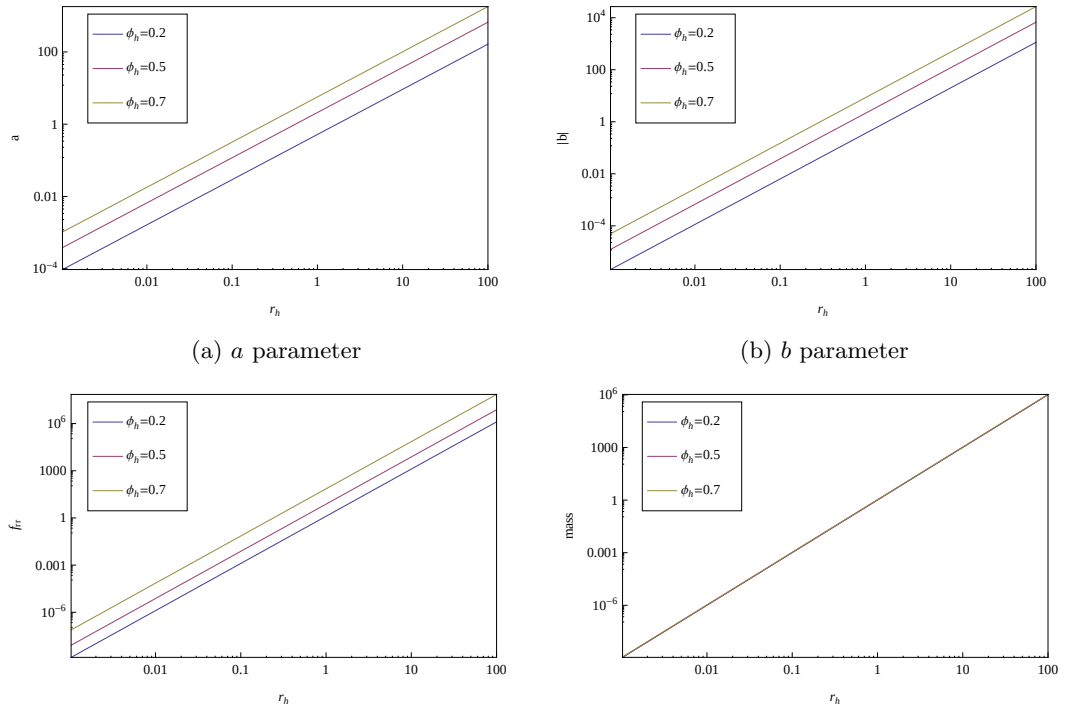

(a) a parameter

(b) b parameter

(c) f_{rr} parameter

(d) Mass plot

Figure 6.11: Subcase 2a for Higgs potential with $k = 0$, $\kappa = 1$, $dm = 1/4L$, $L = 1$, $v = 1$, $\alpha_0 = 35/16L^2v^2$ (a) parameter a as we vary r_h, for three different values of ϕ_h (b) parameter b as we vary r_h, for three different values of ϕ_h (c) parameter f_{rr} as we vary r_h, for three different values of ϕ_h (d) mass plot as we vary r_h, for three different values of ϕ_h.

The plot in Fig. 6.11a shows a increasing monotonically when we vary r_h. The plots for the parameters b and f_{rr} follow a similar behaviour as seen in Figs. 6.11b and 6.11c. This behaviour is also seen for the mass in Fig. 6.11d. When $k = 0$ we have a planar event horizon. There is only one length scale which we have set to 1 by setting $L = 1$. For $k = 0$ we will always have a scale invariance for this reason we do not consider topological black holes with $k = 0$ for the rest of the subcases cases.

$k = -1$

The other case where we have topological black holes is when $k = -1$. We present the graphs when ϕ_h is varied:

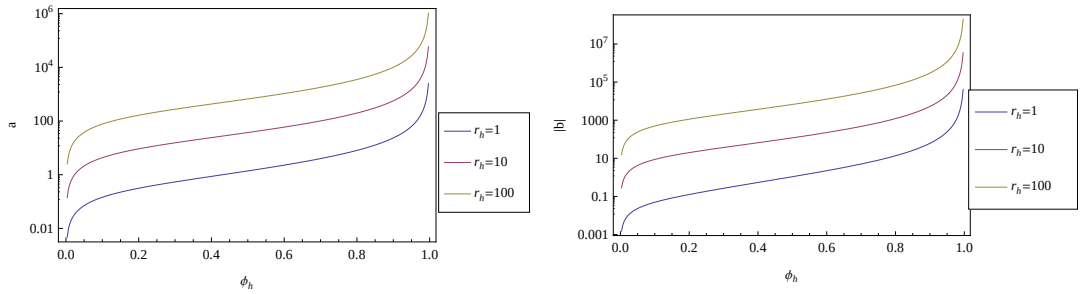

(a) a parameter

(b) b parameter

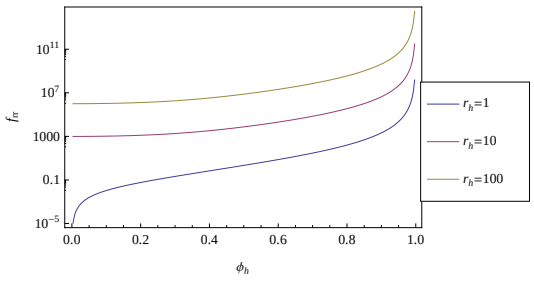

(c) f_{rr} parameter

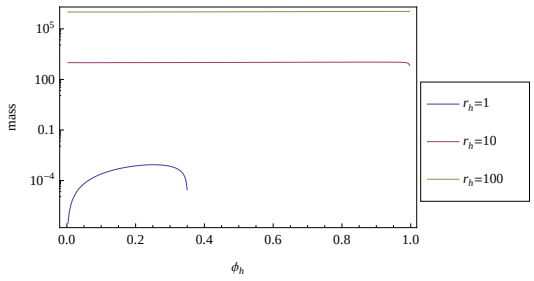

(d) Mass

Figure 6.12: Subcase 2a for Higgs potential with $k = -1$, $\kappa = 1$, $dm = 1/4L$, $L = 1$, $v = 1$, $\alpha_0 = 35/16L^2v^2$ (a) effect on parameter a as we vary ϕ_h for three different values of r_h (b) effect on parameter b as we vary ϕ_h for three different values of r_h (c) effect on parameter f_{rr} as we vary ϕ_h, for three different values of r_h (d) effect on mass as we vary ϕ_h, for three different values of r_h.

The plots for parameters a, b and f_{rr} in Figs. 6.12a-6.12c are similar to the $k = 0$ case. For the mass we see in Fig. 6.12d that when $k = -1$ the mass when $r_h = 1$ has an interesting behaviour. In Figs. 6.13a-6.13c we plot the masses separately for each r_h. We see that for $r_h = 1$ the mass is negative. As for the case where $k = 0$ the mass is of order a thousand for $r_h = 10$ and of order 10^6 when $r_h = 100$.

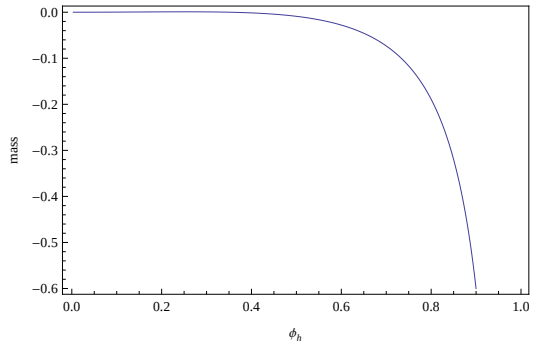

(a) mass for $r_h = 1$

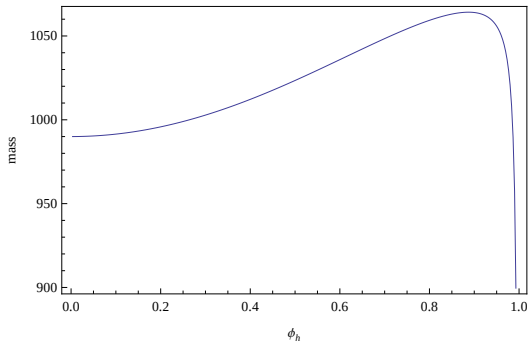

(b) mass for $r_h = 10$

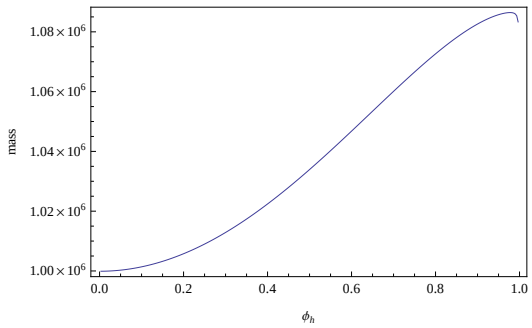

(c) mass for $r_h = 100$

Figure 6.13: Subcase $2a$ for Higgs potential with $k = -1$, $\kappa = 1$, $dm = 1/4L$, $L = 1$, $v = 1$, $\alpha_0 = 35/16L^2v^2$ (a) effect on the mass as we vary ϕ_h, for $r_h = 1$ (b) effect on the mass as we vary ϕ_h, for $r_h = 10$ (c) effect on the mass as we vary ϕ_h, for $r_h = 100$.

When we vary r_h we have:

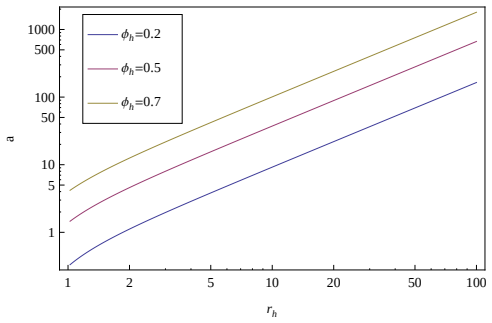

(a) parameter a

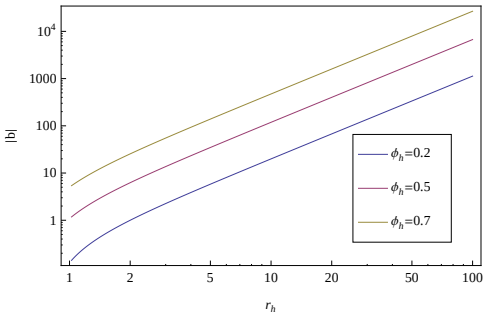

(b) parameter b

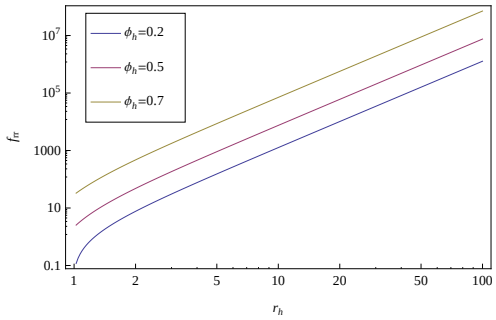

(c) parameter f_{rr}

Figure 6.14: Subcase $2a$ for Higgs potential with $k = -1$, $\kappa = 1$, $dm = 1/4L$, $L = 1$, $v = 1$, $\alpha_0 = 35/16L^2v^2$ (a) effect on the parameter a as we vary r_h, for three different values of ϕ_h (b) effect on the parameter b as we vary r_h, for three different values of ϕ_h (c) effect on the parameter f_{rr} as we vary r_h, for three different values of ϕ_h.

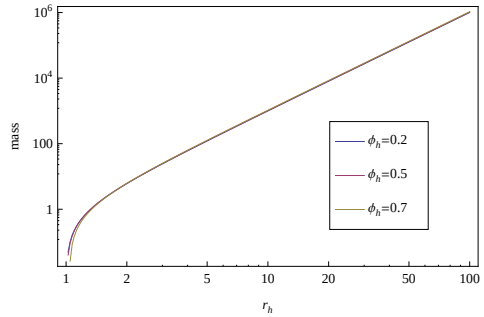

(a) mass

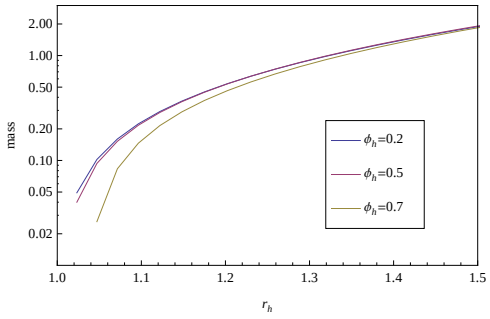

(b) zoom on the mass

Figure 6.15: Subcase $2a$ for Higgs potential with $k = -1$, $\kappa = 1$, $dm = 1/4L$, $L = 1$, $v = 1$, $\alpha_0 = 35/16L^2v^2$ (a) mass as we vary r_h, for three different values of ϕ_h (b) zoom on the mass as we vary r_h, for three different values of ϕ_h.

When we vary r_h in Figs. 6.14a-6.15b, we see that the result we found for $k = 1$ is confirmed, namely, the scalar contribution is negligible for $r_h > 1$. Since the numerical

runs take a long time and the results do not show particularly interesting features we will not consider $k = -1$ for the rest of the subcases.

In this subsection we have thoroughly investigated the results for subcase $2a$. The aim is to have better idea about how the mass is affected when we vary or change parameters such as ϕ_h, r_h and k. We have seen the behaviour of mass parameters and mass when we vary ϕ_h for fixed values of r_h. We have seen that for $r_h > 1$ the behaviour of the mass parameters and the mass parameters does not change. For the rest of the subcases we will consider values of $r_h \leqslant 1$. When we vary r_h with fixed values for ϕ_h we see that the scalar field contribution is negligible for $r_h > 1$. This behaviour is seen for the three fixed values of ϕ_h. For the rest of the subcases we therefore only use one fixed value of ϕ_h. We have seen that when we consider topological black holes with $k = 0$ there is a clear scale invariance. For $k = -1$ we have seen that the mass can be negative as it is the case for $r_h = 1$ when we vary ϕ_h. For this case we also see that for $r_h > 1$ the scalar field contribution to the mass is negligible. Since the main interesting features about topological black holes have been discussed for subcase $2a$, these will not be considered for the rest of the subcases.

§ 6.6 Results for the rest of the cases

We now have a better idea about how the functions ξ and ψ should behave and how the parameters a b and f_{rr} are affected by changes in r_h and ϕ_h. Here we present a selection of results where interesting features appear. This section is split in three parts. We start by presenting the typical behaviour of ξ and ψ functions for selected subcases. We then present the results when we vary ϕ_h with two fixed values for r_h, for $k = 1$. Finally we present the results when we vary r_h with fixed values for ϕ_h for $k = 1$.

6.6.1 Behaviour of ξ and ψ

We consider the higher dimensional subcase $2f$ in $D = 6$. The behaviour of functions ξ and ψ is presented here:

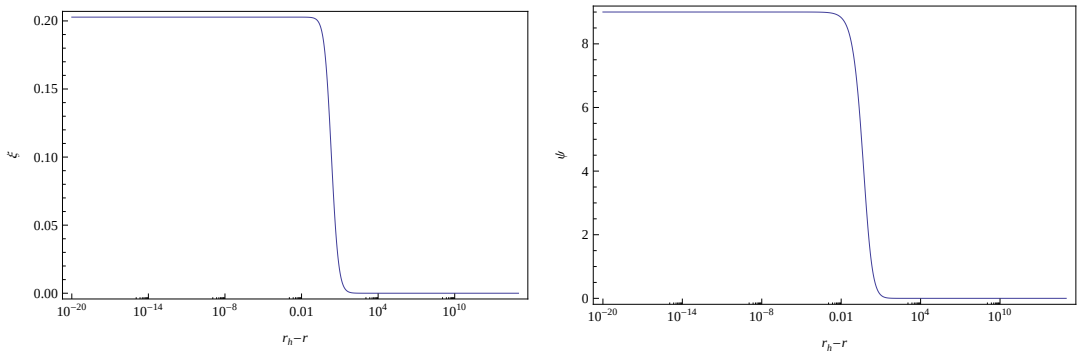

(a) ξ (b) ψ

Figure 6.16: Subcase $2f$ with TWI potential, $D = 6$, $k = 1$, $\kappa = 1$, $L = 1$, $dm = 1/2L$, $r_h = 1$, $\delta_h = 0$, $A = 3$ (a) function ξ (b) function ψ.

We plot functions ϕr^{Delta_-}, ξr^{σ_3} and ψr^{σ_4}:

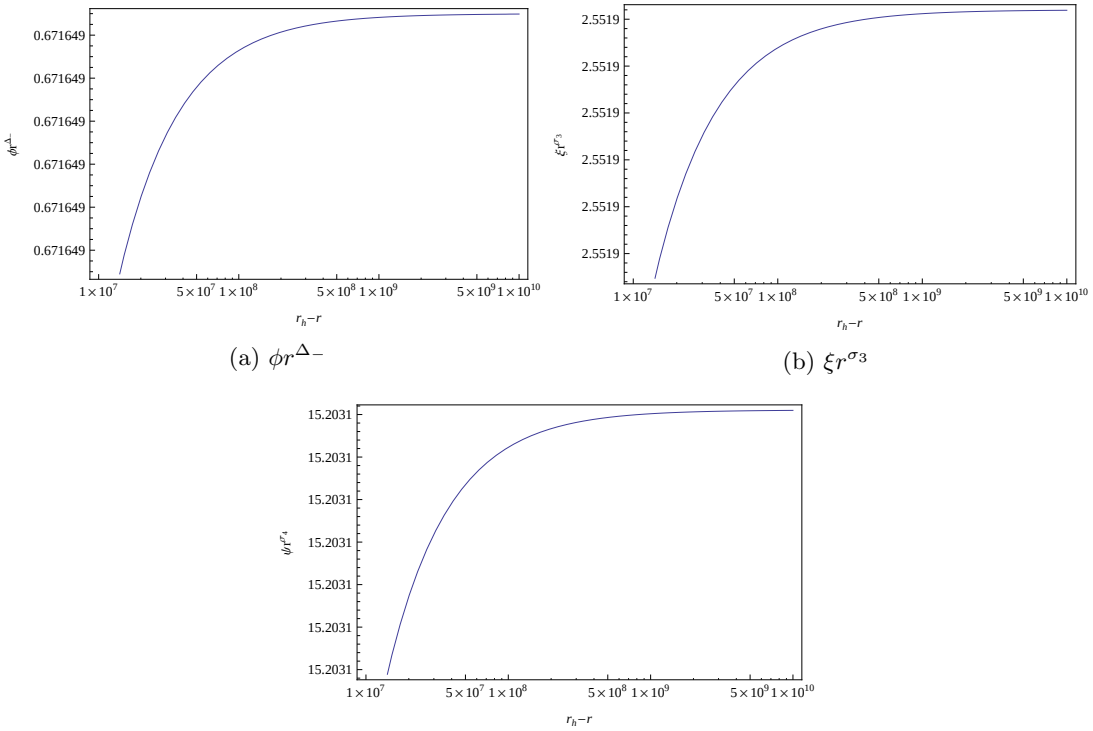

(a) ϕr^{Δ_-} (b) ξr^{σ_3}

(c) ψr^{σ_4}

Figure 6.17: Subcase $2f$ with TWI potential, $D = 6$, $k = 1$, $\kappa = 1$, $L = 1$, $dm = 1/2L$, $r_h = 1$, $\delta_h = 0$, $A = 3$ (a) convergence of ϕr^{Δ_-} (b) convergence of ξr^{σ_3} (c) convergence of ψr^{σ_4}.

The functions ξ and ψ seen in Figs. 6.16a-6.16b vanish at infinity as expected. We see

from Figs. 6.17a-6.17c that there is good convergence for ϕr^{Δ_-}, ξr^{σ_3}, ψr^{σ_4}.

We also want to give an example for a subcase with a logarithmic branch to show that we have good convergence. We consider case $3a$, we present the results for TWI potential.

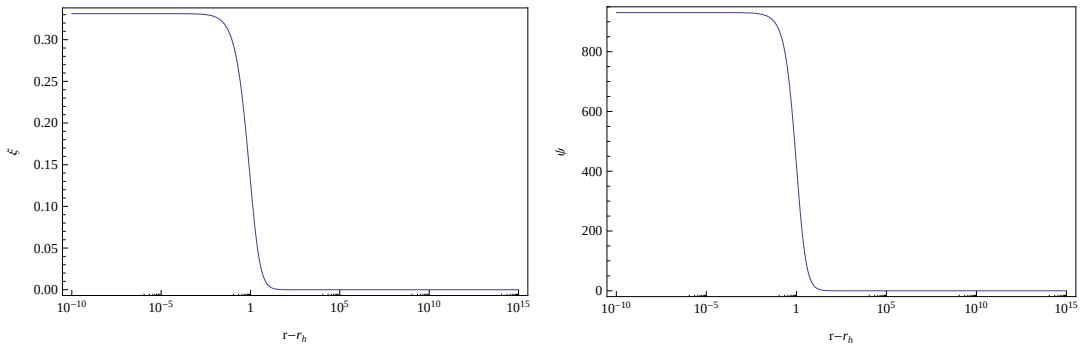

(a) ξ (b) ψ

Figure 6.18: Subcase $3a$ with TWI potential, $D = 4$, $k = 1$, $\kappa = 1$, $L = 1$, $dm = 1/2L$, $r_h = 1$, $\delta_h = 0$, $A = 1$ (a) function ξ (b) function ψ.

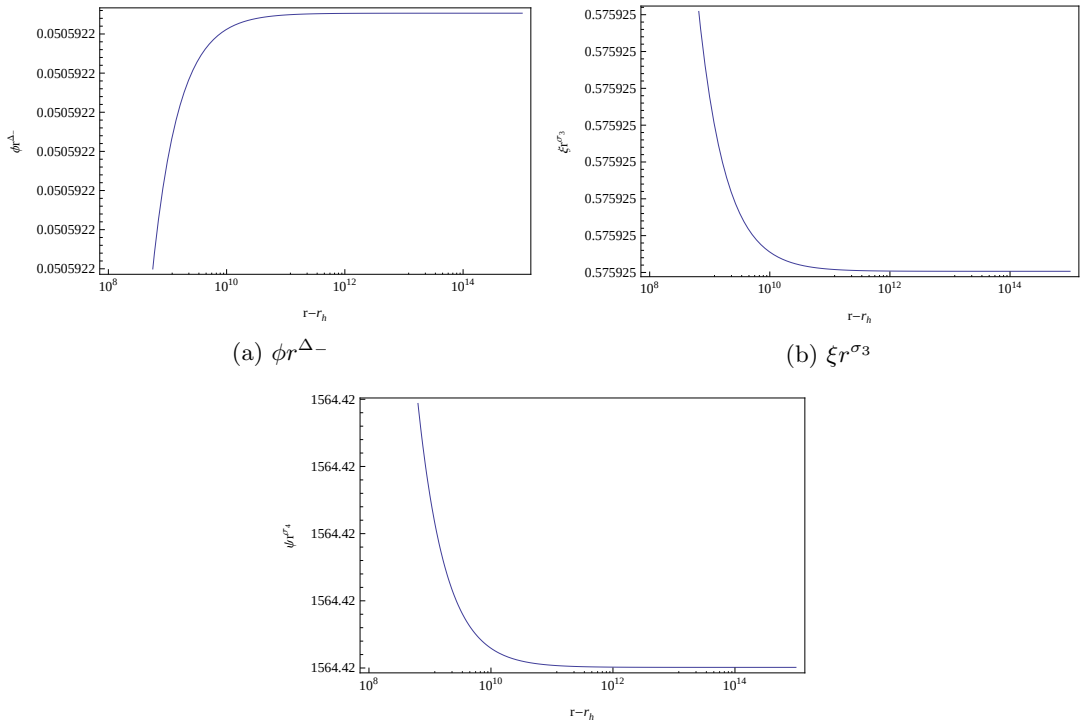

(a) $\phi r^{\Delta-}$ (b) ξr^{σ_3}

(c) ψr^{σ_4}

Figure 6.19: Subcase $3a$ with TWI potential, $D = 4$, $k = 1$, $\kappa = 1$, $L = 1$, $dm = 1/2L$, $r_h = 1$, $\delta_h = 0$, $A = 1$ (a) convergence of $\phi r^{\Delta-}$ (b) convergence of ξr^{σ_3} (c) convergence of ψr^{σ_4}.

The functions ξ and ψ vanish at infinity as expected. We can see from Figs 6.19a-6.19c that there is good convergence for this subcase.

For the rest of the subcases the functions ξ and ψ also go to zero as $r \to \infty$. The functions $\phi r^{\Delta-}$, ξr^{σ_3} and ψr^{σ_4} are found to be convergent as for subcases $2a$, $2f$ and $3a$. For some subcases the convergence is better than others but the general behaviour is the same.

6.6.2 Results when varying ϕ_h

We present a selection of plots when we vary ϕ_h for two fixed values of r_h.

Subcase $2b$ with Higgs potential

We consider subcase $2b$ and we present the plots when we vary ϕ_h:

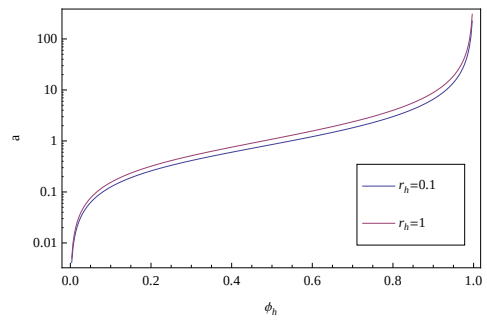

(a) a parameter

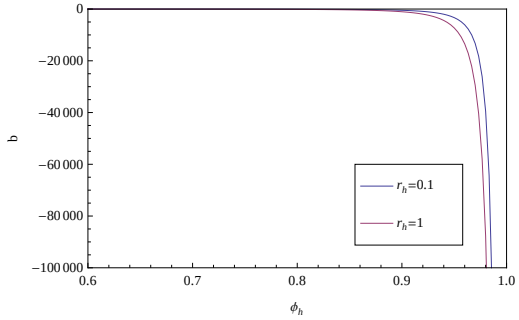

(b) b parameter

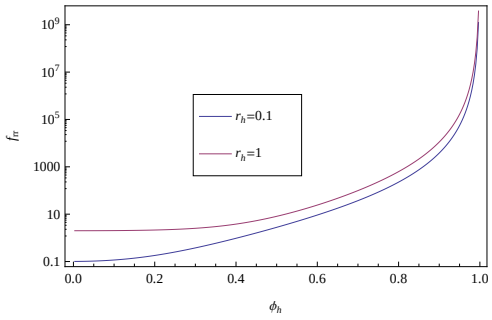

(c) f_{rr} parameter

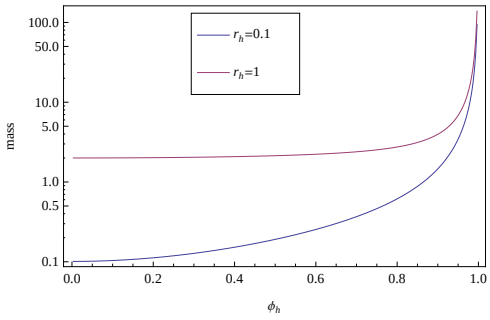

(d) Mass plot

Figure 6.20: Subcase 2b with Higgs potential when $D = 4$, $dm = 2/3L$, $\alpha_0 = 65/(36L^2v^2)$, $k = 1$, $\kappa = 1$, $L = 1$, $\delta_h = 0$ (a) effect on the parameter a as we vary ϕ_h for two different values of r_h (b) effect on the parameter b as we vary ϕ_h for two different values of r_h (c) effect on the parameter f_{rr} as we vary ϕ_h for two different values of r_h (d) effect on the mass as we vary ϕ_h for two different values of r_h.

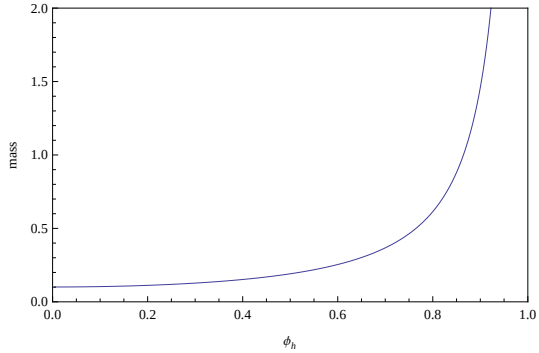

(a) mass for $r_h = 0.1$

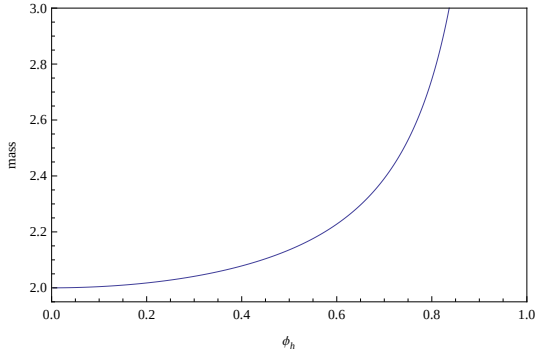

(b) mass for $r_h = 1$

Figure 6.21: Subcase 2b with Higgs potential when $D = 4$, $dm = 2/3L$, $\alpha_0 = 65/(36L^2v^2)$, $k = 1$, $\kappa = 1$, $L = 13$, $\delta_h = 0$ (a) effect on the mass as we vary ϕ_h for $r_h = 0.1$ (b) effect on the mass as we vary ϕ_h for $r_h = 1$.

We see that the features for a, b and f_{rr} in Figs. 6.20a-6.20c are very similar to case $2a$. The parameter a is always positive and increases with increasing ϕ_h. The parameter b is always negative. We see that f_{rr} is also positive and increases with ϕ_h. The mass shown in Figs.6.20d-6.21b is positive. We see that for $r_h = 1$ the mass is bigger than for $r_h = 0.1$. This is because when $r_h = 1$ the black hole is of bigger size and therefore has more mass.

Subcase $2b$ with pseudo-TWI potential

For this case we present the mass plots when we vary ϕ_h:

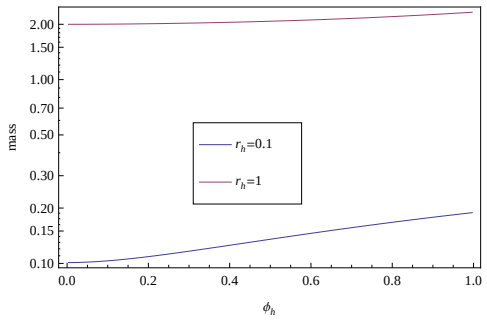

(a) Mass

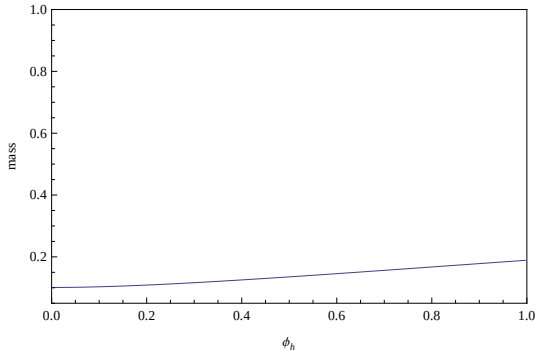

(b) Mass for $r_h = 0.1$

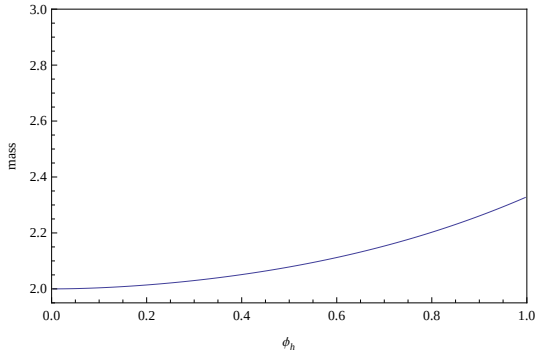

(c) Mass for $r_h = 1$

Figure 6.22: Subcase $2b$ with pseudo-TWI potential for $k = 1$ (a) effect on the mass as we vary ϕ_h (b) effect on the mass as we vary ϕ_h, for $r_h = 0.1$ (c) effect on the mass as we vary ϕ_h, for $r_h = 1$.

The mass shown in Figs. 6.22a-6.22c is positive. We see that for $r_h = 1$ the mass is bigger than for $r_h = 0.1$. This is because when $r_h = 1$ the black hole is of bigger size and therefore has more mass. We see that for $r_h = 1$ the mass increases more rapidly as $\phi_h \to 1$. The plots show typical mass behaviour.

Subcase $2c$ with pseudo-TWI potential

For this subcase, when we vary ϕ_h we have:

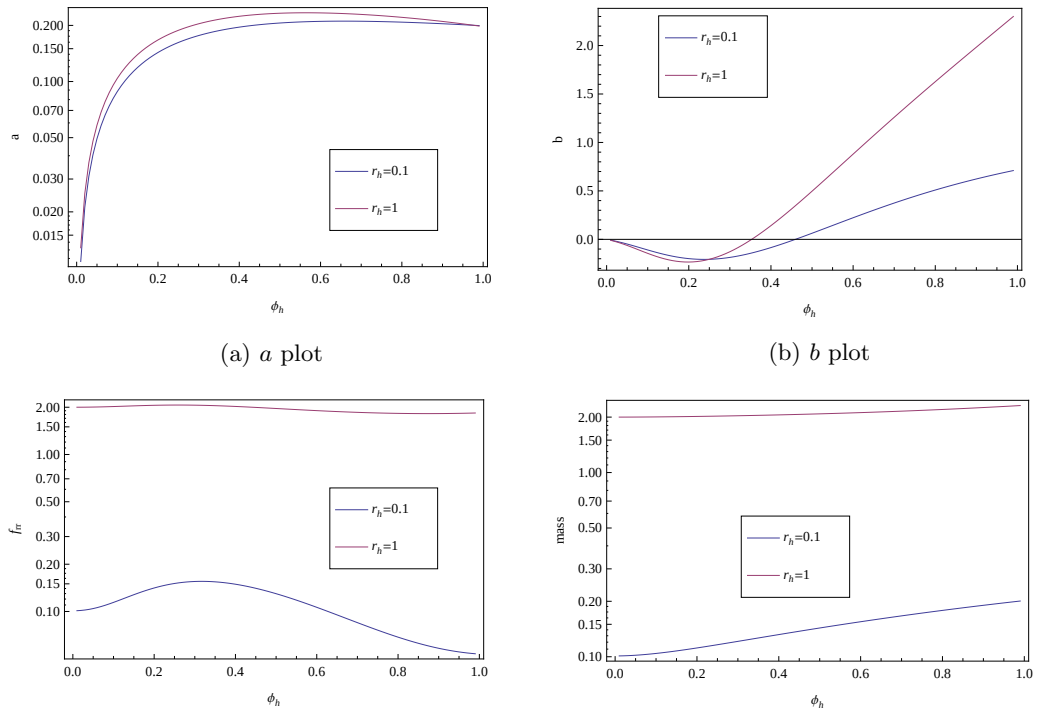

(a) a plot

(b) b plot

(c) f_{rr} plot

(d) Mass plot

Figure 6.23: Subcase $2c$ with pseudo-TWI potential for $D = 4$, $dm = 5/6L$, $A = -7/9$, $k = 1$, $\kappa = 1$, $L = 1$, $\delta_h = 0$ (a) effect on the parameter a as we vary ϕ_h for two different values of r_h (b) effect on the parameter b as we vary ϕ_h for two different values of r_h (c) effect on the parameter f_{rr} as we vary ϕ_h, for two different values of r_h (d) effect on the mass as we vary ϕ_h for two different values of r_h.

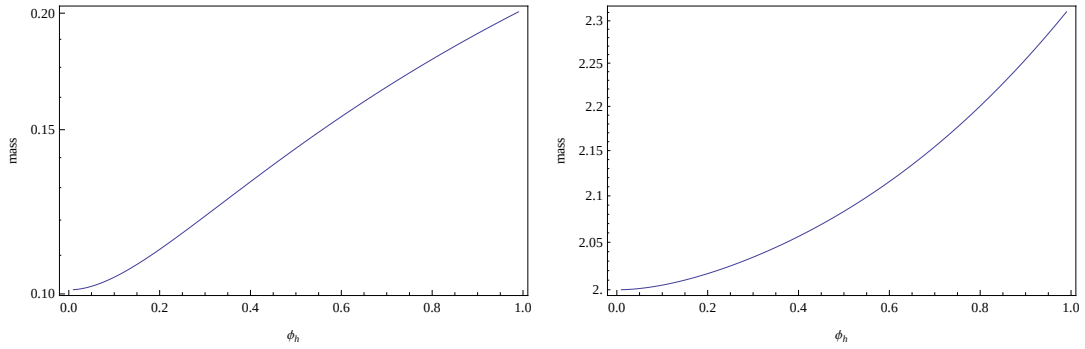

(a) mass for $r_h = 0.1$ (b) mass for $r_h = 1$

Figure 6.24: Subcase 2c with pseudo-TWI potential for $D = 4$, $dm = 5/6L$, $A = -7/9$, $k = 1$, $\kappa = 1$, $L = 1$, $\delta_h = 0$ (a) effect on the mass as we vary ϕ_h for $r_h = 0.1$ (b) effect on the mass as we vary ϕ_h for $r_h = 1$.

In Fig. 6.23a we see that the parameter a is always positive. Fig. 6.23b shows that the parameter b is negative for some region in the parameter space. It is positive and increasing as $\phi_h \to 1$. In Fig. 6.23c we see that the parameter f_{rr} is positive. For $r_h = 1$ the parameter f_{rr} is roughly two. This is also the value of the mass when $r_h = 1$ as can be seen in Figs. 6.23d, 6.24b. When the horizon is small i.e. $r_h = 0.1$ then the mass is small as can be seen in Figs. 6.23d, 6.24a. The parameter f_{rr} seems to have a maximum which we have not previously seen. The mass is however still monotonically increasing as ϕ_h increases.

Subcase 2d with pseudo-TWI potential

We present the results for subcase 2d:

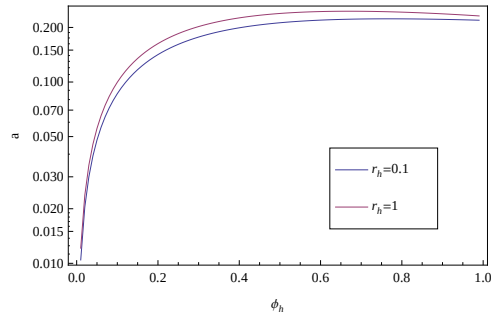

(a) a plot

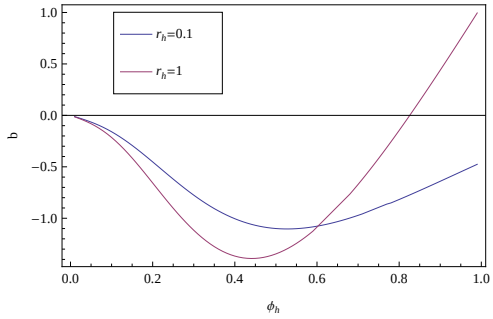

(b) b plot

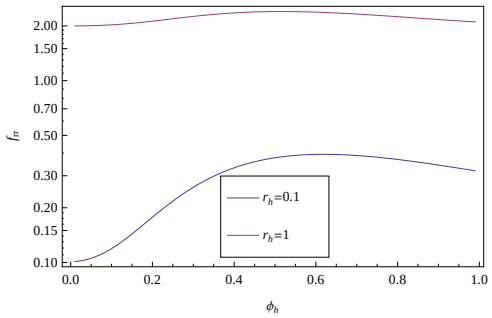

(c) f_{rr} plot

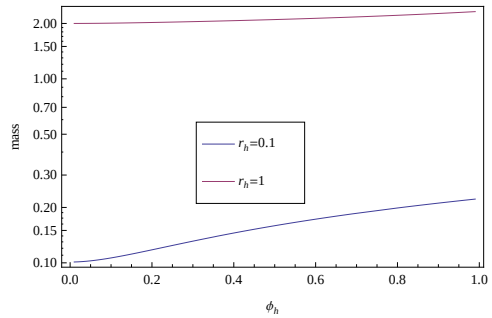

(d) Mass plot

Figure 6.25: Subcase $2d$ with pseudo-TWI potential for $D = 4$, $dm = 12/13L$, $A = -945/1352$, $k = 1$, $\kappa = 1$, $L = 1$, $\delta_h = 0$ (a) effect on the parameter a as we vary ϕ_h for two different values of r_h (b) effect on the parameter b as we vary ϕ_h for two different values of r_h (c) effect on the parameter f_{rr} as we vary ϕ_h for two different values of r_h (d) effect on the mass as we vary ϕ_h for two different values of r_h.

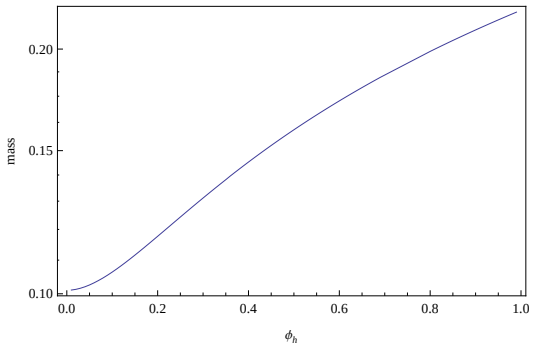

(a) mass for $r_h = 0.1$

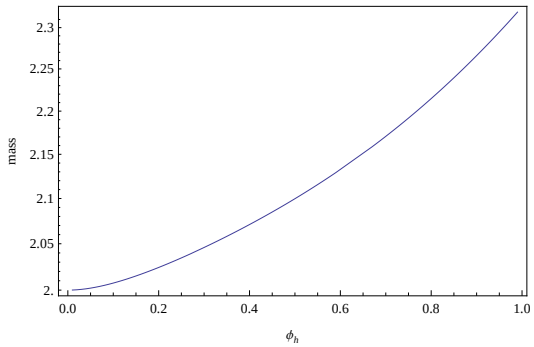

(b) mass for $r_h = 1$

Figure 6.26: Subcase $2d$ with pseudo-TWI potential for $D = 4$, $dm = 12/13L$, $A = -945/1352$, $k = 1$, $\kappa = 1$, $L = 1$, $\delta_h = 0$ (a) effect on the mass as we vary ϕ_h for $r_h = 0.1$ (b) effect on the mass as we vary ϕ_h, for $r_h = 1$.

For this case the results are very similar to case 2c. From Fig. 6.25a we see that a is always positive. In Fig. 6.25b we see that the parameter b is negative over a bigger region of the parameter space compared to case 2c. We also notice that the dip in b is more pronounced. The parameter f_{rr} when $r_h = 1$ is still roughly two. For $r_h = 0.1$ the parameter f_{rr} also has a maximum. We see the shapes of the masses in Fig. 6.25d. The mass is small when $r_h = 0.1$, for $r_h = 1$ is has a value of 2 when $\phi_h \to$ and slowly increases as $\phi_h \to \infty$ (see Figs. 6.26a and 6.26a).

Subcase 2e in $D = 5$ with Higgs potential

We want to show an example of a subcase in a higher dimension:

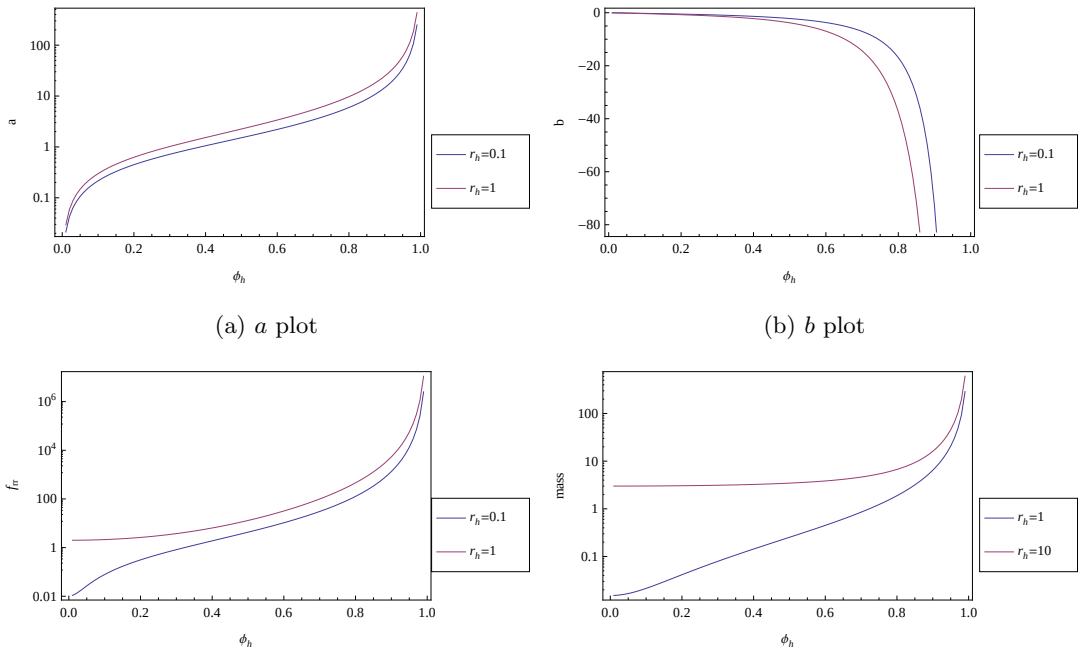

(a) a plot (b) b plot

(c) f_{rr} plot (d) Mass plot

Figure 6.27: Subcase 2e with Higgs potential for $D = 5$, $dm = 1/2L$, $\alpha_0 = 15/(4L^2v^2)$, $k = 1$, $\kappa = 1$, $L = 1$, $\delta_h = 0$ (a) effect on the parameter a as we vary ϕ_h for two different values of r_h (b) effect on the parameter b as we vary ϕ_h for two different values of r_h (c) effect on the parameter f_{rr} as we vary ϕ_h for two different values of r_h (d) effect on the mass as we vary ϕ_h for two different values of r_h.

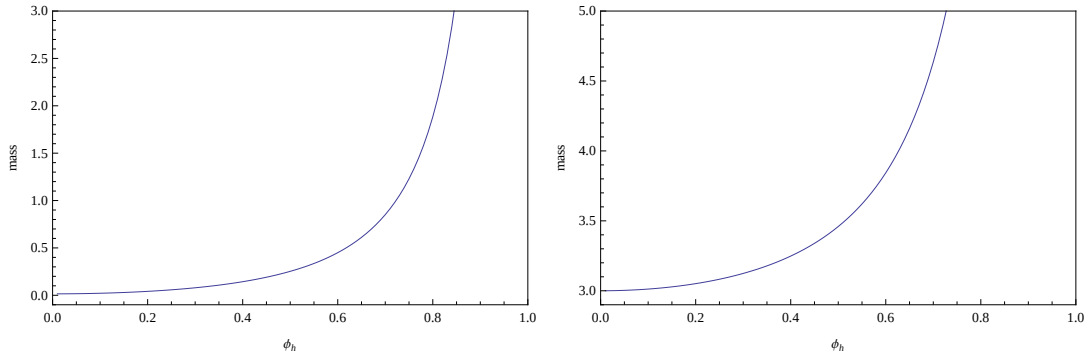

(a) mass for $r_h = 0.1$ (b) mass for $r_h = 1$

Figure 6.28: Subcase $2e$ with Higgs potential for $D = 5$, $dm = 1/2L$, $\alpha_0 = 15/(4L^2v^2)$, $k = 1$, $\kappa = 1$, $L = 1$, $\delta_h = 0$ (a) effect on the mass as we vary ϕ_h for $r_h = 0.1$ (b) effect on the mass as we vary ϕ_h, for $r_h = 1$.

The plots in Figs. 6.28a and 6.28b show interesting features.As $\phi_h \to 1$ the mass seems to diverge more rapidly than in $D = 4$. We notice that the mass for $r_h = 1$ has a value of three.

Subcase $2g$ in $D = 5$ with pseudo-TWI potential

We present the plots for the mass which is very similar to the rest of the cases.

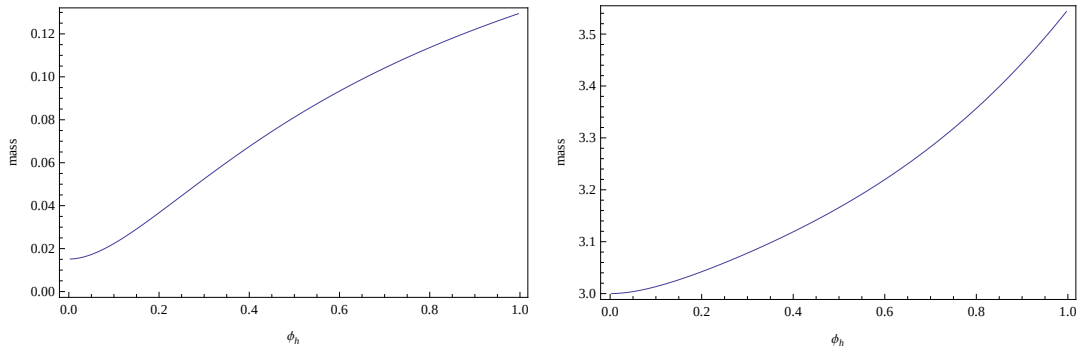

(a) mass for $r_h = 0.1$ (b) mass for $r_h = 1$

Figure 6.29: Subcase $2g$ with pseudo-TWI potential, $D = 5$, $dm = 3/4L$, $A = -55/32$, $k = 1$, $\kappa = 1$, $L = 1$, $\delta_h = 0$ (a) effect on the mass as we vary ϕ_h for $r_h = 0.1$ (b) effect on the mass as we vary ϕ_h for $r_h = 1$.

We see in Figs. 6.29a and 6.29b that the mass is bigger when $r_h = 1$. The mass is always positive and in this case has a value of three when $r_h = 1$. This value is similar to the mass for subcase $2e$. The mass does not seem to diverge as $\phi_h \to 1$.

Subcases $3a, 3d, 3e$ with pseudo-TWI potential

These are subcases with a logarithmic branch.

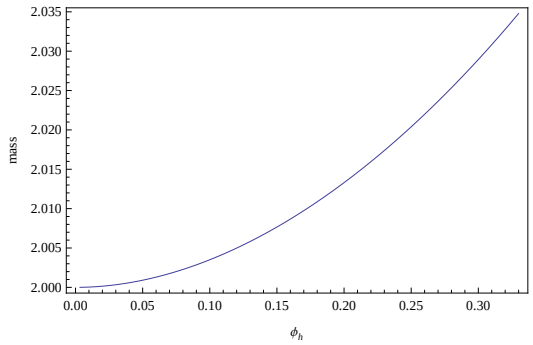

(a) mass for subcase $3a$

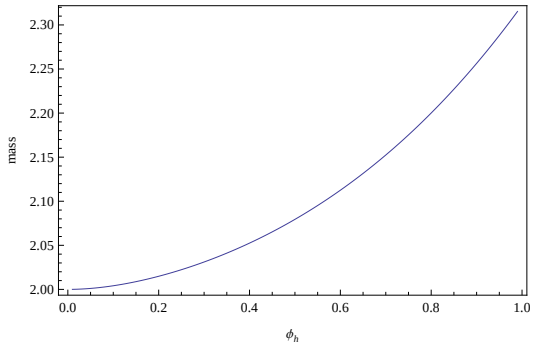

(b) mass for subcase $3d$

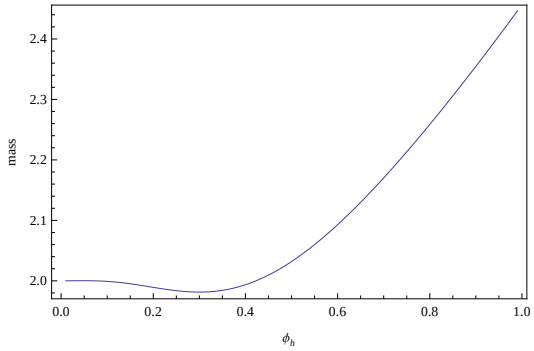

(c) mass for subcase $3e$

Figure 6.30: (a) effect on the mass as we vary ϕ_h with pseudo-TWI potential, $D = 4$, $dm = 1/2L$, $A = -1$, $k = 1$, $\kappa = 1$, $L = 1$, $\delta_h = 0$, $r_h = 1$ (b) effect on the mass as we vary ϕ_h with pseudo-TWI potential, $D = 4$, $dm = 1/2L$, $A = -27/32$, $k = 1$, $\kappa = 1$, $L = 1$, $\delta_h = 0$, $r_h = 1$ (c) effect on the mass as we vary ϕ_h with pseudo-TWI potential, $D = 4$, $dm = 1/2L$, $A = -18/25$, $k = 1$, $\kappa = 1$, $L = 1$, $\delta_h = 0$, $r_h = 1$.

In Figs. 6.30a-6.30c we plots the masses for logarithmic subcases with $D = 4$. We see that all the masses have values around two when ϕ_h is very small. We see that for subcase $3e$ which is the most complicated subcase, the mass is not monotonically increasing as ϕ_h increases. There is also a bit of a dip for which is not seen for subcases $3a$ or $3d$.

6.6.3 Results when varying r_h

Subcase 2b with Higgs potential

We now presents some results for the mass when we vary r_h.

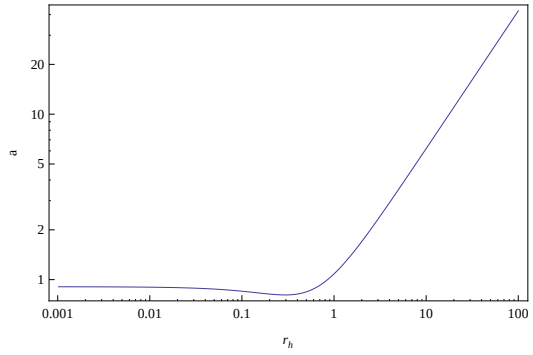

(a) parameter a

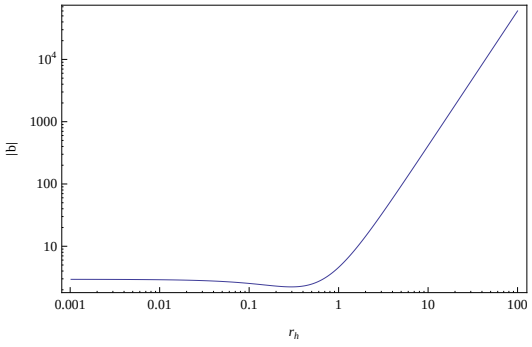

(b) parameter b

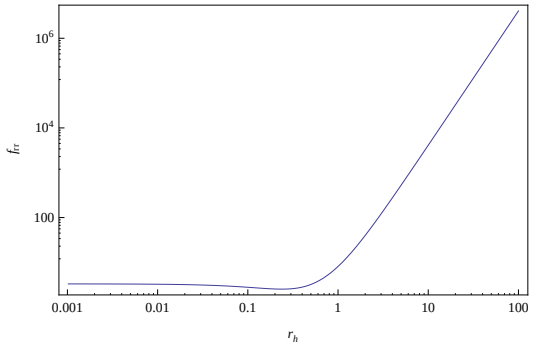

(c) parameter f_{rr}

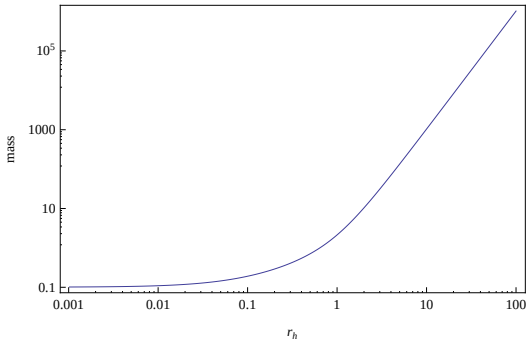

(d) mass

Figure 6.31: Subcase 2b with Higgs potential, $D = 4$, $dm = 2/3L$, $\alpha_0 = 65/(36L^2v^2)$, $\phi_h = 0.5$, $k = 1$, $\kappa = 1$, $L = 1$, $\delta_h = 0$ (a) effect on the parameter a as we vary r_h (b) effect on the parameter b as we vary r_h (c) effect on the parameter f_{rr} as we vary r_h (d) effect on the mass as we vary r_h.

The plots in Figs. 6.31a-6.31d show that there is a change of behaviour in the parameters spaces for a, b and f_{rr} at roughly $r_h \sim 0.5$. There is a slight dip. The magnitudes of the parameters are different. As $r_h \to 100$ parameter a is roughly 30, parameter b is roughly 10^5 and f_{rr} around 10^7. We see that a and f_{rr} are always positive. The parameter b is negative. The mass is positive and does not show any dip.

Subcase 2c with pseudo-TWI potential

For this case when we vary r_h we have:

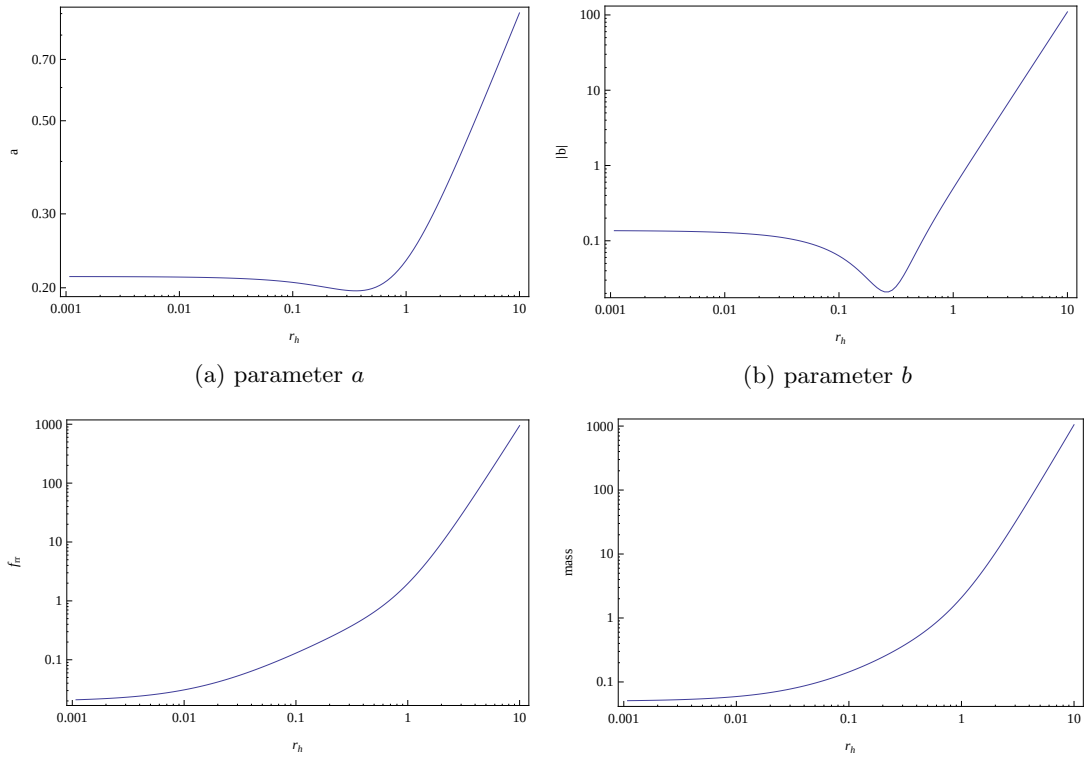

(a) parameter a

(b) parameter b

(c) parameter f_{rr}

(d) mass

Figure 6.32: Subcase $2c$ with pseudo-TWI potential, $D = 4$, $dm = 5/6L$, $A = -7/9$, $\phi_h = 0.5$, $k = 1$, $\kappa = 1$, $L = 1$, $\delta_h = 0$ (a) effect on the parameter a as we vary r_h (b) effect on the parameter b as we vary r_h (c) effect on the parameter f_{rr} as we vary r_h (d) effect on the mass as we vary r_h.

The plots in Figs. 6.32a-6.32d show that there is a change in behaviour at around $r_h = 0.5$. We observe a dip. The change is clearer for parameter b where there is a big dip at $r_h = 0.5$. The mass is still positive. We notice that as $r_h \to 10$ the parameter f_{rr} and the mass increase in a similar way. However f_{rr} increases slightly faster.

Subcase $2e$ with pseudo-TWI potential

In higher dimensions (in this subcase $D = 5$), when we vary r_h we have:

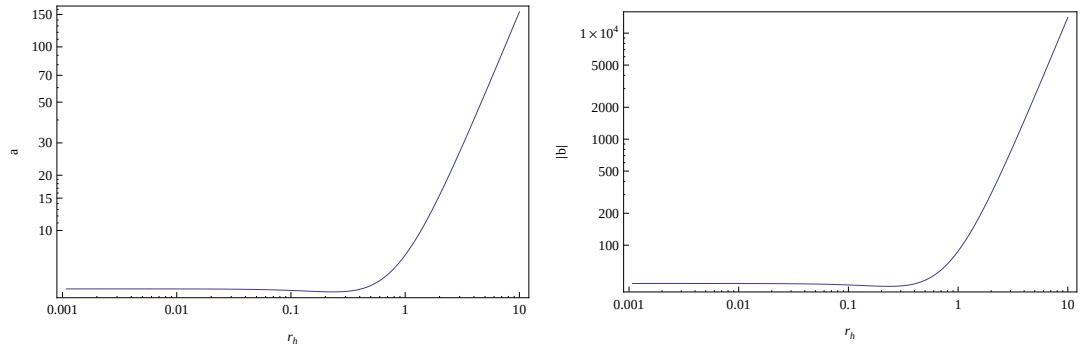

(a) a plot

(b) b plot

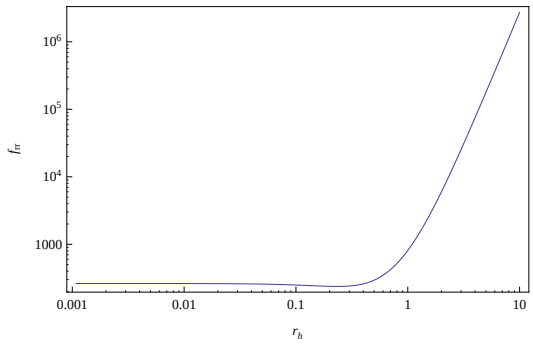

(c) f_{rr} plot

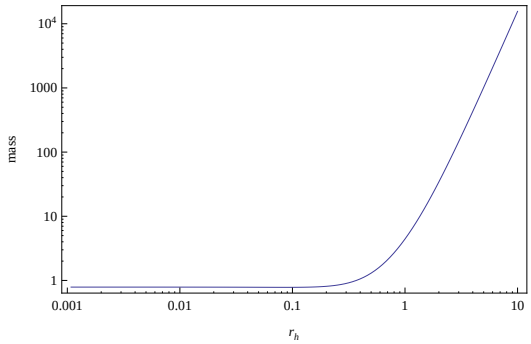

(d) Mass plot

Figure 6.33: Subcase 2e with Higgs potential for $D = 5$, $dm = 1/2L$, $\alpha_0 = 15/(4L^2v^2)$, $\phi_h = 0.5$, $k = 1$, $\kappa = 1$, $L = 1$, $\delta_h = 0$ (a) effect on parameter a as we vary r_h (b) effect on parameter b as we vary r_h (c) effect on parameter f_{rr} as we vary r_h (d) effect on the mass as we vary r_h.

From Figs. 6.33a-6.33d we see that there are no dips in the figures. The shapes look the same. The magnitudes of the parameters are different, the parameter a has the smallest magnitude and the parameter f_{rr} has the biggest magnitude.

Subcase 2g with pseudo-TWI potential

In this subcase we want to illustrate that the scalar field contribution is negligible when $r_h > 1$, we see this in Fig. 6.34:

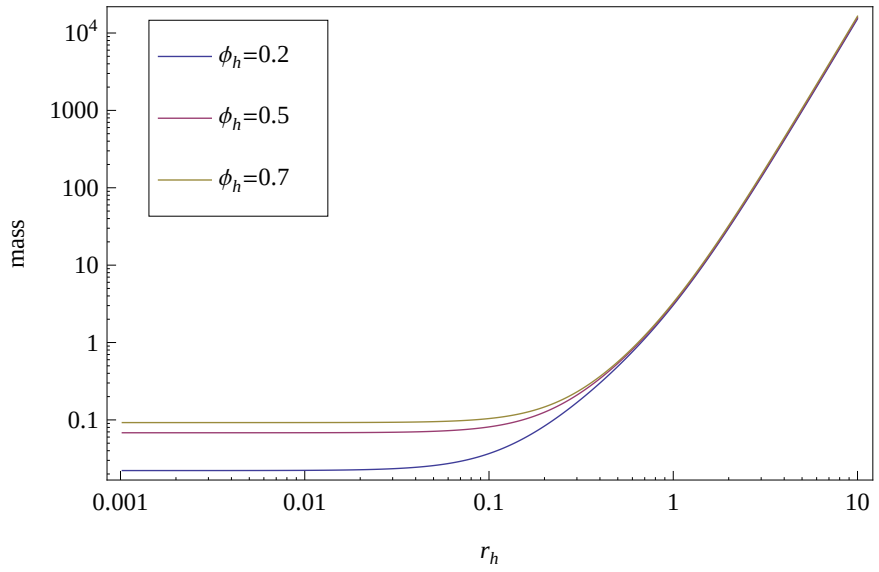

Figure 6.34: Subcase $2g$: effect on the mass as we vary r_h for three different values of ϕ_h with pseudo-TWI potential, $D = 5$, $dm = 3/4L$, $A = -55/32$, $k = 1$, $\kappa = 1$, $L = 1$, $\delta_h = 0$.

This result is similar to subcase $2a$ for Higgs potential.

From all the figures presented above we can say that the results are consistent. They all show that the mass is positive and that for $r_h > 1$ the mass is dominated by the gravitational contribution. The value of the mass increases as we increase r_h.

§ 6.7 Summary

In this chapter we have seen how to obtain the parameters a, b and f_{rr} in order to calculate the mass. We have seen that is not a hard task to solve the differential equation for ϕ and obtain a value for a since a is contained in the leading behaviour of ϕ. However parameters b and f_{rr} are contained in subleading terms which makes them hard to extract. The solution was to define new functions $\xi(r)$ and $\psi(r)$ whose leading behaviour contains b and f_{rr} respectively. We obtained the differential equations for these functions and solved them to obtain b and f_{rr}. We then plotted the mass parameters while varying ϕ_h and r_h. We presented a selection of plots and discussed interesting features.

Conclusion

In this thesis we have studied the mass of black holes minimally coupled to a scalar field in adS spacetime.

We started by reviewing uniqueness and no-hair theorems in chapter 1. We presented two no-hair proofs to understand what lies at the heart of the no-hair theorems. Finally we introduce the ADM mass and the Komar integral.

In chapter 2 we saw how there are several methods to calculate the mass in asymptotically adS spacetime. We considered three methods and decided the Henneaux and Teitelboim method [74] was the most appropriate for our work. We investigated Einstein gravity minimally coupled to a scalar field in chapter 3. We found four possible asymptotic forms for the scalar field. We proved some no-hair theorems when the self interaction potential is convex. When we considered nonconvex Higgs and TWI potentials, soliton and black hole solutions were found and their stability was tested. The stability of case 1 is complicated to determine as the scalar field converges to a non-zero constant at infinity. Cases 2 and 3 were found to be stable, for these cases the scalar field vanishes at infinity as predicted by [129]. Finally case 4 is the oscillatory case and was found to be unstable.

The main focus of our work has been to provide a method to obtain finite expressions of the sapcetimes masses. In order to calculate the mass of the spacetimes the leading order behaviour of the scalar field is not enough. In chapter 4 we present the detailed asymptotics for the scalar field ϕ and the metric perturbation h_{rr}. In this chapter we see that the scalar field has a back reaction on the metric and that different subcases arise as m^2 varies. We used the field equations to calculate important coefficients with own mathematica code.

When the scalar field has a mass above the Breitenlohner-Freedman bound [31], the total mass of the spacetime is the sum of the gravitational contribution and the scalar contribution. Both contributions are divergent but by adding them together using the correct cut-offs, we obtained finite masses. The masses were all calculated using our

own mathematica code. We obtained finite expressions for all the subcases. In [73], Henneaux *et al.* give the explicit expression for one subcase which is in agreement with the expression we found.

The masses were found to depend on three parameters a, b and f_{rr}. The parameters b and f_{rr} are contained in coefficients of subleading terms. In order to extract them, we defined new functions ξ and ψ whose leading order behaviour contain b and f_{rr} respectively. Mass parameters a, b and f_{rr} were found by solving the differential equations for ϕ, ξ and ψ respectively. We used our mathematica code for Higgs potential and a pseudo-TWI potential. We presented detailed results for subcase $2a$. We found that the parameter a is positive and the parameter b is negative for subcase $2a$. These two parameters represent the scalar field contribution to the mass. The parameter f_{rr} which is the gravitational contribution to the mass was found to be larger than a and b. The scalar field contribution was found to be negligible for $r_h > 1$. We presented results for topological black holes. When $k = 0$ the results showed scale invariance. When $k = -1$ we found that the mass can be negative.

We presented results for the rest of the cases. The mass was found to be very similar for all the cases. This shows that the method we used gives sensible results for the mass. Our method can be used to find the mass for spacetimes with gravity minimally coupled to scalar field.

The main direct application is to black hole thermodynamics where the mass of the spacetime is needed to study the thermodynamics stability. Our work can be extended to non-minimally coupled scalar field which is treated in [86] with zero self interaction potential. The thermodynamics could also be studied for this case.

Bibliography

[1] http://grtensor.phy.queensu.ca/.

[2] G. Aad et al. Observation of a new particle in the search for the standard model Higgs boson with the ATLAS detector at the LHC. *Phys.Lett.*, B716:1–29, 2012.

[3] L.F. Abbott and S. Deser. Stability of gravity with a cosmological constant. *Nucl.Phys.*, B195:76, 1982.

[4] A. Acena, A. Anabalon, and D. Astefanesei. Exact hairy black brane solutions in adS_5 and holographic RG flows. *Phys.Rev.*, D87(12):124033, 2013.

[5] A. Acena, A. Anabalon, D. Astefanesei, and R. Mann. Hairy planar black holes in higher dimensions. *JHEP*, 1401:153, 2014.

[6] M. Alcubierre, J.A. Gonzalez, and M. Salgado. Dynamical evolution of unstable self-gravitating scalar solitons. *Phys.Rev.*, D70:064016, 2004.

[7] A.J. Amsel and D. Marolf. Energy bounds in designer gravity. *Phys.Rev.*, D74:064006, 2006.

[8] A. Anabalon. Exact black holes and universality in the backreaction of non-linear sigma models with a potential in adS4. *JHEP*, 1206:127, 2012.

[9] A. Anabalon and D. Astefanesei. On attractor mechanism of adS_4 black holes. *Phys.Lett.*, B727:568–572, 2013.

[10] A. Anabalon, D. Astefanesei, and R. Mann. Exact asymptotically flat charged hairy black holes with a dilaton potential. *JHEP*, 1310:184, 2013.

[11] R.L. Arnowitt, S. Deser, and C.W. Misner. The dynamics of general relativity. 1962. Gravitation: an introduction to current research, Louis Witten ed. (Wilew 1962), chapter 7, pp 227-265.

[12] A. Ashtekar and S. Das. Asymptotically anti-de sitter space-times: conserved quantities. *Class.Quant.Grav.*, 17:L17–L30, 2000.

[13] A. Ashtekar and A. Magnon. Asymtotically anti-de Sitter space-times. *Class.Quant.Grav.*, 1:L39–L44, 1984.

[14] V. Balasubramanian and P. Kraus. A stress tensor for anti-de Sitter gravity. *Commun.Math.Phys.*, 208:413–428, 1999.

[15] M. Banados, M. Henneaux, C. Teitelboim, and J. Zanelli. Geometry of the (2+1) black hole. *Phys.Rev.*, D48:1506–1525, 1993.

[16] M. Banados, C. Teitelboim, and J. Zanelli. The black hole in three-dimensional space-time. *Phys.Rev.Lett.*, 69:1849–1851, 1992.

[17] M. Banados and S. Theisen. Scale invariant hairy black holes. *Phys.Rev.*, D72:064019, 2005.

[18] J.M. Bardeen, B. Carter, and S.W. Hawking. The four laws of black hole mechanics. *Commun.Math.Phys.*, 31:161–170, 1973.

[19] G. Barnich. Conserved charges in gravitational theories:contribution from scalar fields. 2002.

[20] O. Bechmann and O. Lechtenfeld. Exact black hole solution with selfinteracting scalar field. *Class.Quant.Grav.*, 12:1473–1482, 1995.

[21] J.D. Bekenstein. Nonexistence of baryon number for static black holes. *Phys.Rev.*, D5:1239–1246, 1972.

[22] J.D. Bekenstein. Exact solutions of Einstein conformal scalar equations. *Annals Phys.*, 82:535–547, 1974.

[23] J.D. Bekenstein. Novel 'no scalar hair' theorem for black holes. *Phys.Rev.*, D51:6608–6611, 1995.

[24] A. Belhaj, M. Chabab, H. El Moumni, K. Masmar, and M.B. Sedra. Critical Behaviors of 3D Black Holes with a Scalar Hair. *Int.J.Geom.Meth.Mod.Phys.*, 12(02):1550017, 2014.

[25] S. Bhattacharya and A. Lahiri. Black-hole no-hair theorems for a positive cosmological constant. *Phys.Rev.Lett.*, 99:201101, 2007.

[26] M. Bianchi, D.Z Freedman, and Kostas K. Skenderis. Holographic renormalization. *Nucl.Phys.*, B631:159–194, 2002.

[27] M. Bianchi, D.Z. Freedman, and K. Skenderis. How to go with an RG flow. *JHEP*, 0108:041, 2001.

[28] D. Birmingham. Topological black holes in anti-de Sitter space. *Class.Quant.Grav.*, 16:1197–1205, 1999.

[29] P. Bizon. Colored black holes. *Phys.Rev.Lett.*, 64:2844–2847, 1990.

[30] P. Bizon. Gravitating solitons and hairy black holes. *Acta Phys.Polon.*, B25:877–898, 1994.

[31] P. Breitenlohner and D.Z reedman. Positive energy in anti-de Sitter backgrounds and gauged extended supergravity. *Phys.Lett.*, B115:197, 1982.

[32] A.E. Broderick, T. Johannsen, A. Loeb, and D. Psaltis. Testing the no-hair theorem with event horizon telescope observations of Sagittarius A*. *Astrophys.J.*, 784:7, 2014.

[33] K.A. Bronnikov and Yu. N. Kireev. Instability of black holes with scalar charge. *Phys.Lett.*, A67:95–96, 1978.

[34] K.A. Bronnikov and G.N. Shikin. Spherically symmetric scalar vacuum: no go theorems, black holes and solitons. *Grav.Cosmol.*, 8:107–116, 2002.

[35] D. Brown and J. York. Quasilocal energy and conserved charges derived from the gravitational action. *Phys.Rev.D*, 47(4), 1992.

[36] J.D. Brown, J. Creighton, and R.B. Mann. Temperature, energy and heat capacity of asymptotically anti-de Sitter black holes. *Phys.Rev.*, D50:6394–6403, 1994.

[37] A. Buchel and C. Pagnutti. Exotic hairy black holes. *Nucl.Phys.*, B824:85–94, 2010.

[38] M. Cardenas, O. Fuentealba, and C. Martinez. Three-dimensional black holes with conformally coupled scalar and gauge fields. 2014.

[39] S. Carroll. *An introduction to general relativity: spacetime and geometry.* Addison Wesley, 2004.

[40] B. Carter. Axisymmetric black hole has only two degrees of freedom. *Phys.Rev.Lett.*, 26:331–333, 1971.

[41] S. Chadburn and R. Gregory. Time dependent black holes and scalar hair. *Class.Quant.Grav.*, 31(19):195006, 2014.

[42] S. Chatrchyan et al. Observation of a new boson at a mass of 125 GeV with the CMS experiment at the LHC. *Phys.Lett.*, B716:30–61, 2012.

[43] W. Chen, H. Lu, and C.N.Pope. Mass of rotating black holes in gauged supergravities. *Phys.Rev.*, D73:104036, 2006.

[44] D.D.K. Chow and G. Compere. Dyonic adS black holes in maximal gauged supergravity. *Phys.Rev.*, D89:065003, 2014.

[45] A. Corichi, U. Nucamendi, and M. Salgado. Scalar hairy black holes and scalarons in the isolated horizons formalism. *Phys.Rev.*, D73:084002, 2006.

[46] F. Correa, A. Faundez, and C. Martinez. Rotating hairy black hole and its microscopic entropy in three spacetime dimensions. *Phys.Rev.*, D87:027502, 2013.

[47] F. Correa, C. Martinez, and R. Troncoso. Scalar solitons and the microscopic entropy of hairy black holes in three dimensions. *JHEP*, 1101:034, 2011.

[48] F. Correa, C. Martinez, and R. Troncoso. Hairy black Hole entropy and the role of solitons in three dimensions. *JHEP*, 1202:136, 2012.

[49] S. Das, J. Gegenberg, and V. Husain. Scalar field space-times and the adS / CFT conjecture. *Phys.Rev.*, D64:065027, 2001.

[50] J.L. Davis, T.S. Levi, M. Van Raamsdonk, and K.R.L. Whyte. Twisted inflation. *JCAP*, 1009:032, 2010.

[51] S. de Haro, K. Skenderis, and S.N. Solodukhin. Gravity in warped compactifications and the holographic stress tensor. *Class.Quant.Grav.*, 18:3171–3180, 2001.

[52] S. de Haro, S.N. Solodukhin, and K. Skenderis. Holographic reconstruction of space-time and renormalization in the adS / CFT correspondence. *Commun.Math.Phys.*, 217:595–622, 2001.

[53] H. Dennhardt and O. Lechtenfeld. Scalar deformations of Schwarzschild holes and their stability. *Int.J.Mod.Phys.*, A13:741, 1998.

[54] S. Detournay, T. Hartman, and D.M. Hofman. Warped conformal field theory. *Phys.Rev.*, D86:124018, 2012.

[55] P.A.M. Dirac. The theory of gravitation in Hamiltonian form. *Proc.Roy.Soc.Lond.*, A246:333–343, 1958.

[56] G. Dotti, R.J. Gleiser, and C. Martinez. Static black hole solutions with a self interacting conformally coupled scalar field. *Phys.Rev.*, D77:104035, 2008.

[57] T. Faulkner, G.T. Horowitz, and M.M. Roberts. New stability results for Einstein scalar gravity. *Class.Quant.Grav.*, 27:205007, 2010.

[58] X. Feng, H. Lu, and Q. Wen. Scalar hairy black holes in general dimensions. *Phys.Rev.*, D89:044014, 2014.

[59] J. Gegenberg, C. Martinez, and R. Troncoso. A finite action for three-dimensional gravity with a minimally coupled scalar field. *Phys.Rev.*, D67:084007, 2003.

[60] S.A. Gentle, M. Rangamani, and B. Withers. A soliton menagerie in adS. *JHEP*, 1205:106, 2012.

[61] G.W. Gibbons, S.W. Hawking, G.T. Horowitz, and M.J. Perry. Positive mass theorems for black holes. *Commun.Math.Phys.*, 88:295, 1983.

[62] G.W. Gibbons, C.M. Hull, and N.P. Warner. The Stability of gauged supergravity. *Nucl.Phys.*, B218:173, 1983.

[63] S.S. Gubser. Phase transitions near black hole horizons. *Class.Quant.Grav.*, 22:5121–5144, 2005.

[64] S.S. Gubser, A. Nellore, S.S. Pufu, and F.D. Rocha. Thermodynamics and bulk viscosity of approximate black hole duals to finite temperature quantum chromodynamics. *Phys.Rev.Lett.*, 101:131601, 2008.

[65] A.J. Hanson, T. Regge, and C. Teitelboim. *Constrained Hamiltonian systems.* Accademia Nazionale dei Lincei, 1976.

[66] T.J.T. Harper, P.A. Thomas, E. Winstanley, and P.M. Young. Instability of a four-dimensional de Sitter black hole with a conformally coupled scalar field. *Phys.Rev.*, D70:064023, 2004.

[67] M. Hasanpour, F. Loran, and H. Razaghian. Gravity/CFT correspondence for three dimensional Einstein gravity with a conformal scalar field. *Nucl.Phys.*, B867:483–505, 2013.

[68] S.W. Hawking and G.T. Horowitz. The gravitational Hamiltonian, action, entropy and surface terms. *Class.Quant.Grav.*, 13:1487–1498, 1996.

[69] S.W. Hawking and D.N. Page. Thermodynamics of black holes in anti-de Sitter space. *Commun.Math.Phys.*, 87:577, 1983.

[70] M. Henneaux, C. Martinez, and R. Troncoso. More on Asymptotically Anti-de Sitter Spaces in Topologically Massive Gravity. *Phys.Rev.*, D82:064038, 2010.

[71] M. Henneaux, C. Martinez, R. Troncoso, and J. Zanelli. Black holes and asymptotics of 2+1 gravity coupled to a scalar field. *Phys.Rev.*, D65:104007, 2002.

[72] M. Henneaux, C. Martinez, R. Troncoso, and J. Zanelli. Asymptotically anti-de Sitter spacetimes and scalar fields with a logarithmic branch. *Phys.Rev.*, D70:044034, 2004.

[73] M. Henneaux, C. Martinez, R. Troncoso, and J. Zanelli. Asymptotic behaviour and hamiltonian analysis of anti-de Sitter gravity coupled to scalar fields. *Annals Phys.*, 322:824–848, 2007.

[74] M. Henneaux and C. Teitelboim. Asymptotically anti-de Sitter spaces. *Commun.Math.Phys.*, 98:391–424, 1985.

[75] M. Henningson and K. Skenderis. The holographic Weyl anomaly. *JHEP*, 9807:023, 1998.

[76] M. Henningson and K. Skenderis. The holographic Weyl anomaly. *JHEP*, 9807:023, 1998.

[77] T. Hertog. Towards a novel no-hair theorem for black holes. *Phys.Rev.*, D74:084008, 2006.

[78] T. Hertog and K. Maeda. Black holes with scalar hair and asymptotics in N = 8 supergravity. *JHEP*, 0407:051, 2004.

[79] T. Hertog and K. Maeda. Stability and thermodynamics of adS black holes with scalar hair. *Phys.Rev.*, D71:024001, 2005.

[80] M. Heusler. A mass bound for spherically symmetric black hole space-times. *Class.Quant.Grav.*, 12:779–790, 1995.

[81] S. Hollands, A. Ishibashi, and D. Marolf. Comparison between various notions of conserved charges in asymptotically adS spacetimes. *Class.Quant.Grav.*, 22:2881–2920, 2005.

[82] G.T. Horowitz. Introduction to holographic superconductors. *Lect.Notes Phys.*, 828:313–347, 2011.

[83] G.T. Horowitz and R.C. Myers. The adS / CFT correspondence and a new positive energy conjecture for general relativity. *Phys.Rev.*, D59:026005, 1998.

[84] M. Hortacsu, H.T. Ozcelik, and B. Yapiskan. Properties of solutions in (2+1)-dimensions. *Gen.Rel.Grav.*, 35:1209–1221, 2003.

[85] D. Hosler and E. Winstanley. Higher-dimensional solitons and black holes with a non-minimally coupled scalar field. *Phys.Rev.*, D80:104010, 2009.

[86] D. Hosler and E. Winstanley. Higher-dimensional solitons and black holes with a non-minimally coupled scalar field. *Phys.Rev.*, D80:104010, 2009.

[87] W. Israel. Event horizons in static vacuum space-times. *Phys.Rev.*, 164:1776–1779, 1967.

[88] R.A. Matzner J.A.H. Futterman, F.A. Handler. *Scattering from Blak Holes*. Cambridge University Press, 1988.

[89] A. Komar. Positive-definite energy density and global consequences for general relativity. *Phys.Rev.*, 129:1873–1876, Feb 1963.

[90] H.P. Kuenzle and A.K.M. Masood ul Alam. Spherically symmetric static SU(2) Einstein Yang-Mills fields. *J.Math.Phys.*, 31:928–935, 1990.

[91] P.I. Kuriakose and V.C. Kuriakose. Static black hole dressed with a massive scalar field. 2008.

[92] J.P.S. Lemos. Cylindrical black hole in general relativity. *Phys.Lett.*, B353:46–51, 1995.

[93] J.P.S. Lemos. Two-dimensional black holes and planar general relativity. *Class.Quant.Grav.*, 12:1081–1086, 1995.

[94] J.P.S. Lemos and V.T. Zanchin. Rotating charged black string and three-dimensional black holes. *Phys.Rev.*, D54:3840–3853, 1996.

[95] H. Liu and H. Lu. Scalar charges in asymptotic adS geometries. *Phys.Lett.*, B730:267–270, 2014.

[96] H. Lu, C.N.Pope, and Q. Wen. Thermodynamics of adS black holes in Einstein-scalar gravity. 2014.

[97] H. Lu, Y. Pang, and C.N. Pope. AdS dyonic black hole and its thermodynamics. *JHEP*, 1311:033, 2013.

[98] H. Lu and X. Zhang. Exact collapse solutions in $D = 4, \mathcal{N} = 4$ gauged supergravity and their generalizations. *JHEP*, 1407:099, 2014.

[99] K. Maeda, T. Tachizawa, T. Torii, and T. Maki. Stability of non-abelian black holes and catastrophe theory. *Phys.Rev.Lett.*, 72:450–453, 1994.

[100] J.M. Maldacena. The large N limit of superconformal field theories and supergravity. *Adv.Theor.Math.Phys.*, 2:231–252, 1998.

[101] C. Martinez, C. Teitelboim, and J. Zanelli. Charged rotating black hole in three space-time dimensions. *Phys.Rev.*, D61:104013, 2000.

[102] C. Martinez, R. Troncoso, and J. Zanelli. De Sitter black hole with a conformally coupled scalar field in four-dimensions. *Phys.Rev.*, D67:024008, 2003.

[103] C. Martinez, R. Troncoso, and J. Zanelli. Exact black hole solution with a minimally coupled scalar field. *Phys.Rev.*, D70:084035, 2004.

[104] C. Martinez and J. Zanelli. Conformally dressed black hole in (2+1)-dimensions. *Phys.Rev.*, D54:3830–3833, 1996.

[105] P.O. Mazur. Proof of uniqueness of the Kerr-Newman black hole solution. *J.Phys.*, A15:3173–3180, 1982.

[106] L. Mezincescu and P.K. Townsend. Stability at a local maximum in higher dimensional anti-de Sitter space and applications to supergravity. *Annals Phys.*, 160:406, 1985.

[107] Y.S. Myung, W. Hyung Lee, and Y. Kim. Entropy of black holes in topologically massive gravity. 2008.

[108] M. Natsuume and T. Okamura. Entropy for asymptotically adS(3) black holes. *Phys.Rev.*, D62:064027, 2000.

[109] U. Nucamendi and M. Salgado. Scalar hairy black holes and solitons in asymptotically flat space-times. *Phys.Rev.*, D68:044026, 2003.

[110] D.H. Park. Scaling arguments and scalar hairs in asymptotically anti-de Sitter spacetime. *Class.Quant.Grav.*, 25:095002, 2008.

[111] M. Park. Fate of three-dimensional black holes coupled to a scalar field and the Bekenstein-Hawking entropy. *Phys.Lett.*, B597:237–242, 2004.

[112] E. Poisson. *A relativist's toolkit: the mathematics of black-hole mechanics.* Cambridge University Press, 2004.

[113] W.H. Press and S.A. Teukolsky. Perturbations of a rotating black hole. II. dynamical stability of the Kerr metric. *Astrophys.J.*, 185:649–674, 1973.

[114] E. Radu and E. Winstanley. Conformally coupled scalar solitons and black holes with negative cosmological constant. *Phys.Rev.*, D72:024017, 2005.

[115] T. Regge and C. Teitelboim. Role of surface integrals in the hamiltonian formulation of general relativity. *Annals Phys.*, 88:286–318, 1974.

[116] D.C. Robinson. Uniqueness of the Kerr black hole. *Phys.Rev.Lett.*, 34:905–906, 1975.

[117] R. Ruffini and J.A. Wheeler. Introducing the black hole. *Phys. Today*, 30-41, 1971.

[118] A. Saa. New no scalar hair theorem for black holes. *J.Math.Phys.*, 37:2346–2351, 1996.

[119] J. Sadeghi and H. Farahani. Thermodynamics of a charged hairy black hole in (2+1) dimensions. *Int.J.Theor.Phys.*, 53(11):3683–3697, 2014.

[120] M. Sasaki and T. Nakamura. Gravitational radiation from a kerr black hole. 1. formulation and a method for numerical analysis. *Prog.Theor.Phys.*, 67:1788, 1982.

[121] K. Skenderis. Asymptotically anti-de Sitter space-times and their stress energy tensor. *Int.J.Mod.Phys.*, A16:740–749, 2001.

[122] K. Skenderis and S.N. Solodukhin. Quantum effective action from the adS / CFT correspondence. *Phys.Lett.*, B472:316–322, 2000.

[123] A. Strominger. Black hole entropy from near horizon microstates. *JHEP*, 9802:009, 1998.

[124] D. Sudarsky. A simple proof of a no-hair theorem in Einstein Higgs theory. *Class.Quant.Grav.*, 12:579–584, 1995.

[125] D. Sudarsky and J.A. Gonzalez. On black hole scalar hair in asymptotically anti-de Sitter space-times. *Phys.Rev.*, D67:024038, 2003.

[126] T. Tachizawa, K. Maeda, and T. Torii. Non-abelian black holes and catastrophe theory. 2. charged type. *Phys.Rev.*, D51:4054–4066, 1995.

[127] J. Tafel. Static spherically symmetric black holes with scalar field. *Gen.Rel.Grav.*, 46:1645, 2014.

[128] T. Torii, Kengo K. Maeda, and M. Narita. No scalar hair conjecture in asymptotic de Sitter space-time. *Phys.Rev.*, D59:064027, 1999.

[129] T. Torii, K. Maeda, and M. Narita. Scalar hair on the black hole in asymptotically anti-de Sitter spacetime. *Phys.Rev.D*, 64:044007, 2001.

[130] T. Torii, K. Maeda, and T. Tachizawa. Non-abelian black holes and catastrophe theory. 1. neutral type. *Phys.Rev.*, D51:1510–1524, 1995.

[131] P.K. Townsend. Black holes.

[132] L. Vanzo. Black holes with unusual topology. *Phys.Rev.*, D56:6475–6483, 1997.

[133] M.S. Volkov and D.V.Galtsov. Black holes in Einstein Yang-Mills theory. (In Russian). *Sov.J.Nucl.Phys.*, 51:747–753, 1990.

[134] R. Wald and A. Zoupas. A general definition of 'conserved quantities' in general relativity and other theories of gravity. *Phys.Rev.D*, D61:084027, 2000.

[135] R.M. Wald. Final states of gravitational collapse. *Phys.Rev.Lett.*, 26:1653–1655, 1971.

[136] C.M. Will. Testing the general relativistic no-hair theorems using the galactic center black hole SgrA*. *Astrophys.J.*, 674:L25–L28, 2008.

[137] E. Winstanley. Existence of stable hairy black holes in SU(2) Einstein Yang-Mills theory with a negative cosmological constant. *Class.Quant.Grav.*, 16:1963–1978, 1999.

[138] E. Winstanley. On the existence of conformally coupled scalar field hair for black holes in anti de Sitter space. *Found.Phys.*, 33:111–143, 2003.

[139] Elizabeth Winstanley. Dressing a black hole with non-minimally coupled scalar field hair. *Class.Quant.Grav.*, 22:2233–2248, 2005.

[140] E. Witten. A simple proof of the positive energy theorem. *Commun.Math.Phys.*, 80:381, 1981.

[141] E. Witten. Anti-de Sitter space and holography. *Adv.Theor.Math.Phys.*, 2:253–291, 1998.

[142] B. Wu and L. Zhao. Holographic fluid from the nonminimally coupled scalartensor theory of gravity. *Class.Quant.Grav.*, 31:105018, 2014.

[143] W. Xu and L. Zhao. Charged black hole with a scalar hair in (2+1) dimensions. *Phys.Rev.*, D87(12):124008, 2013.

[144] D. Zeng. An exact hairy black hole solution for adS/CFT superconductors. 2009.

[145] X. Zhang and H. Lu. Exact black hole formation in asymptotically adS and flat spacetimes. *Phys.Lett.*, B736:455–458, 2014.

[146] K.G. Zloshchastiev. On co-existence of black holes and scalar field. *Phys.Rev.Lett.*, 94:121101, 2005.